ROLL COMPACTION SCALE-UP: IMPACT OF MATERIAL, EFFECT OF SCALE AND MODELLING OF THE PROCESS TRANSFER

Inaugural Dissertation

for the attainment of the title of doctor
of the Faculty of Mathematics and Natural Sciences
of the Heinrich-Heine University in Düsseldorf

presented by

Ana Pérez Gago
from Luarca, Asturias (Spain)

Düsseldorf, October 2016

From the Institute of Pharmaceutics and Biopharmaceutics

at the Heinrich-Heine-Universität in Düsseldorf (Germany)

Published with the permission of the

Faculty of Mathematics and Natural Science of the

Heinrich-Heine-Universität in Düsseldorf (Germany)

1st Reviewer: Prof. Dr. Dr. h.c. Peter Kleinebudde

2nd Reviewer: Prof. Dr. Jörg Breitkreutz

Date of the oral examination: 05/12/2016

Dedicada a la Dra. María José Campaña Seoane,

por darme el primer empujón en este aventura que ha sido el doctorado en Alemania.

Dedicated to Dr. María José Campaña Seoane,

for giving me the first push towards this adventure that has been the PhD in Germany.

TABLE OF CONTENTS

LIST OF ABBREVIATIONS

The acronyms more commonly used in this thesis are listed below. Other abbreviations or symbols which have been infrequently used, or whose importance is lower, are only described in the text or in the legend of the corresponding equation.

API	Active Pharmaceutical Ingredient
Bm*	Modified Bingham Number
CI	Confidence Interval
Cs	Screw Speed Constant
D	Roll Diameter
D10	Tenth Percentile
D50	Fiftieth Percentile
D90	Ninetieth Percentile
DOE	Design of Experiments
DV	Dimensionless Variable
FA	Feeding Auger
F_{max}	Maximal Force
FS	Feed Screw Speed
G	Gap Width
GSD	Granule Size Distribution
h_{max}	Maximal Height
$h_{max.corr}$	Corrected value of the Maximal Height
HU	Universal Hardness

K	Compressibility
LOD	Loss on Drying
m	Mass Rate or Mass Throughput
Man	Mannitol
MCC	Microcrystalline Cellulose
MLR	Multiple Linear Regression
MP	Mini-Pactor®
PG	Polygran®
P_{max}	Peak Pressure
PSD	Particle Size Distribution
Q3	Cumulative Volume Distribution Curve
q3	Volume Distribution Curve
r	Pearson's Correlation Coefficient
R	Throughput or Production Rate
R2	Coefficient of Determination
r_b	Radius Ball Indenter
RF	Roll Force
RH	Relative Humidity
RMSE	Root-Mean-Square Error
RP	Roll Pressure
RS	Roll Speed
s	Standard Deviation
SA_{roll}	Surface Area of a Roller Compactor Roll

SCF	Specific Compaction Force
t	Value of Student's t-Distribution
TA	Tamping Auger
W	Roll Width
α	Nip Angle
γ_0	Preconsolidation Relative Density
γ_R	Relative Density of the Ribbon Leaving the Rolls
δ_E	Effective Angle of Internal Friction
θ	Angular Roll Position
μCT	Microcomputed Tomography
ρ_{env}	Envelope Density
ρ_{rib}	Ribbon Relative Density
ρ_{true}	True Density
ϕ_W	Angle of Wall Friction

LIST OF PUBLICATIONS

Part of the work collected in this thesis has already been published in journals as research articles, or has been presented at conferences or meetings. The experimental work, data analysis and manuscript writing of the below mentioned "original research papers", have mostly been performed by Ana Pérez Gago under the supervision of Prof. Dr. Dr. h.c. Peter Kleinebudde. For the second article, the collaboration of Dr. Gavin Reynolds was also extremely important, as he has run the model used in that paper, and contributed to it with several ideas. The study performed in the first article is presented in the initial chapter of the thesis, while the work for the publication in preparation can be found as part of the second and third chapters. However, the work corresponding to the "collaboration papers" was mostly developed by the first authors in each case, and therefore, it has not been included as part of this thesis, it has been cited only if applicable.

ORIGINAL RESEARCH PAPERS

A. Pérez Gago, P. Kleinebudde, *MCC–mannitol mixtures after roll compaction/dry granulation: percolation thresholds for ribbon microhardness and granule size distribution,* Pharmaceutical Development and Technology, 2016, published online (doi: 10.3109/10837450.2016.1163388).

A. Pérez Gago, G. Reynolds, P. Kleinebudde, *Impact of the roll compactor scale on ribbon density,* Powder Technology, 2017, accepted.

COLLABORATION PAPERS

L. Pérez-Gandarillas, A. Pérez-Gago, A. Mazor, P. Kleinebudde, O. Lecoq, A. Michrafy, *Effect of roll-compaction and milling conditions on granules and tablets properties*; European Journal of Pharmaceutics and Biopharmaceutics, Volume 106, September 2016, Pages 38-49.

P. Kazemi, M. H. Khalid, A. Pérez Gago, P. Kleinebudde, R. Jachowicz, J. Szlęk, A. Mendyk, *Effect of roll compaction on granule size distribution of MCC-mannitol mixtures: computational intelligence modeling and parametric analysis*, submitted to Drug Design, Development and Therapy, Volume 11, January 2017, Pages 241-251.

ORAL PRESENTATIONS

A. Pérez Gago, P. Kleinebudde, *Porosity of ribbons of MCC, mannitol and binary mixtures obtained by two Freund-Vector roll compactors*, 9th Annual PSSRC Symposium, Ghent, 2015.

A. Pérez Gago, K. Csordas, P. Kleinebudde, *Roll compaction: The impact of system design and scale-up,* International Congress on Particle Technology (PARTEC), Nürnberg, 2016.

POSTERS

A. Pérez Gago, P. Kleinebudde, *Effect of varying process parameters on granule size distribution of roll compacted MCC, mannitol and their mixtures,* 7th International Granulation Workshop, Sheffield, 2015.

A. Pérez Gago, P. Kleinebudde, *Effect of the scale of two Freund-Vector roll compactors on the porosity of ribbons,* DPhG Jahrestagung, Düsseldorf, 2015.

A. Pérez Gago, P. Kleinebudde, *Impact of the scale for two Gerteis roll compactors analyzing the properties of MCC and mannitol ribbons and granules,* AAPS Annual Meeting and Exposition, Orlando, 2015.

A. Pérez Gago, P. Kleinebudde, *Scale-up study using L.B. Bohle roll compactors by characterizing the relative density of ribbons produced from MCC, mannitol and a binary mixture,* 10th World Meeting on Pharmaceutics, Biopharmaceutics and Pharmaceutical Technology, Glasgow, 2016.

1. INTRODUCTION

The production of tablets in the pharmaceutical industry often requires a previous granulation process in order to achieve adequate flowability and compactability of the material by size enlargement. There are two main types of granulation processes: wet and dry. The first type uses a liquid binder for facilitating the production of granules while the dry granulation process uses force to mechanically aggregate the particles (Bryan 2005).

1.1. ROLL COMPACTION/DRY GRANULATION

Roll compaction/dry granulation is a continuous process, in which powder is being compacted while passing through two counter-rotating rolls obtaining a densified ribbon, which is subsequently milled in order to produce granules that can be later compressed into tablets (Guigon et al. 2007). This process is applied not only in the pharmaceutical field but also in mineral, metallurgical, chemical or food industries, and for many types of materials (Dec et al. 2003). Most of the drugs are not suitable for direct compression and thus, a previous granulation process is required. Therefore, this agglomeration process is highly attractive for the pharmaceutical industry and has been growing in importance in the last years (Kleinebudde 2004), as it offers several advantages (Miller 2005; Smith et al. 2009):

- Improvement in the flow properties of the powder
- Prevention of the segregation of components
- Less production of dust, which also positively affects safety
- Increase not only in the bulk density but also in the particle size
- Feasible processability of moisture and heat-sensitive products due to the elimination of aqueous solvents.

However, there are some disadvantages in contrast to wet granulation (Dalziel et al. 2013). The first of them is the lack of fluid binder, what can lead to higher amount of fines or uncompacted material as no liquid bridges are formed. The second problem can be a partial loss of tabletability due to work hardening, which is when the resistance of a material to permanent deformation increases with the amount of deformation (Malkowska et al. 1983), and its future consequence in tensile strength. Finally, formulations containing a high percentage of the active pharmaceutical ingredient (API) are not always adequate for this

process. These disadvantages, and the lack of a deeper understanding of the process itself, which is apparently simple, could be the reasons why this process is less used in the pharmaceutical industry, in contrast to wet granulation.

Although there are several types of roll compactors available on the market, most of them are compounded of three main parts or units: feeding, compaction and granulation (Shlieout 2000). The feeding unit handles all the process from the moment the powder is added to the hopper until it arrives to the compaction part. This means that this unit is responsible for the powder transportation from the chute to the rolls by one or two screws (also known as augers) depending on the feeding design. The compaction unit is where the powder densification process occurs, and includes the rolls and their sealing system as well as the scrapers which facilitate the removing of the ribbon from the roll surface in the case of stickiness. The sealing system avoids the leak of material and sometimes they are equipped with a de-aeration unit that facilitates the elimination of air. Finally, the ribbons are conducted to the granulation area, where a granulator moved by a rotor and a sieve basket mill the compacts into granules with a maximum particle size defined by the sieve. Most of the roller compactors are compounded of these units, which can be different depending on the machine's supplier. Some manufacturers develop their compactors without granulation units, and the milling process is performed separately. Other suppliers use different granulation systems, as is the case with L.B. Bohle compactors, which are equipped with a conical sieve. Furthermore, in the market and even for the same provider, several designs regarding the feeding system (horizontal, vertical or inclined), roll position (horizontal, vertical or inclined), roll surfaces (smooth, knurled, ribbed, serrated, pocketed…) or in some cases, even the sealing systems (side sealing or cheek plates and rim-rolls) are available on the market (Smith et al. 2009).

Even though the principle of the roll compaction is simple, the process is not fully understood. Furthermore, many parameters, configurations and process conditions can be changed in order to obtain different properties of their final and intermediate products (Falzone et al. 1992; Hervieu et al. 1994; Guigon et al. 2003). Several studies have been performed in order to evaluate how the properties of the granules are affected by the roll compaction settings (Inghelbrecht et al. 1998b; Rambali et al. 2001; Weyenberg et al. 2005; am Ende et al. 2007; Souihi et al. 2013b) for different formulations, and in order to prepare diverse final products. However, another critical aspect that has a high impact on the roll compaction process is the mechanical properties of the material which are being compacted.

1.2. COMPACTION BEHAVIOUR

When a material undergoes a compression process, two main behaviours (Ragnarsson 1996) can be identified: elastic deformation and plastic deformation (with or without fragmentation). This allows the classifying of the materials into elastic, plastic or brittle respectively. There is always a combination of different conducts, and therefore, this cataloguing is done according to the predominating behaviour. If force is applied, a displacement will occur to the material (it will be compressed), however, depending on the nature of the substance, ceasing the loading will lead to different reactions. An ideal elastic material will recover its form after releasing the force, while a model plastic substance will maintain the shape given to it by the loading. Nevertheless, the pharmaceutical powders present a combination of both behaviours.

From all these processes that take place during compression, elastic deformation is uninteresting from the point of view of the pharmaceutical industry, as the material returns to its initial shape once the stress applied stops. Therefore, the plastic deformation, both with and without fragmentation, are more attractive in this respect. When a plastic material is being compressed it will keep its form as a compact after finishing the deformation stress. However, a brittle material will suffer fragmentation of its particles before being irreversibly deformed when the stress is being applied.

1.2.1. PURE MATERIALS AND BINARY MIXTURES

Microcrystalline cellulose (MCC) and mannitol are two widely used excipients in the pharmaceutical industry due to their beneficial properties and numerous applications, although they are normally used as diluents (Armstrong 2009; Guy 2009). However, both materials present different behaviour against compression. MCC is a material that principally suffers plastic deformation, while mannitol is a typical brittle material (Bolhuis et al. 1996). These two opposing behaviours, together with their high presence in the pharmaceutical industry, make these materials interesting to develop a study on. Several authors have investigated how the roll compaction of MCC (Falzone et al. 1992; Inghelbrecht et al. 1998a; Herting et al. 2007b; Yu et al. 2013) and mannitol (Souihi et al. 2013a; Wagner et al. 2015) affects the ribbon and granule properties. Nevertheless, all these studies focused on one of these excipients either as a pure material or as a mixture with others powders.

Several authors have also investigated the importance that the mixture composition and their mechanical properties have on the roll compaction process by studying several properties of the ribbons, granules and mostly tablets (Malkowska et al. 1983; Freitag et al. 2005; Herting et al. 2007b; Yu et al. 2013; Souihi et al. 2013a; Pérez-Gandarillas et al. 2015). Some of these studies have been conducted in order to understand the impact of a plastic/brittle-material mixture in roll compaction (Malkowska et al. 1983; Freitag et al. 2005; Yu et al. 2012; Pérez-Gandarillas et al. 2015), but most of the work is focused on the tablet characterization. Malkowska et al. 1983 already observed different behaviour for the plastic/brittle mixture (consisting in MCC and dicalcium phosphate dihydrate) than for the pure materials in the re-working potential. Freitag et al. 2005 studied the plastic/brittle interaction by using mixtures containing magnesium carbonate and powdered cellulose (PC) of different particle sizes. The ranges used were 0, 5, 10, 15, 20 and 25% of PC. After roll compacting these mixtures, they concluded that when using fractions of PC with smaller particle size, greater amounts of fines and lower values of D50 are obtained. The higher proportion of bigger granules and the lower amount of fines were obtained when using a smaller proportion of PC in the mixture. Pérez-Gandarillas et al. 2015 investigated the properties of another plastic/brittle mixture consisting of MCC and lactose in proportions of 25, 50 and 75% of MCC. Regarding granule properties, no great differences in the granule size distribution (GSD) were found.

1.2.2. PERCOLATION THEORY

Binary mixtures can be described using the percolation theory (Blattner et al. 1990; Stauffer et al. 1994; Leuenberger 1999), which basically refers to the interaction between the elements of a system. This theory addresses the formation of clusters inside a lattice, which can connect and affect the behaviour of the system. Those clusters can be either a single particle or a group thereof adjacent, and they can be finite if they are isolated or infinite if they are connected. This change from finite to infinite clusters affects the behaviour of the system and is determined by the percolation threshold or critical concentration. From the pharmaceutical point of view, this theory can refer to the interaction between the powders forming part of a binary mixture. It is possible to apply the percolation theory, if the system is well defined by a lattice.

When a powder A and a powder B are mixed, the particles of both form a lattice by random occupation, resulting in the formation of clusters. At low concentrations of A, the particles of this material will form finite or isolated clusters inside a matrix of B but once the percolation threshold is overcome, the particles of A will form an infinite cluster affecting the behaviour of this whole mixture. For a binary mixture, two percolation thresholds can be defined: a lower threshold where one of the components starts to percolate (form an infinite cluster) and an upper threshold where the other powder stops having an infinitive cluster (Leuenberger 1999). However, on occasions only one percolation threshold can be visualized as Blattner et al. 1990 have shown in their work. They applied the percolation theory to study the properties of tablets prepared from a mixture formed of a hard and brittle material (α-lactose) in three different sieve fractions, and a plastic and soft substance (Polyethyleneglycol or PEG 10,000). They concluded that the percolation threshold is a function of the geometrical packaging which depends on the particle size, particle size distribution (PSD) and shape of the particles. The percolation theory has mostly been applied to studying matrix systems (usually tablets) in order to design the best formulation regarding drug release and tablet disintegration (Bonny et al. 1993; Caraballo et al. 1993; Leuenberger et al. 1995; Fernandez Hervas et al. 1996; Fuertes et al. 2006; Caraballo 2010; Grund et al. 2013). However, not much work applying the percolation theory in roll compaction has been reported in the literature (Boersen et al. 2014; Heiman et al. 2015).

1.3. SCALE-UP

Roll compaction, as any process of high interest for the pharmaceutical industry, has to be scaled-up, as pieces of equipment in different sizes or scales are available on the market. Scale-up or scalability is the transfer of the process from a smaller to a larger scale. This is the definition the present thesis is based on. For achieving this objective of transferring the process between scales, the critical parameters involved in this procedure must be identified and their influence understood, so that it is possible to adapt them in order to obtain the same product quality on both scales. This process is an important point to consider in research and a critical step in the industry, as it is desirable that the results obtained in the laboratory can also be transferred to pilot, production or commercial scale. For the roll compaction process, two scale-up strategies exist, which refer to the pattern that the manufacturers follow to develop the next scale. These approaches are based on how the size of the rolls are modified, although

all the pieces of the roll compactor increase in size. In this manner, change in scale can be achieved by modifying the roll diameter as well as the roll width, or just by varying the roll width while keeping the diameter constant

Nevertheless, it is important to clarify that scale-up can be understood as different concepts which have diverse objectives. On the one hand, scale-up in roll compaction can be understood as the increase in the batch size (Fahmy et al. 2012; Dalziel et al. 2013), i.e. the amount of material produced. Therefore, the scale-up of the roll compaction process can be also performed with the same machine by increasing the throughput (higher roll speed and/or gap) or prolonging the running time of the continuous process. On the other hand, it can also be defined as the investigation of the process by the engineers in order to establish the dimensions and settings of the new machine. The design of the different scales of the roll compactors is an important issue and also a difficult process for the manufacturers, as there are several regulatory demands that need to be fulfilled. One of those is the scaling factor of 10 (or approximately this value) that has to exist between scales in order to define them. This means that if a batch of 1 kg is considered the lab scale, the pilot should be 10 kg and the production 100 kg. Apart from those initial regulations, before the development of a larger-scale compactor, several studies are performed on the smaller-scale machine with the purpose of gaining experience with it. Two possible strategies can be followed (Sprockel et al. 2011). The first approach is a parametric strategy in which equivalency factors are used for calculating the dimensions of the compactor being designed, and the second strategy is an attribute-based strategy which tries to obtain the same ribbon properties in both scales.

On the one hand, the parametric-based strategy uses the experience collected after performing several experiments on the small scale together with its geometry and design to obtain the equivalency factors. These scale-up factors are needed to calculate the parameter values for the larger machine. Pressure can be estimated considering the geometry of the rolls (width and diameter) in order to generate the equivalent force, a fact that can be confirmed by using instrumented rolls. Once the force is known, the corresponding value for the larger scale can be calculated (equation 1, Sprockel et al. 2011).

$$SCF_2 = \frac{D_2}{D_1} \cdot SCF_1 \cdot t_c \qquad \text{Eq. 1}$$

where SCF_2 is the roll force per unit distance of roll width for the new machine, D_2 the roll diameter of the larger scale, D_1 the roll diameter of the laboratory scale, SCF_1 the roll force per

unit distance of roll width for the lab machine and t_c an adjustment factor related to the dwelling time.

Regarding the roll speed, it can be easily transferred to the larger scale also by extrapolation considering the dimensions of the rolls (equation 2, Sprockel et al. 2011). Finally, the relationship between the roll speed and the screw velocity determines the gap for a fixed pressure and material.

$$RS_2 = \frac{R_1 \cdot 5}{D_2 \cdot \pi \cdot W \cdot G_2 \cdot \rho_{rib}} \qquad \text{Eq. 2}$$

where RS_2 is the roll speed in the larger machine, R_1 the throughput or production rate of the laboratory machine, W the roller width (for some machines an adjustment factor may have to be included as well), G_2 the gap width of the new scale and ρ_{rib} the ribbon relative density. This factor of 5 is specific to the example given by Sprockel et al. 2011.

On the other hand, the attribute-based strategy consists in identifying those properties that make a ribbon ideal by extrapolating the development results from the granules. Therefore, it is considered that the optimal ribbons are those which after milling will show the best granule properties regarding flow and compactability. In order to produce these optimum ribbons, the gap and pressure are adapted while using a high roll speed, and keeping the screw speed in the range that adequately maintains the powder feed.

1.3.1. SCIENTIFIC INVESTIGATIONS

Despite its importance, limited work regarding scalability has been published. Although the principal upon which roll compaction is based, is simple, it is not easy to scale the process up, because when the roll diameter increases, the nip area changes unproportionally (Teng et al. 2009). Several authors have performed multiple studies in the roll compaction field which resulted in different tools considered by the investigators as useful for scale-up (Gupta et al. 2004; Zinchuk et al. 2004; Esnault et al. 2013).

Sheskey et al. 2000 and Sheskey et al. 2002 performed a scale-up study using three compactors from Freund-Vector company (TF-Mini, TF-156 and TF-3012) to transfer a drug-containing formulation which production conditions were optimized for the TF-Mini. Freund-Vector Corporation applies the change in roll diameter and width as scale-up strategy. It was observed that the roll force (expressed as tons/inches) and speed can be easily scaled by their

adaptation in order to obtain the same total roll force (depending on the roll width) and the same linear speed (depending on the roll diameter) in all compactors. Furthermore, the authors found that the screw and its relationship with the roll speed should be adapted to a 1.3:1 ratio.

Recently, Allesø et al. 2016 investigated the scale-up between two compactors from the company Gerteis (Mini-Pactor® and Macro-Pactor®) which have the roll diameter in common, thus, only the width of the rolls is different between both scales. A design of experiments (DOE) was performed on the two scales using mainly MCC. Ribbon porosity was determined using two different methods (laser-based technique and an oil intrusion method) and the values obtained for the same process conditions in the two scales were compared, and an excellent correlation was found. They concluded that ribbon porosity was scale-independent when the roll width is used as scale factor and the specific compaction force (SCF) is constant, i.e. when only the roll width differs between both pieces of equipment. The SCF is a parameter that represents the compaction force per cm of roll width, and as it expressed in this manner, the same value can be set in the two different scales.

1.3.2. MODELS

Many of the scale-up studies more recently published include the development of models which allow the prediction of the density of the ribbons, and the parameter settings required for achieving a target value. The models can be primarily classified as mechanistic models and dimensionless variables (DVs). These first are based on physical principles and considerations of the roll compaction process, and most of them rely on Johanson's theory. The second approach consists of the application of dimensional analysis to develop a variable which is independent of the scale, and therefore allows transferring the process.

Many authors have developed other roll compaction approaches, such as other statistical and multivariate models (Mansa et al. 2008; Nkansah et al. 2008; Soh et al. 2008; Cunningham et al. 2010; Peter et al. 2010; Hilden et al. 2011; Michrafy et al. 2011; Muliadi et al. 2012; Esnault et al. 2013; Zheng et al. 2013; Bi et al. 2014; Liu et al. 2016; Tan et al. 2016), which can be normally used to describe how the powder behaves during compaction or to predict the relative density or solid fraction of ribbons. However, those methodologies were not described as being applicable for the scalability of the process, and therefore will be not considered.

1.3.2.1. MECHANISTIC MODELS

Johanson 1965 developed a model which is considered the basis of the roll compaction theory. As this model considers the geometry of the compactor, it could be useful for scale-up predictions. His theory is based on predicting the density of the ribbon by calculating the differences in volume between the slip and nip area in respect to the point of maximal force, i.e. the gap. The nip area is the zone where the densification starts and it is defined by the nip angle (Guigon et al. 2007). In order to calculate the latter, Johanson equates the normal stress generated in the slip (term on the left in equation 3) and the nip (term on the right in equation 3) regions. He proposed that when the pressure gradients for the slip and nip regions are equal, the nip angle can be calculated:

$$\frac{4_\sigma(\pi/2-\alpha-\nu)\ tan\,\delta_E}{\frac{D}{2}[1+G/D-cos\,\alpha]\,[cot(A-\mu)-cot(A+\mu)\,]} = \frac{K_{\sigma_\theta}(2\,cos\,\alpha-1-G/D)\ tan\,\alpha}{\frac{D}{2}[d/D+(1+G/D-cos\,\alpha)\,cos\,\alpha]} \qquad \text{Eq. 3}$$

where σ is the mean normal stress in granular solid, α the nip angle, ν the acute angle between direction of σ_1 and tangent to roll surface, δ_E the effective angle of internal friction, D the roll diameter, G the roll gap, μ the friction coefficient, K the compressibility constant for granular solids, σ_θ the mean normal stress at position θ and d the average thickness of a briquette for zero roll gap. A is defined by equation 4, expression in which θ is the angular position in roll bite:

$$A = \frac{\theta+\nu+\pi/2}{2} \qquad \text{Eq. 4}$$

Once these equations have been solved, the nip angle value is known, thus, it can be used to calculate the roll force (equation 5), and later the volume of the nip region. Then, the density of the ribbon is obtained just by the differences in volume between the nip region and the gap.

$$RF = \frac{P_m WDF}{2} \qquad \text{Eq. 5}$$

where RF is the roll force, P_m the horizontal pressure at θ = 0 = α (nip pressure), W is the roll width and F is the roll force factor and can be calculated according to equation 6:

$$F = \int_{\theta=0}^{\theta=\alpha}\left[\frac{(d+G)/D}{d/D+(1+G/D-\cos\theta)\,\cos\theta}\right]^K \cos\theta\ d\theta \qquad \text{Eq. 6}$$

Nevertheless, the Johanson's model has one weakness. It uses the pressure at the nip angle (nip pressure) to calculate the roll force. However, this value cannot be accurately

estimated and several authors have developed different approaches to overcome this limitation.

Reynolds et al. 2010 proposed a practical approach (also referred as Reynolds' model) in which the need for the nip pressure is avoided by using a preconsolidation relative density that can be used directly to relate the ribbon density to the modelled peak pressure, P_{max}, between the rolls (equation 7). Another novel point is an alternative form of the model that includes the feed screw speed, showing how this has an effect on the incoming material. The model was validated using experimental data obtained from the roll compaction of a formulation (including MCC and dibasic calcium phosphate dihydrate) in an Alexanderwerk WP 120. For this compactor, two roll widths are available: 25 and 40 mm width but both of 120 mm diameters. The relative density of the ribbons was obtained proving that the model provides excellent correlation between the predicted and experimental values. As a starting point, the model needs the compressibility and the preconsolidation relative density. These can be estimated from tabletting after performing a uniaxial compression of the raw powder at different levels of pressure and calculating the density of the resulting compacts. Later, the compressibility and the preconsolidation relative density can be obtained from the plot of the relative density against the pressure applied, as these authors showed in their paper. Although those values can be used as reference for running the tool in the first place, they are not highly accurate, and they normally lead to over-predictions of the ribbon density due to differences in the powder confinement between a die and a roll compactor. For this reason, these parameters need to be estimated from the best fit line obtained from plotting the ribbon relative density against the peak pressure. This best fit line needs to be solved iteratively, as the peak pressure depends on the estimated parameters. Calibrating the compressibility and the preconsolidation relative density this way provides improved ribbon density predictions. From the point of view of the scale-up, the values for the compressibility and the preconsolidation relative density are constant, as the material or formulation is the same, and therefore it is not necessary to calculate them again. Another advantage of this model is the possibility of comparing two compactors at the same time.

$$P_{max} = \frac{2RF}{WD \int_{\theta=0}^{\theta=\alpha(\delta_E,\phi_W,K)} \left[\frac{G/D}{(1+G/D-\cos\theta)\cos\theta}\right]^K \cos\theta d\theta} \qquad \text{Eq. 7}$$

where RF is the roll force, W the roller width, D the roll diameter, θ the angular roll position, α the nip angle, δ_E the effective angle of internal friction, ϕ_W the angle of wall friction, K the compressibility and G the gap or roll separation.

This approach showed not only utility for scale-up, but also for other types of roll compaction transfer. Souihi et al. 2015b used the Reynolds's model to transfer a formulation between two roll compactors using different feeding systems: Alexanderwerk WP 120 and Pharmapaktor C250 (from Hosokawa Bepex company). The poorly compactable paracetamol and four typical excipients for immediate release tablets (mannitol, MCC, croscarmellose and sodium stearly fumarate) were blended. The formulation was roll compacted in the horizontal feed screw roll compactor Alexanderwerk WP 120 following a full factorial design, and in the vertical feeding roll compactor Pharmapaktor C250 guided by a central composite face-centered design. Results in both cases showed an excellent prediction of the ribbon porosity, and therefore, they confirmed the applicability of the model not only for scale-up, but also for process transfer. However, only two formulations were tested in total, although they covered plastic and brittle excipients and a commonly used API.

Another mechanistic model for scale-up was developed by Nesarikar et al. 2012b in which the nip pressure requirement is eliminated. This approach is based on relating the relative density as a function of the gap and the roll force per unit of roll width (RFU in their work and equivalent to SCF), which are two variables independent of the roll compactor. A placebo blend and three different types of active mixtures were roll compacted following different DOEs in an Alexanderwerk WP 120. This compactor was equipped with an instrumented roll (120 mm roll diameter and 40 mm roll width) which allows measuring of the normal stress on the ribbon and the nip angle. In this manner, the nip angle is calculated as a function of gap and RFU, which is subsequently used for calculating the roll force, and therefore, the ribbon density. Placebo data was collected and used to calibrate the model and develop an equation. The three active blends were used for validation of this model, obtaining reasonable accuracy for the ribbon density. Then, a not instrumented Alexanderwerk WP 200 (200 mm and 75 mm of roll diameter and width, respectively) was used for the scale-up study. As no data regarding normal stress or nip angle was collected for the WP 200, the equation obtained for the WP 120 for calculating the latter was used. Considering this assumption, the ribbon densities for a placebo mixture were calculated for the WP 200, and these values compared well with those obtained from the experimental data in the WP 200. The limitations of this approach are the requirement of extensive calibration data using materials with differing compaction behaviour, and the need for an instrumented roll in order to obtain the nip angle.

1.3.2.2. DIMENSIONAL ANALYSIS

Other authors applied a dimensionless number approach. Rowe et al. 2013 developed the called modified Bingham number (Bm*), defined by equation 8. They proposed another model based on the Johanson's theory which included some modifications from Reynolds's approach, especially the consideration of the feeding zone that affects the compaction. The same experimental data collected by Nesarikar et al. 2012b was used (placebo and API blends using the instrumented Alexanderwerk WP 120 and the Alexanderwerk WP 200 roll compactors). In order to scale-up the roll compaction process, the Bm* is established. The Bingham number is a manipulation of the shear stress equation known in the literature. This number has to be modified for the roll compaction process as the pharmaceutical powders normally used do not behave like Bingham materials. The Bm* is plotted against the relative density and a linear correlation was obtained for the two scales considered. The dimensionless expression represents a ratio between yield and viscous stresses, which must be constant in order to get the same solid fraction for the ribbons. Therefore, the Bm* also elucidates the importance of a yield-to-viscous stress relationship to reach a robust roll compaction process. As was the case of the previous model, it covers a broad range of materials and process combinations, however, on this occasion, the authors stress the need for parameters which are easy to measure or obtain.

$$Bm^* = \frac{C_S}{\gamma_0 \cdot \rho_{True} \cdot \pi \cdot D^2 \cdot W} \cdot \frac{(SA_{roll})^{0.5}}{G} \cdot \frac{FS}{RS} \qquad \text{Eq. 8}$$

where Cs is the screw speed constant (kg), γ_0 the preconsolidation relative density (dimensionless), ρ_{true} the true density of the powder (kg/m^3), D the roll diameter (m), W the roll width (m), SA_{roll} the surface area of a roller compactor roll (m^2), G the gap width (m), FS the feed screw speed (s^{-1}) and RS the roll speed (s^{-1}). The Cs is defined in detailed in equations 16-18 (page 159).

More recently, Boersen et al. 2015 proposed another dimensionless relationship, directly known as DV which considered the roll pressure, roll speed, feed screw speed, the true density of the material and the roll diameter as shown in equation 9. This variable was correlated with the ribbon density, obtaining a linear relationship. This DV was used to transfer the process from an Alexanderwerk WP 120 to a Fitzpatrick IR220. The roll compaction was first run with the Alexanderwerk and using the equation, the corresponding DV was obtained and used to calculate back the process conditions for the Fitzpatrick. A small percentage of error was found between the ribbon relative densities obtained in both machines after

performing the adaptation with the DV. Although this model was mostly applied to different sieve fractions of MCC and their mixtures with APIs, and therefore requires further validation, it looks promising, in particular because of the limited effort required to calculate the DV. The authors concluded that it could be a first good approach for process transfer, and also for scale-up.

$$DV = \frac{RP}{RS \cdot FS \cdot \rho_{true} \cdot D^2} \qquad \text{Eq. 9}$$

where RP is the roll pressure (Pa), RS the roll speed (1/min), FS the feed screw speed(1/min), ρ_{true} the true density of the powder (kg/m^3) and D the roll diameter (m).

1.3.2.3. OTHER MODELS

Other techniques or approaches can be used in order to predict the ribbon relative density in larger scales. Shi et al. 2016 developed a practical approach to scale-up the roll compaction process from the Alexanderwerk WP 120 to the Alexanderwerk WP 200 roll compactor. This methodology consists of the development of a linear equation which describes the target property and which is later adapted for the large scale. They started with the performance of a central composite design on the Alexanderwerk WP 120 with a formulation containing plastic and brittle excipients as well as API. The authors defined ribbon thickness and density as reference attributes. According to the experience learnt from the statistical evaluation, it is possible to establish two linear equations for each of these properties. In these equations, apart from the numerical slopes and Y-intercepts, the pressure and, for the thickness the gap, are also involved. The authors considered that the slopes of these equations are powder-dependent (remain constant for the same formulation) while the Y-intercepts are compactor-dependent. In this sense, the slope can be maintained to develop the linear equation on a larger scale. A calibration batch was conducted on the Alexanderwerk WP 200 in order to obtain the Y-intercepts. The roll pressure and gap for this new batch were known and the ribbon thickness and density were measured. With this information, the authors adapted the previous equations and obtained the ones for the Alexanderwerk WP 200. The success of this methodology was later confirmed by running new experiments on the large-scale compactor. The great advantage of this approach is its simplicity.

Another tool was proposed by Liu et al. 2011. In this work, a new statistical methodology is used to scale-up a roll compaction process between the Fitzpatrick IR220 and

the Fitzpatrick IR520. A joint-Y partial least squares (JYPLS) was proposed by García Muñoz et al. 2005 and applied by the authors in their study for scaling-up the roll compaction process. This model has the pre-requirement that the attributes of the products (Y for both scales which can be for example ribbon density) must have a common correlation. Historical data consisting of different combinations of four APIs and nine excipients compacted in one or another compactor was used to fit a JYPLS model. The JYPLS model is later inverted by a constrained optimization in order to find the settings that should be selected for the Fitzpatrick IR 520 to obtain the same quality of the ribbons. The results confirmed that this methodology could be used for scaling-up, however, this model requires high amount of data to perform its calibration.

1.4. DIMENSIONAL ANALYSIS

Most of the processes implemented in the chemical or pharmaceutical industry are scale-dependent. In order to solve this scale-up problem, in the engineering field and physical science the dimensional analysis (Zlokarnik 1991; Levin 2005; Zohuri 2015) is widely used and considered as the basis of the scale-up methods. For this reason, it has been already applied in the literature, as well as also being used in the present work. Dimensional analysis is a method which consists on the development of dimensionless numbers by establishing an equation which as a whole lacks the dimensions. It is based on the assumption that any phenomenon can be described by a dimensionally homogeneous equation in which the relevant variables of the process are involved. Therefore, dimensional analysis leads to an equation or relationship named DV, which allows the transfer of the process of interest between scales or even different operating units.

Before starting to apply this methodology, it is necessary to understand that every physical variable can be expressed as the basic dimensional qualities which are e.g. mass (M), length (L) and time (T). Although there are in total 7 of those basic dimensional qualities, only those 3 (M, L and T) are required to face most of the cases in the pharmaceutical field. In this sense, any variable involved in one of those processes can be expressed using these 3 magnitudes. For example, a diameter is a physical quality which has dimensions of L. In the same manner, the speed is defined as the distance covered per unit of time, and therefore, it has the dimensions of L divided by T (LT^{-1}). It is important to consider these basic dimensional

qualities, because the objective of the dimensional analysis is to develop a DV in whose equation all the variables are dimensionally homogenous (Levin 2005).

1.4.1. BUCKINGHAM'S Π THEOREM

The key theorem of the dimensional analysis is the Buckingham's π theorem (Zlokarnik 1991; Zohuri 2015), which is a methodology that allows the development of DVs. This objective is achieved by the construction of π-products or dimensionless groups, which are grouping variables that as a whole have no dimensions. This theorem starts with a list of relevant variables expressed as MLT dimensions. In it, the target variable has to be also considered for the development of the π-products. Choosing the variables that enter the problem is a difficult step, as including wrong factors will lead to a wrong DV in the majority of cases. Gathering information from experimental work, would allow for the detecting of the important variables and thus, reduce the number of them in the problem. However, not all the variables that experimentally seem to be important are relevant in the end. For example, selecting variables whose influence is already considered in others, should be avoided, as could lead to incorrect DVs.

Once this relevant list is prepared including the variables and their dimensions, Buckingham's theorem states that the number of independent dimensionless groups that can be obtained is defined by equation 10:

$$m = n - r \qquad \text{Eq. 10}$$

where m is the amount of dimensionless groups or π-products, n the number of variables or physical quantities considered on the process and r the number of basic dimensional qualities or rank of the dimensional matrix. The amount of π-products should be low (ideally not higher than 3) in order to reduce the problem and to simplify the interpretation of the results.

In order to facilitate the understanding of the methodology followed, an example will be provided. In this case, the π-products would be obtained for the flow of a fluid located over a spherical solid. In Table A, the list of relevant variables as well as the target one is presented. In this case, the force would be the variable of study. Apart from that, in Table B, all the base quantities are collected by this example.

Table A: Target and relevant variables for the case study together with the symbol and the dimensions.

NUMBER	VARIABLES	SYMBOL	DIMENSIONS
1	Force	F	MLT^{-2}
2	Density	ρ	ML^{-3}
3	Viscosity	μ	$ML^{-1}T^{-1}$
4	Diameter	D	L
5	Velocity	V	LT^{-1}

Table B: Basic dimensional qualities and symbol thereof involved in this example.

NUMBER	DIMENSION	SYMBOL
1	Mass	M
2	Length	L
3	Time	T

According to these tables and using equation 10, the number of dimensionless groups (m) is equal to 2. This results of the deduction from the 5 variables involved in this study, of the 3 basic dimensions required for this example (MLT). In order to obtain these two π-products, several methods can be followed, such as the use of dimensional matrix or by establishing a function. The example provided will continue with the application of the latter approach.

First of all, a function including all the variables considered is defined as equal to 0. From this formula, it is possible to affirm that the target variable is also a function of all the others factors included:

$$f(F, \rho, \mu, D, V) = 0 \qquad \text{Eq. A}$$

$$F = f(\rho^a, \mu^b, D^c, V^d) \qquad \text{Eq. B}$$

Afterwards, both sides of the equation are substituted by the dimensions. The exponents already given in equation B, must be maintained when replacing the variables for

the dimensions presented in Table A. The next step is to group the products that have the same dimensions. The mathematical calculations thus, continue as follows:

$$MLT^{-2} = (ML^{-3})^{a} \cdot (ML^{-1}T^{-1})^{b} \cdot L^{c} \cdot (LT^{-1}) \qquad \text{Eq. C}$$

$$M^{1}L^{1}T^{-2} = M^{a+b} \cdot L^{-3a-b+c+d} \cdot T^{-b-d} \qquad \text{Eq. D}$$

Once the groups have been defined as in equation D, the next step is to equate the exponents in both sides of the formula for the same dimension (colors in equation D are used in order to facilitate the identification of the different groups). The resolution of the formulas will lead to the calculation of the unknown exponents. Nevertheless, it will be only partial in order to group the factors in different π-products, as will be shown below. Depending on the complicity of the equations obtained, different calculations can be performed.

$$\begin{aligned} a + b &= 1 \\ -3a - b + c + d &= 1 \\ -b - d &= -2 \end{aligned} \qquad \text{Eq. E}$$

In order to calculate the exponents, a system of linear equations is used in this example, taken two of the unknown formulas from equation E. After performing all the calculations, the resulting values are:

$$\begin{aligned} a &= 1 - b \\ d &= 2 - b \\ c &= 2 - b \end{aligned} \qquad \text{Eq. F}$$

Once, the exponents values are calculated, they can be substituted on the initial equation B set at the beginning of the process:

$$F = \rho^{1-b}, \mu^{b}, D^{2-b}, V^{2-b} \qquad \text{Eq. G}$$

As can be seen, not all the exponents were obtained. In this case, one (b) was not calculated. The reason for this is that when substituting in the initial equation considered, b will defined one π-product, while the other dimensionless group will be determined by the exponents which have a specific value:

$$F = (\rho^{-1}, \mu, D^{-1}, V^{-1})^{b} \cdot \rho\, D^{2}\, V^{2} \qquad \text{Eq. H}$$

$$\frac{F}{\rho\, D^{2}\, V^{2}} = \left(\frac{\mu}{\rho D V}\right)^{b} \qquad \text{Eq. I}$$

Therefore, the two π-products that according to the theorem should be calculated in this case are those below:

$$\pi_1 = \frac{F}{\rho\, D^2\, V^2} \qquad \text{Eq. J}$$

$$\pi_2 = \left(\frac{\mu}{\rho D V}\right)^b \qquad \text{Eq. K}$$

Apart from this methodology, other techniques can be followed to obtain the π-products. They can even be defined by trial-error methods. Nevertheless, there are some rules which facilitate the establishment of the π-products:

- The first dimensionless group should include the target variable (force in the example described).
- Any factor presenting units that are not shared with other variables cannot be included in any π-product.
- Any variable which is already dimensionless is automatically a dimensionless group.
- Two factors having the same dimensions (for example, two types of length, like thickness and diameter) will be another π-product expressed as their ratio.
- Any dimensionless product multiplied by numbers or exponents will remain dimensionless, thus, these mathematical operations are allowed.

Independent of the mode to obtain the π-products, the different dimensionless groups defined are related between each other in the final equation of the DV. The problem is to find the relationship established between them. Therefore, the last step consists of representing the different dimensionless groups against each other, in order to see what kind of relationship they have between themselves. For example, for another case with 3 π-products, it could be possible to prepare a graph in which π_1 is plotted in the X-axis and π_2 is plotted in the Y-axis. Different π_3 can be represented on the graph and for example, if for the diverse π_3 a parallel line to one of the axis is observed, it can be concluded that it has no effect and be deleted. Nevertheless, the process of developing a DV equation is not always easy or even feasible.

2. OBJECTIVES

The current thesis has been performed as in individual project within the IPROCOM (the development of in silico process models for roll compaction) Marie Curie initial training network. This project was funded by the European Commission under the FP7-PEOPLE-2012-ITN Programme. This multidisciplinary consortium, as can be seen in Figure 1, is composed of a total of 15 projects grouped in 3 work packages (WP) depending on the research goals and 4 strands (S) classified according to a specific part of the roll compaction process investigated. In that sense, the present work, which corresponds to project number 3, is focused on roll compaction scale-up and it belongs to the WP1 and the S2. Therefore, most of the work presented in this thesis refers to the roll compaction process from the point of view of the ribbon characterization.

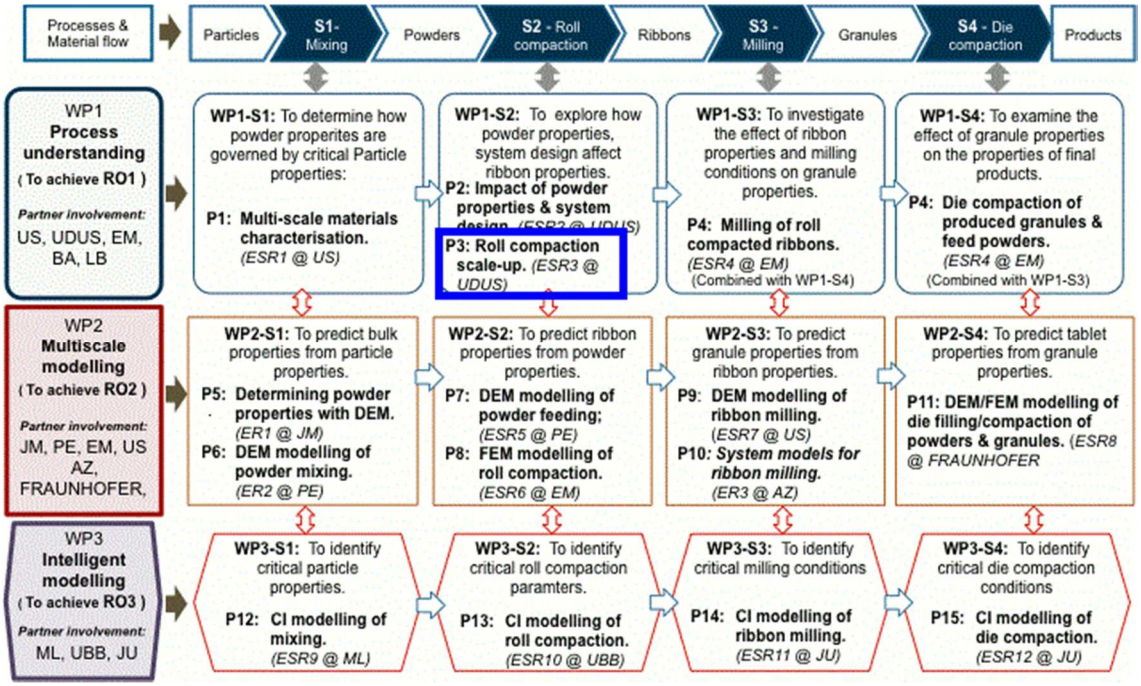

Figure 1: General plan of the IPROCOM consortium where the present individual project is marked.

The main objective of this work is to study the scale-up of the roll compaction process from the point of view of the process understanding. With this purpose, it is necessary to investigate the influence of the different production conditions, the powder properties of the raw materials and the effect of the roll compactor scale on the attributes of mainly the intermediate products (ribbons) in order to successfully transfer the process between scales.

A total of 7 binary plastic/brittle mixtures were roll compacted following a common DOE using 3 couples of compactors provided by Gerteis, L.B. Bohle and Freund-Vector companies. This means a total of 6 machines classified in 3 compactor lines. MCC and mannitol were selected as model excipients in order to study the plastic/brittle behaviour. Ribbons, and to a lesser extent granules, from MCC, mannitol and 5 binary mixtures (15, 30, 50, 70 and 85% MCC) were produced at all the scales and later characterized. Due to its importance, pure MCC, mannitol and the 50% mixture (or 1:1 blend) were considered as the main materials, and therefore, deeply studied. The compactors involved in this work were classified in 3 individual scale-up studies according to the supplier. The different manufacturers provide machines with diverse designs (feeding system, roll position, scale-up strategies...) and therefore, this allows a general overview of the scale-up of the roll compaction process. Furthermore, the scalability of the specific compactors used in this work has been poorly investigated in the literature, and currently, for the specific case of the L.B. Bohle compactors, no scale-up studies have been yet published, according to the author's knowledge. Finally, some of the scale-up models described in the literature were fed with the data collected in order to evaluate, on the one hand, the accuracy of these models, and on the other hand, if the model shows enough precision to make predictions and successfully transfer the process between scales. Due to the availability or complexity of using the different models, only 3 of those approaches were studied.

Therefore, this thesis will be divided in three main chapters: The first part mostly focused on the effect of the properties of the powder compacted and process parameters, a second one on the combined impact of the mixture composition, production conditions and the scale, and finally the last part, in which different models described in the literature are applied to the data collected in order to successfully scale-up the process.

3. MATERIALS AND METHODS

3.1. MATERIALS

MCC (Avicel® PH 101, FMC Bio Polymer, USA) and mannitol β-modification (Pearlitol® 200 SD, Roquette, France) within the consortium of the IPROCOM project, were used to perform all experiments for the Gerteis (Mini-Pactor® and Macro-Pactor®), L.B. Bohle (BRC 25 and BRC 100) and Freund-Vector (TFC-Lab Micro and TF-Mini) scale-up studies. In the case of MCC, the lots used were: P113825620, P114857702, 61333C and 61351C (Gerteis line), P114827702 (L.B. Bohle line) and P113825526 and 61407C (Freund-Vector line). Regarding mannitol, the batches utilized were: E430G, E988G, E355G and E884G (Gerteis), E430G (L.B. Bohle) and E288G and E372G (Freund-Vector).

No lubricant was used in any of the compactions as it can drastically affect the process (He et al. 2007; Miguélez-Morán et al. 2008; Dawes et al. 2012; Yu et al. 2013; Mosig et al. 2014). The moisture content can also influence the roll compaction (Gupta et al. 2005a; Wu et al. 2010; Osborne et al. 2013), and as MCC is an hygroscopic powder, the raw materials were stored in a climate room at 21°C and 45% of relative humidity (RH) whenever it was possible.

3.2. METHODS

3.2.1. PRODUCTION

3.2.1.1. DESIGN OF EXPERIMENTS

DOE has been proven to be a useful tool for the study of the roll compaction process (Souihi et al. 2013a) and thus, it was used to investigate how different compaction conditions, materials and compactors' scales affect the properties of ribbons and granules. Although different DOEs were later modified and applied to study specific aspects, two original designs were implemented: a multilevel and a simple full factorial design. Those DOEs were afterwards modified by adding other factors depending on the objective of the evaluation. The statistical evaluations were always performed using Modde 9.0 (Umetrics, Sweden) and applying a multiple linear regression (MLR). The non-significant factors were always deleted from the model before presenting the results. This software provides coefficient and response contour plots, useful for a visual understanding of the data.

Table 1: Description of the multilevel DOE performed.

FACTORS	LEVELS				
	– 1		**0**		**+ 1**
Gap (mm)	1.5		2.25		3
Roll Speed (rpm)	2		3		4
Specific Compaction Force (kN/cm)	2	4	6	8	10

The multilevel full factorial design (Table 1) consists in 2 factors in 2 levels and 1 factor in 5 levels plus 3 repetitions of the centre point meaning a total of 23 runs. The full factorial design (Table 2) is a reduced version of the previous one and it has 3 factors in 2 levels together with the 3 replications of the zero level, what leads to 11 runs in total. The factors considered in all these designs are the gap width, roll speed and the SCF, and this last one, due to its importance, is investigated in 5 levels on the first case. In order to facilitate the distinction between both DOEs, the multilevel design was also called as 23-runs DOE and the simple full factorial design was normally named as 11-runs DOE or also 2^3 design. The levels that appear in the tables were chosen according to the limitations of the process, as some combinations of gap width and roll speed were not feasible. Those DOEs were performed during the production of the different mixtures, and they were randomized in order to avoid that the manufacturing order could have a systematic influence on the resulting products and therefore, on the models derived from the data.

Table 2: Description of the 2^3 DOE performed.

FACTORS	LEVELS		
	- 1	**0**	**+ 1**
Gap (mm)	1.5	2.25	3
Roll Speed (rpm)	2	3	4
Specific Compaction Force (kN/cm)	4	6	8

The multilevel design was carried out only when investigating the Gerteis compactors, while the 2^3 design was used also in case of some parts of the Gerteis study and for the main materials (MCC, mixture 50% and mannitol) in case of the L.B. Bohle line. For the Freund-

Vector compactors, and due to the design limitations of the machines (especially the lack of gap control system), no DOE was applied. In this manner, only the roll pressure was studied in 3 different levels (2, 5 and 8 MPa) for the main materials while maintaining as constant as possible the roll speed and the gap width at 2 rpm and 1.5 mm respectively. The mixtures (15, 30, 70 and 85% MCC) were produced under only 5 MPa roll pressure, 2 rpm roll speed and 1.5 mm gap, which could be considered as the "centre point" for the study of these compactors.

3.2.1.2. PREPARATION OF MIXTURES

For each individual scale-up study, a total of 5 weight/weight mixtures were prepared. In the case of the blends compacted with the Gerteis compactors, a mixing-sieving-mixing process was followed in order to ensure the appropriate ratio between the materials, as several agglomerates were observed in the raw powders. For the studies performed using the compactors provided by L.B. Bohle and Freund-Vector, a direct mixing process was performed, and only when necessary, the powder was previously sieved. The amounts of mixture prepared also differ depending on the line studied and the number of experiments planned.

Regarding the Gerteis line, for the large scale compactor, approximately 35-40 kg were prepared. The corresponding amounts of powder were weighed using a ground balance (Mettler ID5 MultiRange, Mettler Toledo, Germany) and blended in a drum hoop mixer (Rhönrad RRM 100, J. Engelsmann AG, Germany) equipped with a motor (RF40DT80K4BMG/TF, Sew-Eurodrive, Germany). The mixer was set at 29 rpm for 10 min time. After that, the powder was sieved in a Frewitt mill (GLV ORV, Frewitt, Switzerland) using a 1mm mesh sieve and the speed chosen was 154 rpm in the oscillation mode. When the powder has passed through the sieve, the mixing process was repeated under the same conditions. For the small scale, around 18-20 kg mixture were required. The materials were weighed on a benchtop balance (Precisa 16000D, PAG Oerlikon AG, Switzerland) and introduced into a L.B. Bohle mixer (LM40, L.B. Bohle Maschinen + Verfahren GmbH, Germany) during 20 min at approximately 28 rpm. This change in time was made according to the size difference between the container used for the large (160 l capacity approximately) and the small scale (20 l capacity). Once this time had finished, the powder was manually sieved using 1mm mesh sieve, and the blending process was repeated afterwards.

The mixtures prepared to perform the L.B. Bohle experiments followed a common process, however, for the BRC 25 about 10 kg of main materials and 3 kg of the other mixtures were blended, while for the BRC 100, approximately 20 kg for the MCC, 50% mixture and mannitol and 6 kg for the other mixtures were prepared. The raw materials were weighed with a benchtop balance (XP32001LDR, Mettler Toledo, Switzerland) and the resulting amounts of powders were mixed only once on a L.B. Bohle mixer (LM40 NIR, L.B. Bohle Maschinen + Verfahren GmbH, Germany). The mixing conditions in both cases were 29 rpm during 10 min, and depending on the amount prepared, the containers of 10 and 20 l capacity were used. Similarly, for the Freund-Vector line a common procedure was used, although for the TFC-Lab Micro approximately 2 kg for MCC, the 50% mixture and mannitol, and 0.5 kg for the other materials were required, while for the TF-Mini, around 4 kg for the main materials and 1 kg for the other mixtures were prepared. The corresponding amounts of materials were weighed with the benchtop balances Kern (CB 12K1N, Kern & Sohn Gmbh, Germany) for the small scale and Satorius (Sartorius Universal U4100S, Sartorius GmbH, Germany) for the large scale. In the case of the small compactor, the powder was previously sieved. In order to mix the amounts weighed in a 1 or 2 l container, the Turbula® mixer was in both cases used (Turbula® T2F, Wab, Willy A. Bachofen AG Machinenfabrik, Switzerland) during 10 min at 34 rpm.

3.2.1.3. ROLL COMPACTION

A total of three individual scale-up studies were performed in order to get a general overview about the scalability of the roll compaction process. With the intention of evaluating only the effect of the scale excluding the impact of other design features, the roll compaction conditions were kept as similar as possible. In this respect, the same sealing system and roll surface were used for each couple of compactors as their change can have effects on the properties of the products (Rambali et al. 2001; Cunningham et al. 2010; Akseli et al. 2011; Dawes et al. 2012; Nesarikar et al. 2012a; Iyer et al. 2014b; Mazor et al. 2016; Wiedey et al. 2016). Similarly, in all the cases no lubricant was used during the production, and the temperature and relative humidity were measured. When possible, also the process data were collected. There were some differences in the diverse studies performed, but mostly the main materials (MCC, mannitol and 50% mixture) were investigated more comprehensively than the other mixtures. Nevertheless, for all the lines, at least one batch per blend was produced in both scales. And in every case, all samples collected were stored in a climate-controlled room

at 21°C and 45% RH for a minimum of 24 hours before performing any further characterization.

3.2.1.3.1. GERTEIS LINE: MINI-PACTOR® VS. POLYGRAN®

The Gerteis line was the most complete of all the studies and it was performed by comparing the Mini-Pactor® 250/25 and the 3-W-Polygran® 250/50/3 (Gerteis Machinen + Processengineering AG, Switzerland) from this moment on, referred as Mini-Pactor® and Polygran® respectively (Figure 2). As scale-up strategy, Gerteis keeps the diameter constant and only changes the roll width between scales. Both compactors have a roll diameter of 250 mm, however, the Mini-Pactor® has a roll width of 25 mm (small scale) while for the Polygran® is 50 mm instead (large scale). Another typical characteristic from these compactors is the position of the rolls, which in both cases is inclined, as well as the use of two feeding screws. Therefore, the transportation of the powder from the hopper to the gap is performed by a feeding auger (FA) and a tamping auger (TA). Both scales were assembled with knurled roll surface and side sealing system (or cheek plates). Gap control was activated, so the speed of both screws was automatically adjusted. Nevertheless, the ratio FA:TA was pre-set to 1:2 for the Mini-Pactor® and 1:3.5 to the Polygran®, what assures that the right gap value is achieved. The agitator on the chute was set at 3 rpm, value constant for the Mini-Pactor®, but automatically readapted in the case of the Polygran® due to the gap control.

a b

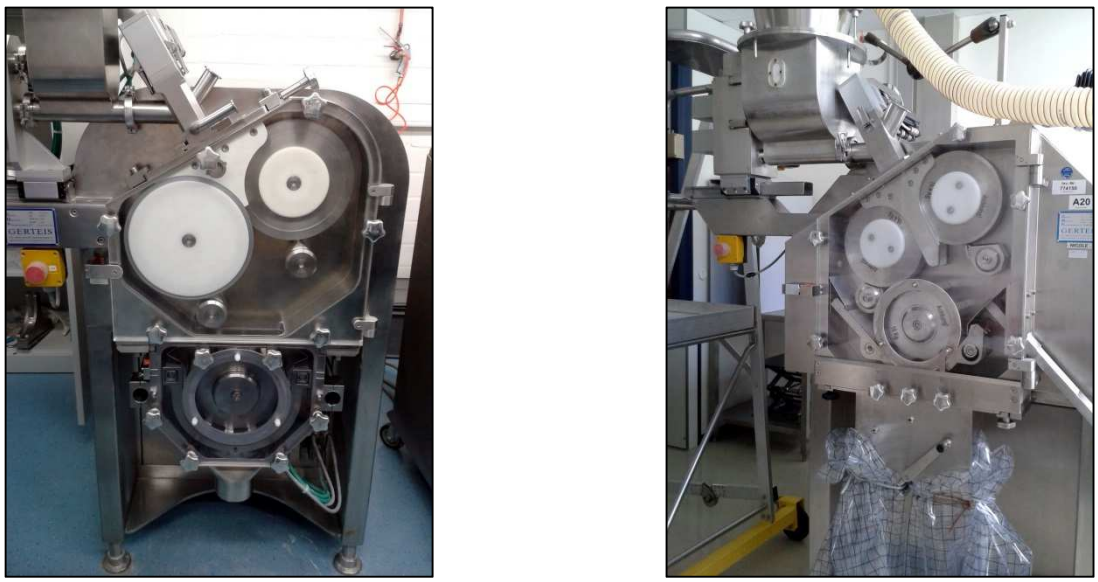

Figure 2: Pictures of the Mini-Pactor® (a) and the Polygran® (b) compactors used in this study.

A minimum of 500 g of ribbons were collected at the moment the steady-state conditions were achieved. This amount was confirmed with a benchtop balance Sartorius Excellence (Sartorius Universal MA AF 200, Sartorius GmbH, Germany) for the Polygran® and with the Sartorius Universal (Sartorius Excellence E5500S, Sartorius GmbH, Germany) for the Mini-Pactor®. During the production the temperature and RH were measured using a humidity and temperature indicator (Hygromer® A2, Rotronic, Germany) in the case of the Polygran®. The Mini-Pactor® is placed in a climate room which was set at 21°C and 45% RH. Nevertheless, the conditions in the room during production were checked for every batch.

A small study was performed for the Mini-Pactor® in order to evaluate how reproducible is the compaction with this machine. The first trial was performed by producing another random lot of MCC (4 kN/cm SCF, 3 mm gap and 4 rpm roll speed) together with the rest of the batches. A second trial was carried out with the 85% mixture of MCC in order to evaluate the reproducibility of the compaction with the Mini-Pactor® together with the mixture composition. Two lots were compacted with one year difference in respect to the complete DOE (the same mixture was used after remixing it for 5 min in order to avoid the segregation that could have occurred). The batches repeated were the lot at 8 kN/cm SCF, 1.5 mm gap and 2 rpm roll speed as well as one from the centre point conditions. The ribbons produced were collected as usual.

3.2.1.3.2. L.B. BOHLE LINE: BRC 25 VS. BRC 100

The second scale-up study was carried out with the BRC 25 and BRC 100 (L.B. Bohle Maschinen + Verfahren GmbH, Germany) whose pictures can be found in Figure 3. These two machines are relatively new on the market. L.B. Bohle uses the same scale-up strategy as Gerteis, so both compactors have a diameter of 250 mm and they only differ on the roll width. The BRC 25 has a roll width of 25 mm (small scale) while for the BRC 100 it is 100 mm (large scale). However, the main difference between Gerteis and L.B. Bohle families of compactors is the roll position, which is horizontal for the latter. Although both compactors expressed the force as SCF, Gerteis compactors apply it through a hydraulic system, while L.B. Bohle compactors have a spindle motor. The feeding is also carried out by a FA and a TA, although for the BRC 100, due to the throughput requirement, a double TA is necessary. Both machines were assembled with smooth surface rolls and rim rolls as sealing system. Gap control was activated and thus, the pre-set ratio FA:TA was for both machines 1:2.5, although in practice, the relationship was 1:4 for the BRC 25. The agitator on the chute is automatically adjusted according to the speeds of the feeding screws.

a b

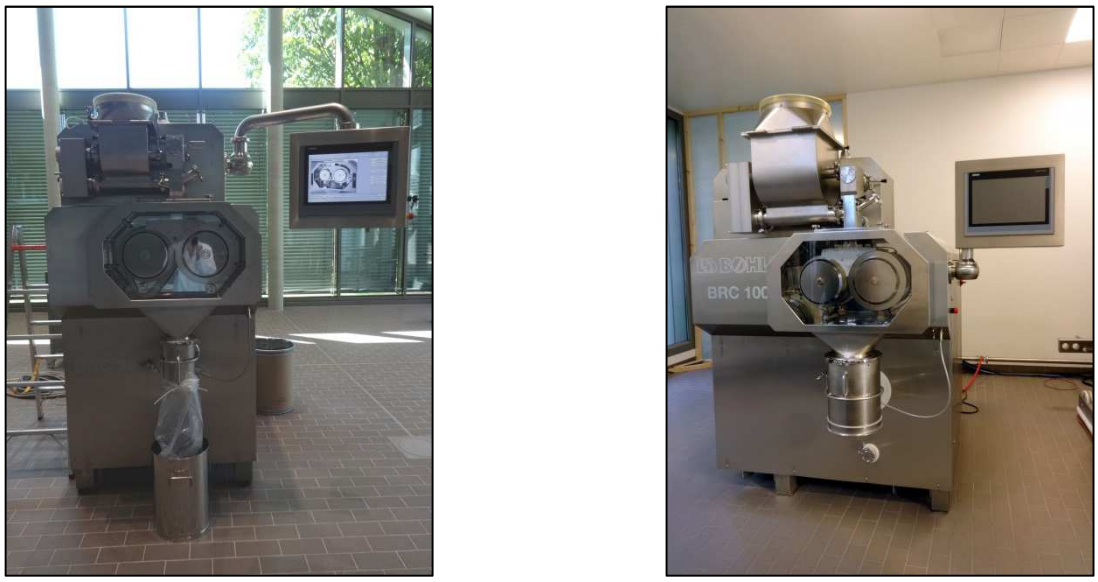

Figure 3: Pictures of the BRC 25 (a) and the BRC 100 (b) used on this study.

Approximately 500g of ribbons were also collected with the help of a ground balance (Kern DE150K5N, Kern & Sohn Gmbh, Germany) and at the same time, the temperature and RH were recorded using a humidity and temperature indicator (Hamster EHT1, ELPRO-BUCHS AG, Switzerland). The BRC 100 was installed in a room where the RH was controlled. This fact led to values between 41% and 48% for all the batches, instead of over 60% as were registered for the BRC 25.

3.2.1.3.3. FREUND-VECTOR LINE: TFC-LAB MICRO VS. TF-MINI

The Freund-Vector line was the last scale-up study performed, and due to the lack of gap control, it was less widely investigated than in the previous cases. Furthermore, the fact that these compactors use roll pressure instead of SCF leads to some difficulties when scaling the process up, as the units have to be converted. However, the interest of this study lies in the different scale-up strategy followed by the supplier. In this case, both the roll diameter and width change from one machine to other. The two scales involved in this work were the TFC-Lab Micro and TF-Mini (Vector Corporation, USA) which can be seen in the Figure 4. The TFC-Lab Micro is the smallest compactor available on the market, as it has 50 mm of roll diameter and 24 mm of roll width. The TF-Mini has 100 mm of diameter and 37 mm of roll width. Both machines were built up with ribbed roll surface and rim-rolls as sealing system. In the case of these compactors, the feeding is performed by one single screw. As no gap control system is available, it is only possible to adjust the screw speed in order to get the desirable gap width by feeding more or less material. In this respect, its value was controlled by measuring

the thickness of the out-coming ribbons with a digital calliper for the TFC-Lab Micro (Absolute Digimatic Series 500-171U, Mitutoyo (UK) Ltd., UK.) as well as for the TF-Mini (Absolute Digimatic Series 500-191, Mitutoyo Corporation, Japan).

a b

Figure 4: Pictures of the TFC-Lab Micro (a) and the TF-Mini (b) used on this study.

When the process was stable, a minimum of 300 g of ribbons were collected. This amount was confirmed with the benchtop balance Sartorius (Sartorius Universal U4100S, Sartorius GmbH, Germany) for the TFC-Lab Micro and with the Kern (Kern CB 12K1N, Kern & Sohn Gmbh, Germany) for the TF-Mini. The temperature and RH were also checked during the production either by monitored rooms for the TFC-Lab Micro or by using a commercial humidity and temperature indicator (Alarma-Hygromer testo 608-H2, Tesco, UK) in the case of the TF-Mini.

3.2.1.4. GRANULATION

Some authors have reported that the properties of the granules are an extrapolation of the ribbons' characteristics when milling them under similar conditions (Campbell et al. 2001; Morrison et al. 2007). Changing the process and the machine can drastically affect the characteristics of the granules obtained (Sakwanichol et al. 2012). Therefore, a standard granulation was performed in order to assure that the milling process was not a source of variability in the properties of the resulting granules. Nevertheless, two types of granulation

were performed in this work. In both occasions, the idea was to carry out a post-compaction granulation in an independent mill, so the different granulators in the compactors have no effect on the granules obtained. As was the case for the ribbons, the granules produced were also kept in a climate-controlled room below 21°C and 45% RH at least 1 day before characterization.

3.2.1.4.1. MIXTURES STUDY AT THE POLYGRAN®

This granulation procedure was performed only for the ribbons produced at the Polygran® in order to develop a general study focused on the plastic/brittle behaviour of the roll compacted mixtures. Approximately 300 g of ribbons from every batch collected at the Polygran® were weighed with the same balance used for their production and milled in a Frewitt sieving machine (GLA ORV 0215, Frewitt, Switzerland) under standard conditions. This mill was assembled with a 1 mm mesh sieve and the speed was set at 154 rpm, in oscillation mode. The ribbons were milled following the same randomization order as for their production, and the machine was cleaned after granulating each batch with a vacuum cleaner to minimize inter-batch contamination.

In order to simulate a real roll compaction process, the ribbons were not previously cleaned regarding fines, trying in this manner to mimic their fall into the granulator. However, it is important to point out that this lack of ribbon pre-treatment has one inconvenience. When characterizing the granules, it is no longer possible to know if the fines measured belong to the uncompacted material from the roll compaction process, or if they are generated when milling the ribbons

3.2.1.4.2. SCALE-UP STUDY

This milling process was performed only for the MCC and mannitol from the centre point produced at the Gerteis compactors and the main materials compacted at 5MPa at the Freund-Vector line. In this case, the granulation process is different although the conditions were similar to the previous procedure. This fact leads to different results and therefore, not comparable to the previous ones. That is the reason why both processes were separately classified.

For this study, the selected ribbons were milled with the granulator Erweka (AR 400, Erweka Apparatebau GmbH, Germany) using a middle oscillation speed and a 1 mm mesh sieve. A total amount of 50 g assured using a benchtop balance (Sartorius 3826 oo4-2, Sartorius

GmbH, Germany) were always milled and afterwards, a vacuum cleaner was used in order to eliminate residual granules or ribbon's fragments before the next milling.

The aim of the study with the Freund-Vector samples was not only to evaluate the different granules properties obtained when changing the scale, but also to investigate the importance of fines generated during the roll compaction process. In this sense, two different pre-treatments of the ribbons were performed, meaning that the ribbons from the same batch were separated into two groups: one milled with fines and the other after cleaning them. In the first case, the ribbons were taken directly from the bag including the powder accumulated during the compaction process, with the intention of trying to reproduce a continuous roll compaction process. In the second case, the granulation was performed after removing the fines with a brush and manually taking out the softer edges formed during the compaction due to the design of the rim rolls. The reason for this latter pre-treatment was to obtain granules whose properties are exclusively affected by the ribbon attributes.

3.2.2. CHARACTERIZATION

3.2.2.1. POWDER

The powders compacted at the Polygran® were taking as reference to characterize the different properties of the starting mixtures. The reason for choosing these raw materials is that the mixing conditions followed when preparing the mixtures for the other compactors, were based on the ones used for the preparation of the present blends.

3.2.2.1.1. TRUE DENSITY

The true density or helium density is defined as the particle density of a powder and it was measured with a helium pycnometer (AccuPyc 1330, Micromeritics Instrument Corp., USA). The raw materials were previously acclimatized for at least 24 hours in the climate-controlled room below 21°C and 45% RH. The amount required was weighed on a high precision balance (MC 210 P, Sartorius AG, Germany) and the measurement was performed in triplicate. The 3.5 cm^3 chamber was used for the calibration as well as for the measurements.

3.2.2.1.2. PARTICLE SIZE DISTRIBUTION

The PSD was characterized using a dynamic image analyser (Camsizer® XT, Retsch Technology GmbH, Germany). Approximately 2 g of the raw material was used for the

characterization. A minimum of 2 but mostly 3 replicates, depending on the reproducibility of the results, were performed.

Although this is not the most appropriate method to evaluate the size distribution of such a fine powder, this technique was chosen in order to make the results of raw powder and granules comparable. The same procedure was followed on both occasions. Therefore, further details can be found in the section 3.2.2.3.1. (pages 38 and 39).

3.2.2.1.3. LOSS ON DRYING

The loss on drying (LOD) is a value expressed in a percentage that corresponds to the amount of material which is lost when a certain quantity of powder is submitted to elevated temperature. The LOD was measured with a moisture analyser (Mettler LP16-M, Mettler Waagen GmbH, Switzerland) in combination with a high precision balance (Mettler PM460/9 DeltaRange®, Mettler Instrumente, Switzerland). A minimum of 4.5 g were weighed and distributed along the surface of a metal plate latterly introduced in the moisture analyser. The machine heats the powder until a prefixed temperature of 105ºC is reached. Once this value is achieved, the balance checks every 30 seconds if a new change in weight occurs, and therefore, if after this time no change in the mass is detected by the balance, the measurement finishes.

3.2.2.2. RIBBONS

3.2.2.2.1. APPEARANCE

Due to the different process conditions set, diverse sealing systems and roll surfaces assembled, the 6 types of compactors used and the 7 kinds of powders roll compacted, the resulting ribbons show completely different aspects when comparing them. This can strongly affect the feasibility of the characterization, and it was one of the reasons why some characterization methods were not applied. Therefore, ribbon appearance was collected as a qualitative attribute considering its length and structure, as can be seen in Figure 5a and 5b respectively. It was considered, on the one hand, the fact that the ribbons compacted kept as one long unit or broken into small pieces (a), and, on the other hand, it was also taken into account if the ribbon was produced as one piece or if it was divided in two parts following a lengthwise cut in their laterals by bilamination (b).

a b

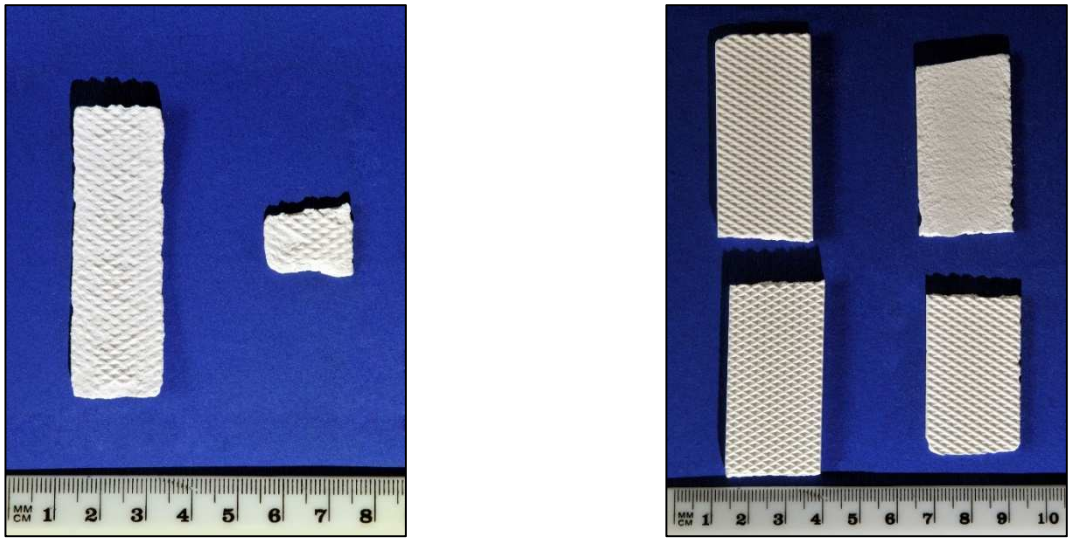

Figure 5: Example pictures of ribbons long and short (a) and integrate and laminated (b). For this latter picture, the same ribbon was cut on the middle, so both sites can be observed. Furthermore, the material used for their compaction is different, mannitol (a) and MCC (b).

3.2.2.2.2. RELATIVE DENSITY

The average ribbon relative density or solid fraction was expressed in percent and calculated according to equation 11. It was obtained based on the envelope density measured at the envelope and T.A.P. density analyser (GeoPyc® 1360, Micromeritics Instrument Corp., USA). This piece of equipment was assembled using a 25.4 mm chamber what requires a consolidation force of 51 N and a conversion factor of 0.5153 cm^3/mm. The medium used to perform these measurements is called DryFlo™ which consists of a mixture of particles of different sizes and a graphitic lubricant. The volume of the ribbons in respect to the total content of this medium was kept at 20%, which reduces the error in the measurements (Micromeritics 2001). As true density of the raw materials, the average value measured with the helium pycnometer obtained for the Polygran® powders was used for all the mixtures and compactors.

$$\rho_{rib} = \frac{\rho_{env}}{\rho_{true}} \cdot 100 \qquad \text{Eq. 11}$$

where ρ_{rib} is the ribbon relative density, ρ_{env} the envelope density and ρ_{true} the true density of the powder.

The GeoPyc® allows for the measuring of the ribbons independent of their size, surface or material used, as the samples are cut in small pieces. In this manner, a minimum of 5 ribbons

depending on their size were randomly sampled and manually cut off. Depending on the batch, the amount of sample needed could vary from a minimum of 3.5 g to a maximum of 5 g approximately, in order to keep the 20% of sample volume. The objective of this measurement was to have a representative value of the mean relative density of a batch, and therefore, pieces from all parts of the ribbon (edges and centre) were taken. A 3-cycles blank with only the DryFlo™ and a 3-cycles measurement were performed for each of the 3 replicates from batch analysed.

3.2.2.2.3. DENSITY DISTRIBUTION

An X-ray microcomputed tomography (μCT) system (CT alpha, Procon X-Ray, Germany) was used to measure the density distribution of the ribbons. One representative sample from one of the centre point batches for MCC and mannitol was chosen. In this manner, for each line, 2 ribbons (small and large scale) were measured for MCC and mannitol. However, in the case of the L.B. Bohle compactors, the measurement was excluded as it was not possible to reconstruct a complete ribbon, losing in this manner, the crosswise distribution. The ribbons were stored in the climate room at 21ºC and 45% RH for at least 24 hours before performing the measurement. However, as one analysis lasts around 3 hours, some changes in the density distribution could be due to the hygroscopicity of the material, although it will not be considered in detail in the discussion.

Regarding the measuring conditions, the X-ray beam was set with an acceleration voltage of 80 kV and a current of 80 μA. The detector was configured with a number of projections of 1600, each of those is an average of 5 or 10 images, and an exposure time of 500 ms was set. However, the resolution was changed depending on the sample analysed from a minimum voxel size of 25 μm to a maximum of 65 μm. The resulting data was reconstructed as a 3D image using a commercial software (VG Studio, Volume Graphics, Germany) and visualized using another program (Avizo Fire 9.0, FEI, USA). Several photos were taken considering crosswise (ribbon width, i.e. sample observed from the top) and lengthwise along the gap width (ribbon length, i.e. sample observed from the side) planes either in coloured scale, or black and white. The latter were used to calculate the so-called grey value, which correlates to the density distribution. This grey value is calculated with an experimental software which obtains the average of a column of pixels. In order to avoid miscalculations in the relative density, grey values under 50 were excluded. If this had not been done, the black background and the borders limiting the ribbons analysed would have had an effect which would have led to an underestimation of the density. These 50 grey values correspond to

relative densities between 28 and 41% depending on the material and calibration. This value has been chosen after testing the results obtained with other bounds. Nevertheless, establishing any limit can lead to an under or overestimation of the relative density.

Table 3: Relative density of the calibration tablets used for the μCT measurement.

TABLET NUMBER	RELATIVE DENSITY MCC (%)	RELATIVE DENSITY MANNITOL (%)
1	42.6	60.0
2	50.6	63.2
3	55.5	65.6
4	62.1	67.2
5	67.4	70.9
6	72.0	71.7
7	73.9	75.6
8	82.9	88.4

In order to transform the grey value into real density, a calibration has to be performed using tablets of known solid fraction. Therefore, when performing any measurement, between 5 and 8 reference tablets were used. Those were produced using a hydraulic press (062566, Perkin-Elmer & Co GmbH, Germany), which allows obtaining tablets with a homogenous and uniform density distribution. This is due to the fact that the matrix diameter is large (13 mm) and also because long dwell times were applied (1 min). The amounts of raw material were weighed on a benchtop balance (Sartorius Extend ED224S, Sartorius Weighing Technology GmbH, Germany) previous compression. In order to obtain a relative broad range of densities, the initial powder weight varied from 200 to 500 mg. In the case of mannitol, on some occasions, it was necessary to use magnesium stearate Parteck® LUB MST (Merck KGaA, Germany) as lubricant to avoid the stickiness of the tablet to the punch. After 24 hours equilibration time in the climate-controlled room, the relative density was mathematically calculated. The dimensions were measured using a digital calliper (Absolute Digimatic Series 500, Mitutoyo Corporation, USA), the weight obtained from a high precision balance (Sartorius AC 121S, Sartorius AG, Germany) and the true density of the raw powder were used to obtain the density of the tablets. The relative density values of the tablets for both materials are presented in Table 3 and are used to calculate the equivalence between the grey value and

the real density. As the range of the grey scale depends on the sample analysed, it is necessary to readapt the grey value-relative density correlation for each measurement. In order to prepare the latter, the grey value of the tablets is obtained and the mean for the whole data set is calculated, which is afterwards plotted against the density presented in Table 3. This fact also explains why the calibration tablets have to be included every time a measurement is performed.

3.2.2.2.4. MICROHARDNESS

The microhardness is the resistance, in a microscopic level, of a material to permanent penetration. It was measured by indentation using a commercial microindenter (Fischerscope Hm 2000 Microhardness System, Helmut Fischer, Germany) equipped with a ball indenter of 0.4 mm diameter. For all the experiments performed, the force was linearly increased to 1000 mN (1 N) during 20 seconds followed by 5 seconds of loading. The ball indenter consists of a metal piece which has a sphere on its tip which penetrates the surface of the ribbon. After descending until the sample's surface and establishing a zero point, the indenter starts penetrating by loading the predetermined force during the fixed time. At the end of this time, the distance penetrated within the sample or maximal height (h_{max}) is collected and used to calculate the universal hardness (HU) as is shown in equation 12 (N/mm^2). This equation is only used when assembling the ball indenter and thus, in this case, the microhardness is expressed as HU.

$$HU = \frac{F_{max}}{2 \cdot \pi \cdot r_b \cdot h_{max.corr}} \qquad \text{Eq. 12}$$

where F_{max} is the maximal force applied (which in this case is constant, 1 N), r_b the radius of the ball that is 0.2 mm for the indenter used (although this value can slightly change based on the penetration area) and $h_{max.corr}$ which represents the depth reached inside the ribbon, considering its surface as the starting point, and it is obtained at the end of the 5 seconds of loading. However, a correction was performed in order to avoid some errors that occurred during measuring. As a result, it was decided to subtract the height reached at 10 mN force from the original h_{max} and, hence, $h_{max.corr}$ was obtained.

Probably due to the irregular surface of the ribbons and the problems to establish the zero point, for some of the samples low forces were generating extremely high values of h_{max}. In Figure 6, an example graph of a ribbon showing this problem (a) is presented together with a typical measurement with the variability in the curves that could be expected (b). Therefore,

the resulting h_{max} was treated. From this value, the height reached after applying 10 mN of force was subtracted in order to avoid this drastic variation of the height-force curves in the first sector of the representation. This correction was performed for all samples analysed.

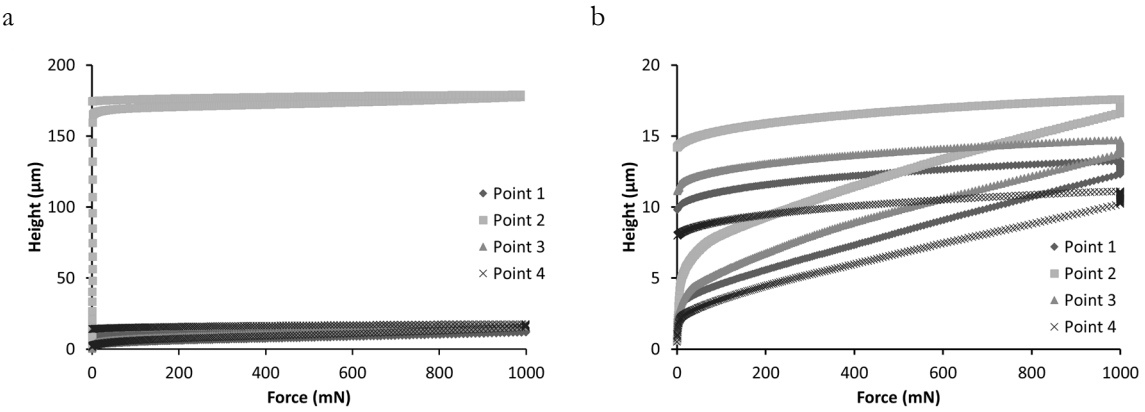

Figure 6: Two examples of indentation curves: a case with the problem of high height reached at low values of force (a) and normal case showing the expected variability between the curves (b).

Two methods were performed depending on where the measurement points were located, as variations in the results were observed when using one technique or another. In order to understand the differences between both these approaches, it is necessary to first consider the surface of the ribbons. In Figure 7, two schemes of the ribbons obtained at the Polygran® are presented as an example of the measuring methodologies followed. On the one hand, a first approach was named as "rhombus method", because the measurement points were located in the middle of the rhombus drawn by the knurled roll surface (Figure 7a). On the other hand, a second system called "cross method" was performed on the intersections between the rhombuses, as can be seen at the Figure 7b. If this pattern is considered from a lateral perspective, the rhombuses are the deepest areas of this surface, while the crosses are the highest. Therefore, when the measuring points set correspond to the rhombus, as those zones are profound, on several occasions the microindenter is not able to properly descend and establish the zero point from which the penetration should start, because the crosses obstruct the access. This fact at the end indicates that not all the points set were measured, and it is one of the reasons that justifies why most of the samples were analysed using the cross methodology.

Independent of the approach used, a total of 3 ribbons per batch were measured at a minimum of 4 different points in the centre along their surface, by applying 1 N force increasing during 20+5 seconds. In the case of the rhombus technique, a common measuring

pattern could not be followed as it depends more on the feasibility of the measurement. However, for the cross method, the points analysed were always equidistant for the same ribbon, although, depending on its length, the distance between them could change.

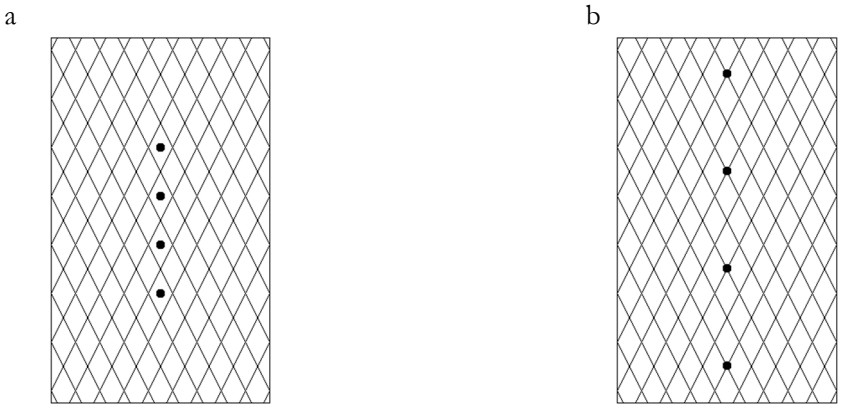

Figure 7: Representation of the two knurled ribbons produced with the Polygran® together with the measuring points for the rhombus (a) and the cross (b) techniques.

The rhombus methodology was only performed for the centre point ribbons (6 kN/cm SCF, 2.25 mm gap and 3 rpm roll speed) produced from all the mixtures at the Polygran®, although those samples were also characterized using the cross technique in order to compare both methods.

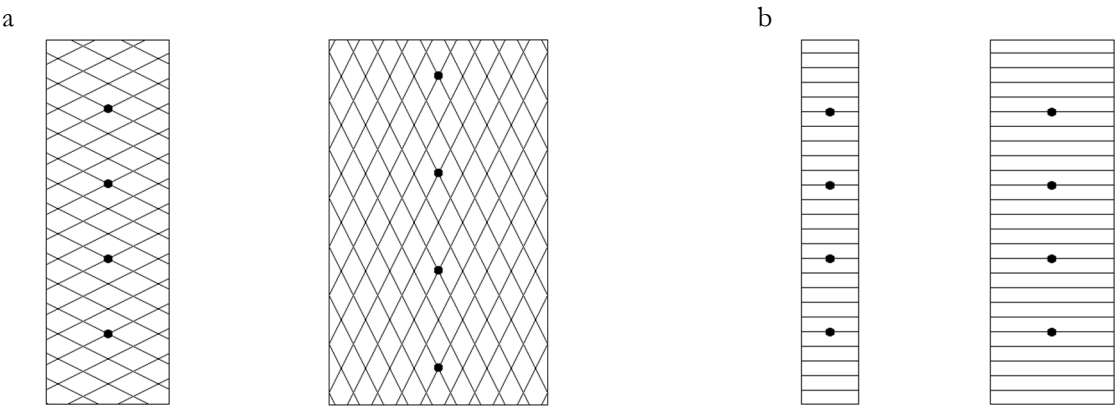

Figure 8: Scheme of the measuring points at the ribbons produced with the two scales of Gerteis (a), i.e. Mini-Pactor® and the Polygran® (left and right respectively) and Freund-Vector (b) compactors, i.e. TFC-Lab Micro and TF-Mini (left and right respectively). Please note the different roll surfaces for both families of compactors, knurled for Gerteis and ribbed for Freund-Vector machines.

Therefore, the cross methodology was carried out on the centre point ribbons collected from the Mini-Pactor® and the Polygran®. Apart from these conditions, HU was also measured for MCC, mannitol and the 50% MCC mixture ribbons produced following the 2^3 or 11-runs

DOE for both Gerteis compactors. Although the cross technique cannot be applied to the characterization of the ribbons produced at the Freund-Vector compactors, a similar principle was followed. In this case, the roll surface was ribbed, and thus, the measurement was also performed on the highest zones of the ribbons, which in this case, are the lines generated by the roll surface. In Figure 8, a scheme of all the ribbons measured is presented. Although in both cases of the Gerteis compactors the surface of the roll was knurled and the drawing represents a rhombus, the pattern is slightly different. However, the rhomboidal areas always correspond to the deeper zones of the surface, while the crosses in between are the hills of this structure. Those produced with the L.B. Bohle compactors were unfortunately too small to perform the measurement, and therefore, it was decided not to characterize them regarding this property.

3.2.2.3. GRANULES

3.2.2.3.1. GRANULE SIZE DISTRIBUTION, PERCENTILES AND AMOUNT OF FINES

The Camsizer® XT was used for characterizing the GSD, which was described with the volume distribution curve (q3) and its cumulative version (Q3) together with the percentiles tenth, fiftieth and ninetieth (D10, D50 and D90 respectively). The q3 and Q3 curves were calculated using the Xc min diameter as basis. This value is the most similar to the diameter which would be obtained by sieving/screening process. It is defined as the diameter of a circle that has the same area as the particle being characterized, calculated as the shortest chord of all the chords projected by the particle (Retsch 2012). The percentiles can be defined as the limit in size presented by a determined percentage of particles, meaning for example that the D50 represents the size under which the 50% of the particles are included. They are thus, the values under which a certain percentage of particles are contained. For the specific case of the D50, it can be also called medium particle size. The amount of fines was also determined by establishing the lower limit according to the particle size of the mannitol powder, as it is the material which has the bigger starting particles, and whose mean size is according to the supplier, 180 µm (Roquette 2006).

The absence of a liquid binder in the roll compaction process is the cause of the higher amount of fines in comparison to the wet granulation techniques (Dalziel et al. 2013). Starting with this premise, the Camsizer® XT was built with x-jet modulus, which applies 30 kPa

pressure in order to break the agglomerates that could have been formed during the storage of the granules. The size of the classes were defined at 0-1, 1-10, 10-31, 31-45, 45-63, 63-90, 90-125, 125-180, 180-250, 250-355, 355-500, 500-710, 710-1000, 1000-1400 and 1400-2000 μm (these last two set as security intervals). In order to obtain representative samples of a batch, the granules were sampled using a rotary sample divider (PT, Retsch Technology GmbH, Germany). Each batch was measured at least 3 times, although for some cases, 4 replicates were performed.

3.2.3. MODELLING

In recent years, the interest in developing models for pharmaceutical processes has grown as they are useful tools that allow the predicting of product properties without the need for performing heavily time and material-consuming experiments. For the roll compaction process, those models can also be used to successfully scale-up the process, as it is possible to predict the ribbon properties that would be obtained in the next scale.

With the intention of transferring the process between the scales, some of the models already described in the introduction were tested regarding utility and accuracy of prediction. The data used to feed and fit the models was the ribbon relative density obtained from the main materials (MCC, mannitol and 50% MCC mixture). Depending on the requirements of the approach, i.e. if using pressure or force units, data collected from Freund-Vector or Gerteis and L.B. Bohle was used. In most of the cases, only the ribbon relative densities for Gerteis and L.B. Bohle compactors were considered. The data used corresponds to the 11-runs DOE, because this design was performed in both compactor lines.

The models useful for scale-up that will be tested in this work are classified in two main groups depending on the methodology followed on their development. In this sense, a mechanistic model and two dimensional analysis equations can be defined. Those models have been chosen either because they have shown a high utility for the scalability of roll compaction (mechanistic model) or as they are dimensionless equations that can be easily and rapidly applied to scale the process up. Furthermore, another approach based on dimensional analysis will be proposed in this thesis.

3.2.3.1. MECHANISTIC MODELS

Many models described in the literature are based on the theory developed by Johanson 1965 and the consequent mathematical approach. This "rolling theory for granular solids" as was named by the author, was used by several scientists to develop models valid for scaling-up the roll compaction process (Reynolds et al. 2010; Nesarikar et al. 2012b). The approach developed by Reynolds et al. 2010 has been tested by using the ribbon relative density data collected at the Gerteis and L.B. Bohle compactors for the main materials produced by following the 2^3 DOE.

3.2.3.1.1. REYNOLDS'S APPROACH

Before being able to apply this model, it is necessary to obtain some flow properties of the starting powder. This information was kindly provided from an internal database in AstraZeneca in Macclesfield (UK). The frictional properties of the starting materials were measured using a ring shear tester (RST-XS, Dietmar Schulze, Germany) by using a standard shear testing procedure (Peschl et al. 1977). In this manner, the effective angle of internal friction (δ_E) and the angle of wall friction (ϕ_W) were measured. The latter was obtained by performing the analysis against a stainless steel coupon with roughness average (Ra) value of 0.4. The measurements were made using preconsolidation loads of 4 kPa and pre-shear stress of 1, 1.4, 2 and 2.6 kPa.

Once this data is collected, the model can be applied. The approach developed by Reynolds et al. 2010 was used to calculate the peak pressure (P_{max}) imposed by the roll compactors and to provide a mechanistic analysis of the influence of the different governing factors on ribbon density. This model is based on that proposed by Johanson to solve the pressure gradients in the slip and nip regions between the rolls. The relative density of the ribbon leaving the rolls (γ_R), is related to the calculated P_{max} at minimum gap by the following power law presented in equation 13:

$$\gamma_R = \gamma_0 \ {P_{max}}^{1/K} \qquad \text{Eq. 13}$$

where γ_0 is the preconsolidation relative density and K is the material compressibility, both are compaction parameters depending on the materials. P_{max} was described in equation 7 (page 10).

3.2.3.2. DIMENSIONAL ANALYSIS

Another option to model the roll compaction process in order to scale it up is to use the dimensional analysis and obtain a DV from it. In the literature, two DV were described (Rowe et al. 2013; Boersen et al. 2015). In both cases, the equation of the DV is given and used to transfer the process between two different compactors and/or scales. All these DVs are always correlated to one property in order to evaluate their utility or efficiency, which is the ribbon relative density in these cases.

3.2.3.2.1. MODIFIED BINGHAM NUMBER

Rowe et al. 2013 proposed a modified version of the Bingham number, which is a relationship already known to express the shear stress. As the materials during the roll compaction process suffer high levels of shear stress, they proposed this equation to examine the ratio of yield-to-viscous stresses experience by the Bingham materials when flowing. The original equation was modified resulting in the Bm* which can be found in equation 8 (page 12). The reason for this adaptation is that most of the pharmaceutical powders behave differently to the Bingham materials. Those materials have the capacity of acting as a solid or rigid body when they suffer low stresses, but under high ones, they behave like liquids.

As no units directly related to roll pressure or compaction force were used, this approach could be applied to all families of compactors. This DV was tested for the ribbon relative density data collected from the Gerteis and L.B. Bohle compactors for the 11-runs DOE. In both cases, only the data for the main materials was used.

3.2.3.2.2. BOERSEN'S DIMENSIONLESS VARIABLE

Another DV for scaling-up or transfer the roll compaction process was proposed by Boersen et al. 2015. After a previous study (Boersen et al. 2014) and literature comparison (Falzone et al. 1992; Inghelbrecht et al. 1997; von Eggelkraut-Gottanka et al. 2002; Guigon et al. 2003), they identified the roll pressure, speed and horizontal feed screw as the critical parameters of the roll compaction process from the point of view of the operation. In order to make the relationship truly dimensionless, the authors also included the true density of the raw powder, although this property is constant between the compactors for the same formulation. Furthermore, the DV should also consider a parameter that refers to the piece of equipment used. Therefore, roll diameter was chosen as a scaling factor. The final formula of the DV can be found in equation 9 (page 13).

In this case, the DV can only be applied to the Freund-Vector compactors. First of all, because the authors considered the roll pressure, and in the case of the Gerteis and L.B. Bohle compactors, it is not possible to transform the SCF in roll pressure. Secondly, the equation only includes the roll diameter, which remains constant (250 mm) for the 4 compactors of those two companies. And finally, this DV is developed considered that only one feeding screw belongs to the compactor, however, Gerteis and L.B. Bohle ones have the FA and the TA.

3.2.3.2.3. PÉREZ GAGO'S APPROACH

Another DV aside from the models available in literature was proposed in this work. The principals on which it relies will be presented together with the results in the corresponding part (section 4.3.3. in pages 162-168). Nevertheless, the main reason why this approach was developed was the need for a DV that can be applied to the compactors developed by Gerteis and L.B. Bohle, as they have different peculiarities in comparison to other manufacturers. First of all, they used SCF in kN/cm to express the force applied to the powder. Secondly, the different scales of these compactors keep the diameter constant and only the roll width varies between pieces of equipment. Finally, the feeding system is composed of two feeding screws instead of one. Therefore, and based on the work of Boersen et al. 2015, another DV was developed in order to apply this methodology to these compactors. In this manner, a list of variables affecting the roll compaction process was prepared. Following the methodology performed by these authors, the equation was organized in order to obtain a dimensionless relationship. The DV was found by trial-and-error approaches and it is described in equation 14. The Buckingham's theorem was also applied with the intention of justifying mathematically and experimentally the equation. However, some data requirements were incomplete and this leads to the lack of sufficient information to test the π-products. Although the Buckingham's theorem was unsuccessfully applied, some knowledge was extracted from this trial.

$$DV_{PG} = \frac{RF \cdot \rho_{true} \cdot D^2}{R^2} \cdot \frac{RS}{TA} \qquad \text{Eq. 14}$$

where RF is the roll force calculated as the product of the SCF and the roll width (N), ρ_{true} is the true density of the powder (kg/m^3), D is the roll diameter (m), R is the throughput or production rate (kg/s), RS is the roll speed (rpm) and TA is the tamping auger speed (rpm). This variable was tested for the main materials produced with the Gerteis and L.B. Bohle compactors following the 11-runs DOE.

4. RESULTS AND DISCUSSION

4.1. MIXTURES BEHAVIOUR

4.1.1. INTRODUCTION AND OBJECTIVES

In roll compaction, the SCF, the gap width and the roll speed are the most important operating settings. They have a high impact on the characteristics of the resulting products obtained. Different combinations of these three parameters can lead to ribbons and granules with diverse properties. Therefore, investigating how they affect the resulting products is the first step for proper process understanding. However, the effect of the operating conditions is highly dependent of the mechanical properties of the blend compacted. Different materials react in diverse manners to the same production settings and therefore, remarkable differences regarding product attributes can be obtained for diverse materials compacted under the same conditions. Nevertheless, not only the effect of the pure materials is critical, but the mixing of different powders in several percentages will bring mixtures with different starting characteristics.

Two main behaviours against compaction are described according to the interest they have for the pharmaceutical industry: plastic deformation and brittle character. Nevertheless, powders compacted in the pharmaceutical industry do not present either of these pure behaviours, as they are the result of a mixture of two or more materials, and each of those has its own properties. Therefore, the plastic/brittle behaviour of mixtures for the roll compaction process is of high interest when investigating this procedure. Actually, not always is there a linear or proportional behaviour, but some synergistic interactions which end in unexpected results. The percolation theory describes this phenomenon by the formation of clusters within the blend, which are determined by the percolation threshold. These clusters will lead to a behaviour mostly affected by one or another powder which compounds the mixture.

The aim of this first part of the present thesis is to investigate how MCC (plastic) and mannitol (brittle) and their 5 binary mixtures (0, 15, 30, 50, 70, 85 and 100% MCC) behave against different roll compaction conditions. A multilevel full factorial design consisting of gap width and roll speed in 2 levels, SCF in 5 levels and 3 repetitions of centre point was performed. This DOE consists in a total of 23 runs and it was carried out 7 times for each of the combinations of pure materials and mixtures. These 7 blends (named according to the fraction of MCC) were compacted at the Polygran® and the ribbons were collected and milled into

granules. Although this part of the study is mainly focused on granule characterization from the point of view of the mixture proportion influence, some starting powder and ribbon properties were also measured. With the intention of further understanding the behaviour of the mixtures, some of the properties of the out-coming ribbons and granules were analysed by applying the percolation theory.

4.1.2. POWDER CHARACTERIZATION

4.1.2.1. TRUE DENSITY

The true or helium density of the starting material was the first powder attribute considered to evaluate the quality of the mixing procedure. Furthermore, the values obtained were later used for the calculations of the ribbon density. In Table 4, an average true density is presented. The standard deviations are not collected in the table as their values were between 0.00 and 0.01 for all the cases.

Table 4: Average value of true density (n = 3) for the different starting powders.

PROPORTION OF MCC (%)	**TRUE DENSITY (g/cm^3)**
0	1.47
15	1.49
30	1.51
50	1.53
70	1.55
85	1.57
100	1.59

The true density values measured lead to a minimum of 1.47 g/cm^3 to a maximum of 1.59 g/cm^3 for mannitol and MCC respectively, while the values of the mixtures are in between. This means, that the mixing process was successfully performed, and that there is a linear correlation between the proportion of MCC and the helium density, with a Pearson's correlation coefficient (r) of 0.9966 value.

4.1.2.2. PARTICLE SIZE DISTRIBUTION

The PSD for the raw powder was measured using the same procedure and parameters than for the granule characterization. In Figure 9, the mean q3 representation is presented. From the graph is possible to observe that the pure MCC is the powder which has smallest particles (D50 = 55.0 μm) while the mixtures increase this size until reaching the maximum value with the mannitol (D50 = 146.2 μm).

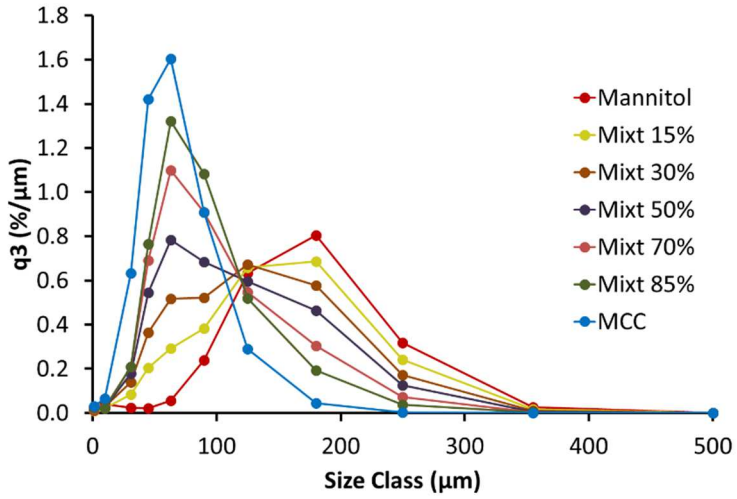

Figure 9: Volume size distributions of the raw powder later used for roll compaction, mean (n ≥ 3).

The PSD profile confirms the proper preparation of the mixture, as the particle mean size increases with the proportion of mannitol. It also proves that there is a linear relationship between the PSD and the MCC fraction, with a -0.9986 value of r (negative due to the slope of the line) for the correlation between the D50 and the proportion of MCC.

4.1.2.3. LOSS ON DRYING

MCC is a hygroscopic material, i.e. it is able to catch water molecules from the air in the room in which it is being stored. According to the supplier, the moisture content is between 3.0% and 5.0% depending on the batch (FMC BioPolymer 2008). Conversely, mannitol is slightly affected by the changes in RH and temperature (Bolhuis et al. 1996). Therefore, it was interesting to measure the LOD of the pure materials and mixtures (Figure 10), because the moisture fraction of the starting powder has an impact on the compaction (Gupta et al. 2005a; Wu et al. 2010; Osborne et al. 2013). Furthermore, it is also a quality indicator of the mixture preparation.

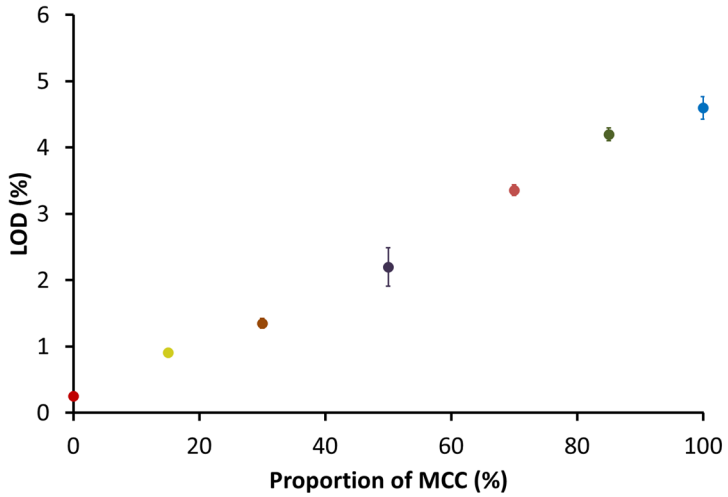

Figure 10: LOD for the different starting powders, mean±s (n = 3).

The temperature and RH in the room where the materials were stored were not constant, varying between 23.2 ºC and 26.2ºC and between 28.3% and 57.6% respectively. From this figure, it is possible to conclude that the higher the percentage of MCC, the greater the LOD, emphasizing again the successful mixing process as well as the linear relationship, with an r value of 0.9960, between MCC fraction and LOD. This value is changing from a minimum of 0.25% (mannitol) to a maximum of 4.60% (MCC). The tendency was expected considering the hygroscopicity of this latter material.

4.1.3. RIBBON CHARACTERIZATION

In order to focus on the effect of the material in the attributes of the resulting ribbons, the centre point ones were selected and characterized. They were produced under a 6 kN/cm SCF, 2.25 mm gap and a 3 rpm roll speed. As the roll compaction conditions were kept constant, this allowed for the studying of the effect of the material only. The reason for selecting those ribbons is based on the fact that they were produced in triplicate, giving also an idea about the reproducibility of the process, which can be a source of variability. Therefore, this section will be mostly focused on investigating how varying the MCC/mannitol fraction affects the ribbon properties.

4.1.3.1. RELATIVE DENSITY

The relative density of the centre point ribbons was measured using the true density value previously obtained. The 3 repetitions of the centre point were individually characterized, and each of those batches was measured in triplicate. In Figure 11, the mean relative density for each of the 3 centre point batches is presented together with the standard deviation. Nevertheless, later an average of the 3 means was calculated and named as a global mean, which will be used for further investigation of the material impact.

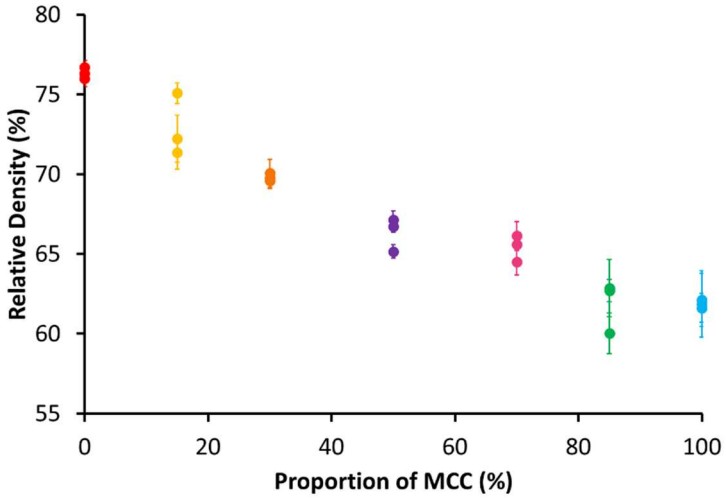

Figure 11: Relative density of the centre point ribbons for each of the 3 repetitions, mean±s (n = 3).

The ribbon relative density tends to decrease with the increase in MCC percentage. When calculating the global relative density, it can be observed how it changes from a maximum of 76.3% for mannitol to a minimum of 61.9% for pure MCC and 85% MCC. Although the global mean is the same for these latter mixtures, as can be seen in the figure, for the 85% MCC there is one point notably separated from the others. These means lead to two conclusions. First, that during the production some settings were not properly controlled by the machine (process data for this compactor is not available to prove what has been observed during the production), and this could also justify the separated points from 15, 50 and 85% MCC. Thus, the reproducibility of the process is not always accurate. And secondly, that it can be affirmed that the mixtures are showing intermediate densities. Therefore, and although the correlation is poorer than for the powder characterization (r = -0.9649, value that rises to -0.9796 when considering the global mean only), for the same compaction conditions, the higher the proportion of MCC, the lower the ribbon relative density.

4.1.3.2. MICROHARDNESS

The HU based on the $h_{max.corr}$ for the ribbons of the centre point was measured in order to study the material effect using the two different methods, described in section 3.2.2.2.4. (pages 35-38). Those techniques are the "Rhombus Method" and the "Cross Method". Independent of the approach, the same measuring conditions were followed.

The global HU mean for all the ribbons from the centre point was calculated and plotted together with the confidence interval (CI) against the percentage of MCC in order to evaluate the material effect. This value of HU is calculated as the average of all the individual points measured for the 3 repetitions of the centre point, i.e. there is no classification depending on the ribbon which was measured, thus, all the points are considered equal. The CI is calculated using the Student's t-distribution for an error of $\alpha = 0.05$ using this equation:

$$CI = \bar{x} \pm t \cdot \frac{s}{\sqrt{n}} \qquad \text{Eq. 15}$$

where $\bar{x}$ is the mean HU value of the sample, s its standard deviation, t the value of Student's t-distribution and n the size of the sample. As the standard deviations obtained in all the cases were high, it was decided to use the CI instead.

The measurements were always performed in the middle of the ribbon and along its surface as the density distribution changes across the width (Farber et al. 2008; Miguélez-Morán et al. 2008). Nevertheless, several authors have also investigated how the density varies lengthwise along the ribbon (Simon et al. 2003; Lim et al. 2011; Nesarikar et al. 2012b; Souihi et al. 2015a, Wiedey et al. 2016) and it was found out that the screws belonging to the feeding system generate a spiral distribution of the density along the ribbon. This fact could be one source of variability which explains the high CI values obtained.

4.1.3.2.1. RHOMBUS METHOD

The microhardness results presented in Figure 12 were collected following this methodology. These values are the global average of all the measurements performed, which means that at least 4 points were analysed in 3 ribbons from the 3 centre point batches, although this number of experiments is normally overcome. It was especially difficult to obtain these values, as this approach is based on performing the measurement on the deepest parts of the ribbons.

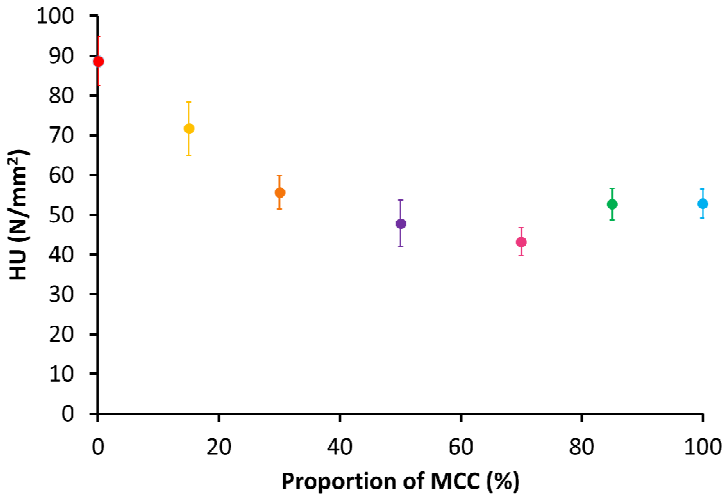

Figure 12: Representation of the average HU with the CI against the proportion of MCC for the centre point ribbons measured with the rhombus method, mean±CI ($n \geq 37$, $\alpha = 5\%$).

In this figure, it can be observed a general tendency of decreasing the HU as the percentage of MCC is increasing until reaching the 70% mixture. From this point on, the HU value rises slightly. Therefore, a clear impact of the composition is observed. MCC, as a plastic material is softer while mannitol is harder due to its brittle character (Ragnarsson 1996). A high proportion of mannitol leads to harder ribbons while pure MCC to softer ribbons. However, the combination between these two materials can even result in softer ribbons, being those from mannitol the hardest ones with an average value of 88.6 N/mm^2 and the softest ones from the 70% mixture with a mean of 43.2 N/mm^2. This stresses how the interaction between both materials affects the final behaviour of the mixture.

4.1.3.2.2. CROSS METHOD

In Figure 13, the global HU results for this alternative methodology are presented together with the CI. As opposed to the previous technique, the measurements were performed with ease and speed, although relatively high CI was still obtained. The results with this methodology show the effect of the material on the resulting HU value as well. An especially high HU for mannitol was found, while the other mixtures evaluated varied in a much smaller range (minimum of 28.9 to maximum of 33.4 N/mm^2) reaching almost a plateau. In this sense, the maximum HU value is 61.9 N/mm^2, while the minimum of 28. 9 N/mm^2 is obtained for the ribbons produced of the 85% mixture. As it was also observed for the previous method, the microhardness evolves differently depending on the MCC/mannitol fraction but to a much more minor extent.

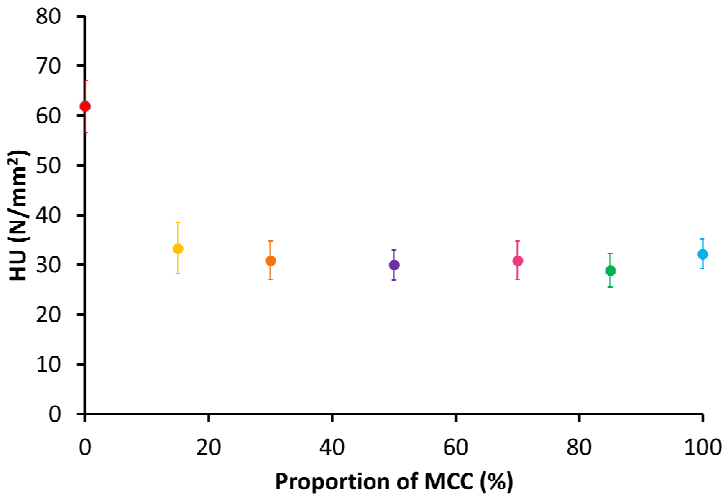

Figure 13: Representation of the average HU with the CI against the proportion of MCC for the centre point ribbons measured with the cross method, mean±CI (n = 36, α = 5%).

When comparing this methodology with the rhombus technique, the first conclusion that can be extracted, is that much lower HU values are obtained from the present method, giving initial evidence of the differences between both methods. Different densities are observed when the knurled surface is used, resulting in higher values in the crosses than in the rhombus as can be seen in some of the pictures obtained by Souihi et al. 2015a. The highest differences between the two methods were obtained with the ribbons of 15% mixture, while the closest HU values were found with the 70% MCC. Nevertheless, the HU obtained for the rhombus method may be too high. Freitag et al. 2004 also determined the microhardness by following a similar procedure to the one used in this work (excluding the issues with the ribbon surface, as they used smooth rolls) for magnesium carbonate ribbons, which is also a brittle material like mannitol. The values they obtained, depending on the SCF applied for the samples production, were between 5 and 32 N/mm^2 approximately. Although both materials are different, this is the first clue that indicates that probably the results for this method are more reliable than when using the rhombus system. Regarding the CIs, although slightly lower values were obtained for the present technique, they are high for both cases. Finally, both methodologies agree that mannitol ribbons are the hardest ones, however the softer ones are those from 85% MCC in this case. In general, the cross method, due to its faster and easier application was chosen as the representative method for microhardness characterization.

4.1.4. GRANULE CHARACTERIZATION

The ribbons collected were milled into granules using the Frewitt mixing machine. However, no pre-treatment of the sample was performed, in order to mimic the normal flow of a roll compaction process. Conversely, this means that the fines measured can have their origin during the roll compaction process (uncompacted material) or on the milling procedure (real fines of the granules). No differences regarding nomenclature will be done in this section, also because it cannot be addressed which amount of fines is generated for one or the other process. "Uncompacted material" and "fines" will be treated as synonyms in the present chapter.

The ribbons which were granulated are all those produced according to the 23-runs DOE (Table 1, page 22) which was performed for each mixture involved in this study. Therefore, the granule characterization was focused not only on the material effect, but also on the impact of the different combinations of the process parameters of the DOE. The GSD of all granules was measured and both the graphical representation and the statistical analysis were performed considering the 23 individual results obtained per material.

4.1.4.1. GRANULE SIZE DISTRIBUTION

All granules produced were analysed in the Camsizer® XT. Due to the high amount of measurements performed, an average curve was prepared for each one of the 23 batches produced per mixture. If the q3 curve is taken into consideration, in all batches a bi-modal distribution is observed. This pattern is characteristic to the granules obtained in roll compaction, as no liquid binder is used during the production. Therefore, the amount of fines, represented by the first component or peak in the curves, is higher than in a wet granulation process. In order to facilitate the outlook of this first element, the q3 curve (left) together to its logarithmic representation (right) were represented in Figure 14 and classified depending on the mixture.

a

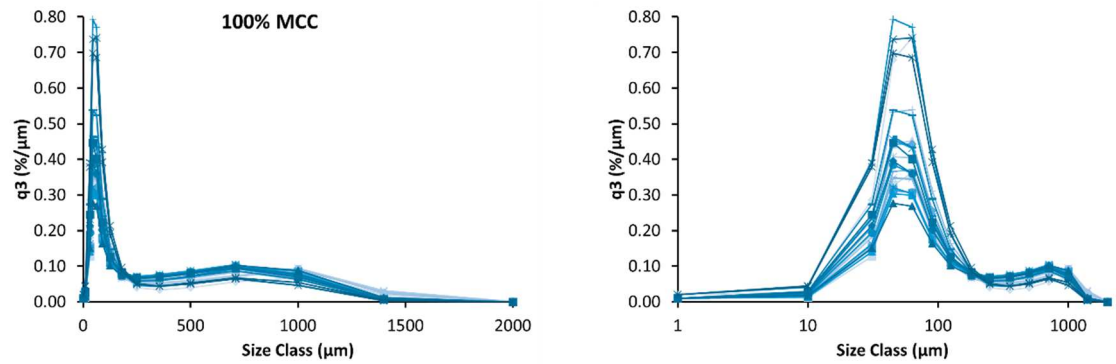
100% MCC
q3 (%/µm)
Size Class (µm)
0.00
0.10
0.20
0.30
0.40
0.50
0.60
0.70
0.80
0
500
1000
1500
2000
1
10
100
1000

b

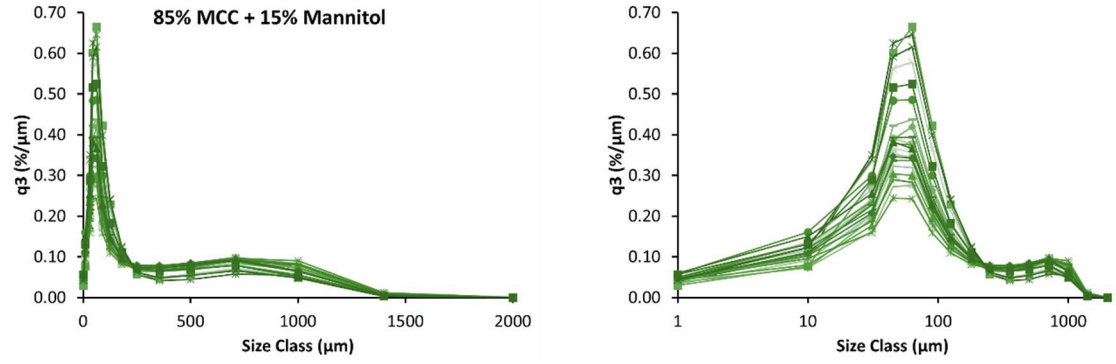
85% MCC + 15% Mannitol
q3 (%/µm)
Size Class (µm)
0.00
0.10
0.20
0.30
0.40
0.50
0.60
0.70
0
500
1000
1500
2000
1
10
100
1000

c

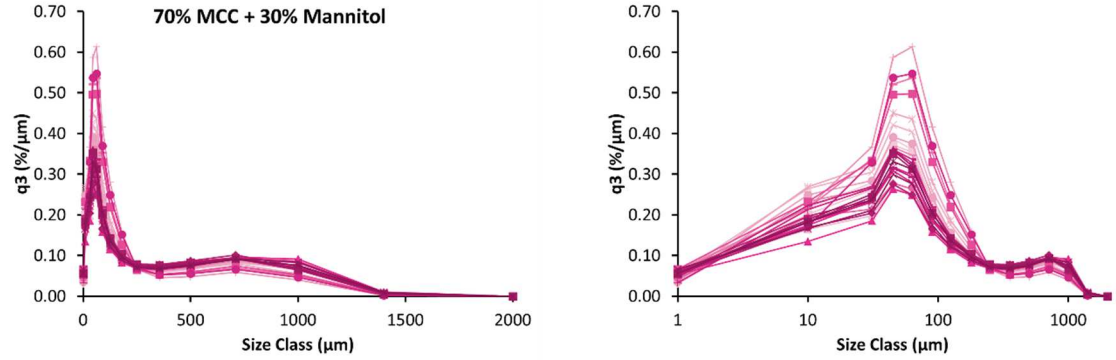
70% MCC + 30% Mannitol
q3 (%/µm)
Size Class (µm)
0.00
0.10
0.20
0.30
0.40
0.50
0.60
0.70
0
500
1000
1500
2000
1
10
100
1000

d

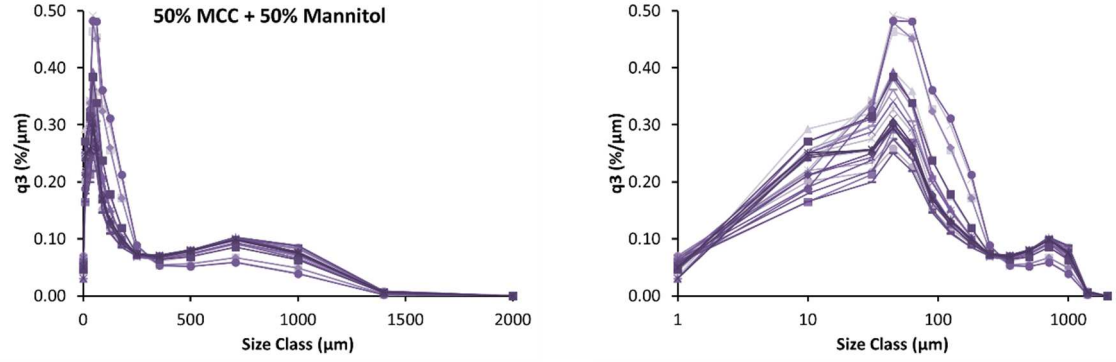
50% MCC + 50% Mannitol
q3 (%/µm)
Size Class (µm)
0.00
0.10
0.20
0.30
0.40
0.50
0
500
1000
1500
2000
1
10
100
1000

e

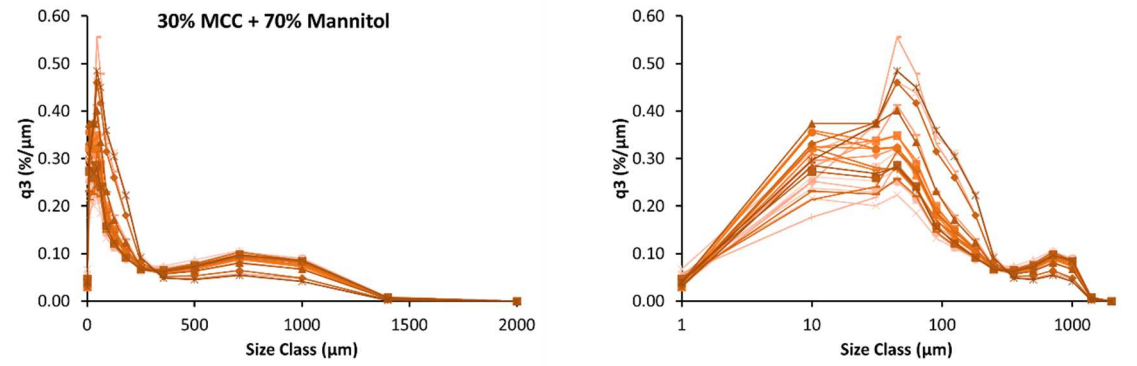

f

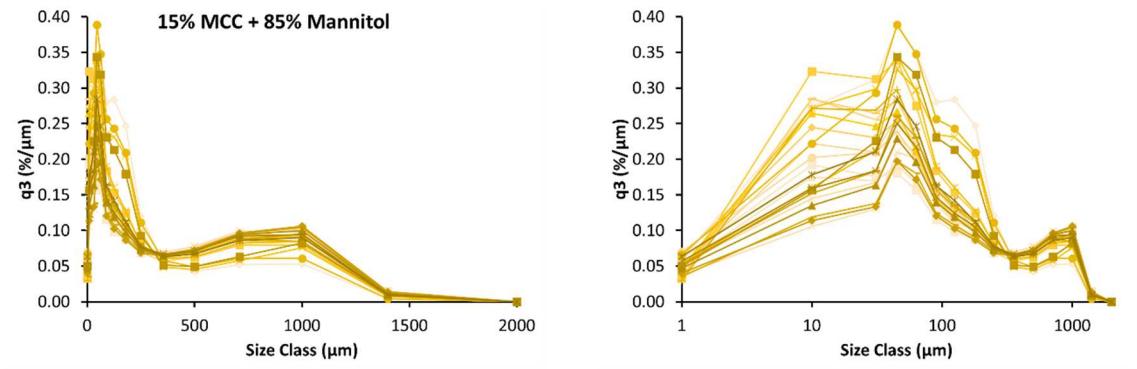

g

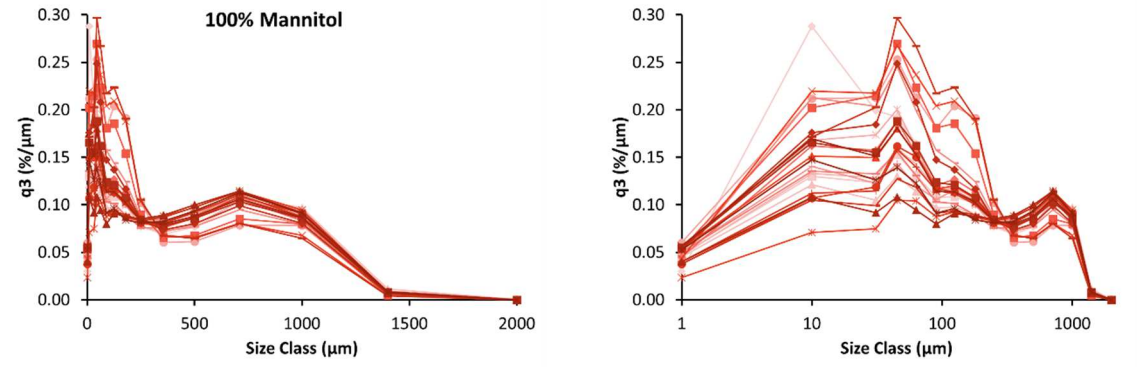

Figure 14: Linear and logarithmic q3 curves for mixtures of: 100% (a), 85% (b), 70% (c), 50% (d), 30% (e), 15% (f) and 0% MCC (g), mean ($n \geq 3$).

As all combinations of parameter settings evaluated are plotted together, it cannot be addressed any mixture effect. Nevertheless, the q3 representation permits a perception of how the first component decreases, as well as how the amount of bigger particles increases with the proportion of brittle material on the mixture. In general MCC shows a high amount of fines from 10 to 250 µm, and lower proportion of larger particles from 500 to 1400 µm, while

mannitol presents a more homogenous distribution as there are similar proportions of granules for each interval.

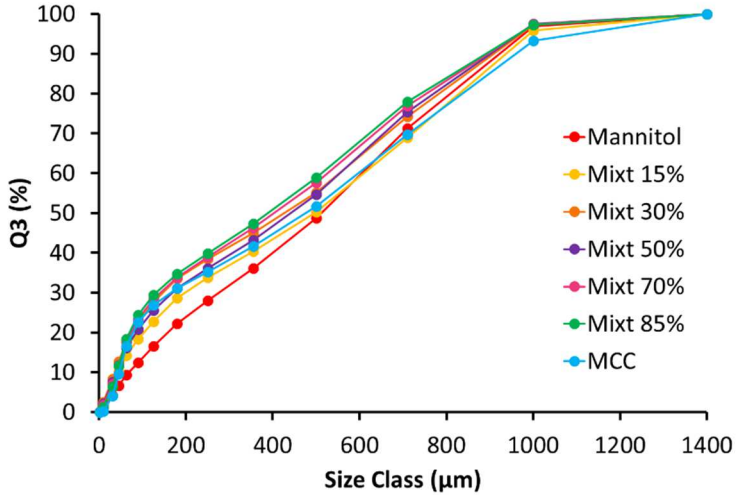

Figure 15: Average cumulative curves Q3 for the centre points of each mixture, mean (n = 3).

For a better understanding of how the different materials respond to the milling process, an average Q3 curve of the granules obtained at the centre point conditions was calculated for each material and plotted in Figure 15. The mixtures show a non-linear or synergic behaviour in respect to the proportion of MCC, as has been also observed for the microhardness of the ribbons. Only the 15% mixture presents an intermediate behaviour in respect to the pure materials. The differences between the mixtures depend on the segment from the whole distribution taken into consideration. Thus, below 250 µm the mixtures show behaviour more similar to MCC. However, from 800 µm, the tendency of these mixtures is closer to the mannitol, i.e. more brittle. In the middle sector, around 500 µm the higher differences for the mixtures (from 30 to 85% MCC) in respect to the pure materials are observed.

4.1.4.2. AMOUNT OF FINES

In the q3 curve the amount of fines is represented by the first peak on the representation, although it also comprises small granules. This is due to the fact that the limit for distinguishing between granules and fines was established at 180 µm (particle size of mannitol according to the distributor) although for MCC the particle size is, according to the supplier, 50 µm (FMC BioPolymer 2008). The logarithmic form of the q3 (see Figure 14, pages

52 and 53) is used for facilitating the understanding of this first peak, which is almost illegible in the linear representation.

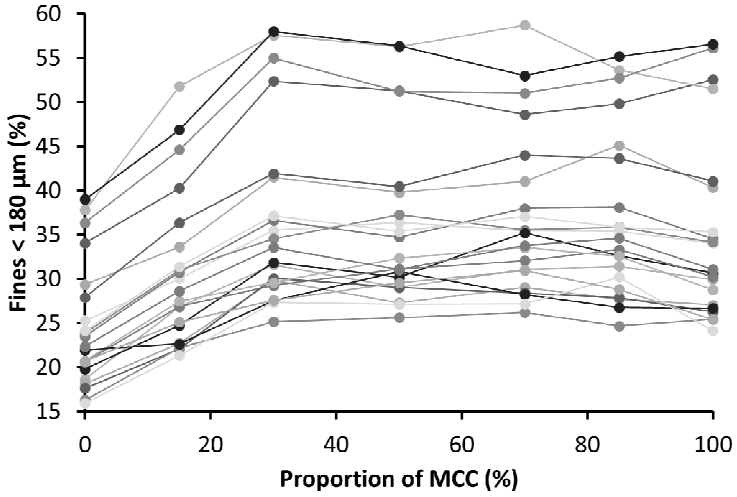

Figure 16: Percentage of fines smaller than 180 µm obtained for all the DOEs against the proportion of MCC. Please note that the lines connect the mixtures for the same factor level, mean (n = 3).

However, in order to have an idea of the range in which the percentage of uncompacted material is varying, the fines fraction for the 23 runs is plotted against the proportion of MCC in Figure 16. In this graph, a joining line for the same process conditions (same SCF, gap and roll speed) is depicted. Although some lines tend to cross, in general, they are parallel and in some instances they are even grouped, as is the case with the points corresponding to the 2 kN/cm that show the highest values of fines. Based on that, the first conclusion that can be extracted from the graph is that there are some trends, and a similar change in process conditions leads to a comparable variation of the uncompacted material. The fraction of fines considering all conditions and materials varies in total, from a minimum of 16% (mannitol) to a maximum of 59% (mixture 70% MCC). In general, MCC has higher amount of uncompacted material than mannitol batches. The combination of the mixtures results in higher or lower values than the pure materials, highlighting again an interaction between MCC and mannitol.

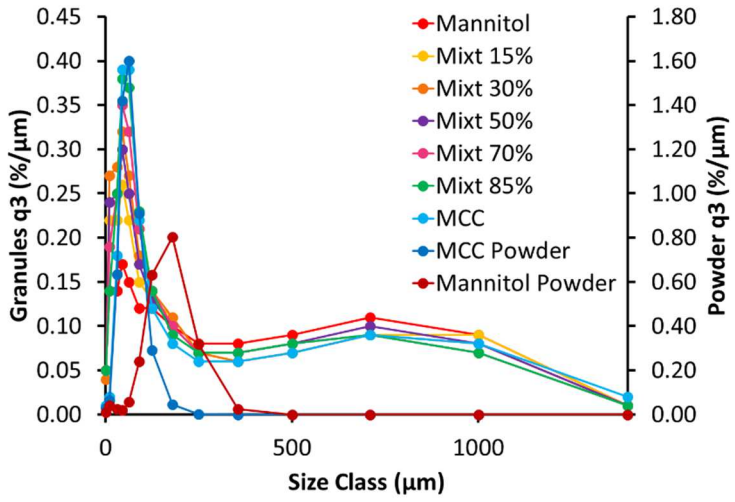

Figure 17: Representation of the q3 curves for the centre point of each mixture together with the pure materials so that the size enlargement can be observed. Please note that the raw powder is represented on the right Y-axis, mean (n = 3).

As the fine fraction exceeded in some cases a value of 50%, as it was observed in Figure 16, it might be questioned, whether the roll compaction process is really achieving the goal of size enlargement. For this purpose, Figure 17 shows an average q3 curve for the centre point granules of each mixture together with the ones obtained for the raw MCC and mannitol powder analysed on the Camsizer® XT under the same conditions as the granules. The starting materials are represented in a second Y-axis which allows for observation of both mixtures and powders on a visible scale. In this representation, it is possible to observe that in spite of the high amount of fines previously mentioned, it is also clear that roll compaction increases the particle size of the raw powder, and therefore is a useful process for obtaining granules.

4.1.4.3. PERCENTILES

A new and summarized DOE was prepared for the study of the D10, D50, D90 and fines, including the percentage of MCC as a new quantitative factor, in order to evaluate the importance of the mixture compacted in the resulting GSD. The percentiles give another point of view, as they are another way of expressing the distribution curve, and here the effect of the mixture composition can be clearly evaluated. After the statistical analysis performed by Modde, it can be concluded which are the factors that affect the variation of these responses. In Figure 18 the coefficient plot is presented. Only the significant responses are shown, therefore, the roll speed and its interactions were deleted. On some occasions, the coefficient of determination (R^2) is slightly higher than 0.6 and 0.7, although a 0.9 value is overcome for

the models of D50 and fines. According to the software Modde, up to 0.5 values, a model is considered with relatively low significance.

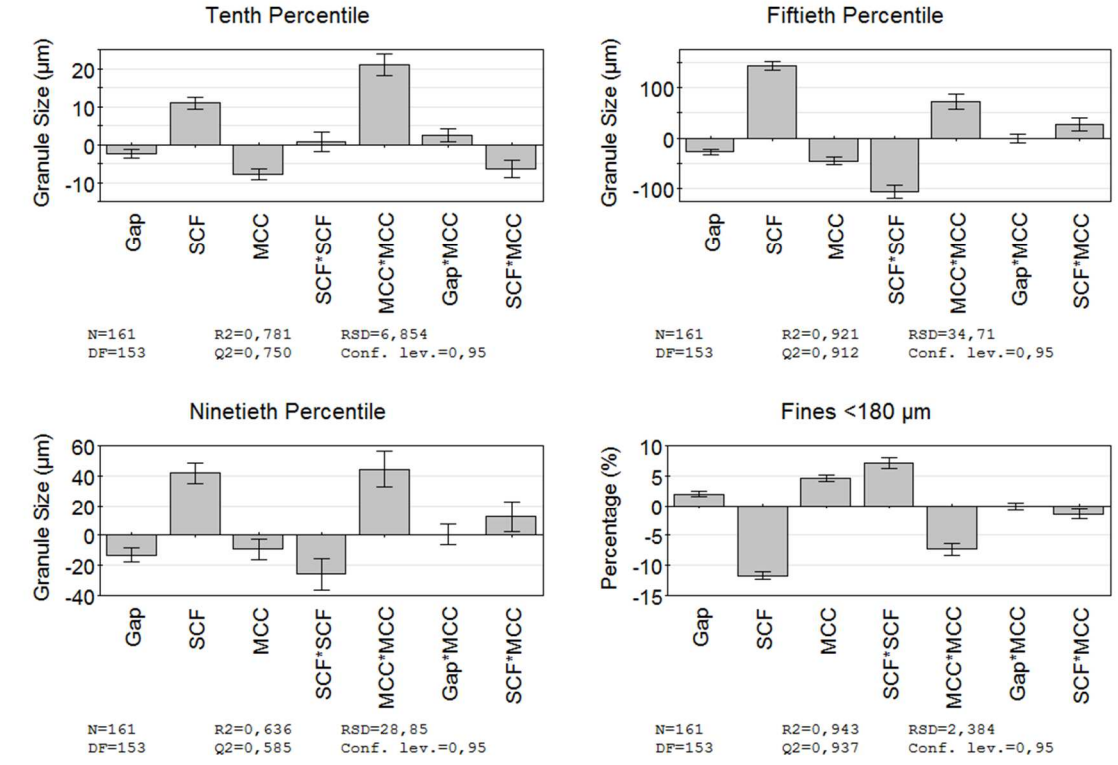

Figure 18: Coefficient plots for the D10, D50, D90 and fines for the modified version of the DOE including material (the proportion of MCC) as a factor (MLR).

A factor or interaction is significant when the error bar is not cutting the X-axis. If the bar for a specific factor is in the positive part of the Y-axis, this means that it has a proportional or direct effect on the property of interest, i.e. the higher the value of the factor, the higher the one of the property. If the bar is in the negative part of the Y-axis, then the factor has an inverse or indirect influence on the property of study, i.e. the lower the factor, the higher the property. For the present case, the SCF and the quadratic effect of the percentage of MCC have a proportional influence on all percentiles and an indirect effect on the fines. On the contrary, the gap and the proportion of MCC have an inverse effect but a direct influence on the fines. The interaction between force and MCC is also significant for all responses, but with an inverse effect on the D10 and fines, and a proportional influence on the D50 and D90. Similarly, the interaction between gap and MCC is significant with a proportional effect only on the D10. However, the quadratic effect of the SCF has no significant influence on this response but it does have it on the D50 and D90 with an inverse relationship and a direct effect on the fines. Therefore, from this statistical analysis it can be basically concluded that

the higher the SCF, the smaller the gap, and the lower the proportions of MCC, the larger the granules. This is in good agreement according to the results observed for ribbon relative density. Denser ribbons will be more difficult to mill, which will lead to larger granules (Gamble et al. 2010; Samanta et al. 2012; McAuliffe et al. 2015; Freeman et al. 2016; Pérez-Gandarillas et al. 2016). In other words, denser ribbons are also obtained for high SCFs, low gaps and proportions of MCC. Furthermore, this direct effect of the SCF and the gap on the GSD was already described in the literature (Rambali et al. 2001; von Eggelkraut-Gottanka et al. 2002; am Ende et al. 2007). Nevertheless, the roll speed showed no significant effect on the tested speed values although in the literature has been found to have an influence on the GSD (Weyenberg et al. 2005; Souihi et al. 2013b). This difference with the bibliography may be explained by the fact that the roll speed varies in a narrow range, only from a minimum of 2 to a maximum of 4 rpm.

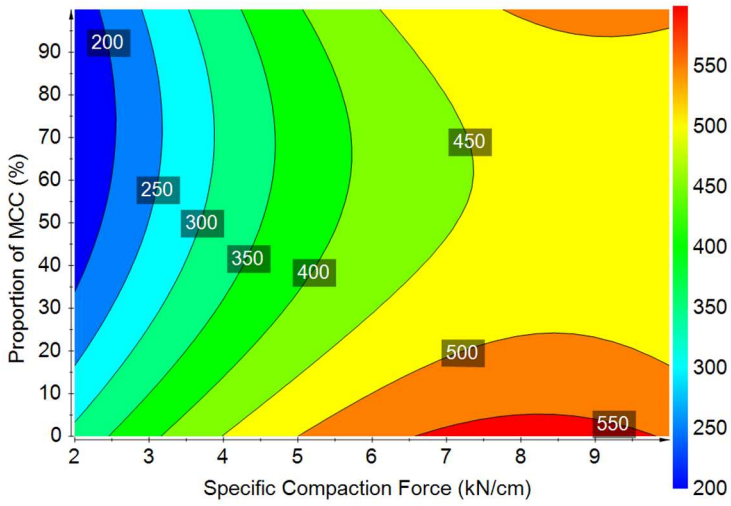

Figure 19: Response contour plot for D50 including the proportion of MCC and SCF for the summarized DOE prepared including the MCC fraction as a factor (MLR).

The response contour plots is another tool that Modde offers to visualize the results. It gives the factor space, i.e. the prediction of the values of property of interest within the factor levels investigated. This figure also allows for easier interpretation of the interactions, and from the previous coefficient plot, the most interesting one is the relationship between the proportion of MCC and SCF. The response which is more informative is the D50 as it gives an average value of the size of the granules. In Figure 19, the contour plot for D50 was prepared as an example considering the MCC fraction and the SCF in their axis. This plot was obtained from the summarized DOE previously discussed. As can be seen from this contour plot, the interaction between the MCC fraction and the SCF set, follows a non-linear tendency.

For low SCF values, the D50 tends to decrease almost linearly when rising the proportion of MCC. However, the D50 evolves differently for SCF values from 4 kN/cm on, having beyond 7 kN/cm the peak values for especially low or high percentages of MCC. This pattern in the figure stresses the importance of the MCC fraction through the synergic effect of the mixtures.

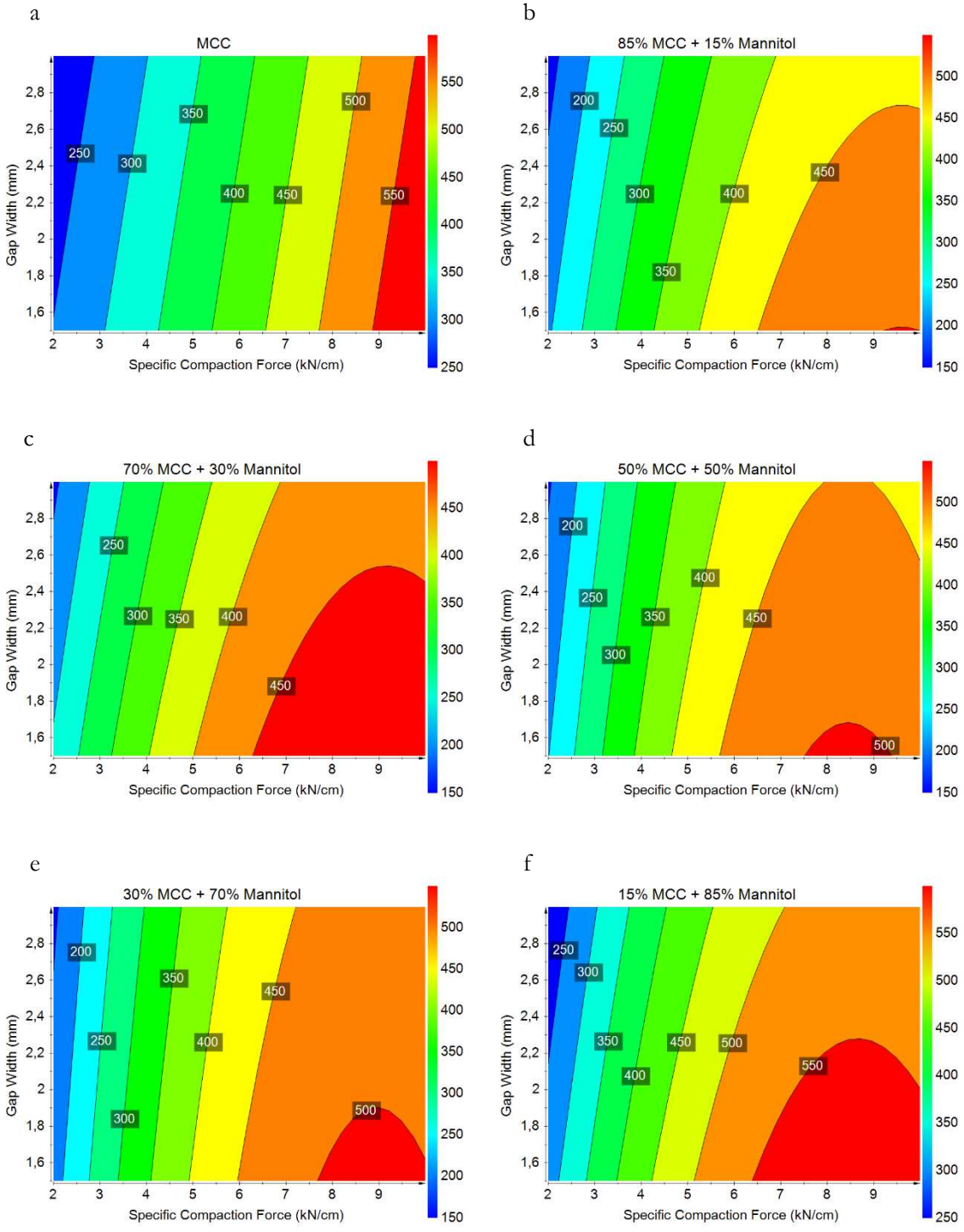

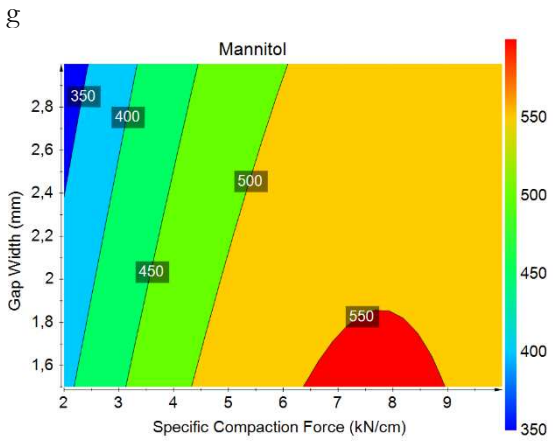

Figure 20: Response contour plots for D50 of the mixtures: 100% (a), 85% (b), 70% (c), 50% (d), 30% (e), 15% (f) and 0% MCC (g).

Similarly, the 7 individual DOEs were statistically analysed and the D50 contour plots for the most important factors (SCF and gap) were prepared. In Figure 20, the contour plots for D50 of all blends were collected in order to compare them. All mixtures but the pure MCC are influenced by the gap and the quadratic effect of the SCF indirectly, while the force itself has a proportional relationship with the D50. For mannitol (0% MCC), the interaction between gap and SCF shows a direct effect, although not significant for the specific case of the D50. Similarly, for the 70% MCC, the speed has an inverse influence slightly significant for this percentile. Finally, for pure MCC the only factor significant is the SCF, as the gap presents an indirect influence not significant, which justifies the pattern (Figure 20a). The analysis of these contour plots leads to a similar conclusion, the higher the SCF and the lower the gap, the larger the granules. However, depending on the material, the pattern is different, and the highest D50 values may not be found for those extreme conditions of SCF and gap (Figure 20d and 20g).

4.1.4.4. CORRELATION RELATIVE DENSITY-AMOUNT OF FINES

In order to also evaluate the relationship of the granule properties to the ribbon attributes, a correlation between relative density of the ribbon and the amount of fines was prepared. In Figure 21, the correlation for the ribbon density against the amount of fines is presented for the 3 repetitions of the centre point ribbons. As expected, the slope of the best fit line for all the data points is negative, meaning that the denser the ribbons the lower the amount of fines. A separation between the mannitol and all the others points occurs. For the

fines fraction, this distance is more than a 5% which is relatively high considering the distribution of the mixtures and MCC points. This means, however, that a small decrease on the relative density leads to a high increase in the amount of fines.

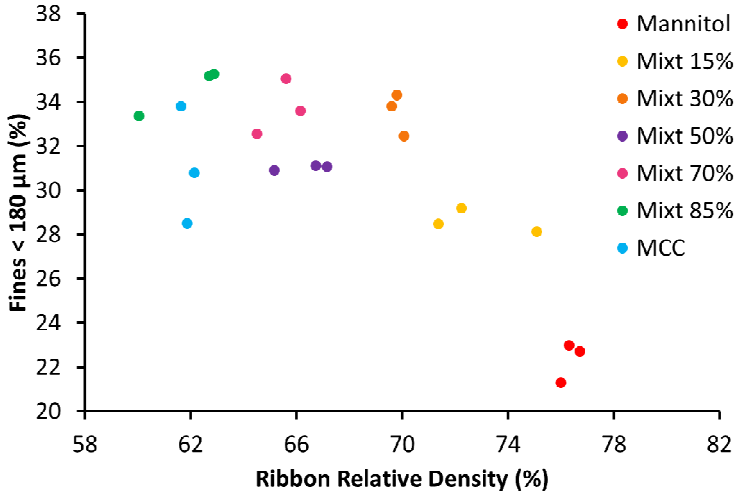

Figure 21: Correlation for the ribbon density and the amount of fines of the granules, mean (n = 3).

Despite the distribution of the points which may suggest that the points are grouped in two lines, the t-test was performed for $\alpha < 0.1\%$ and 20 degrees of freedom in order to confirm that this trend is significant from a statistical point of view. The r value is for this case -0.739 whose absolute value is higher than the 0.652 tabulated. Therefore, both properties are related not only from the theoretical point of view, but also the statistical perspective.

4.1.5. PERCOLATION THEORY

The plastic/brittle material fraction for the mixtures has shown a clear impact on the properties of ribbons and granules. For the raw materials, no synergic effect due to the interaction between mannitol and MCC has been observed for any of the characteristics evaluated. This means that the non-linear effect that the plastic/brittle fraction exerts on some of the ribbon and granule properties is coming from the roll compaction process. However, not all properties are affected in the same manner by the fraction plastic/brittle. For the ribbon relative density, no percolation is observed, as a linear relationship between this property and the percentage of MCC was obtained. However, for all other properties involved in this study, a non-linear behaviour was observed. Thus, the percolation theory was used in order to further understand the relationship between material composition and mechanical behaviour. The

percolation thresholds were identified for the microhardness (both methods), percentiles and fines. As it has been already reported in the literature (Sinko et al. 1995; Castellanos Gil et al. 2009; Boersen et al. 2014), the percolation threshold can be obtained by calculating the intersection point of the best fit lines depicted by dividing the data in two sets. Although the points chosen to calculate all these lines may be questionable and other possibilities could be established, considering the values of the data points and the trend observed during the previous discussion, it seems reasonable to make the fits presented below. Furthermore, for the specific case of the HU, the same best-fit line pattern was followed for both methods.

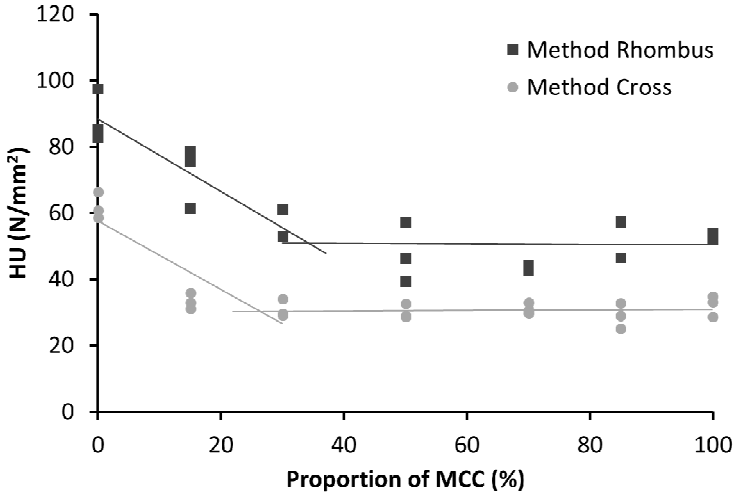

Figure 22: Percolation thresholds for the microhardness comparing both methods of determination, calculated by intersection of the best fit lines, mean ($n \geq 12$).

In Figure 12 and 13 (pages 49 and 50 respectively) the global mean for the microhardness of all ribbons of the centre point was presented for both methodologies. Now in Figure 22, the mean HU value for each of the 3 replicates is used to draw the best fit lines. The intersection between these two lines occurs at 34% of MCC for the rhombus method and 26% for the cross system. The same procedure was followed for the percentiles and the fines fractions. Similar percolation thresholds were found for D10 and the fines as well as for the D50 and D90, so the data was paired in two groups. A graph containing both calculations of the percolation threshold was prepared for both pairings. Figure 23 shows the graphical calculation of the percolation thresholds for D10 and the fines (a) as well as for D50 and D90 (b). In the case of D10 and the fraction of fines, the values for the intersection between the two best fit lines are 27% and 28% respectively. This percolation threshold is similar to the value obtained for the microhardness measured with the cross method. Below the percolation threshold of MCC, the fraction of fines decreases and D10 increases with the mannitol

fraction. However, in the case of D50 and D90 the percolation threshold is 84% and 85% respectively, so the differences in behaviour are due to the percolation of mannitol.

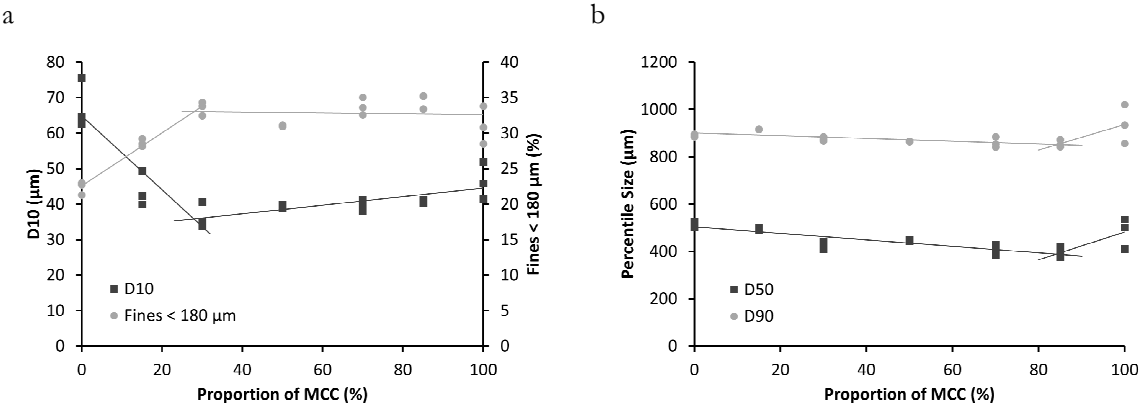

Figure 23: Percolation thresholds for D10 and fines (a) and D50 and D90 (b) calculated by intersection of the best fit lines, mean (n = 3).

These percentages referred to the limit above which the behaviour of the whole mixture changes. In that sense, a percolation threshold of 34%, means that until this amount of MCC is reached, it predominates a behaviour mostly affected by mannitol, i.e. the powder percolating is MCC. In the mixture small clusters of MCC are being formed and once this example percentage of 34 is overcome, the clusters connect. This leads to an alteration of the system and its subsequent predominance of the behaviour of MCC. From this point, the mannitol would be isolated in clusters (percolation of this material) that will have a lower influence on the mixture properties. Although for this case one percolation threshold can be visualized, theoretically (Leuenberger 1999), there are two percolation thresholds: one for MCC and one for mannitol, and in between, both materials can percolate.

4.1.6. SUMMARY

In this first part of the thesis, the effect of the proportion of MCC on the properties of ribbons and granules was investigated. A DOE consisting in a multilevel full factorial design plus 3 repetitions of the centre point was performed for 7 binary mixtures of MCC and mannitol. It was evaluated how the plastic/brittle material fraction (variation of the proportion of MCC) affects the relative density and microhardness of the produced ribbons, as well as the GSD of the granules, when varying the roll compaction conditions.

A bi-modal GSD was found independently of the roll compaction settings and the material used. The individual DOEs were merged into one, which included the proportion of MCC as a new factor. The percentiles D10, D50 and D90 as well as the amount of fines were studied through this combined DOE to identify the most critical factors affecting them. On the one hand, the SCF and the quadratic effect of the proportion of MCC showed a clear direct relation to the evolution of the percentiles, as well as an indirect effect on the amount of fines. On the other hand, for the gap and proportion of MCC an indirect influence was also detected on the percentiles while on the fines it was a proportional effect. Thus, the higher the SCF, the smaller the gap and the lower the proportions of MCC, the larger are the granules.

In order to have a first idea of this material effect already observed for the percentiles and fines, powder properties regarding true density, PSD and LOD were measured. For all these attributes a linear relationship was found, i.e. the higher the proportion of MCC, the lower or higher the property of interest. Therefore, in order to evaluate the impact of the plastic/brittle fraction after roll compaction, the centre point ribbons and granules were selected as the production conditions were the same for all these batches. Ribbons were characterized regarding relative density and microhardness (expressed as HU and measured by two methodologies) and for the granules the GSD was measured. Although an almost linear relationship between the ribbon density and the proportion of MCC was found, for the HU and the GSD a clear synergic effect was observed. This means that the interaction between MCC and mannitol results in values even higher or lower than the pure materials.

The importance of the proportion of the two excipients in the plastic/brittle mixture was further evaluated by application of the percolation theory. The percolation thresholds for the microhardness (both methodologies), the percentiles and the fine fraction, were identified by calculating the intersection point from the best fit lines of the data divided in two sets. A proportion of MCC of 34% and 26% was obtained as percolation threshold for the HU (rhombus and cross method respectively). D10 and the fines fraction as well as D50 and D90 were paired according to the threshold values, which were 27% and 28% (percolation of MCC) and 84% and 85% (percolation of mannitol) respectively. The importance of the plastic/brittle fraction was proven when preparing a mixture for roll compaction. Depending on the proportion of MCC the behaviour of a hypothetical mixture will be more similar to the profile observed for MCC or for mannitol, which will be reflected on most of the properties of ribbons and granules.

4.2. SCALE-UP

4.2.1. INTRODUCTION AND OBJECTIVES

Roll compaction/dry granulation is a process of high interest for the pharmaceutical industry, and as such, it is necessary to investigate its scalability. Scale-up is the transfer of a process from a smaller to a larger scale, i.e. from lab to pilot, production or commercial scale. For achieving this objective, the critical parameters involved in this procedure must be identified and their influence understood, so that it is possible to adapt them in order to obtain the same product quality on both scales. This is important to consider in research and a critical step in the industry, as it is desirable that the results obtained in the laboratory can also be transferred to a larger scale. For the roll compaction process, vendors use two scale-up strategies based on how the size of the rolls is modified between scales: by changing the roll diameter together with the roll width or by just varying the roll width while keeping the diameter constant. This last technique is used in order to facilitate the change in scale. On the one hand, using the same diameter will facilitate the calculations of forces that will be used in the new scale, leading to the use of the SCF for those suppliers who have chosen this strategy (Gerteis and L.B. Bohle). With this approach, the idea is that the same SCF can be applied in both compactors, avoiding transformations of values, although the total roll force will be different. On the other hand, maintaining the roll diameter reduces the need to adapt the roll speed either, as the linear speed will be the same in both scales. Therefore, these providers make great efforts to easily transfer the roll compaction process between their pieces of equipment, evading calculations or transformations when changing the scale.

As it has been illustrated in the previous chapter, different combinations of process parameters, as well as mixture composition, affect the roll compaction process. In this manner, those factors should also be considered in the individual scale-up studies, as they can also be diversely affected by the change in the roll compactors' scale. Furthermore, different roll surfaces, sealing systems and feeding configurations are available on the market. These characteristics of the roller compactors can also have an impact on the products. And finally, the differences between suppliers can be another source of variability between machines, for example, different scale-up strategies or diverse systems to apply the force. Thus, and in order to have a general overview of the scalability of the roll compaction process, all these factors should be considered. However, this part of the thesis will be mostly focused on ribbon properties and therefore, the scalability of the granulation process will be not evaluated in detail.

Therefore, in the present part of the thesis, a total of three individual scale-up studies will be performed for a couple of compactors developed by Gerteis, L.B. Bohle and Freund-Vector companies. This first provider has an inclined feeding system, while it is vertical for the other suppliers. Gerteis and L.B. Bohle use as scale-up strategy, the exclusive change of the roll width, while Freund-Vector varies both roll width and diameter between scales. Apart from that, depending on the line, different roll surfaces and sealing systems are used. For each individual scale-up study, different combinations of process parameters and mixtures are evaluated. For all studies pure MCC and mannitol together with 5 mixtures thereof are investigated. As a larger study for the granules properties has been presented in the previous chapter, this section will be mainly focused on the ribbon characterization. It is also important to consider that powder characterization was not performed for all the lines (only for the Polygran®, as shown in the previous section). It is assumed that, as the mixing conditions are similar for all the blends prepared independent of the compactor later used, their properties should be also comparable to those obtained for the mixtures of the Polygran®. This could be a source of variability, although it will be excluded from the interpretation of the results. Therefore, the scalability of the roll compaction process will be mostly studied through the ribbon characterization.

4.2.2. GERTEIS LINE

This first and most complete scale-up study will cover the transfer of the roll compaction process between the Mini-Pactor® and the Polygran® developed by Gerteis. Both compactors have a 250 mm roll diameter while the Mini-Pactor® has a 25 mm roll width (small scale) and 50 mm for the Polygran® (large scale). In order to keep the process as constant as possible, both machines were assembled with knurled roll surfaces and with cheek plates. For this study, both DOEs defined were used. The 23-runs DOE was performed for the main materials (MCC, mannitol and 50% mixture) and its reduced version (11-runs DOE) was carried out for the 4 mixtures of MCC left. The same batches were produced in both scales. Aside from the larger amount of samples, more characterization methods were applied to the Gerteis line than to the following scale-up studies.

4.2.2.1. PROCESS DATA

The Mini-Pactor® was equipped with a real-time monitoring system, which allows for observation on the computer's screen of the real SCF and gap width, although the roll speed is not displayed. This is not only useful to control the production conditions, but also permits the collecting of the process data. Unfortunately, the Polygran® only shows the real-time values while production, and it is not possible to copy this information. In Figure 24, a complete profile of a DOE production is plotted, although sample collecting took place only in certain periods of time (when the steady-state conditions were achieved). In this sense, the changes in SCF and gap are presented for the 23 runs compacted for the 50% mixture.

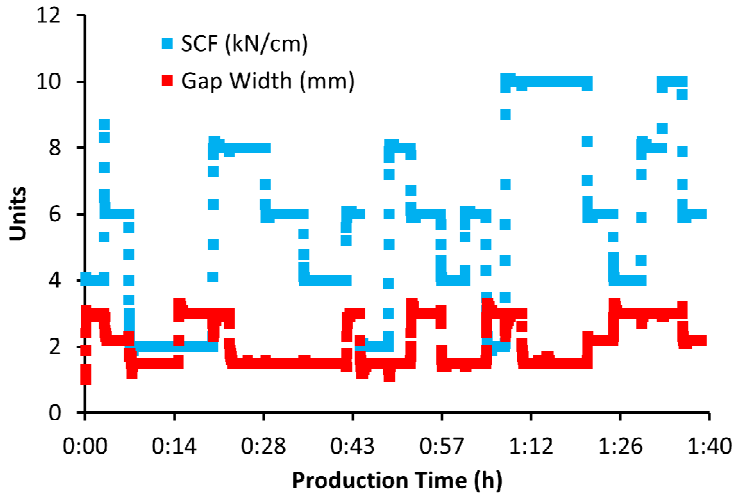

Figure 24: Example graph for the complete compaction of the 50% mixture in the Mini-Pactor®, in which it can be seen how the SCF and gap width vary during the process.

The first main conclusion that can be extracted from the graph is the fast adaptation of the process and the efficient gap-control and SCF system. Nevertheless, plotting this amount of results together avoids evaluating the variation within one batch. Thus, Figure 25 was prepared with 2 examples considering the moment in which the sample collection started or few seconds before. One corresponds to one batch from the figure above (left) and the other one is an example for MCC compacted under different conditions (right).

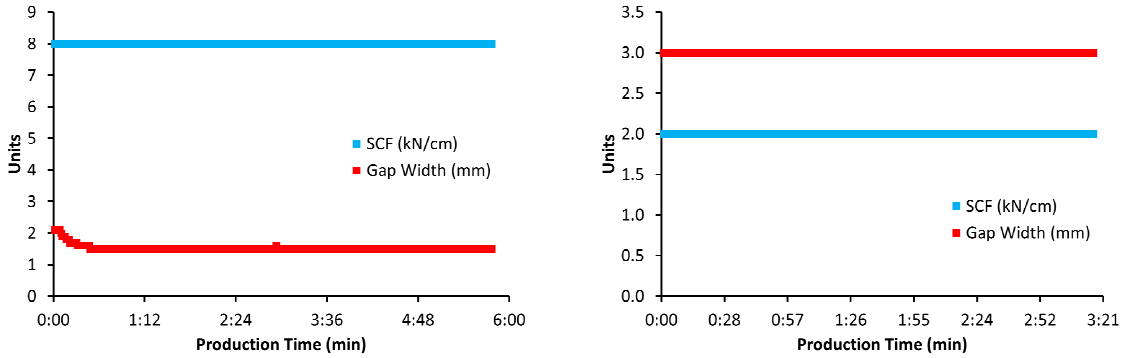

Figure 25: Example graphs in which it can be seen how the SCF and the gap width evolve during a normal compaction process for the 50% mixture (left) and MCC (right) on the Mini-Pactor®.

From this figure it can be easily seen that the control of the process is excellent, keeping the SCF and gap width constant. In the case of the left-hand side figure, the initial adaptation of the gap width is also presented. It must be mentioned as well that such a control is observed for some other batches. Nevertheless, for some lots, small deviations in respect to the set value could occur, which varies on a range not greater than ±0.1 for most of the cases. Furthermore, it is important to consider that for this compactor one data point is generated each second, meaning that in the graphs there is no lack of information. For all these reasons, it can be concluded that the Mini-Pactor® has an excellent control system for both SCF and gap.

4.2.2.2. RIBBON CHARACTERIZATION

In the scale-up studies, most of the efforts were concentrated on the ribbon properties. Their characterization is especially problematic as no standard methods are available and the wide range of sizes and shapes of the ribbons increases the difficulties of finding suitable methods for all samples. Several authors in this situation, opted for the production of simulated ribbons normally by uni-axial compression (Zinchuk et al. 2004; Gupta et al. 2005b; Patel et al. 2010; Peter et al. 2010; Zheng et al. 2013; Bi et al. 2014) in order to correlate the results to compacts produced by roll compaction.

Nevertheless, in the literature different techniques to characterize the ribbons can be also found. One of the most interesting attributes is the relative density, which has been widely determined by using the GeoPyc® (Ghorab et al. 2007; Chang et al. 2008; Gamble et al. 2010; Dumarey et al. 2011; Hilden et al. 2011; Lim et al. 2011; Nesarikar et al. 2012a; Austin et al. 2013; Souihi et al. 2013a; Iyer et al. 2014a; McAuliffe et al. 2015). However, other methods

have been also described in the literature, such as the mathematical calculation according to dimensions and weight (Gupta et al. 2005b; Nkansah et al. 2008; Osborne et al. 2013; Iyer et al. 2014a), the sectioning method (Miguélez-Morán et al. 2009; Golchert et al. 2013), mercury intrusion porosimetry (Dalziel et al. 2013) or other techniques (Herting et al. 2007a; Iyer et al. 2014a; Allesø et al. 2016). Furthermore, density distribution has been determined by several methods, like μCT (Miguélez-Morán et al. 2009; Akseli et al. 2011; Wiedey et al. 2016), near-infrared or NIR (Dawes et al. 2012; Samanta et al. 2013; Khorasani et al. 2015), ultrasonics (Akseli et al. 2011) or terahertz pulsed imaging (Zhang et al. 2016). Microhardness has been also measured and collected in the literature, although not widely (Wöll 2003; Freitag et al. 2004; Miguélez-Morán et al. 2009). Finally, tensile strength has been also determined by the three-point beam test (Chang et al. 2008; Hamad et al. 2010; Kushner et al. 2011; Osborne et al. 2013; Iyer et al. 2014b). However in this section, ribbons would be characterized regarding physical appearance, relative density (measured with the GeoPyc®), density distribution (with μCT) and microhardness.

4.2.2.2.1. APPEARANCE

As many samples were prepared and the ribbon appearance is a qualitative property, only a few select ribbons were characterized. This decision was taken in order to give just an idea of how the roll compaction process in different scales affects this attribute. In this manner, only the ribbons of pure MCC and mannitol for the 11-runs DOE were considered. As an example, two pictures of those ribbons produced on both scales are presented in Figure 26 as an example. In particular, the samples photographed belong to the centre point.

a b

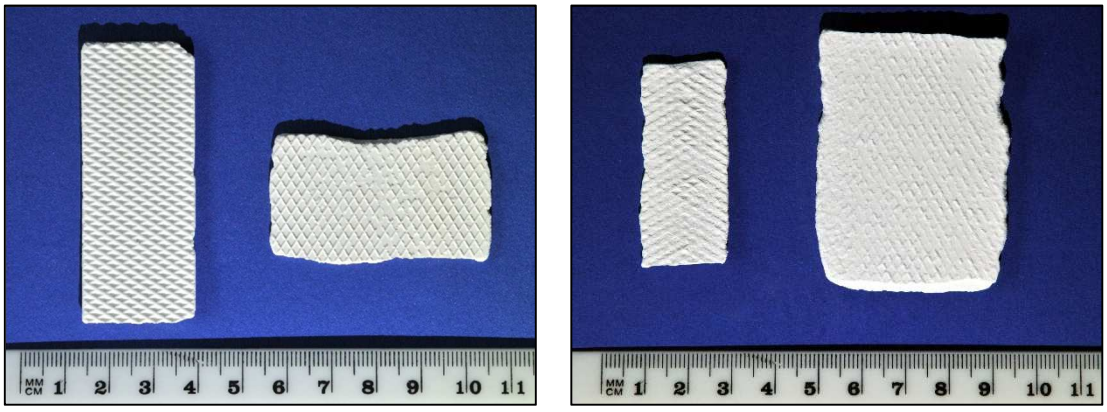

Figure 26: Example of two pieces of ribbons from MCC (a) and mannitol (b) produced with the Mini-Pactor® (ribbon on the left) and the Polygran® (ribbon on the right).

Although, these images only show one of the sides, they give an idea of what the ribbons look like depending on the material and scale. All other ribbons selected were judged regarding the length and structure of the coming pieces from the gap. In this sense, the length was described by defining "long" and "short" ribbons. The limit was stablished at 2.5 and 5 cm for the Mini-Pactor® and Polygran® respectively. These lengths correspond to the width of the rolls, meaning that a ribbon is considered long when it overcomes the size of a square. Regarding the structure, it was defined as "integrated" and "laminated" ribbons. The first ones come out of the gap as one unique piece and, therefore, in both sides the drawing of the knurled design can be seen. However, in other situations, two pieces are coming out as they stick to the surface of both rolls (Figure 5b, page 32). This lamination results, on the one hand, in ribbons with only one knurled side and, on the other hand, in a certain curvature.

Table 5: Physical appearance of the MCC and mannitol ribbons produced in both compactors. Please note that the roll speed was shortened as RS and mannitol as Man, as well as the Mini-Pactor® which was abbreviated as MP and the Polygran® as PG.

DOE CONDITIONS			**APPEARANCE RIBBONS**			
SCF (kN/cm)	**GAP (mm)**	**RS (rpm)**	**MCC MP**	**MCC PG**	**MAN MP**	**MAN PG**
4	**1.5**	**2**	1L	2S	2S	1L
4	**3**	**2**	2L	2S	2L	1S
4	**1.5**	**4**	1L	2S	2S	1L
4	**3**	**4**	2L	2S	2L	2S
8	**1.5**	**2**	2L	2S	2S	1L
8	**3**	**2**	2L	2S	2L	1S
8	**1.5**	**4**	2L	2S	2L	1L
8	**3**	**4**	2L	2S	2L	1S
6	**2.25**	**3**	1L	2S	2L	1S
6	**2.25**	**3**	1L	2S	2L	1S
6	**2.25**	**3**	2L	2S	2L	1L

In Table 5 all the information regarding the appearance of the ribbons of both materials and scales is collected. Numbers 1 and 2 refer to the structure (integrate or

bilaminated respectively) and S and L to the length (short or long correspondingly). It is important to point out, that this cataloguing was made considering the majority of the ribbons and situations like storage or transport could affect the preservation of the samples. The main conclusion is that regarding structure, length or even both, the appearance of the ribbons from the same material in the two scales is always differing. However, there is not a clear explanation why the visual properties of the ribbons change drastically when scaling up the process. It could be possible that the slightly different design of the knurled roll surface could lead to a different graving of the powder in both scales. Furthermore, the cheek plates were in proportion longer on the Polygran® than on the Mini-Pactor®, so the powder may be differently canalized. These facts, in combination with the higher roll width and therefore surface, could explain these differences. Nevertheless, Bultmann 2002 also considered the visual ribbon properties after multiple recompaction of MCC at the Polygran® and bilamination was not addressed in the paper. Independent of that, it is clear that the scale of the roll compactor has a clear effect on the appearance, leading in some occasions to opposite visual characteristics.

4.2.2.2.2. RELATIVE DENSITY

Ribbon relative density is a key property which correlates to other attributes of the ribbons, but also granules and tablets (Miguélez-Morán et al. 2009; Reynolds et al. 2010). Therefore, all samples produced were characterized regarding this property. Furthermore, the methodology is feasible for all samples, independent of their dimensions or structure. The density characterization was divided in three sections, two of them defined by the DOE performed, and the last one as a small isolated study, but which gives interesting information regarding reproducibility. For the two first parts, there is some data overlapping but focused on different perspectives. Please note that in this section, only the ribbon density results are included.

The measurement at the GeoPyc® could be a source of variability within the ribbon relative density. The sampling could lead to the exclusion of representative pieces and furthermore, the bilamination and internal cuts of the ribbons may also have an impact. Ribbons including mannitol are brittle and this predisposition to break, makes that the more the manipulation of those samples, the higher the loss of material. Therefore, the difficulties while handling ribbons containing mannitol (especially the sampling of the pieces which would be characterized) could have had an impact on the measurement with the GeoPyc®. Nevertheless, considerable effort was taken to obtain a representative sample and the low

deviations in some of the measurements would suggest it is suitable. Furthermore, its wide use in the literature also supports this methodology. Therefore, during the coming discussion, the evaluation will be done excluding the possible variations existing on the technique, especially because in the literature comparable results when using this machines and other methodologies were found (Iyer et al. 2014a).

4.2.2.2.2.1. MAIN MATERIALS

This section is mostly focused on the effect of the process conditions (especially the SCF) and the scale. In this manner, here are collected the results corresponding to the 23-runs DOE performed for MCC, mannitol and the 50% mixture. In Table 6, all results collected are presented. The first conclusion that can be extracted from this table, and as was also observed in the previous chapter, is that for all cases and the same conditions, the ribbon density tends to decrease with the increase of MCC percentage. The plastic MCC generates lower densities while mannitol as a brittle material leads to higher values. In the literature, Golchert et al. 2013 observed how for the same formulation in which only the type of excipient is changed, the ribbon relative density is lower when using a plastic material like MCC, than when including other brittle powders like lactose or dicalcium phosphate anhydrous. In fact, Chang et al. 2008 found similar ribbon solid fractions when for a particular formulation, mannitol or lactose are used, meaning that one or other brittle material lead to similar ribbon densities.

Similarly, Iyer et al. 2014b investigated the ribbon relative density for two excipients and their 1:1 mixture compacted also at the Mini-Pactor® under fixed conditions of 2.5 mm gap width and 2 rpm roll speed. The SCF was varied between 5 and 10 kN/cm and the machine was assembled with both types of smooth and knurled rolls. The first material is a commercial available mixture, i.e. a co-processed excipient especially designed for dry granulation, which consists on MCC (at 75%) and anhydrous dibasic calcium phosphate (25%) and is known as Avicel® DG. The second excipient is lactose. When comparing the pure materials and the mixture, for the same conditions the relative density tends also to increase from the minimum observed for Avicel® DG to a maximum for lactose. Although neither the production conditions nor the materials are comparable, the values found by these researchers seem to be in good agreement with those obtained in the present thesis, which varies between 65 and 78% approximately for Avicel® DG, 71 and 81% for the mixture and finally 80 and 85% for lactose.

Table 6: Average ribbon relative density values for the main materials compacted under the conditions of the 23-runs DOE (n = 3) together with the production conditions for the Gerteis compactors.

CONDITIONS			**AVERAGE RELATIVE DENSITY (%)**					
SCF (kN/cm)	**GAP (mm)**	**RS (rpm)**	**MCC MP**	**MCC PG**	**MIXT MP**	**MIXT PG**	**MAN MP**	**MAN PG**
2	1.5	2	50.2	46.7	55.8	52.2	67.1	67.8
2	3	2	45.9	46.9	53.6	50.6	65.2	65.3
2	1.5	4	50.4	48.9	54.5	53.1	65.2	65.8
2	3	4	44.3	46.1	48.7	51.4	64.2	64.9
4	1.5	2	58.3	55.7	63.6	62.5	72.3	73.6
4	3	2	54.3	54.9	61.4	59.7	69.6	71.4
4	1.5	4	56.6	55.4	63.0	62.2	71.8	73.2
4	3	4	52.4	53.0	61.8	60.0	71.0	71.7
6	1.5	2	65.7	63.1	66.4	68.7	75.6	78.1
6	3	2	61.0	59.9	67.0	66.3	75.6	75.9
6	1.5	4	63.5	63.1	65.1	67.0	74.0	77.7
6	3	4	61.4	59.6	66.8	64.1	73.9	75.2
8	1.5	2	66.8	65.8	71.1	70.1	77.9	80.1
8	3	2	63.2	65.6	72.5	69.8	76.7	78.4
8	1.5	4	68.1	65.3	68.6	70.6	75.7	80.5
8	3	4	64.4	63.6	71.9	68.7	77.0	77.7
10	1.5	2	71.4	69.8	74.0	73.7	79.3	82.8
10	3	2	69.9	68.2	76.0	73.2	79.2	79.9
10	1.5	4	69.9	69.9	74.8	73.7	77.7	82.1
10	3	4	67.8	68.2	74.5	71.9	77.8	79.6
6	2.25	3	62.1	62.1	67.6	66.7	75.6	76.7
6	2.25	3	58.2	61.9	67.2	67.1	74.4	76.3
6	2.25	3	61.4	61.6	64.6	65.2	75.5	76.0

From the data presented in the table, a second conclusion can be extracted regarding acceptability of the ribbons produced. According to Zinchuk et al. 2004, the ribbon relative density for obtaining satisfactory products (granules and tablets) regarding quality should be between 60 and 80%. Although the range to establish the acceptability of the products depends on the material and therefore, this can be a risky estimation, it will be considered in order to have an initial idea of the product quality. Therefore, for MCC in both compactors, SCF under 6 kN/cm leads to ribbons with a relative density lower than 60%, and for the mixture, 4 kN/cm is the minimum SCF which can be used to produce good-quality ribbons, also in both scales. For mannitol no lower limit needs to be established, however, compacting using the Polygran® under 8 and 10 kN/cm using a gap of 1.5 mm width, leads to ribbons with densities higher than 80% independently of the roll speed used. In other words, the SCFs that can be configured to produce ribbons between 60 and 80% relative density, are between 6 and 10 kN/cm for MCC regardless of machine and conditions used. In the case of the mixture, from 4 to 10 kN/cm can also be applied independent of the scale and other process parameters. Finally, for mannitol compacting at the Polygran®, high SCF values of 8 and 10 kN/cm can only be used for gaps larger than 1.5 mm or the ribbons obtained will overcome the 80% established. Furthermore, there is a small exception for one batch of MCC at the Mini-Pactor® for the centre point, which results in ribbons with a density slightly lower than the limit.

In order to identify which factors are affecting the process, several statistical evaluations were performed. First of all, the original DOEs were analysed individually considering the different combinations of materials and compactors. For all models, the R^2 values overcome the 0.96 meaning a good fitting. As the SCF was studied in 5 levels, it was possible to add its quadratic effect to the model. The SCF showed a significantly proportional relationship together with the inverse influence of its quadratic effect for all cases (this means that the higher the SCF, the denser the ribbons). In the case of MCC, for both compactors, also the gap showed an indirect effect on the relative density (the lower the gap, the denser the ribbons). In the case of the mixture, the gap also had an inverse influence only for the Polygran®, however, for the Mini-Pactor®, the interaction of gap and SCF showed a proportional effect. Finally for mannitol, in both scales, the roll speed was also indirectly significant, and furthermore, for the Polygran® also the gap. The non-significant factors and interactions were deleted from the models.

This already gives a first impression of the effect of the scale, but it has to be further investigated, as the study of the effect of the scale together with process parameters and

mixture compositions is of high interest. Additionally, those effects of the SCF and the gap in the ribbon density were also identified by Allesø et al. 2016, as well as in the previous chapter through the granules evaluation. These authors observed also that the higher the SCF and the lower the gap, the denser (or less porous) the ribbons. Some other researchers observed similar influence of the SCF (Dalziel et al. 2013; Souihi et al. 2013b; Iyer et al. 2014b; Khorasani et al. 2015) and the gap width (Miguélez-Morán et al. 2009) in the ribbon relative density, although these studies included other formulations and factors in their DOEs. This general effect of increasing the ribbon density while rising the SCF and decreasing the gap was presented is Figure 27 with a contour plot as an example, where a linear profile can be observed.

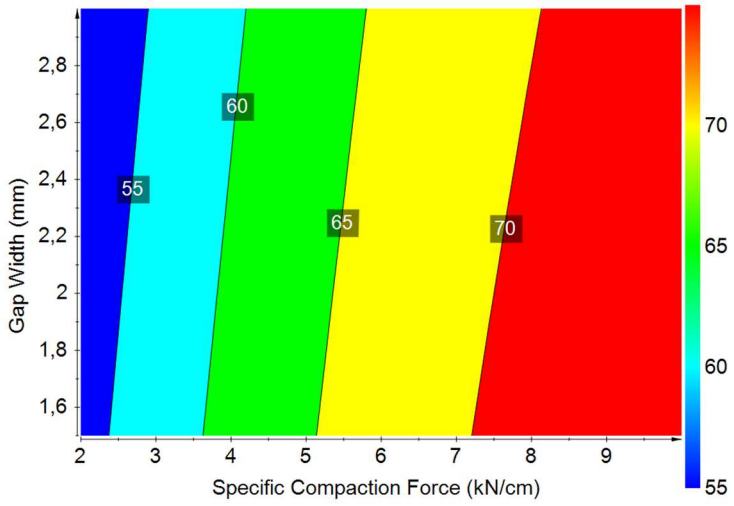

Figure 27: Example of a contour plot for the mixture compacted at the Polygran® in which the effect of SCF and the gap on the relative density is shown (MLR).

Nevertheless, the objective of this part of the thesis is to further investigate the effect of the scale in combination with process parameters and material effect, although to a lesser extent. With this intention, a total of three DOE modifications were performed. The first one was performed by including the scale as a factor, represented by the roll width. This can be made as the diameter is constant in both machines, and additionally, allows for expression of the scale as a quantitative factor. In Figure 28, the coefficient plot is presented. The models obtained results in high R^2, always exceeding 0.97, which is considered as an indicator of a good approach.

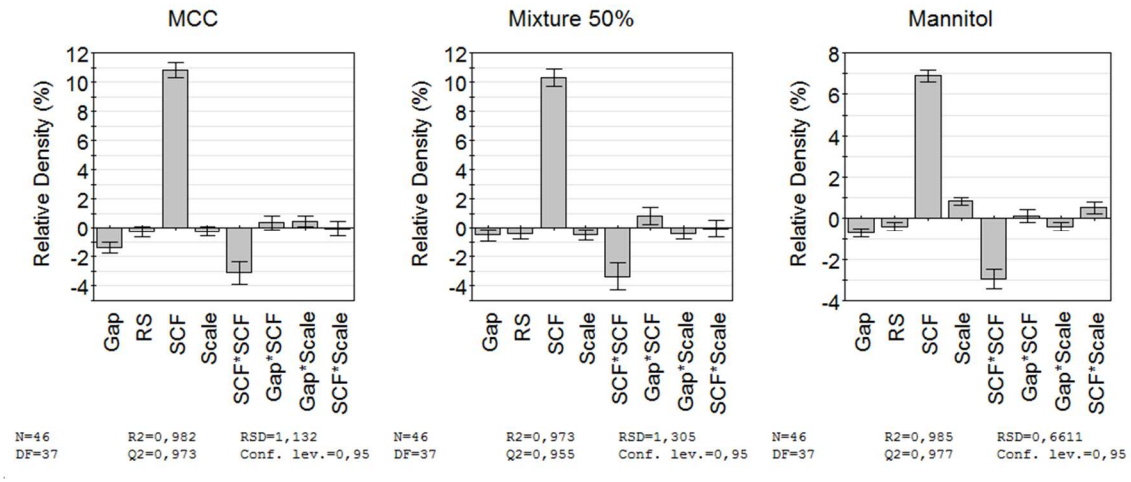

Figure 28: Relative density coefficient plots for the first modification of the DOE including the scale as a factor (MLR).

From this first analysis, it can be concluded that for all the cases, the SCF has a direct effect and the gap and quadratic effect of the SCF show an inverse influence on the relative density. This confirms what is already concluded from the last coefficient plots, that the higher the SCF and the lower the gap, the harder the ribbons, which are the largest effects by far. Furthermore, the other factors are significant or not, depending on the material considered. Roll speed (RS in the figure) is only inversely significant for mannitol. The scale is significant with an indirect and proportional effect for mixture and mannitol respectively. The gap-scale interaction is directly significant for MCC while inverse for mannitol. Apart from that, there are other interactions that are only affecting one material. This is the case of the interaction gap-SCF which has a direct effect on the mixture and the interaction of SCF and scale, which also has a proportional influence on the compaction of mannitol. Therefore, all materials are affected by the scale directly or as part of an interaction. Nevertheless, at this point it is important to stress the difference between "significant" and "relevant". From the coefficient plot, it can be concluded that the scale and/or its interactions are significant, however, it is possible that at the end and from a practical point of view, their effect, especially on the properties of the resulting granules and tablets, will not be relevant. Nevertheless, the scientific discussions will be based mainly on the significance.

A second modification of the original DOE was performed by adding to the initial design the material composition, expressed as percentage of MCC. In Figure 29, the corresponding coefficient plot can be found. These models have again a high R^2 value, 0.972 for both. In this case, the scale effect can also be evaluated by comparing the factors which have an impact on each compactor. For both machines a proportional relationship of the SCF

together with the inverse influence of the gap and the quadratic effect of the SCF is again identified. However, for this study including the proportion of MCC, an indirect impact on the material proportion and its interaction with the SCF with a proportional relationship are observed. This means that denser ribbons are obtained not only with low gaps and high forces but also with low proportions of MCC, as has already been discussed when plotting the density of different mixtures compacted under similar conditions. However, the differences between both scales are reflected by the factors which are significant only for the Mini-Pactor®. The roll speed and the gap-MCC interaction show a significant inverse effect only for the small scale, as well as the combination of gap and SCF with a direct relationship. In other words, the compaction in both scales is influenced by different factors.

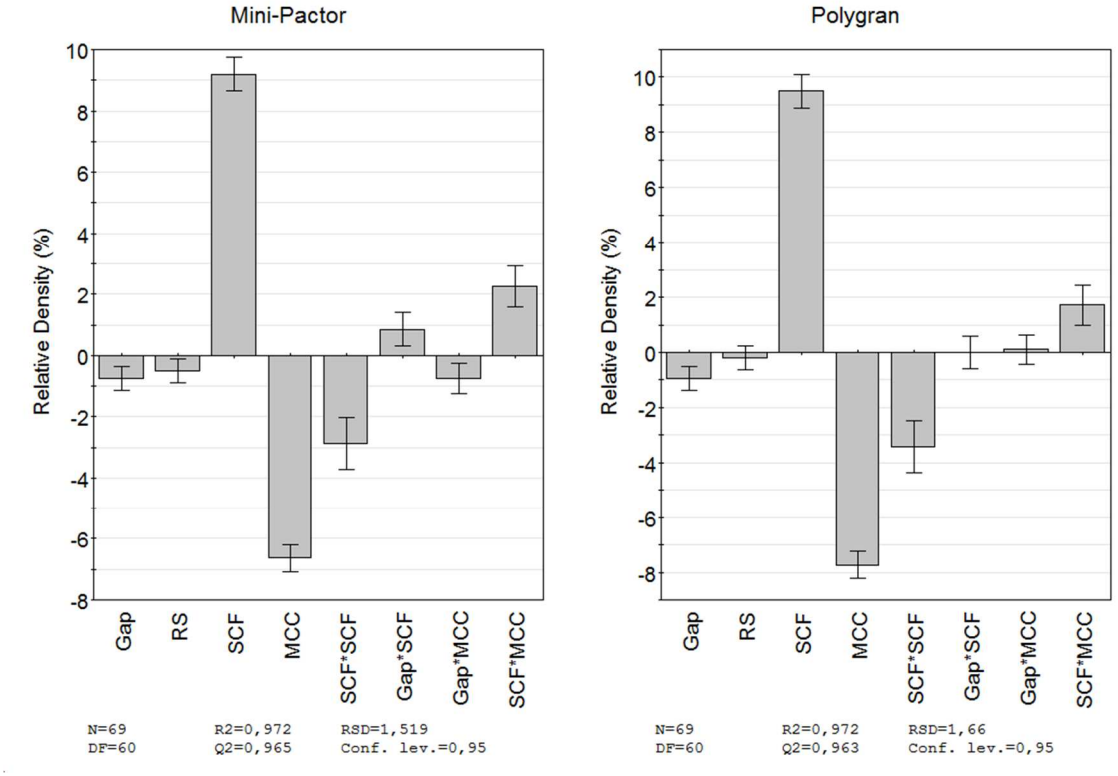

Figure 29: Relative density coefficient plots for the second modification of the DOE including the proportion of MCC as a factor (MLR).

In order to visually explain the interaction between SCF and MCC, contour plots for the Mini-Pactor® and the Polygran® were prepared and presented in Figure 30. These representations allow better understanding of how the factors relate to each other. As can be seen, although the pattern looks linear for low SCF, when reaching high values of force, the relative density tends to increase to a minor extent in respect to the proportion of MCC. This

means that higher values of relative density can only be achieved with high SCFs and low fractions of MCC. For both compactors, a slightly different pattern is observed.

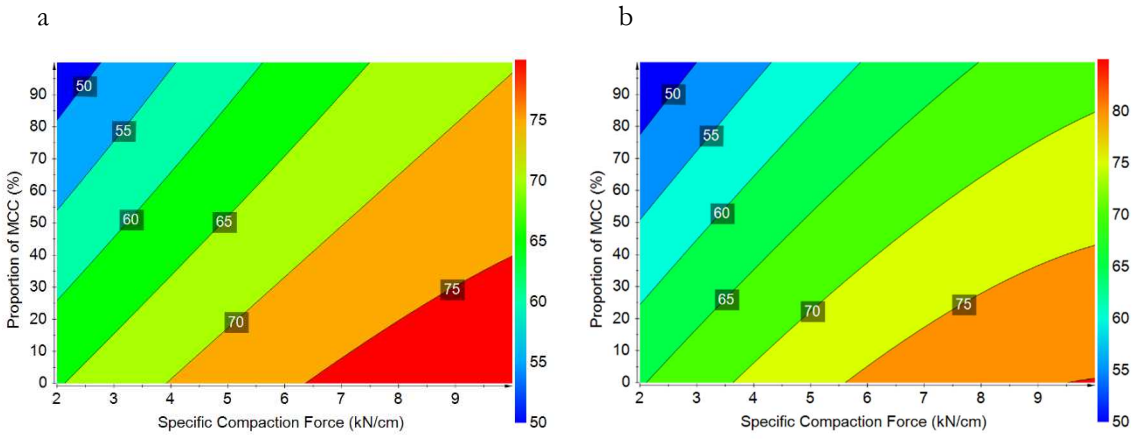

Figure 30: Response contour plots for relative density including the proportion of MCC and SCF for the Mini-Pactor® (a) and the Polygran® (b) for roll speed of 3 rpm and gap of 2.25 mm (MLR).

Finally, a last DOE was prepared, in this case, including both scale and MCC proportion as factors. As it has been already seen, diverse DOEs provide different information, and that is the reason why the evaluation of a complete DOE is also interesting.

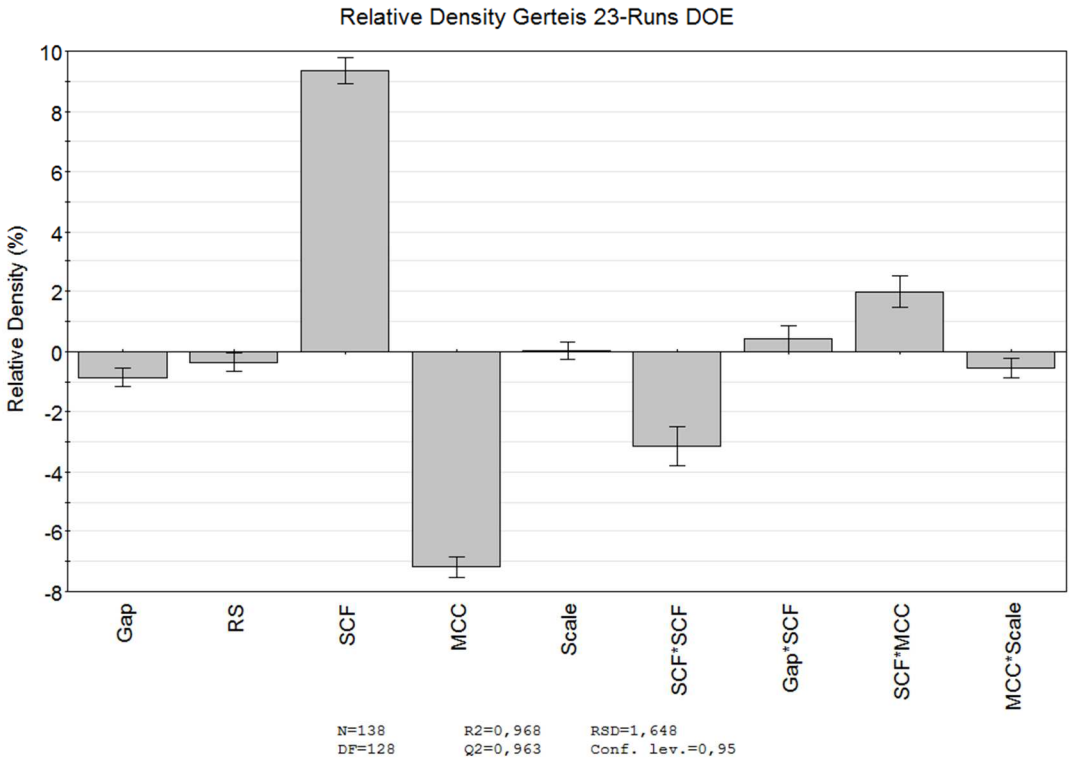

Figure 31: Relative density coefficient plot for the third modification of the DOE including the proportion of MCC as a factor (MLR).

The coefficient plot for this last DOE modification was prepared in Figure 31, which gives a general overview of the compaction of different materials under a broad range of process conditions. The R^2 value (0.968) is again high. The SCF and the interactions gap-SCF and SCF-MCC have a direct influence on the relative density, while the gap, roll speed, MCC, quadratic effect of the SCF and the interaction MCC-scale are inversely significant. In general, this means that the higher the SCF, the lower the gap, roll speed, and proportion of MCC, the denser the ribbons. The scale by itself is not significant, however, it can be seen its importance as part of its interaction with the proportion of MCC, meaning that the combination of certain proportions of MCC with the change of scale, are significant. This has already been observed in Figure 28 (page 76) with the lack of significance of the scale factor only for MCC.

The contour plot in Figure 32 shows the influence of the proportion of MCC and the scale, expressed as roll width. This plot gives the prediction of the relative density depending on those factors for fix conditions corresponding to the centre point. The density would change by approximately 62% and 74% with the MCC percentage. Although the interaction between scale and MCC was proven to be significant, as the lines are almost parallel, it can be call into question whether it would be relevant from a practical point of view, especially in the next products, i.e. granules and tablets. Keeping this in mind but, as discussed, focusing on the significance of the effect, it could be also affirmed, that MCC has a greater effect on the relative density on the larger scale than on the smaller one. This is defined by the separation between the lines that are slightly larger at lower values of roll width.

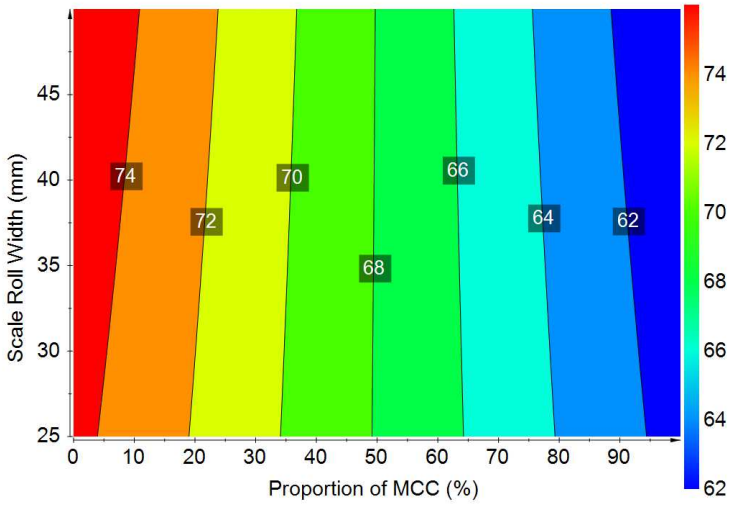

Figure 32: Response contour plot for relative density including the proportion of MCC and the scale on the axes for the centre point conditions of 6 kN/cm of SCF, 2.25 mm gap and 3 rpm roll speed (MLR).

In a recent publication, Allesø et al. 2016 plotted the porosity of the ribbons produced with the same material and under the same conditions in the Mini-Pactor® (small-scale compactor) against the Macro-Pactor® (large scale). An excellent correlation was found, meaning a successful direct scale-up, i.e. setting the same production conditions leads to the same product properties on both scales. Ideally, the correlation should have a slope equal to 1 and a Y-intercept of 0 in order to obtain the same relative density in both scales for the same conditions. However, the slope and Y-intercept found by these authors deviated slightly from those values. Independent of that, this type of correlation was also obtained for the relative density data collected in the present thesis and depicted in Figure 33. The average ribbon density was plotted together with the standard deviation as well as the equations of the best fit lines and the corresponding r value. As there are 3 repetitions of the centre point, the average was calculated, meaning that 21 points instead of 23 are used for the representation.

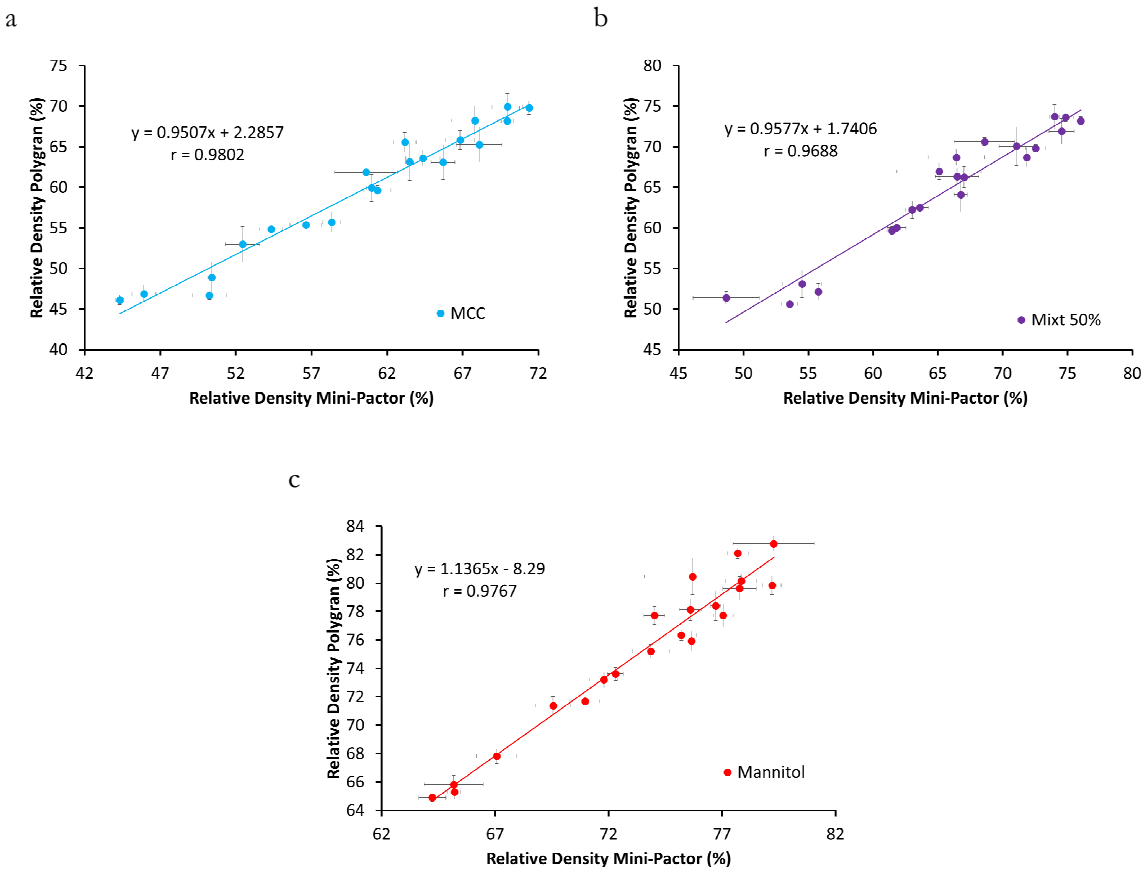

Figure 33: Correlation for relative density of ribbons produced at the same manufacturing conditions between the Polygran® in the Y-axis and the Mini-Pactor® in the X-axis for MCC (a), the 50% mixture (b) and mannitol (c). The best fit line equation and the correlation coefficient are also presented, mean±s (n = 3).

For all cases presented, an r value higher than 0.9 is obtained. There is no clear relationship between the quality of the correlation and the material composition, as for this complete dataset, the value of the coefficient does not decrease or increase proportional with the percentage of MCC. Good correlations are obtained, and in all cases, they overcome by far the tabulated value of 0.652 (for $\alpha < 0.1\%$ and 20 degrees of freedom). However, on the one hand, the standard deviations are in some occasions relatively high, and on the other hand, these results are poorer in comparison to the excellent correlation obtained by Allesø et al. 2016. A possible explanation of the differences between their study and the present work may be the number of points considered. In the current evaluation, 21 points were taken into account, while these researchers considered 5 instead. Nevertheless, if the equation of the best fit line is evaluated, the slope for all cases is close to the ideal value of 1, as the authors also obtained, but the Y-intercept overcomes by far the 0 (between 1.7 and 8.3), while they found a 2.3 value. In this sense, the best correlation would be the one obtained for the mixture as it combines a high r value, with a slope of almost 1 and the Y-intercept is the lowest out of all the ones obtained. In conclusion, these correlations, although good, are not perfect, as they are still far from the ideal situation, and thus, the scale has an effect.

A deeper study can be done by performing an F and t-test for an $\alpha = 0.05$ and $n = 3$ (the 3 measurements on the GeoPyc®). Firstly, the F test is applied in order to see if the variances obtained for the 3 measurements of each batch are statistically equal or unequal for both scales. After this first classification, the corresponding one-tail t-test is applied. Although this evaluation was carried out for all batches, an unclear pattern was identified, and statistically equal and unequal densities between both scales were found. Therefore, only the results for average of the 3 repetitions of the centre point would be considered. For these conditions and all materials compacted, the ribbon relative densities obtained in both scales resulted in values statistically equal.

With the objective of concluding this first study, mostly focused on the change in scale together with the effect of process parameters, a representation of the variation in relative density depending on the SCF for fix conditions of gap and roll speed was prepared and plotted in Figure 34. The idea of these graphs is to try to identify if there is a general trend when the SCF, which is the most important factors affecting the density, varies for constant conditions of gap and roll speed.

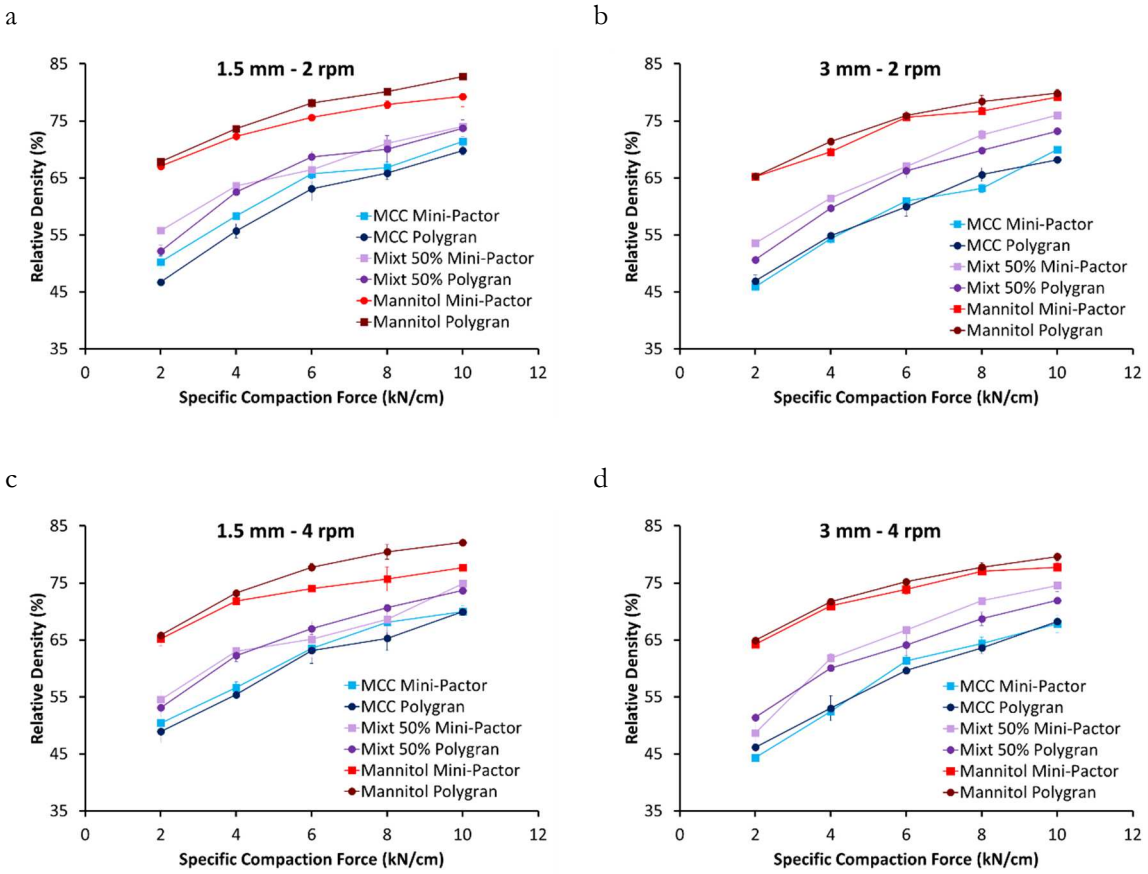

Figure 34: Representation of the ribbon relative density against different SCFs for different materials and compactors when producing under constant conditions of gap width and roll speed: 1.5 mm and 2 rpm (a), 3 mm and 2 rpm (b) 1.5 mm and 4 rpm (c) and 3 mm and 4 rpm (d), mean±s (n = 3).

As expected to a greater or lesser extent, the relative density always increases when rising the SCF. When comparing the same compactor, the first conclusion is that the density always decreases with the increase in the proportion of MCC, a fact already observed in previous data analysis. If the scale is taken into consideration and both lines are compared, in most of the cases, the curves are similar. Actually, for the same conditions, differences not higher than 4.8% has been found for the same material between both compactors. Furthermore, the error bars are normally lower than 3.0%, value overcome in just two occasions. Nevertheless, if a deeper analysis were to be performed, some patterns could be observed. Some batches of MCC and the mixture reach similar or close values when compacting using 1.5 mm gap. This can be observed in the graphs (a and c), where the distances between the MCC lines and the mixture curves are shorter than when using 3 mm. When considering only the scale, it can be concluded that the value of mannitol compacted at the Polygran® is always higher than in the small scale. However, for the mixture and pure MCC, in most of the cases, the Mini-Pactor® produces denser ribbons than the Polygran®. In the case

of MCC, the batches whose densities are higher at the large scale, have in common the production with 3 mm gap and the use of low (2 and 4 kN/cm) or high SCFs (8 or 10 kN/cm), i.e. no intermediate forces. For the mixture, a similar pattern can be identified. The batches with densities higher for the Polygran® are those produced with intermediate-high forces (6 and/or 8 kN/cm) with 1.5 mm gap. However, a small exception occurs for the 2 kN/cm compacted at 3 mm gap and 4 rpm roll speed. Nevertheless, this discussion has been made without bearing in mind the results of the F and t-test, and thus, in some occasions the differences are almost imperceptible and the batches are considered as statistically equal.

The main conclusion that can be taken from this first section regarding the scale-up of the batches considered, is the need of adapting the production conditions in order to reach a target ribbon density while changing the scale. However, these are not the desired results. Gerteis develops its compactors based on different approaches which can permit scaling-up the process directly or at least facilitating the transfer between scales. In this manner, the objective of this provider is that setting the same conditions in both scales leads to same ribbon properties, and it has been proven that this is not always the case.

4.2.2.2.2.2. MIXTURES

In this section, the effect of the scale is investigated in combination with the material composition. The results already presented in the previous section for the 11-runs DOE are considered together with the equivalent ones obtained for the 15, 30, 70 and 85% mixture that was compacted following this same design. In Table 7, the average of the ribbon relative density is presented only for the mixtures mentioned (for the main material, please go back to Table 6, page 73). If again the criterion of relative density values between 60 and 80% is taken into consideration, all ribbons produced from 15 and 30% MCC at both scales are in this range. However, those produced with 4 kN/cm for the 70 and 85% mixtures are under the 60%, with the exception of one batch of 70% compacted at the Polygran® under 1.5 mm and 2 rpm. In this manner, in general, the low limit for producing ribbons which result in good-quality granules and tablets will be 50% MCC, and if higher percentages have to be used, then the minimum force that should be set is 6 kN/cm in order to obtain densities higher than this 60% value.

Table 7: Average ribbon relative density values for the mixtures compacted under the conditions of the 11-runs DOE (n = 3) together with the production conditions for the Gerteis compactors. Please note that the mixtures are just named as the percentage of MCC.

CONDITIONS			**AVERAGE RELATIVE DENSITY (%)**							
SCF (kN/cm)	**GAP (mm)**	**RS (rpm)**	**15% MP**	**15% PG**	**30% MP**	**30% PG**	**70% MP**	**70% PG**	**85% MP**	**85% PG**
4	1.5	2	67.8	71.4	66.4	66.6	59.0	61.2	57.3	58.2
4	3	2	67.1	67.7	65.1	63.2	59.1	58.3	56.0	56.7
4	1.5	4	66.4	69.5	61.4	65.0	57.6	58.6	56.2	57.8
4	3	4	67.4	67.2	64.7	62.7	58.6	57.6	56.5	56.4
8	1.5	2	72.8	75.2	75.0	75.4	69.9	68.2	67.5	70.7
8	3	2	74.3	74.5	72.8	72.4	69.7	69.1	67.9	68.3
8	1.5	4	74.4	76.1	73.9	74.7	67.9	68.3	68.4	67.0
8	3	4	73.8	74.9	72.6	72.1	69.1	68.6	66.2	67.1
6	2.25	3	73.5	71.4	67.6	69.8	65.6	66.1	63.7	62.9
6	2.25	3	72.8	72.2	69.4	69.6	63.8	64.5	63.1	60.0
6	2.25	3	71.7	75.1	67.0	70.1	64.8	65.6	60.7	62.7

In the literature, Dalziel et al. 2013 performed a study in which several levels of SCF (3, 5, 7, 10 and 15 kN/cm) were investigated. An API formulation containing almost a 70% of MCC was compacted at the Macro-Pactor® under constant conditions of 2 mm gap width (for one particular batch 3 mm) and 3 rpm of roll speed. A linear correlation between SCF and ribbon relative density was found. The densities obtained by these researchers cannot be compared to those found in the present thesis due to formulation composition, compactor and conditions used to the production of the samples. Nevertheless, in order to have an idea, the values in this study were 60.6, 61.8, 71.3, 73.7 and 83.5% (for the latter, the gap was increased to 3 mm), meaning that for the 70% mixture values in good agreement with those were obtained.

In order to have a first impression of the material effect together with the scale, the global mean of the relative density obtained for the centre point conditions was plotted against the proportion of MCC in Figure 35. In general, the value changes from a minimum of 60.6%

to a maximum of 76.3% for all materials and scales. Depending on the MCC fraction, the value of the Mini-Pactor® is larger than the one for the Polygran®, although the values are statistically equal on both scales according to the F and t-test ($\alpha = 0.05$). However, the clearest fact that can be extracted from this graph is the tendency to decrease the relative density with the increase of the proportion of MCC. If the best fit lines are calculated, both the r and slope values are similar for both scales. The correlation coefficient is equal to -0.9813 for the Mini-Pactor® and to -0.9796 for the Polygran®. The slopes have for both cases almost the same value, -0.140 for the Mini-Pactor® and -0.145 for the Polygran®. Furthermore, if the t-test for the trend of the line is performed for an $\alpha < 0.1\%$ and 6 degrees of freedom (n = 7), the tabulated t-test value is 0.925, and thus, the tendency of both lines is statistically significant.

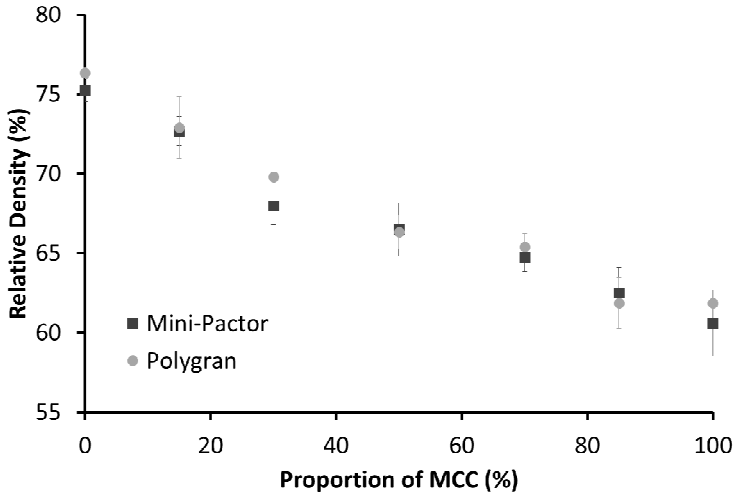

Figure 35: Relative density for all the mixtures for the centre point conditions comparing the two scales of Gerteis supplier, mean±s (n = 3).

As was the case of the previous section, several statistical analyses have been performed. First of all, the original DOE was individually studied for the different combinations of materials and compactors. All models have R^2 which overcome the 0.78 value. All of them have in common the SCF as a directly significant factor. However, for most of the models, only this factor was identified as significant. For mannitol, 30% and 50% mixtures compacted at the Polygran® and MCC at the Mini-Pactor®, the gap was found as indirect significant factor. Finally, and only for the case of the 50% mixture produced at the Mini-Pactor®, the interaction between SCF and gap was also proportionally significant. At this point, some differences between scales can be appreciated through the different coefficient plots obtained for the same material. For this reason, a first modification of the original 11-runs DOE was performed by including again the scale as a factor. The coefficient plot

corresponding to this analysis is collected in Figure 36. All the models present high values of R^2, being the lower one 0.873 for the mixture of 15% MCC.

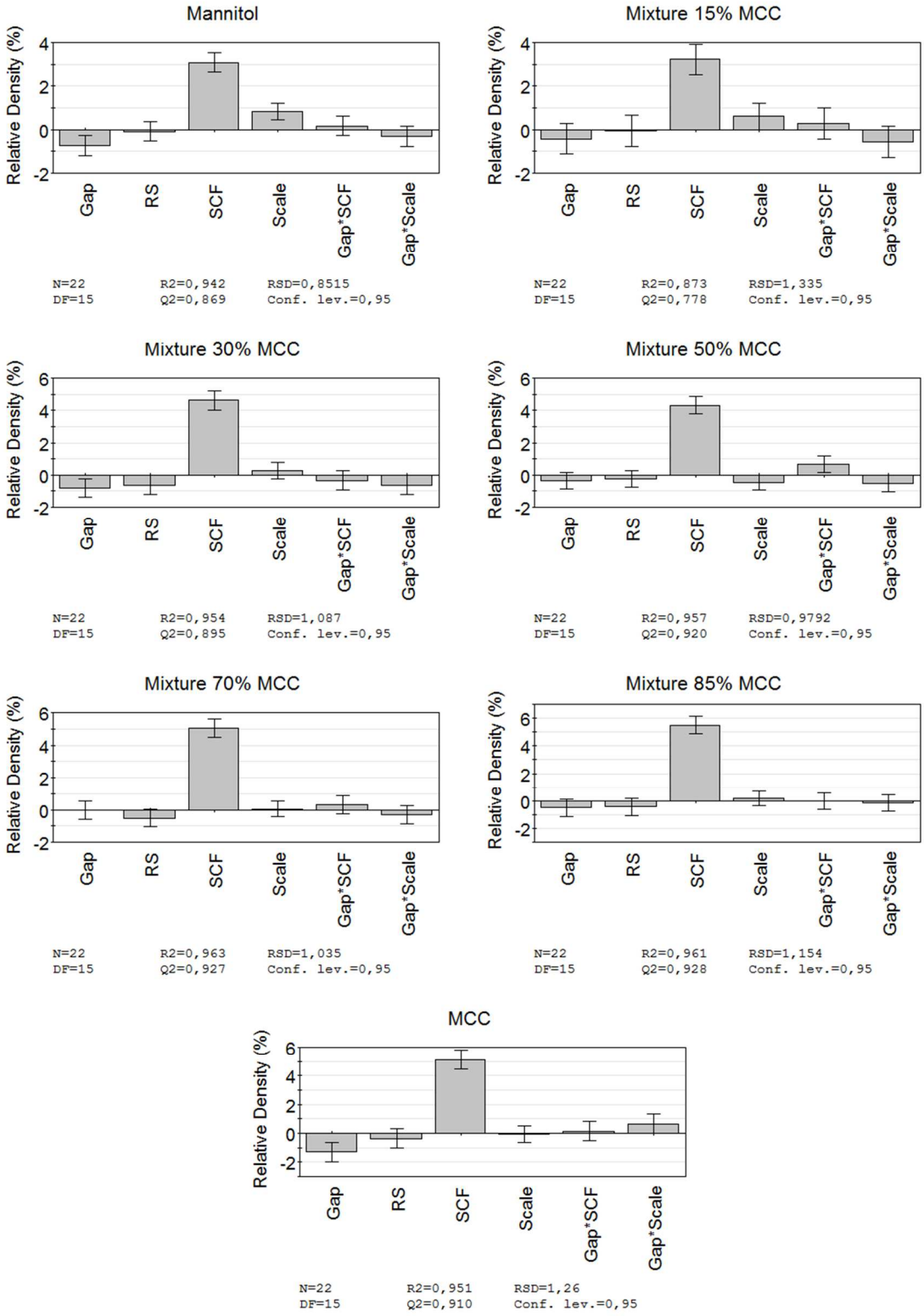

Figure 36: Relative density coefficient plots for the first modification of the DOE including the scale as a factor (MLR).

The models become now more complex than before. The SCF is again the most important factor with a direct influence for all the materials. Gap has an inverse effect only for the pure materials and the 30% mixture, and for the latter, roll speed is also indirectly significant although it is on the limit. Similar case occurs with the interactions. The combination of gap and SCF is only proportionally significant for the 50% mixture and the gap-scale for the 30% mixture. As it was the case of the roll speed, the significance is not pronounced. Regarding the most interesting factor for this study, the scale is only significant with a direct influence for mannitol while for the 50% mixture with the opposite effect, as also observed in the previous section (Figure 28, page 76). In this sense, the impact of the scale has not a clear relationship with the proportion of MCC, i.e. the direction of the influence does not evolve with the proportion of MCC. Finally, and although the scale as a factor shown no significant effect, its interaction with the gap for the 30% mixture and MCC did, meaning that these blends are also affected by the change in scale.

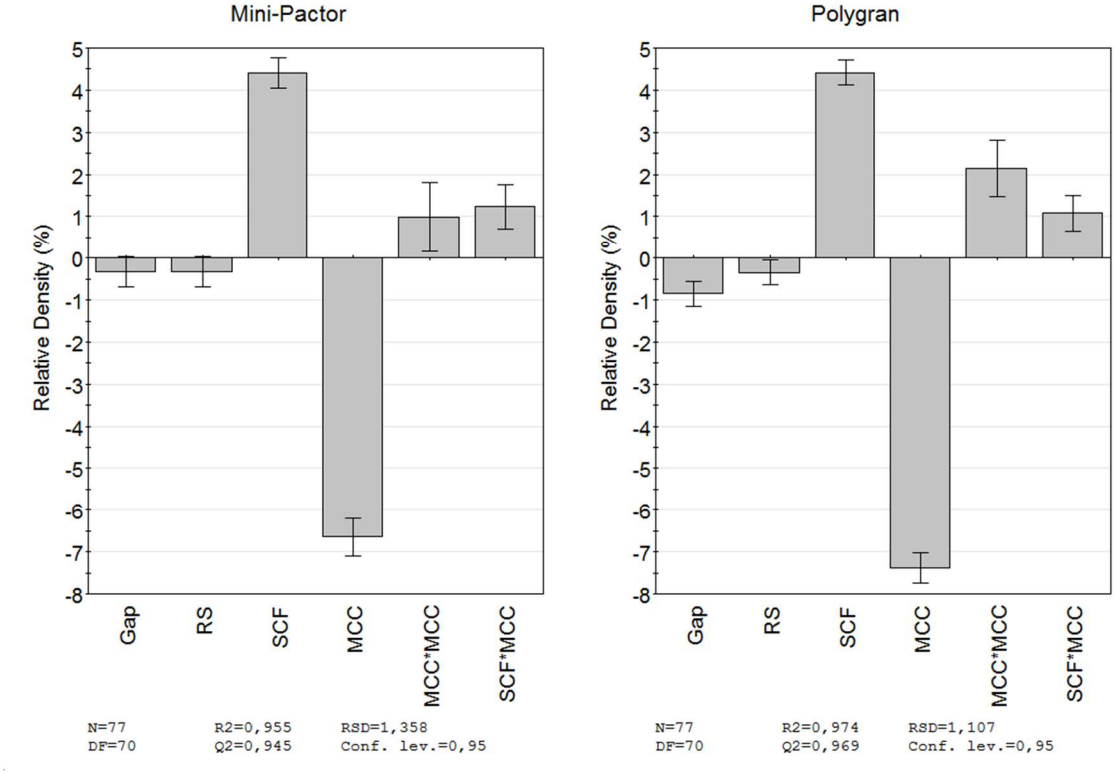

Figure 37: Relative density coefficient plots for the second modification of the DOE including the proportion of MCC as a factor (MLR).

Continuing with the statistical evaluation, a new modification of the original DOE was performed with the inclusion of the material as a factor. As there are a total of 7 mixtures, the proportion of MCC can be included also as a quadratic effect. The corresponding coefficient

plot is collected in Figure 37. The models obtained show a high R^2 value which overcomes the 0.95 for both cases. As it was the case of the same DOE investigation performed in the previous part, this version allows indirectly for the studying of the scale by considering the differences in both compactors. The SCF is having, as always, a direct effect on the relative density for both compactors. However, in this occasion, the inverse impact of the proportion of MCC shows the most important influence on the ribbon density for both machines, although it is slightly higher for Polygran® than for the Mini-Pactor®. This means that the relative density depends more on the material or proportion of MCC than on the SCF applied. Furthermore, the quadratic effect of MCC and the interaction SCF-MCC have a direct influence on both scales. Apart from that and only for the Polygran®, the gap and the roll speed have an inverse effect. This fact also gives an idea of the differences between the compaction in one or another machine.

Finally, a last complete analysis was made including both scale and material as factors. This evaluation through its coefficient plot in Figure 38, gives a general overview of the whole process when all the mixtures prepared are compacted. The model obtained shows a 0.964 value of R^2 confirming its consistency.

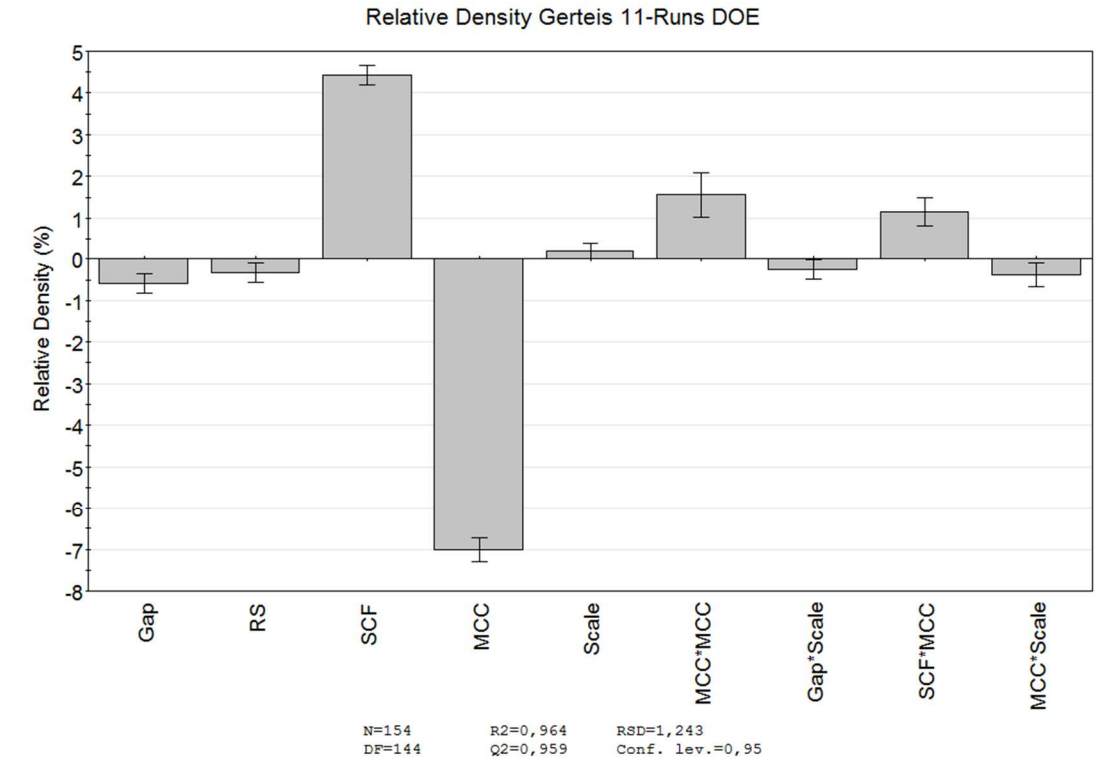

Figure 38: Relative density coefficient plot for the third modification of the DOE including the proportion of MCC as a factor (MLR).

As direct factors affecting the process, SCF, quadratic effect of the proportion of MCC and the interaction between SCF and material can be identified. Inverse factors are the gap, roll speed, proportion of MCC and the interactions gap-scale and MCC-scale. The results are similar to those previously obtained and presented in Figure 31 (page 78), although on this occasion the compactor scale as its own interaction is significant. However, the proportion of MCC shows the greatest impact on the ribbon density, and furthermore this coefficient plot adds the interactions of the scale with the gap and the material as significant. In general, once again it can be concluded that the higher the SCF, the lower the gap, roll speed, and proportion of MCC, the denser the ribbons. Nevertheless, the impact of the scale by its combination with other factors has been again identified as significant, highlighting the problem of scaling-up.

Although the complexity of the process has been confirmed, an example contour plot has been prepared. In Figure 39 the most important factors, SCF and proportion of MCC have been included for a fix gap of 2.25 mm, roll speed of 3 rpm and a potential intermediate scale of 37.5 mm roll width. As can be seen, the density would change between 60 and 75% drawing an exponential profile on the contour plot. This pattern is slightly different than the one observed for the main materials in Figure 30 (page 78).

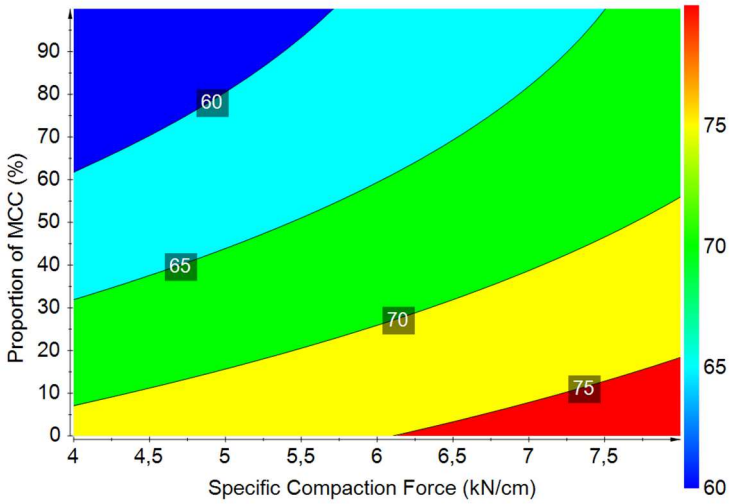

Figure 39: Example of a relative density response contour plot including the proportion of MCC and the SCF on the axes and for constant conditions of 2.25 mm gap, 3 rpm roll speed and a potential compactor with 37.5 mm roll width (MLR).

In order to further investigate the scale-up of the mixtures, the same correlations as prepared in the previous section were again represented. In Figure 40, only those corresponding to the 15, 30, 70 and 85% mixture were presented, as the correlations of the

main materials were already discussed. In general, relatively high values of r are obtained, as all of them overcome the 0.9, however, the large standard deviation proves the lack of adjustment to a straight line. Regarding the slope of the curves, it seems that there is no clear relationship between its value and the percentage of MCC, especially, if the main materials are also considered. For all cases, the slope is close to 1 (for these mixtures the value changes from 0.90 to 0.99), while the Y-intercepts are deviating from 0 with values between 1.2 and 8.6 approximately. In this manner, the best correlation would be the one for the 85% mixture. These results resemble those obtained for the previous correlations (Figure 33, page 80) although no clear relationship between the proportion of MCC and the values for the slope of the different best-fit lines can be established. The t-test can be performed to confirm if the trend of the lines is statistically significant. For an $\alpha < 0.1\%$ and 8 degrees of freedom (9 points) the tabulated value is 0.872 which is overcome by all the graphs, passing then this test.

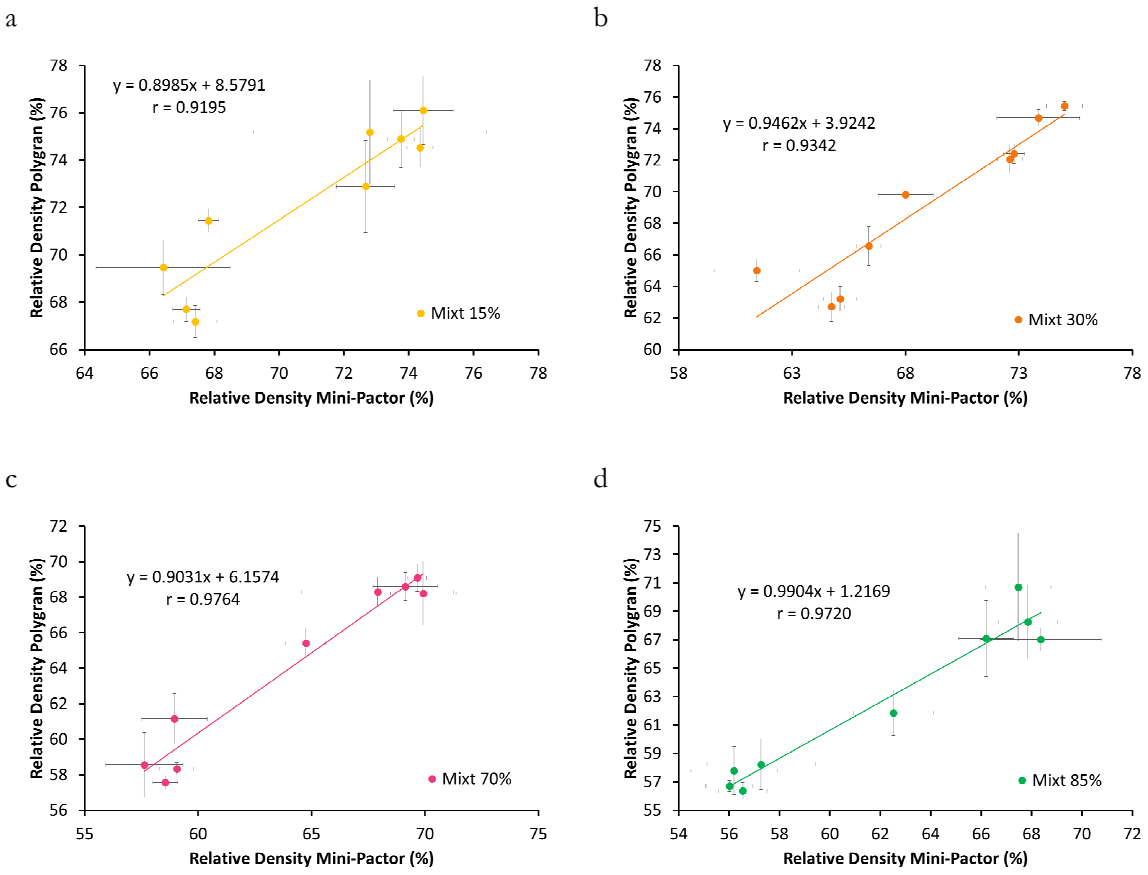

Figure 40: Correlation for relative density of ribbons produced at the same manufacturing conditions between the Polygran® in the Y-axis and the Mini-Pactor® in the X-axis for the mixtures of 15% (a), the 30% (b), the 70% (c) and the 85% MCC (d). The best fit line equation and the correlation coefficient are also presented, mean±s (n = 3).

With the objective of further evaluating each data point, an F and t-test for $\alpha = 0.05$ and $n = 3$ was performed for the complete 11-runs DOE. In this case, for the 70 and 85% mixture, no statistically significant differences were found for any of the batches, what can be considered as a direct scale-up. However, for the 15% and 30% mixture some batches resulted in ribbons with statistically different densities. It could be concluded that for mixtures up to 70% MCC, the scalability is almost direct, although, for MCC some batches are giving statistically unequal densities, and the interaction gap-scale has been identified as significant.

Finally, and in order to conclude this second part of the ribbon density of the Gerteis line, a graph in which the relative density is plotted against the proportion of MCC for different SCFs was prepared. This section has been mainly focused on the effect of the scale as well as the mixture composition, and the representations presented in Figure 41 will give new information about the roll compaction process.

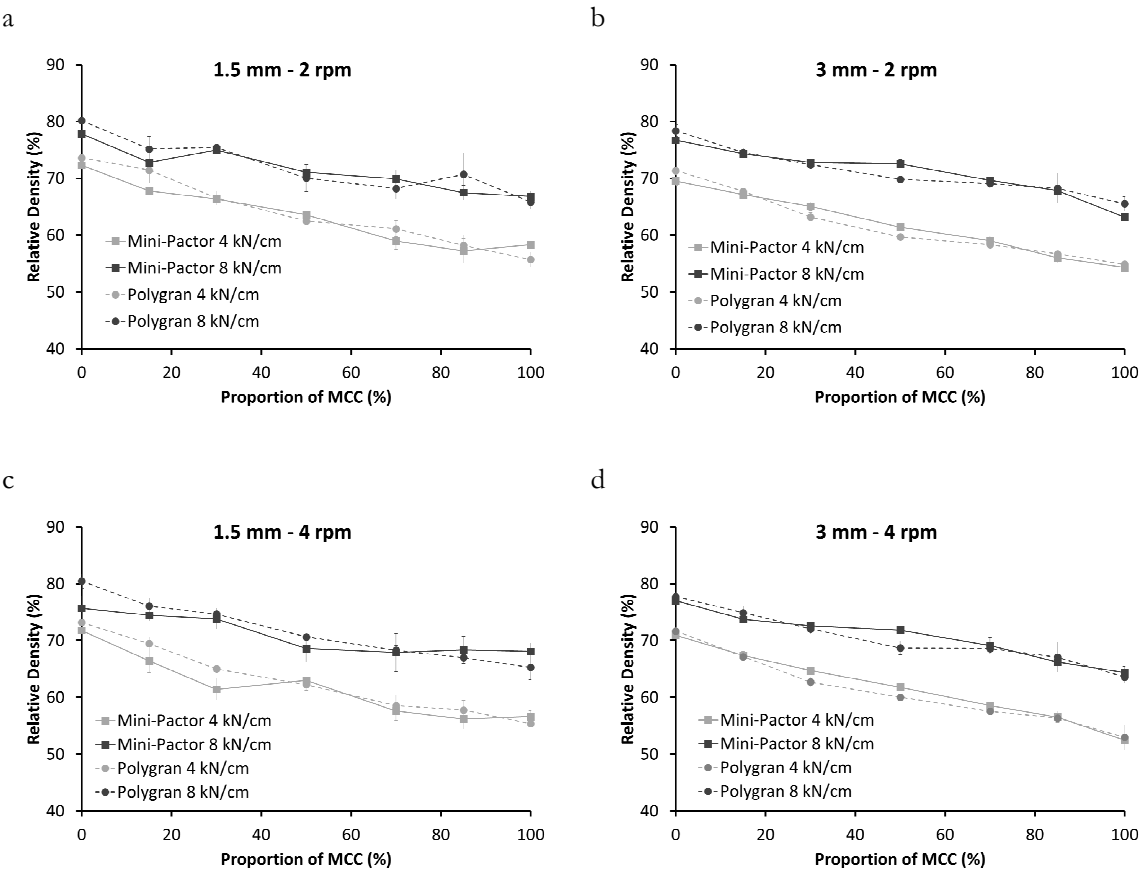

Figure 41: Representation of the ribbon relative density against different proportions of MCC for different SCFs and compactors when producing under constant conditions of gap width and roll speed: 1.5 mm and 2 rpm (a), 3 mm and 2 rpm (b) 1.5 mm and 4 rpm (c) and 3 mm and 4 rpm (d), mean±s (n = 3).

The first conclusion, and as expected, is that the higher the SCF and the lower the MCC fraction, the higher is the relative density value. If a general evaluation is made and similarly to what has been observed in the previous section, the curves are in general leading to similar values for both scales, with differences in percent no greater than 4.8, and with standard deviations of 3.8% as maximum. But, if the data is evaluated further, it can be seen that the relative densities obtained for the ribbons compacted at large gaps seem to present in general higher differences between the densities obtained at lower and higher forces for the same compactor. Similarly, for these conditions, only the 50% mixture for the Mini-Pactor® results, in few occasions, in ribbons denser than those of 70%, altering the linearity of the decrease in density with the increase of the proportion of MCC. Other small exceptions affecting the linear decrease can be found. For the batches compacted at 1.5 mm gap, again the Mini-Pactor® shows some lots with higher density although the proportion of MCC increases, and even some also for the Polygran®, especially in the case of combining the low gap with also slow speeds. If the impact of the scale is taken into consideration, the higher differences are found for the small gaps independent of the SCF used. This may be also justified by the fact that the Polygran® seems to have some problems to properly control such a low gap and some variations during the production may have occurred.

This second part of the study of the relative density of the Gerteis line, ends also up with the main conclusion that the scalability of the roll compaction is not as simple as desired. Nevertheless, some mixtures showed few problems to be scaled. For this reason and due to its importance, most of the following studies will be mainly focused on the named main materials.

4.2.2.2.2.3. TEST REPRODUCIBILITY

In order to prove the reproducibility of the roll compaction process with the Mini-Pactor®, two small tests were performed. The objective was on the one hand to prove the reproducibility of the process itself and on the other hand, the evaluation of not only the compaction but also the mixture composition. Please note, that the repetition of the MCC batch was performed immediately after finalizing the production of the DOE. However, the compaction of the new batches of the 85% mixture was performed with a one year difference in respect to the rest of the DOE and after remixing the blend for a few minutes in order to avoid its segregation.

Table 8: Ribbon relative density values for the repetitions produced for the Mini-Pactor® reproducibility study.

BATCH	ORIGINAL DENSITY (%)	NEW DENSITY (%)
MCC Repetition	52.4	52.1
Mixt 85% Repetition 1	67.5	66.4
Mixt 85% Repetition 2	62.5	62.7

In Table 8 the relative density for the ribbons obtained after repeating the batches is presented together with the initial value measured for the lots produced in first place. If both values are compared, for the 3 batches, the differences are always lower than a 1.1%, being for 2 of the 3 batches 0.2 and 0.3%, and therefore, this confirms the reproducibility of the process when using the Mini-Pactor® for the compaction of not only a pure material but also a binary mixture.

4.2.2.2.3. DENSITY DISTRIBUTION

The results measured with the GeoPyc® give a general overview of the ribbon relative density of a complete batch. As several ribbons and pieces belonging to diverse parts are considered for the measurement, no differences within the ribbon can be addressed. Although the mean relative density is a key property, the density distribution within a ribbon is also highly interesting. Therefore, one centre point ribbon for each scale was selected as representative sample to investigate not only the density distribution within the sample for a compactor, but also in order to compare the profiles when changing the scale. In particular, the ribbons chosen belong to the last repetition of the centre point. In Figure 42 a 3D image of the samples from MCC (a) and mannitol (b) measured using μCT are presented. Although the software sometimes has problems to load such a great amount of information in one image of high quality, this picture permits observation of the aspect of the knurled and laminated surface of the ribbon. Furthermore, the differences in size between both compactors can be also observed in these images. Please note that the calibration tablets included in every measurement and used to transform the grey value into relative density can also be seen in these pictures.

a b

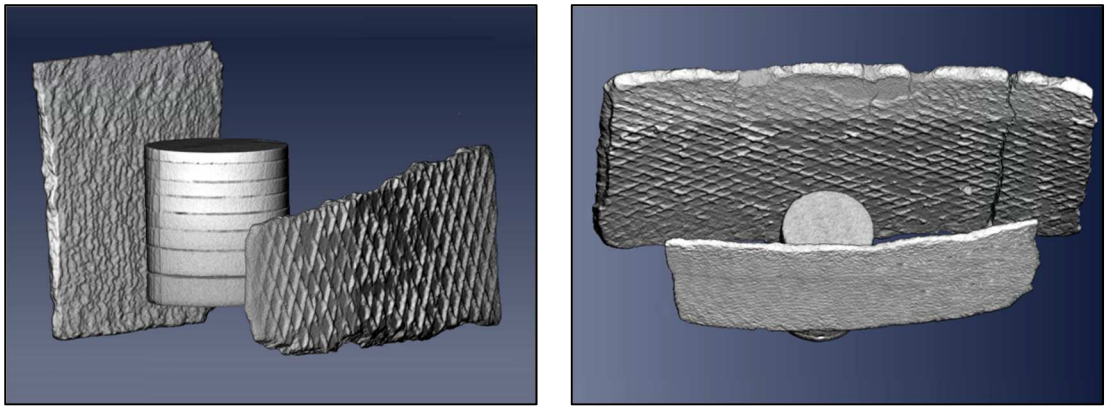

Figure 42: Picture in 3D of the ribbons compacted from MCC (a) and mannitol (b) at both scales of Gerteis compactors analysed using μCT.

Nevertheless, these pictures do not give information about the density distribution within the sample and neither a value in percentage. In order to obtain those, these pictures are cut in different crosswise planes and analysed. These planes are the result of looking at the ribbon from above, so that its width can be observed. In Figure 43, an example cut along the width of the ribbons is presented for MCC (a) and mannitol (b) in colour scale. Please note that the images were edited in order to always keep the large scale ribbon on the left side of the picture and the small scale one on the right part. Although, the colour scale changes for each measurement and therefore, both images cannot be compared, blue and red always represent lower and higher relative density values respectively.

a b

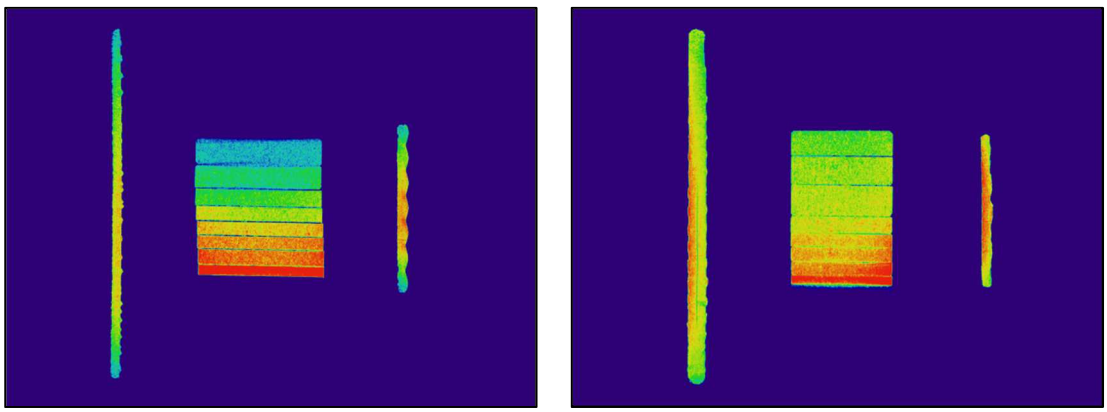

Figure 43: Crosswise cuts in colour of the ribbons from MCC (a) and mannitol (b) compacted at both scales of Gerteis compactors. Please note that the ribbon on the left was produced at the Polygran® and the one on the right at the Mini-Pactor®.

In general, it can be seen how the relative density tends to be higher in the middle than in the edges for both scales and materials. This is due to the use of the cheek plates, which leads to ribbons which are softer on the sides and harder on the centre, while the rim rolls results in ribbons harder on the edges and softer on the middle (Cunningham et al. 2010; Akseli et al. 2011; Nesarikar et al. 2012a; Mazor et al. 2016; Wiedey et al. 2016). In the case of MCC, both ribbons are laminated and the profiles are similar, however it is interesting how for mannitol, only the ribbon produced in the small scale was divided in two pieces while the one compacted with the Polygran® is intact. This latter ribbon seems to have a small lamination inside that does not reach a total separation of both parts, and one of these sides shows higher density. Although both rolls should apply the same force, there seems to be a harder side, that may correspond to the movable roll on which the hydraulic pressure is acting. Furthermore, it is possible that this movement and gravity could also have an effect. Finally, when comparing the density for each pair, it seems that the ribbons produced at the Mini-Pactor® at least for these specific samples and crosswise cuts reach higher values than its equivalent in the large scale. However, if the average relative density obtained on the GeoPyc® would be taken into consideration (Table 6, page 73) it is seen how the values for the last repetition of the centre point are slightly higher in the Polygran® than in the small scale.

In order to know exactly which ranges of densities are presented in the ribbons, the calibration tablets were used to transform the grey values obtained from the analysis of several black and white crosswise cuts like the previous ones into relative density. A minimum of 3 crosswise cuts were used to obtain a density distribution curve along the width of the ribbons. As an example, the correlations between the grey value and the relative density calculated for the calibration tablets for MCC (a) and mannitol (b) are presented in Figure 44. Excellent correlations are obtained with high r values, low standard deviations in general and homogeneous distribution of the points. This means that the equations collected also on the graphs can be used to transform the grey values for the ribbons into relative density. Nevertheless, for the correlation of mannitol, the tablet with the highest density (number 8 in Table 3, page 34) was excluded, as it seemed to have problems to properly correlate to the grey value, not only for this case, but for the other samples analysed. These tablets were used to perform all measurements in other lines, and therefore, these correlations now shown are taken just as an example. Depending on the grey scale the r value can slightly increase or decrease, but excellent correlations are always obtained.

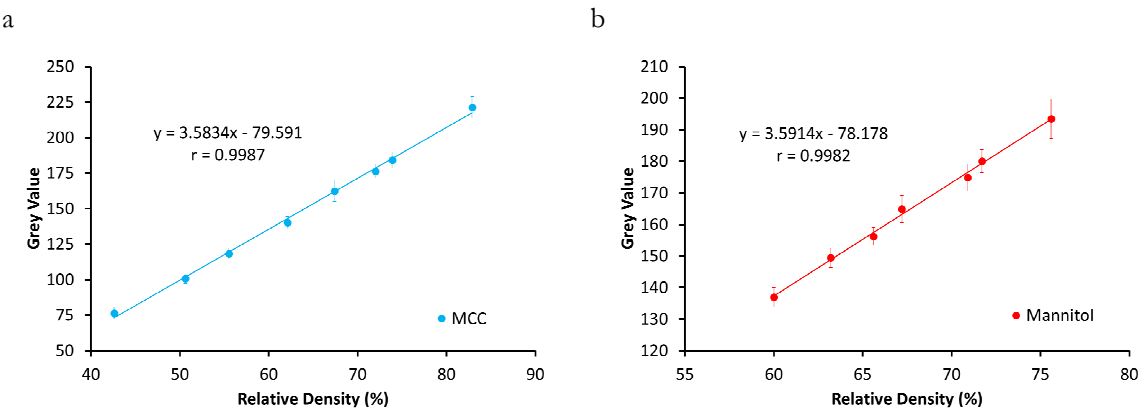

Figure 44: Correlation between the grey value obtained for the tablets and the real relative density calculated used for the treatment of the ribbons from MCC (a) and mannitol (b) compacted at the Gerteis compactors.

In Figure 45 the density distribution for the selected ribbons of MCC and mannitol compacted in the Gerteis machines is depicted. In order to facilitate the visualization of the results, the width of the ribbon was represented with positive and negative values, where 0 corresponds to the middle of the sample. This allows plotting the centre of both ribbons (with different widths) at the same point. These curves, which confirm the profile already observed in the colour crosswise cuts, permit observing the way the values change across the width with high detail. The general tendency is that the density rises from a minimum value on the edges until a maximum in the centre. This increase is not completely symmetric and in the case of MCC at the Mini-Pactor® and mannitol at the Polygran®, a small peak alters the progressive decrease. These differences are probably due to the distribution along the length of the ribbon. Independent of that, both scales lead to similar density distribution profiles.

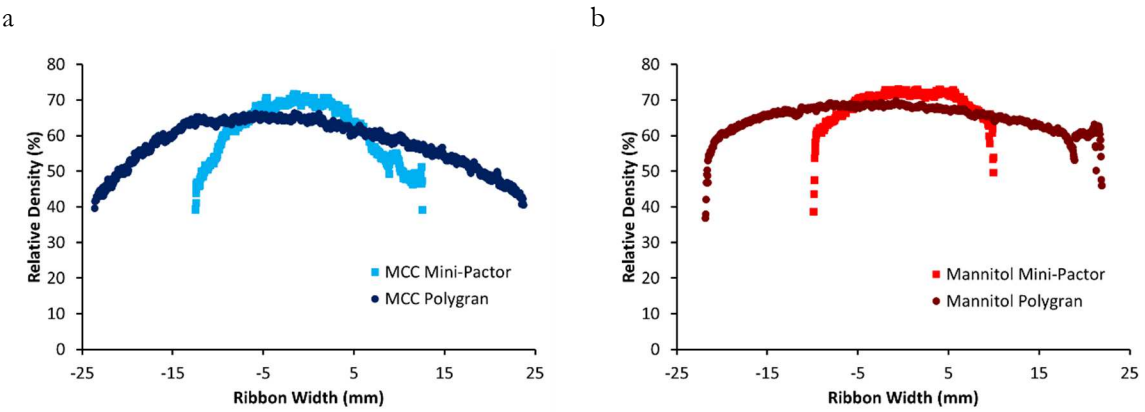

Figure 45: Density distribution along the width of the ribbons from MCC (a) and mannitol (b) compacted at the Mini-Pactor® and the Polygran®, mean ($n \geq 3$).

In the literature, Akseli et al. 2011 investigated the density distribution in MCC ribbons produced with and without lubrication (external or internal) in a Fitzpatrick IR520 assembled with cheek plates. They also found a similar profile of density distribution. Nevertheless, the range in which the densities varied was slightly narrower. For the conditions used (65.9 MPa roll pressure, 2 mm gap and 10 rpm roll speed) and when no lubricant was used, the relative densities changed from a lower value of 53 and 57% in the edges to a 70% in the middle of the ribbon. For the present case of the thesis, the relative density for MCC varies from a minimum of almost 40% for both scales to a maximum of 65% and 70% approximately for the large and small compactor respectively. However, these authors calculated these values considering the dimensions of the ribbons after cutting them in 3 pieces. Recently, Wiedey et al. 2016 investigated the density distribution for several ribbons of MCC compacted at the Mini-Pactor® using μCT, and they observed not only similar profiles for density distribution along the ribbon, but also how when considering the lengthwise plane, the density changes following a spiral, profile also found by other authors but for other compactors and/or materials (Simon et al. 2003; Lim et al. 2011; Souihi et al. 2015a).

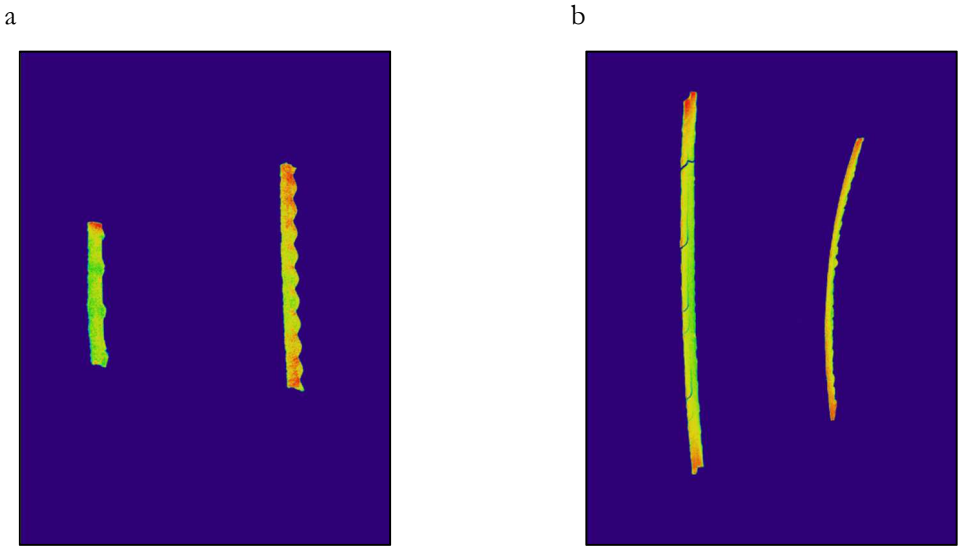

Figure 46: Lengthwise cuts in colour of the ribbons from MCC (a) and mannitol (b) compacted at both scales of Gerteis compactors. Please note that the ribbon on the left was produced at the Polygran® and the one on the right at the Mini-Pactor®.

Therefore, lengthwise colour pictures were taken and collected in Figure 46. As it was the case for crosswise cuts, the large-scale ribbon is always presented on the left side of the picture. As expected, there are differences in the density distribution along the ribbon length for all the samples analysed. However, the density variation is a narrower range than when considering the ribbon width. Furthermore, for the mannitol ribbon compacted at the

Polygran®, the internal lamination that does not end up in two separate pieces can again be seen. In general, the upper and lower edges of the ribbons show higher densities than in the middle. It could be though that some of these differences are due to the changes over the time during the performance of the measurement, as consequence of the hygroscopicity of the material. However, mannitol should not be affected by this fact, and even though, this profile is obtained. Therefore, it could be possible that in these areas are determined by the spiral distribution previously discussed. In this sense, the MCC ribbon compacted at the large scale is too short to show the next harder zone.

If a comparison between the value obtained at the GeoPyc® and the resulting mean of all the densities from the μCT measurement was performed, for most of the cases, some differences would be observed. In principle, it would be expected that the GeoPyc® underestimates the relative density, as the internal pores cannot be measured with this method, and therefore, they are excluded from the value. However, as can be seen in Figure 47, the GeoPyc® leads to higher values than the ones obtained when using μCT. It is important to point out that the standard deviation for μCT is calculated considering the whole curve and therefore, the values are especially high. This also means that depending on the curve, more than 500 points are considered to obtain the standard deviation.

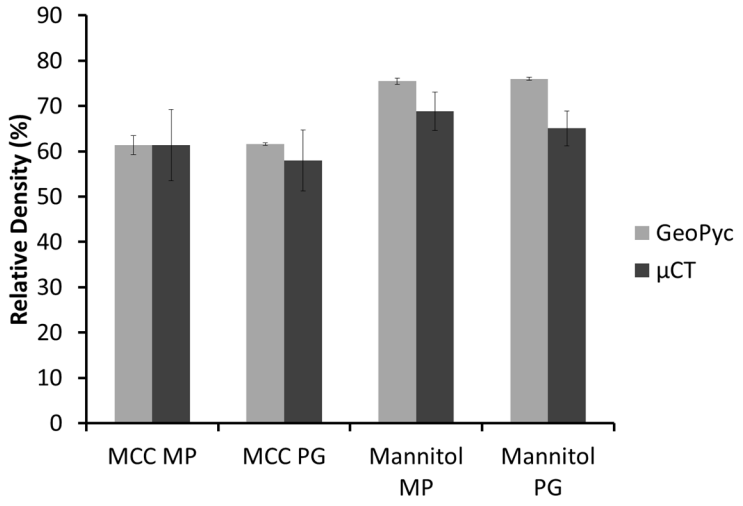

Figure 47: Comparison between the relative density results obtained using the GeoPyc® and the μCT. Please note that MP refers again to the Mini-Pactor® and PG to the Polygran®, mean±s (n ≥ 3).

Up to 11.3% higher values are obtained when using the GeoPyc®, however, it is not clear where these differences are coming from. Although grey values under 50 were excluded from the calculations, this would lead to even lower relative densities for μCT. The lamination and breakage of the ribbons can have also an effect on the values, as the column of pixels

considered to calculate the average would have parts that do not really correspond together. However, this fact would not generate such large differences. Most probably, these variations between both techniques are that the μCT takes only one sample into consideration, while for the GeoPyc®, at least 3 measurements with a minimum of 5 ribbons are analysed. Therefore, the limitation of the μCT is that the results mostly depend on the ribbon sampled, which may not be a representative one, and, as has been also seen, the crosswise planes considered for the density distribution calculations. Although the values differed in comparison to the relative density obtained on the GeoPyc®, it is an excellent tool to learn about density distribution.

4.2.2.2.4. MICROHARDNESS

A large discussion about the microhardness measurement has been made in the previous chapter. The most important conclusion from that study affecting the current one is the fact that all samples which will now be presented have been measured using the called "cross method". The microhardness has been only measured using this method for the mixtures produced at the centre point conditions, and the main materials compacted following the 11-runs DOE. The global HU mean obtained for all mixtures produced at the centre point conditions in both scales are plotted in Figure 48.

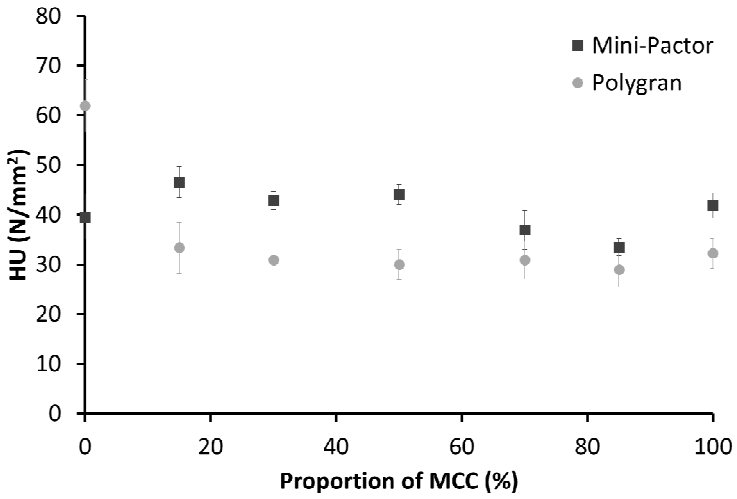

Figure 48: Microhardness for all the mixtures for the centre point conditions comparing the two scales of Gerteis supplier, mean±CI (n = 36, α = 5%).

For this graph, the first main conclusion that can be extracted is that, the HU values are always higher on the Mini-Pactor® than on the Polygran® but for mannitol. It is especially noteworthy the fact that, if the pure mannitol is again ignored, the points follow the same trend for both compactors, although the distance between the small and the large scale can vary.

Nevertheless, a plateau could be identified, especially considering the relative high CI obtained for the present results. These high error bars (with values between 1.7 and 4.5 for the Mini-Pactor® and 3.0 and 5.2 for the Polygran®) may have their origin on the methodology in combination with the density distribution along the ribbon, what probably leads to important differences in HU for small distances on the ribbon surface. These high deviations have been also observed in the work of Wöll 2003. However, no other explanation has been found for the microhardness obtained for mannitol, which is especially remarkable for the Polygran®, as this value is the highest of all the mixtures, and by far. Controversially, maybe the low values of microhardness for mannitol at the Mini-Pactor® could be suspicious, although for brittle materials could be more probable to have lower values (Freitag et al. 2004). But for any of those possible scenarios, no clear reason for those differences has been found.

The HU values for the main materials compacted under the 11-runs DOE conditions were statistically analysed. The coefficient plots were presented in Figure 49. The model fit is in general acceptable, although some of them have R^2 values relative low, even 0.560 is found for the ribbons from mannitol compacted at the Polygran®. This, in combination with the fact that some of the models are affected only by one factor, reduces the trustworthiness thereof.

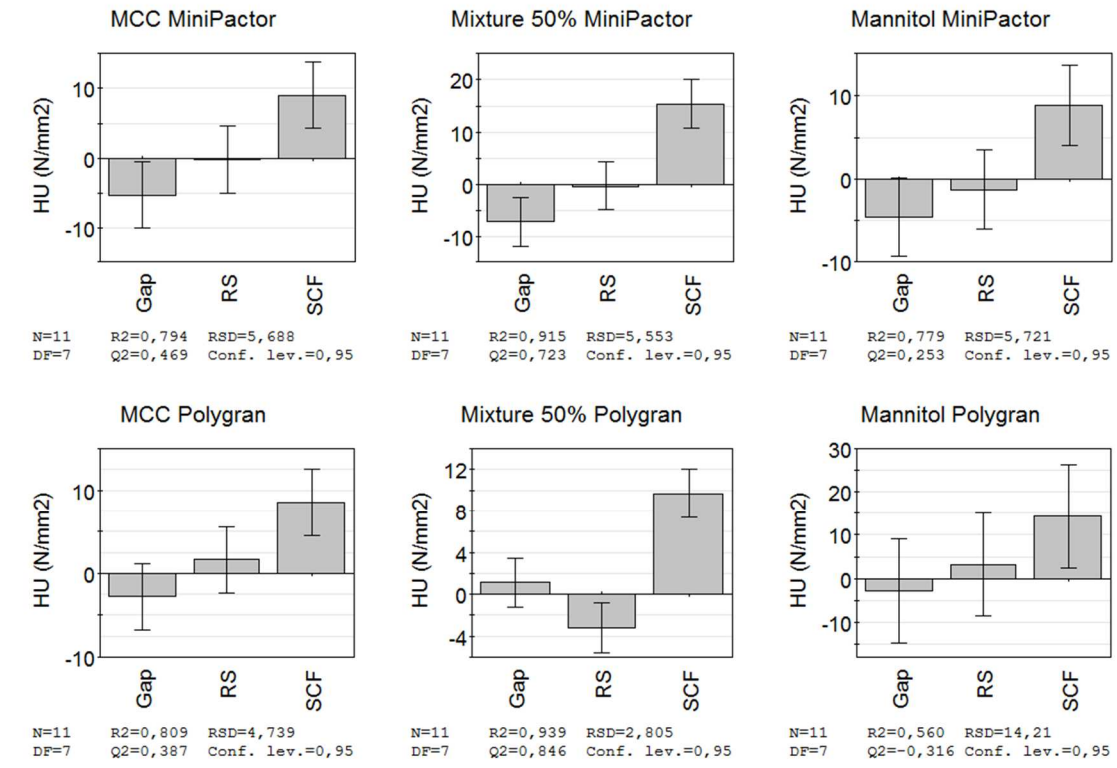

Figure 49: Coefficient plots for the ribbon microhardness analysing every combination of material and scale separately for both scales of Gerteis compactors (MLR).

All models are directly influenced by the SCF, however, the gap is only inversely significant for the MCC and mixture compacted at the Mini-Pactor®. Similarly, the mixture compacted at the Polygran® is also indirectly influenced by the roll speed. From the relative density studies, it has been learnt that in most of the cases, the higher the SCF and the lower the gap and the proportion of MCC, the higher is the relative density, which would lead also to a higher microhardness. However, for the present study, this fact is not clearly reflected in all cases.

A modification of the original DOE was made by including the scale (again represented as roll width) as a factor. This resulted in a new DOE which will allow the study of the scale effect. The corresponding coefficient plot is depicted in Figure 50 and the R^2 values are relatively high, although again the predictability for mannitol is poor.

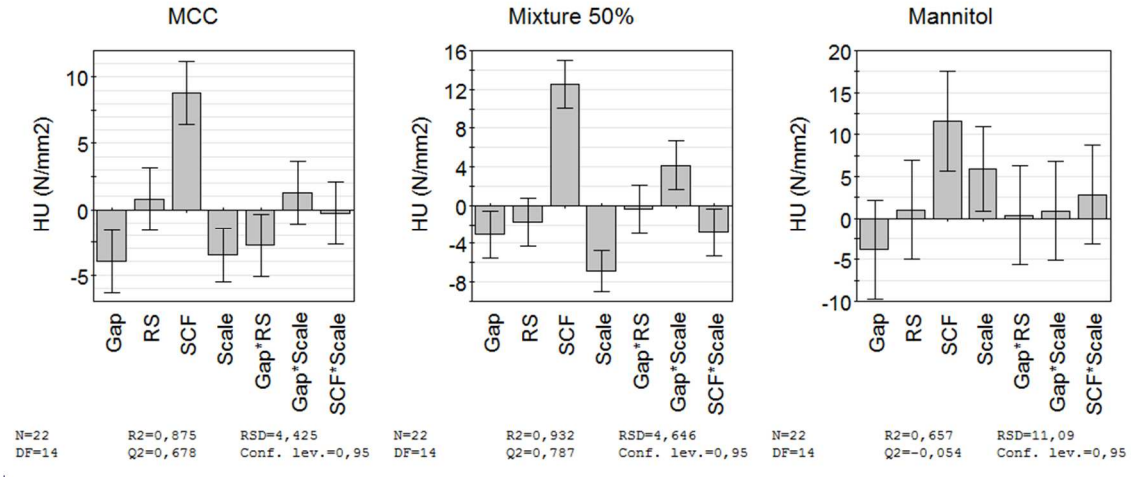

Figure 50: Coefficient plots for the new design including the scale as a factor for both scales of Gerteis compactors (MLR).

From this analysis, it can be seen that the SCF with a direct effect is the only factor common for all the models. The scale itself is also significant for all materials. As it has been observed for the same coefficient plot of the relative density (Figure 28, page 76) the direction of the responses is different for MCC and the mixture than for mannitol. Although for the relative density, the scale was not significant for MCC, for this material as well as for the mixture, the influence was inverse, while for mannitol it was the opposite. For the microhardness, this behaviour is again observed, giving confidence to the results obtained for both properties. Continuing with the discussion for the current coefficient plot, the gap is inversely significant for pure MCC and the mixture. Then, the combination of gap and roll speed is indirectly affecting the microhardness for MCC, while for the mixture the interactions

gap-scale and SCF-scale are proportionally and inversely significant respectively, for the mixture. This stresses the importance of the scale, which seems to have a stronger effect on the microhardness than on the relative density. In any case, those models show difficulties to be clearly interpreted, and the reliability of the results is not clear.

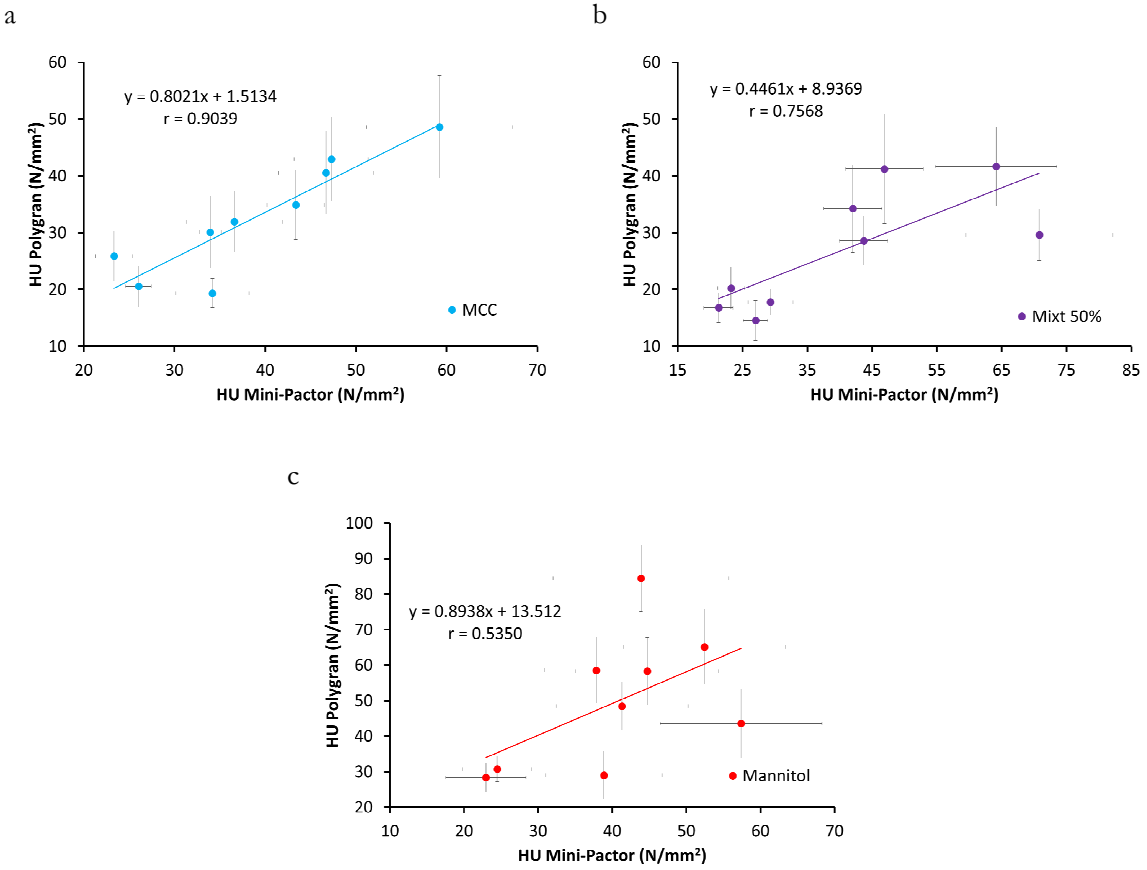

Figure 51: Correlation for microhardness of ribbons produced at the same manufacturing conditions between the Polygran® in the Y-axis and the Mini-Pactor® in the X-axis for MCC (a), the 50% mixture (b) and mannitol (c). The best fit line equation and the correlation coefficient are also presented, mean±CI (n = 36, α = 5%).

Finally, the same type of correlation as the one obtained for the relative density was prepared for the microhardness. The graphs are presented in Figure 51. In general, the correlations are poorer than for the relative density, especially if the CI is considered. The slopes are in general also lower than for the density results, and therefore, further away from 1. Regarding the Y-intercepts, although a 1.5 value is obtained for the pure MCC, the other main materials show larger values (8.9 and 13.5). The r values of the best fit lines decrease with the content of MCC, having this material a value of 0.9039, the mixture 0.7560 and mannitol 0.5350, what means that if the t-test is performed, only MCC would pass it. The t value for an $\alpha < 0.1\%$ and 8 degrees of freedom is 0.872, and thus, the mixture and mannitol are far from

reaching this value. For this reason and considering the slope and Y-intercept, MCC has the best correlation. Nevertheless, the high CI calls into question the quality of the correlation, especially after observing the significance of the change in scale in the DOE evaluation.

In summary, it can be concluded that the microhardness is more strongly affected by the scale than the density. However, and although the reliability of the results obtained is in question, the tendency of them follows the same direction as the relative density.

4.2.2.2.5. CORRELATION RELATIVE DENSITY-MICROHARDNESS

As the results regarding microhardness were difficult to interpret and in order to statistically confirm that they are reliable, a correlation considering the relative density and the HU was prepared. In Figure 52, the correlation between density and HU for the main materials and both scales of Gerteis is presented. One best fit line will be calculated for each material and compactor.

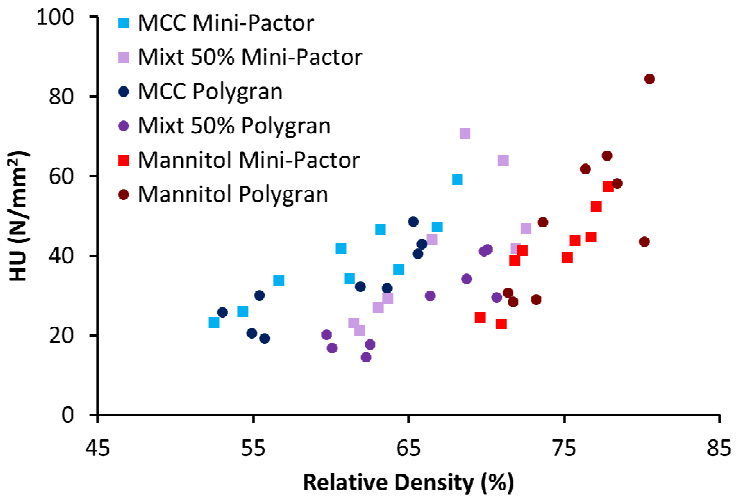

Figure 52: Microhardness results against the relative density for the main materials and both scales of Gerteis compactors, mean (n = 3).

For all correlations a positive slope is obtained, as expected. This means that the higher the relative density, the greater the microhardness value. However, the slope tends to increase with the decrease of the content of MCC. This also means that for mannitol small changes in relative density increase the microhardness in a higher proportion. It has been previously confirmed that both properties are correlated (Wöll 2003; Miguélez-Morán et al. 2009). However, the relationship between both can be different. Wöll 2003 found in his work, that for MCC ribbons compacted at the Mini-Pactor®, an exponential relationship exists between the Martens hardness (another type of microhardness used when the pyramid or the Vickers

indenter is assembled) and the ribbon porosity. Similarly, the same type of relationship was found between this microhardness and the SCF applied, as Freitag et al. 2004 also found for their brittle materials. Miguélez-Morán et al. 2009 used also the microindentation to establish a correlation between the logarithm of the indentation area and the relative density, which for this case was linear. The relative density extrapolated from the microhardness results was in good agreement with the values observed for μCT.

Apart from that, it is interesting to evaluate if the trend of those lines is statistically significant, because this will provide a stronger support to the results of HU. The tabulated value of r for 8 degrees of freedom (9 points) and an $\alpha < 0.1\%$ is 0.872, and considering this coefficient, only for the MCC compacted at the Mini-Pactor®, the mixture at the Polygran® and mannitol at the Mini-Pactor® the trend is statistically significant. However, if the range is decreased to an $\alpha < 1\%$ (99% of confidence), the value falls to a 0.765 which also includes the MCC and mannitol compacted in the Polygran®, only the mixture in the Mini-Pactor® remains out of the acceptance with an $r = 0.753$ which excludes this correlation for a small difference. As the work of Wöll 2003 showed that the relationship between both curves is exponential instead of linear, the R^2 for the exponential curve was calculated and it resulted in a small increase of this value in respect to the one obtained in for linear correlation for MCC at the Mini-Pactor® and the mixture compacted at both scales. However, for mannitol the behaviours seem to be better described by a line. Independent of this last result, it can be concluded that in general, and considering a wider or narrower range of confidence, the relative density and the HU are statistically significantly correlated, which means that although there are difficulties to interpret the results of microhardness, they are still in agreement with those of density.

4.2.2.3. GRANULE CHARACTERIZATION

The granule characterization has been drastically limited after the investigation described in the previous chapter. Nevertheless, in this section, a brief study performed with non-pre-treated ribbons granulated in another miller (Erweka) is collected, and only related to the GSD of the samples.

4.2.2.3.1. GRANULE SIZE DISTRIBUTION

MCC and mannitol ribbons belonging to the centre point were chosen for this small study. The GSD was measured using the Camsizer® XT and the same method as in the previous chapter. In Figure 53, an average q3 curve for the granules of MCC (a) and mannitol (b) produced at the two scales is plotted together with the standard deviation. Actually, these error bars give a fast impression of the reproducibility of this methodology, and, as can be seen in the graph, for the fines higher variabilities are found, probably due to the lack of ribbon pre-treatment before milling.

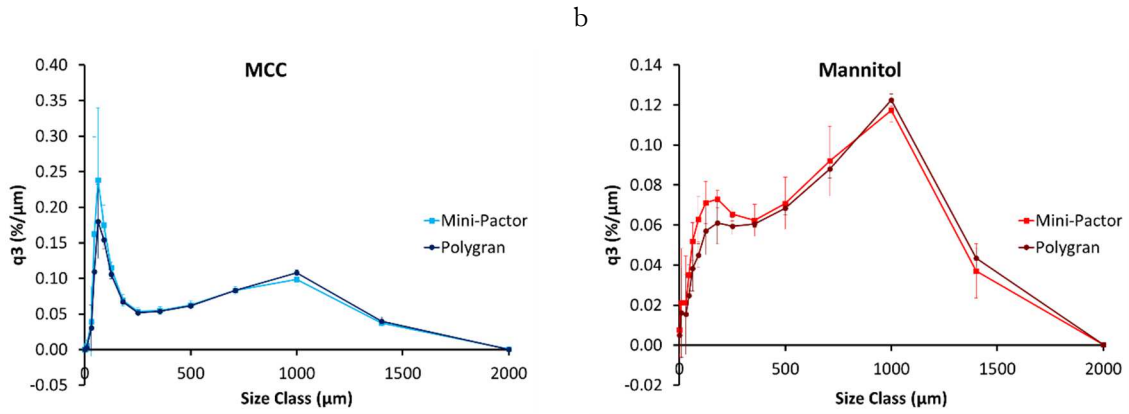

Figure 53: Representation of the curve q3 for MCC (a) and mannitol (b) considering the scale of the Gerteis roll compactor used for their production, mean±s ($n \geq 2$).

The first conclusion that can be extracted, is that after the roll compaction process a notable amount of fines is found, represented by the first peak. However, as the ribbons were not previously cleaned in an effort to mimic a natural compaction, it is not possible to distinguish between uncompacted material originated from the compaction, and fines produced during the milling. If the compactor scales are compared, it can be observed not only that the trend of the curve is similar for both machines (they almost overlap perfectly), but that the amount of small particles, is comparable. Although no remarkable differences in GSD exist between the two scales, the Mini-Pactor® shows a slightly higher amount of fines for both materials. It is in this sector where the higher differences are presented. However, the variations are not that notable. The fines were defined at 180 µm as it is the mean particle size of the mannitol which has bigger starting particles than MCC. This assures that all the uncompacted material is encompassed by this limit. For this value, MCC showed 20.0% in the Mini-Pactor® and 17.0% at the Polygran®, while for mannitol the fraction of uncompacted material was 10.3% and 8.1% for the Mini-Pactor® and the Polygran®, respectively.

A comparison between the Q3 curves of MCC and mannitol for both scales is presented in Figure 54. As the differences between the two scales are not substantial, the both materials were plotted together with the intention of seeing how they behave. From this graph, it is clear that the MCC has higher proportion of fines (up to 200 μm) while mannitol shows a greater amount of larger particles (between 700 and 1000 μm). This fact has been already observed in the preceding chapter. Mannitol ribbons are always denser than those from MCC, and this results in larger granules, as they are more difficult to mill.

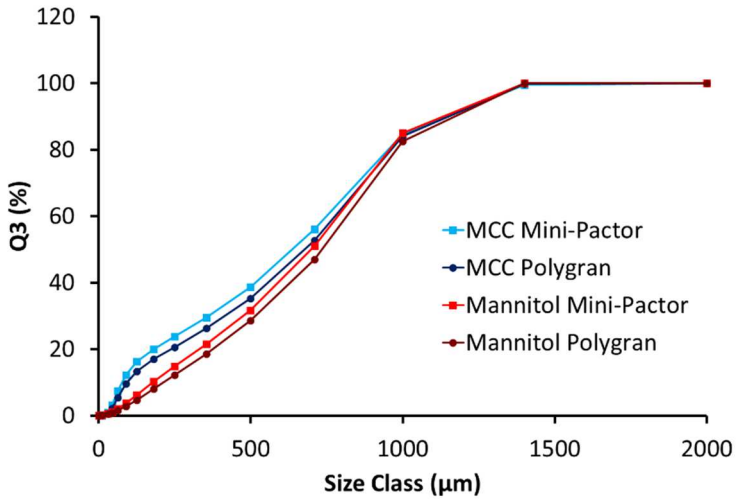

Figure 54: Comparison of the Q3 curve for all the materials and scales, mean ($n \geq 2$).

In general, what can be extracted from these graphs is that the change in scale does not seem to have an effect on the GSD of the granules and even if this could be questionable, the pre-treatment of the ribbons would probably lead to the complete overlapping of the profiles. This is expected, especially if the relative density is taken into account. For the centre point ribbons of MCC and mannitol, no statistically significant differences were found, and this is also reflected in the GSD. The relevance of the relative density on the GSD should be also considered, although a first assessment has been already performed in the section 4.1.4.4. (pages 60 and 61). In Figure 55, a correlation between the relative density and D50 for MCC and mannitol is presented for the ribbons produced at the Polygran® and later milled. This representation considered the 23-runs DOE results for both properties, with an average value for the centre point.

Although the correlations seem to be not highly accurate due to the scattering of the points, if the t-test is performed, both r values overcome the tabulated 0.652 for $\alpha < 0.1\%$ and 20 degrees of freedom. This means that both properties are statistically significantly correlated. This fact was already expected, because, as also described in the literature, harder ribbons are

more difficult to mill and lead to granules with higher amounts of larger particles (Gamble et al. 2010; Samanta et al. 2012; McAuliffe et al. 2015; Freeman et al. 2016; Pérez-Gandarillas et al. 2016). However, it is especially noteworthy that the best correlation is obtained for mannitol. Probably due to the brittle nature of this material, an easier break of the ribbons takes place, leading to broader range of results, as can be also seen in the wider interval of D50 values in comparison to MCC. Independent of that, it can be affirmed that the relative density of the ribbons and the GSD of the granules obtained after milling them are proportionally correlated.

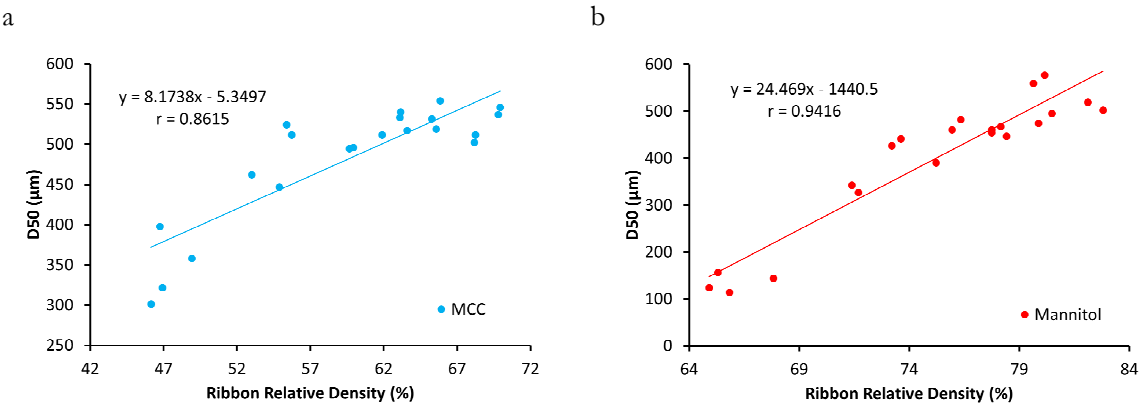

Figure 55: Correlation for the ribbon relative density and the D50 of the granules for MCC (a) and mannitol (b), mean ($n \geq 3$).

In order to investigate this connection more deeply, the coefficient plot of the ribbon relative density and the D50 of the granules measured for the 11-runs DOE for all the mixtures was prepared and presented in Figure 56. This allows for more detailed observation of the factors affecting both responses, the more similar both coefficient plots are, the more related both properties would be. High model fit (R^2 of 0.976 for the relative density and 0.856 for the D50) was obtained. As can be seen, both properties are inversely affected by the gap and proportionally by the SCF and quadratic effect of the MCC. Roll speed and MCC is only inversely significant for the relative density, while the interaction between SCF and the proportion of MCC is directly affecting this property. For D50, this latter interaction has an indirect effect, while MCC and Gap-SCF and Gap-MCC, as well as the percentage of MCC are proportional affecting the percentile. Nevertheless, it has been especially surprising that MCC showed a direct effect while in the previous investigation of the percentiles (Figure 18, page 57) the proportion of MCC had a clear inverse effect. This may be explained by the exclusion of all batches compacted at 2, 6 (but the centre point) and 10 kN/cm, which could have balanced out the effect. However, the differences between both properties in the

direction of the effects do not mean that they are not related, but that they are affected differently. For example, also when the percentiles were investigated in detail in Figure 18, the amount of fines was shown to have the opposite effect of most of the factors in respect to the other percentiles, however, they are related as it is another way to express the GSD.

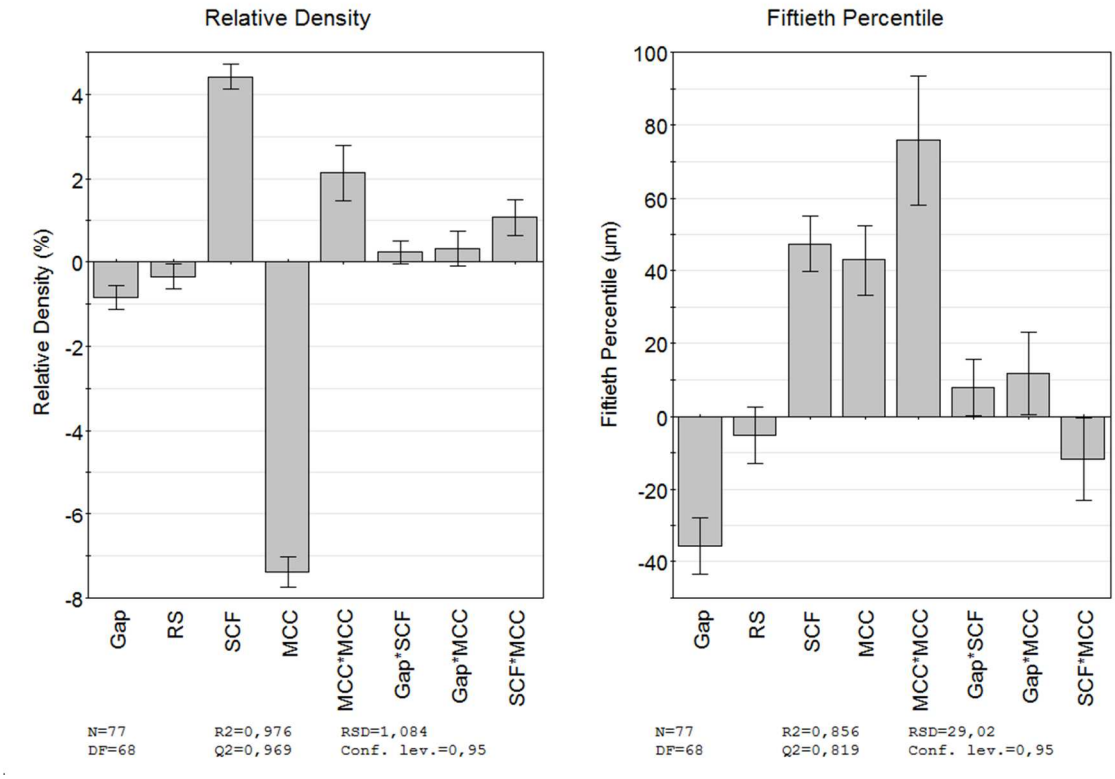

Figure 56: Coefficient plots for the relative density and D50 for the 11-runs DOE performed for all the mixtures at the Polygran® (MLR).

The most important factors, i.e. SCF, gap and MCC affect both relative density and D50. Therefore, it can be in general concluded that both properties are related and thus, the density of the ribbons would determine the properties of the granules obtained after milling, but always when the same granulation conditions are used, as has been also described in the literature (Campbell et al. 2001; Morrison et al. 2007). However, the imperfect correlation and the coefficient plot stress that some other factors affect the properties of the granules apart from the relative density, although this impact is less pronounced.

4.2.3. L.B. BOHLE LINE

The L.B. Bohle scale-up study includes the comparison between the BRC 25 and BRC 100, which are the most modern compactors involved in this thesis, and therefore, especially interesting to investigate. These compactors follow the same scale-up strategy as the Gerteis ones, i.e. the diameter in both scales is the same, while the roll width is changing from scale to scale. Both compactors have 250 mm of roll diameter (as Gerteis machines) and 25 mm roll width for the BRC 25 (small scale) and 100 mm for the BRC 100 (large scale). In particular, the BRC 100 is the largest compactor used in this thesis. Both machines were built up with rim rolls as sealing system and smooth rolls. However, the roll surface for the BRC 25 was pre-treated, giving it a certain roughness, although this aspect will not be addressed during the discussion. For this scale-up study, the DOE was smaller than in the case of the Gerteis line. The 11-runs DOE was performed for the main materials (MCC, mannitol and 50% mixture) and 3 repetitions of the centre point were also run for the other mixtures. In order to produce the latter batches, the machine was set in between under different conditions until a new steady-state was achieved and then, the centre point parameters were re-established. All the experiments described were run in both machines.

4.2.3.1. PROCESS DATA

For both compactors it was possible to collect process data, but only at each 10 seconds approximately. This is especially problematic for the case of the BRC 100, in which, due to the high throughput, collecting 500 g lasts even less than 1 min time.

a

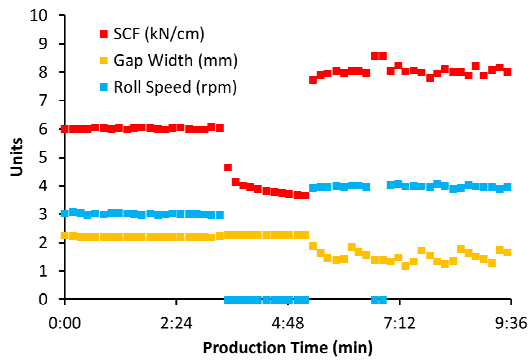

b

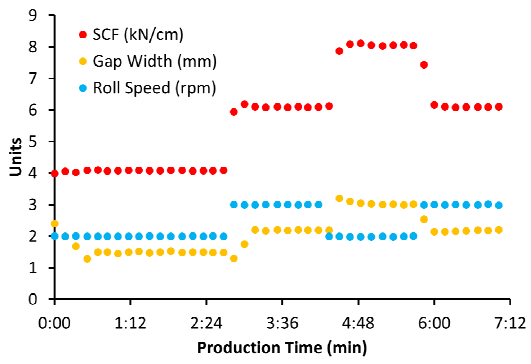

Figure 57: Example graphs for the BRC 25 (a) and BRC 100 (b) in which it can be seen how the SCF, gap width and roll speed evolves during a compaction process.

In Figure 57, an example of the process data for the BRC 25 (a) and the BRC 100 (b) is presented, where the evolution of the SCF, gap and roll speed can be seen. From these graphs, it can be concluded that the BRC 25 seems less stable than the BRC 100. However, it is important to point out, that, as was the case for the Mini-Pactor®, the whole process for several batches is presented in the graphs. In the case of the BRC 25, it is easy to identify when no collection was performed, as it corresponds mostly to the moments in which the roll speed is 0 rpm. Nevertheless, for the BRC 25 some variations on the collection times also happened. For example, the gap width changed during collection from 1.38 to 1.85 mm (for a set value of 1.5 mm), the roll speed between 3.94 to 4.02 rpm (4 rpm were configured) and the SCF for the same batch varies from 7.91 and 8.06 kN/cm (for 8 kN/cm). Although those values are still in an acceptable range, for the BRC 100 better control is obtained, especially for the roll speed and the SCF. For example, the gap width changed from 1.45 to 1.54 mm (for 1.5 mm), the roll speed changed from 2.00 to 2.02 rpm (2 rpm set) and the SCF from 4.07 to 4.10 kN/cm (4 kN/cm desired value). Those are just examples and it is entirely possible that better or worse profiles were obtained. Another important aspect is the rapidness of the machine to achieve the next conditions set. Although, the graphs only give information each 10 seconds, it confirms this fact already observed during the experimental performance. It can be concluded that both compactors have not only a stable process, but also, from the graphs, the fast adaptation to the new conditions set can be seen. Nevertheless, and in comparison to the Mini-Pactor® the process control is slightly poorer.

4.2.3.2. RIBBON CHARACTERIZATION

For this scale-up study, the sample characterization was focused on ribbons. Furthermore, the small investigation in the Gerteis section, showed that the scale has no effect on the GSD when ribbons with similar density are milled, as their properties seem to correlate with those obtained for the granules. Therefore, all efforts were concentrated on density characterization of the ribbons. The microhardness was excluded, not only because of the difficulties for its interpretation, but due to the size of some of the ribbons, which would have been an impediment for the characterization.

4.2.3.2.1. APPEARANCE

Rim rolls were used as a sealing system, whose use leads to ribbons which break into small pieces. In Figure 58, two example pictures of ribbons from both compactors for MCC

(a) and mannitol (b) are presented. Not only can the small pieces of ribbons obtained be noted, but also the differences in size for both scales. In the case of MCC, it was possible to reconstruct a ribbon from the BRC 100, which gives an impression of what the largest ribbons look like.

a b

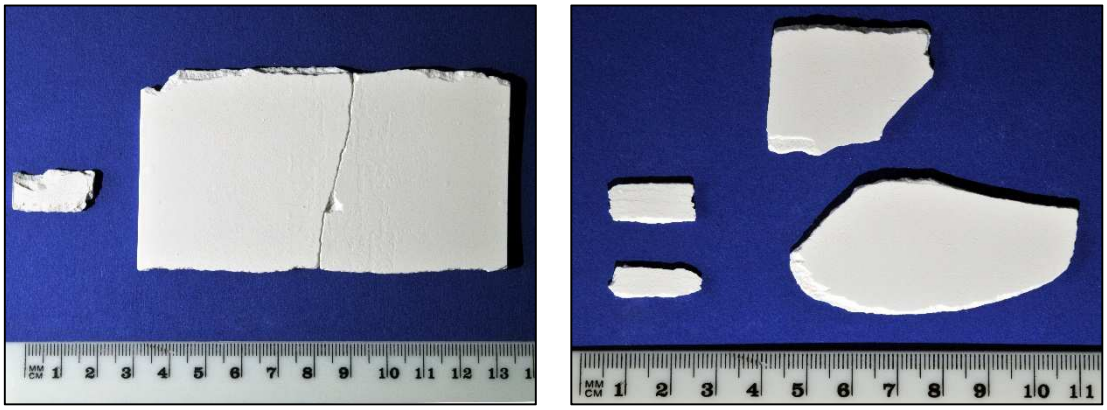

Figure 58: Example of several pieces of ribbons from MCC (a) and mannitol (b) produced with the BRC 25 (ribbon on the left) and the BRC 100 (ribbon on the right).

Those in the pictures are just examples, however, the general aspect of the ribbons is similar. Although this was not clear for the Gerteis samples, MCC as a plastic material tends to keep the shape after compaction, while mannitol as brittle normally results in smaller pieces. This has been already observed in the literature when ribbons made of both types of materials are visually compared (Yu et al. 2012; Pérez-Gandarillas et al. 2016). As was the case for Gerteis, all ribbons produced were classified according to the structure and length. The ribbons were categorized considering the general aspect of the batch, and of course, facts like transport and storage can also affect the physical integrity of the samples. Nevertheless, in this case, the limit to distinguish between short and long ribbons was established again according to the roll width, meaning that up to 2.5 cm for the BRC 25 and 10 cm for the BRC 100 ribbons would be considered as short.

There is no need to present the results in a table, as most of the ribbons produced were intact or integrated and divided in small pieces, i.e. short. This means that no bilamination occurred and the sealing system used leads to the breaking of the ribbons during production. Only those of mannitol produced at the BRC 100 under 4 kN/cm, 1.5 mm and 2 rpm; under 8 kN/cm, 1.5 mm and 2 rpm and under 8 kN/cm, 1.5 mm and 4 rpm bilaminated. It can be possible that other batches produced showed also bilamination, but as the ribbons broke into small pieces, wrong judgments regarding the aspect could have been made. Anyway, in general,

it can be said that there are no differences regarding ribbon appearance when compacting with one or other machine, although this is probably more related to the sealing system assembled than to the compactor line used.

In any case, all ribbons have a size that complicates the characterization of the microhardness, especially for the BRC 25 samples. Therefore, due to the short length of the ribbons and the difficulties that this methodology has already shown, it was decided to exclude it from the ribbon characterization.

4.2.3.2.2. RELATIVE DENSITY

The relative density results could be focused on different manners. In this section although with less detail than in the previous one, the effect of the scale will be evaluated together with the process parameters and mixture proportion impact. The density of all the ribbons produced was characterized and presented in Table 9.

Table 9: Average ribbon relative density values for the main materials compacted under the conditions of the 11-runs DOE (n = 3) together with the production conditions for the L.B. Bohle compactors.

CONDITIONS			**AVERAGE RELATIVE DENSITY (%)**					
SCF (kN/cm)	**GAP (mm)**	**RS (rpm)**	**MCC BRC25**	**MCC BRC100**	**MIXT BRC25**	**MIXT BRC100**	**MAN BRC25**	**MAN BRC100**
4	1.5	2	59.1	57.9	65.5	63.5	67.8	71.7
4	3	2	55.6	54.5	59.6	59.8	62.4	67.4
4	1.5	4	58.9	58.4	59.5	62.6	67.2	65.5
4	3	4	55.3	53.4	57.1	59.6	67.1	65.1
8	1.5	2	67.8	70.7	70.9	72.5	73.3	78.0
8	3	2	66.4	65.2	67.7	70.6	72.8	75.1
8	1.5	4	68.0	70.3	67.5	73.4	74.1	74.3
8	3	4	66.9	65.7	68.8	69.5	72.6	75.4
6	2.25	3	63.8	62.8	66.9	67.6	67.5	69.5
6	2.25	3	63.0	64.9	65.3	69.1	71.9	72.4
6	2.25	3	62.9	62.3	64.0	68.2	69.9	67.1

As these compactors are relatively new on the market, no publications have been found involving any of these machines. Nevertheless, it can be again compared to the literature in relation to how the density decreases with the increase of the plastic material MCC (Chang et al. 2008, Golchert et al. 2013; Iyer et al. 2014b). For the whole scale-up study, the majority of the ribbons showed densities between 60 and 80%, although few exceptions occurred. MCC ribbons were below this 60% value, but also some of the batches from the mixture produced at 4 kN/cm, mainly those compacted using large gap widths.

A first statistical evaluation of the original 11-runs DOE was performed for the different compactors and material. The coefficient plots presented in Figure 59 confirm the already observed tendency of increasing the relative density when rising the SCF and decreasing the gap. However, the gap width is not a significant factor for mannitol compacted at both scales, as well as the mixture compacted at BRC 25. The models obtained show a R^2 value higher than 0.7, even than 0.9 for some of them.

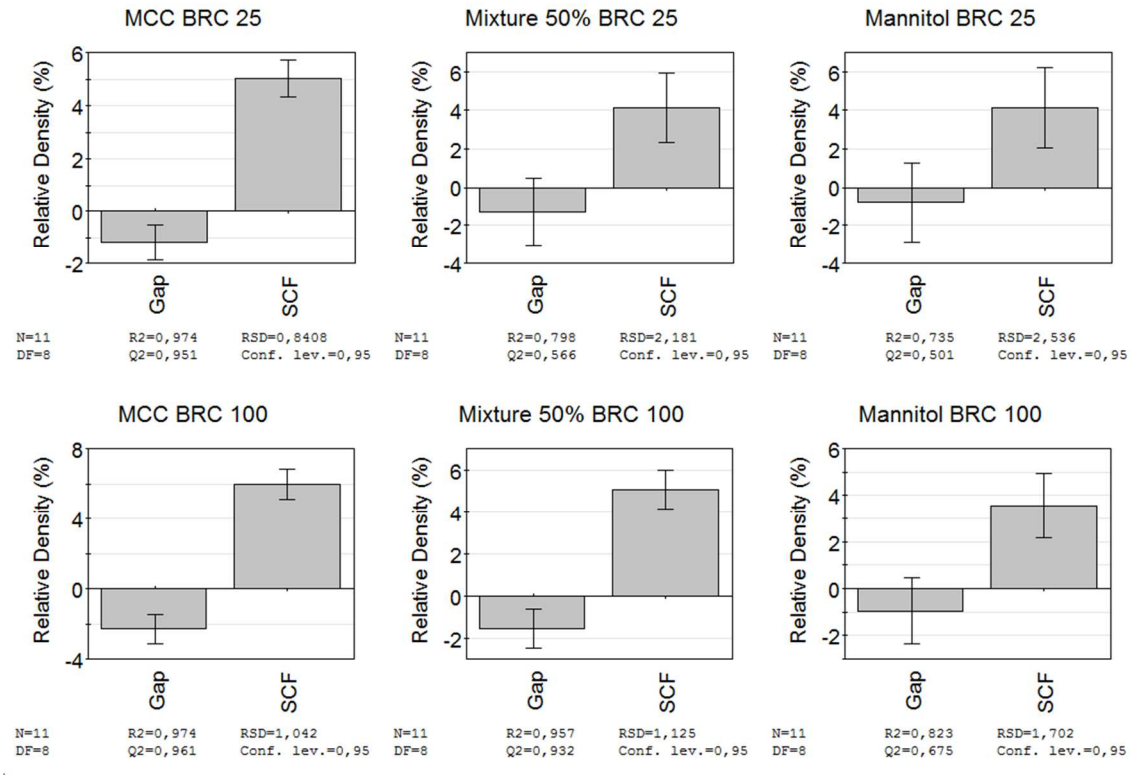

Figure 59: Coefficient plots for the ribbon relative density analysing every combination of material and scale separately for the L.B. Bohle compactors (MLR).

This DOE was later modified and the scale was included as a quantitative factor by using the roll width of the compactor. The scale changed from 25 to 100 mm. If this new design is analysed, the coefficient plot presented in Figure 60 is obtained. In this case, the

coefficient of determination is also higher than 0.8, and most of them overcome the 0.9 already, which gives significance to the models.

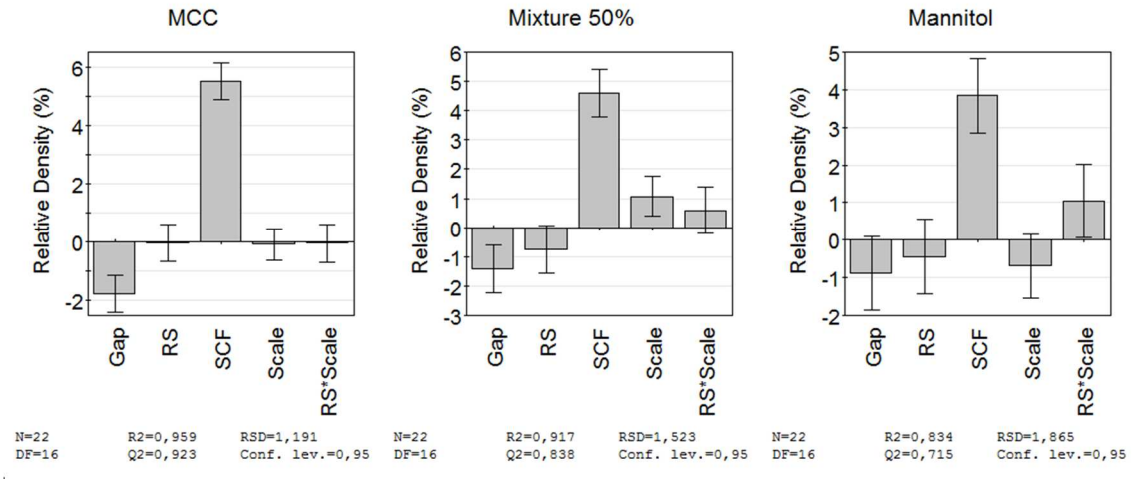

Figure 60: Coefficient plots for the new design including the scale as a factor for the L.B. Bohle compactors (MLR).

In this new version of the 11-runs DOE, the direct effect of the SCF and the inverse of the gap is observed, although for mannitol the latter is not significant. Similarly, the scale for the mixture and its interaction with the roll speed for mannitol are directly significant. In other words, this coefficient plots proves that the change of compactor has an effect for the mixture and mannitol. However, MCC is not affected, meaning that similar densities are obtained in both scales. Although no significant effect of the scale as a single factor was observed for mannitol, it is interesting how for the mixture the relationship with the density is direct while inverse for this brittle material. The idea behind this fact is that for the mixture the higher the scale, the higher the density, however, for mannitol, the change to a larger scale leads to lower density. This different influence of the scale on the mixture than on mannitol was already observed for Gerteis compactors but with the opposite effect (Figures 28 and 50, pages 76 and 101 respectively).

This impact of the scale has been further investigated by preparing a correlation for the same material in which the ribbon relative density obtained in both compactors is compared. The best fit line is plotted for the data together with its equation as well as the r obtained. All correlations are presented in Figure 61, where one per material is prepared. The correlation with the highest r value of 0.9799 is the one from MCC, as expected according to the results obtained during the statistical evaluation. However, this relationship is still not perfectly linear and relatively high standard deviation is obtained for some points, stressing the

effect of the scale, although it was not found to be significant in the DOE evaluation and it is not as strong as it is with the other materials. The correlation coefficient becomes lower when decreasing the proportion of MCC, reaching the worst value of 0.8203 for mannitol. If the equation of the best fit line is taken into consideration, the slope tends to also decrease together with the proportion of MCC, although the value is close to 1.2 for pure MCC and 1.0 for the 50% mixture. For the latter, also the Y-intercept is almost ideal with a value of 0.8, the lowest obtained for this type of correlations. Considering these aspects together with the r value, the mixture would have the best correlation, as was also the case for the Gerteis line. For the pure materials, the Y-intercept value changes between 13.2 and 21.1 for MCC and mannitol respectively. In conclusion, these correlations again prove the effect of the scale on the ribbon relative density, as they are far from the ideal situation.

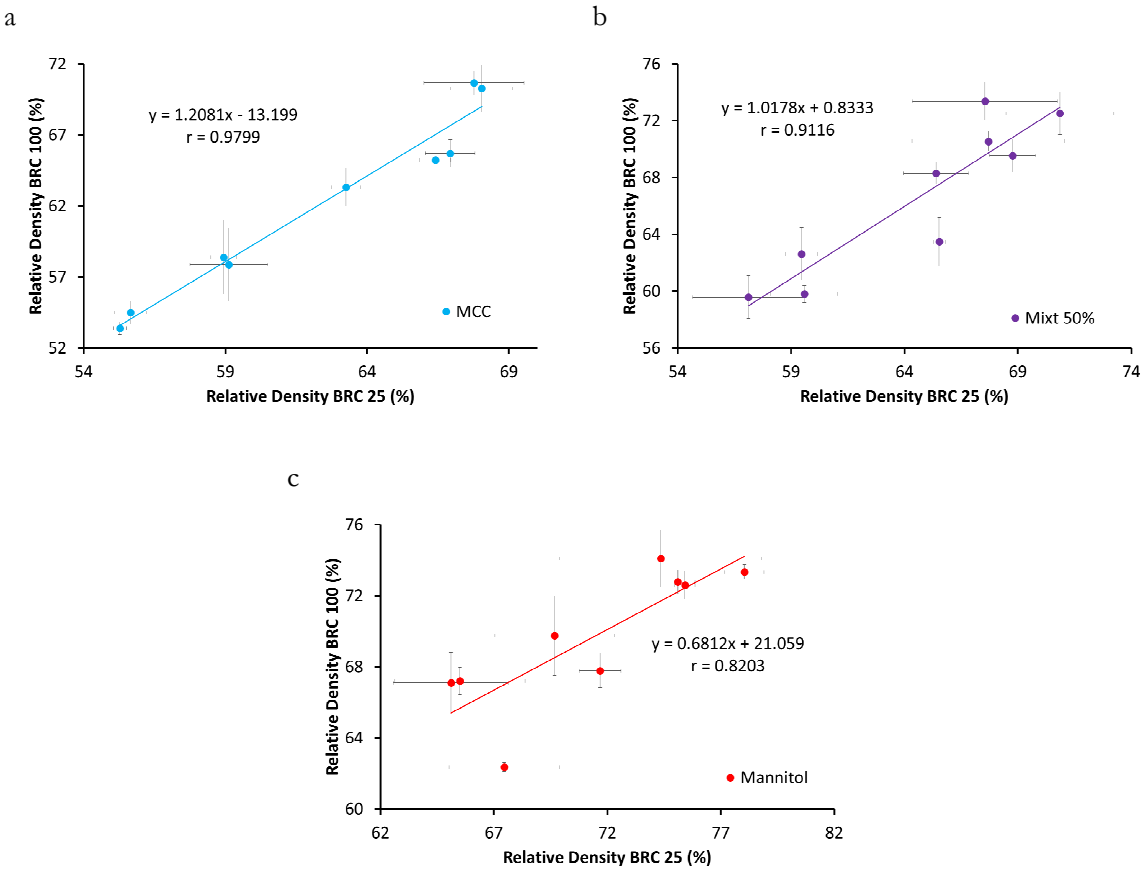

Figure 61: Correlation for relative density of ribbons produced at the same manufacturing conditions between the BRC 100 in the Y-axis and the BRC 25 in the X-axis regarding the compaction of MCC (a), the 50% mixture (b) and mannitol (c). The best fit line equation and the correlation coefficient are also presented, mean±s (n = 3).

Apart from the 11-runs DOE, 3 repetitions of the centre point (6 kN/cm SCF, 2.25 mm gap and 3 rpm roll speed) were also produced for the mixtures of 15, 30, 70 and 85%

MCC and characterized regarding ribbon density. The global means obtained are presented in Figure 62, where both scales are compared. The first main conclusion is that, as has been already observed previously, the higher the content of MCC, the lower the relative density of the ribbons. Actually, this relationship is almost linear, although less pronounced than in the case of Gerteis compactors (Figure 35, page 85). However, the most interesting fact from the point of view of the scale, is that for these batches the density value is always higher on the BRC 100 than on the BRC 25, even for the pure materials, where the differences come closer. Nevertheless, this may be influenced by the fact that the ribbons obtained for the BRC 100 were larger and therefore, also the pieces used for the analysis were bigger.

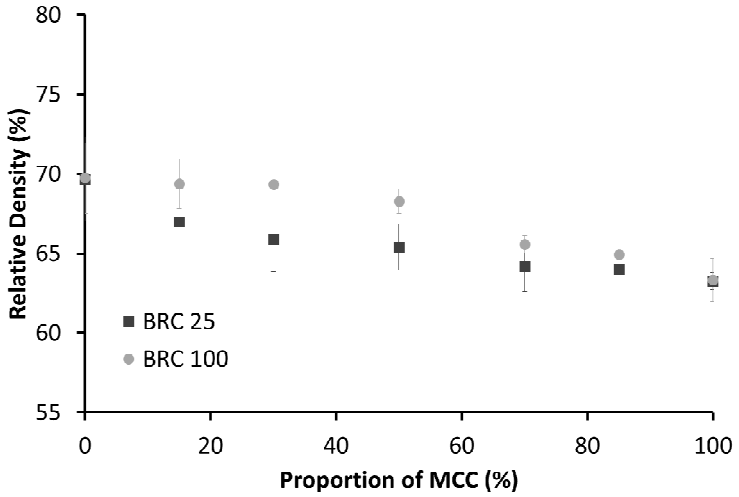

Figure 62: Relative density for all the mixtures for the centre point conditions comparing the two scales of L.B. Bohle supplier, mean±s (n = 3).

Finally, and in order to investigate individually the effect of the scale for each data point, the F and t-test for an $\alpha = 0.05$ and $n = 3$ was performed. For the majority of the batches, no statistically significant differences were observed. However, for mannitol, almost half of the batches were statistically different, while for the mixture of 50%, also two lots were unequal. For MCC, only one lot was identified. Regarding the centre point, only the 50 and 85% mixtures resulted statistically unequal in both scales. No common pattern was observed for those batches which were not statistically reproducible, therefore, no problem of the machines to set some conditions can be addressed.

4.2.3.2.3. DENSITY DISTRIBUTION

As rim rolls were used to perform the compaction in the L.B. Bohle pieces of equipment, the ribbons broke in small fragments. However, for the BRC 100, it was possible to reconstruct one ribbon of MCC belonging to the last repetition of the centre point and it was analysed using μCT. Unfortunately, reconstructing a piece of ribbon in the case of the corresponding mannitol batch was not possible, and as this would have meant that the density distribution across the ribbon width would be lost, no mannitol ribbons were analysed with this technique. Similarly, this reconstruction was not feasible for the equivalent centre point batch of MCC in the BRC 25 either, and a small piece was taken instead. This broken ribbon has the border of the sealing system marked, and therefore, at least it can be affirmed that it belongs to the edge and also includes part of the middle. The 3D picture of both ribbons together to the calibration tablets is presented in Figure 63. In this image, it can be seen not only the cut on the centre of the ribbon from the large scale, but also the irregular shape of the BRC 25 piece.

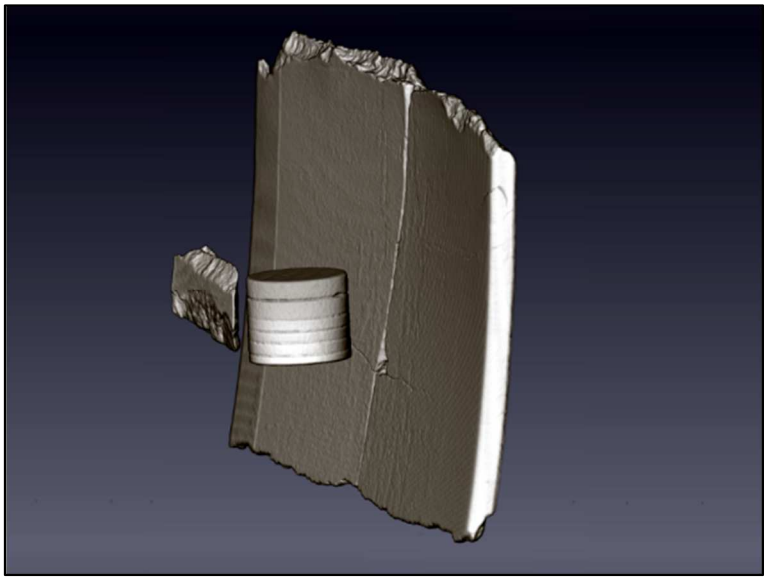

Figure 63: Picture in 3D of the ribbons compacted from MCC at both scales of L.B Bohle compactors analysed using μCT.

However, the most interesting aspect is the density distribution within the ribbons. In Figure 64, the colour cuts of the crosswise (a) and the lengthwise (b) planes are collected. For the distribution across the ribbon width, and as expected due to the sealing system used, a different profile than the one observed for the Gerteis compactors can be seen. In this case, the rim rolls result in denser edges while the density in the centre of the ribbon is lower, as was expected considering the literature (Mazor et al. 2016; Wiedey et al. 2016). This profile is

clearly observed for the MCC ribbon compacted at the BRC 100. However, the density distribution for the BRC 25 sample is not so evident, probably because part of it is missed, although the well-defined edge seems to be harder than the rest of the ribbon. Furthermore, this piece is extremely irregular, having also some cuts inside. Independent of that, the large-scale ribbon reaches lower density than the sample from the BRC 25.

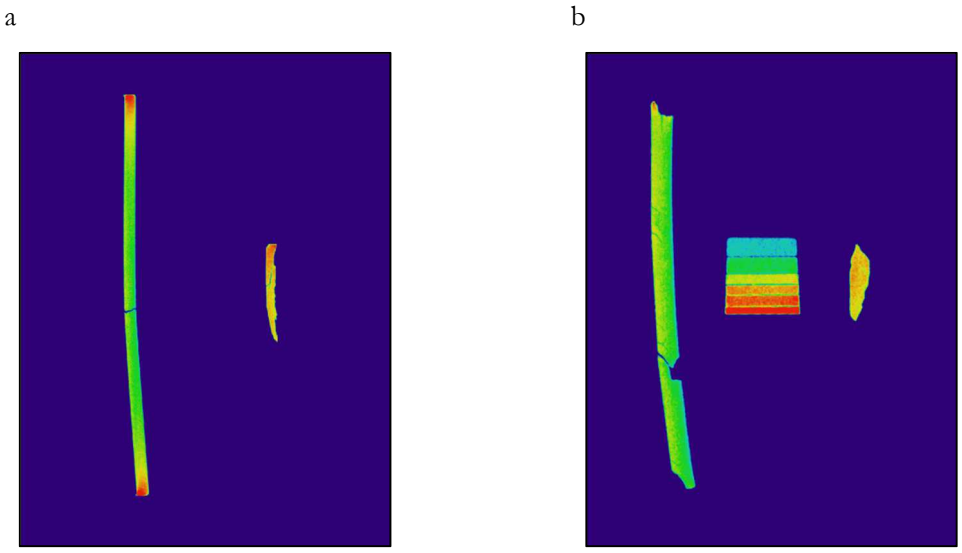

Figure 64: Crosswise (a) and lengthwise (b) cuts in colour of the ribbons from MCC compacted at both scales of L.B. Bohle compactors. Please note that the ribbon on the left was produced at the BRC 100 and the one on the right at the BRC 25.

If the lengthwise cut is referred to, the distribution along the ribbon compacted at the BRC 100 seems to be relative constant for the dimensions considered, having lower values on the right border and the middle (green colour) than in the left edge (yellow colour). This again means that one of the rolls may exert a slightly higher force, most likely the movable or floating one with which the L.B. Bohle compactors are also equipped. The ribbon from the small scale seems to change in a similar range although the density is higher, but with a different profile. It seems that the superior part is denser than the lower site. However, the size of the sample and the fact that is broken and laminated in some areas, could explain why these differences between both pieces are observed. Furthermore, the hygroscopicity of the MCC together with the long measuring time when using μCT, could also have an effect on the lengthwise density distribution.

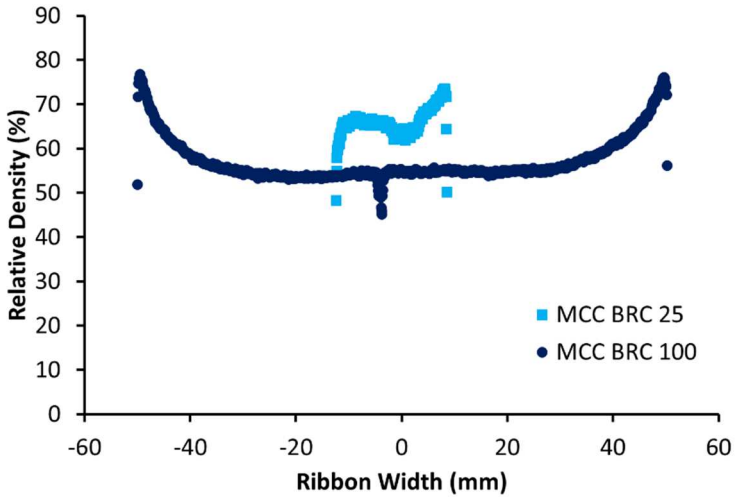

Figure 65: Density distribution along the width of the ribbons from MCC compacted at the BRC 25 and the BRC 100, mean ($n \geq 2$).

The profile along the ribbon width was taken to transform the grey value into real relative density, in the same manner as for the Gerteis compactors. The resulting densities were plotted in Figure 65 where both ribbons are compared. The curve observed for the BRC 100 ribbon shows clearly this tendency of decreasing the relative density from the edges until reaching a value more or less constant in the middle. The ribbon here presented broke into two pieces that were found to belong together, and therefore, this drastic decrease in the density in the centre proves the effect of cuts in the calculations of the density distribution already discussed for the Gerteis samples. However, in the profile obtained for the BRC 25 ribbon no similar behaviour can be inferred. Actually, the density seems to only increase from the edge to the middle with a small fall before achieving the maximum. This result is probably highly affected not only by the irregular and incomplete shape of the ribbon, but by the internal cuts and laminations within its structure. Therefore, no clear conclusions can be extracted aside from the fact that the profile obtained for the BRC 25 is unexpected and not comparable with the one observed for the BRC 100. However, it cannot be assured that these differences between both profiles are exclusively due to the change in scale. This fact, together with what has been observed for the cross and lengthwise cuts, proves why this measurement was discarded for the mannitol ribbons. As those also broke into small pieces and it was impossible to match them, no density profiles could have been derived without knowing where the pieces belonged.

Finally, a comparison between the average relative density obtained with μCT and the value measured with the GeoPyc® can be established. In this case, the BRC 25 results in a value

a 3.0% higher for the μCT than for the GeoPyc®, while for the BRC 100, the density is a 5.1% lower on the μCT. Therefore, again important differences are found, emphasizing that both techniques cannot be compared. Nevertheless, both methods give different advantages: GeoPyc® provides a general overview for many samples, while allows clear observation of the distribution within a smaller amount of ribbons.

4.2.4. FREUND-VECTOR LINE

This last scale-up study consists of the evaluation of the effect that using the TFC-Lab Micro (small scale) and the TF-Mini (large scale) has on the properties of the products when setting the same manufacture conditions. These compactors use the other scale-up strategy: they differ not only in roll width, as in the previous cases, but also in roll diameter. The TFC-Lab Micro, which is the small scale, has a roll diameter of 50 mm and 24 mm of roll width, while the TF-Mini, which is the large scale in this study, has 100 mm of diameter and 37 mm of roll width. The compactors were assembled with rim rolls and ribbed roll surface. A total of 13 batches from different mixtures were produced in each of these compactors. All ribbons were produced using 2 rpm of roll speed and trying to reach a gap width of 1.5 mm. All 7 mixtures were compacted at 5 MPa roll pressure, and the main materials also using 2 and 8 MPa, reaching in this manner, the total of 13 batches per compactor.

Before starting to discuss the results obtained, it is important to make an initial criticism of the experiments performed. The first point to consider, is that both machines have no gap control system or even an in-line system which can show the gap in real time, which already complicates the production and decreases its precision. However, two other points were not considered when defining the experiments: the conversion of the roll pressure into roll force and the linear speed. These adaptations were performed by Sheskey et al. 2000 and Sheskey et al. 2002, and they concluded that the scale-up of their formulation had minimal problems.

On the one hand, although the same pressure can be set on both compactors, this hydraulic pressure has to be converted into roll force in order to know the real force applied to the powder in the gap. In other words, applying 5 MPa in both compactors result in different roll forces. In order to perform this transformation, the suppliers provide conversion factors which are 0.93 and 0.31 kN/bar for the TFC-Lab Micro and TF-Mini respectively. Therefore, 5 MPa, i.e. 50 bars, in the TFC-Lab Micro are equivalent to 46.5 kN, while for the TF-Mini is 15.5 kN. This means that the real roll force is always higher on the TFC-Lab Micro. Furthermore, if a proper scale-up is considered, i.e. the change from small to large scale, in order to reach the 46.5 kN in the TF-Mini, it would have been necessary to set 15 MPa instead. However, the maximum pressure that can be set is approximately 14 MPa, thus, it would have been not possible to adapt this parameter. These roll forces can also be converted into SCF by dividing the value by the roll width, and then for the TFC-Lab Micro, 5 MPa would be equivalent to approximately 19.4 kN/cm while for the TF-Mini, it would be around 4.2 kN/cm, so the differences become even larger.

On the other hand, the roll speed is expressed as rpm, i.e. rounds per minute. These units depend on the diameter of the roll, as the time that a disc needs to complete one turn depends on how large is it. Therefore, if the speed was recalculated according to the diameter of the rolls, the linear roll speed would be obtained. The roll diameter of the TFC-Lab Micro is 50 mm (0.05 m), while for the TF-Mini is 100 mm (0.1 m). This means that 2 rpm in linear speed are equivalent to 0.0052 m/s for the TFC-Lab Micro and 0.0105 m/s for the TF-Mini. Therefore, the latter is twice faster (also because the diameter is twice larger), which will lead to a lower dwell time in the gap. This parameter would have been easily adapted by setting 4 rpm in the TFC-Lab Micro. However, reaching a 1.5 mm gap was already difficult for the 2 rpm roll speed, meaning that probably, it would have not been feasible if the material is passing through the gap twice faster.

These two points were initially not considered as the intention for this scale-up study, like for the previous ones, was to assess the scale effect when entering exactly the same conditions without any transformation. However, for Gerteis and L.B. Bohle compactors, there is no need to adjust neither the roll force (always using SCF) nor the roll speed (diameter is the same). These providers do this in order to facilitate the scalability of their compactors. Nevertheless, the pressure and the linear speed for Freund-Vector compactors should have been considered before performing the study. It would have been possible to understand if the adaptation of these parameters (when possible), would have led to the same ribbons and granules properties in both scales.

4.2.4.1. PROCESS DATA

The process data was only possible to be gathered for the TFC-Lab Micro, which is equipped with an access to a system that allows collecting the real pressure and the feeding screw speed during the roll compaction process after performing the experiments. Unfortunately, in some occasions it was necessary to stop the process by decreasing the feeding screw speed to 0 rpm. But if this interruption of the process was not required, the profiles presented in Figure 66 are obtained, where both roll pressure and feeding screw speed are plotted. These graphs were prepared considering the moment in which the sample collection process starts and ends, although for the other compactors lines, several batches were represented together in the same graph. In the present case, the production of every lot was done separately (not continuously), therefore in the graphs only the considered steady-state

conditions for ribbon collection are plotted. Due to absence of gap control system, during the first minutes running the machine, it was necessary to play with the screw speed in order to reach the desired gap.

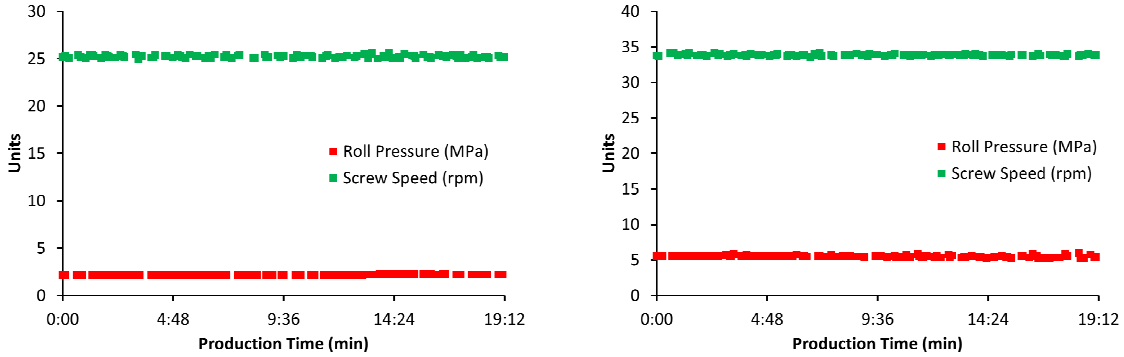

Figure 66: Example graphs in which it can be seen how the roll pressure and the screw speed evolve during a normal compaction process on the TFC-Lab Micro.

These graphs are proof that the process is controlled and the steady-state conditions are possible to reach. However, and although it seems to be a stable process, the scale of the graph has to be considered. In Figure 67, one of those previous representations (right) was split in two independent graphs, one for the pressure (a) and other for the screw speed (b). Now, it is possible to see, how the process is not so well-controlled, having a coefficient of variation of 2.79% and 0.37% for the roll pressure and screw speed respectively.

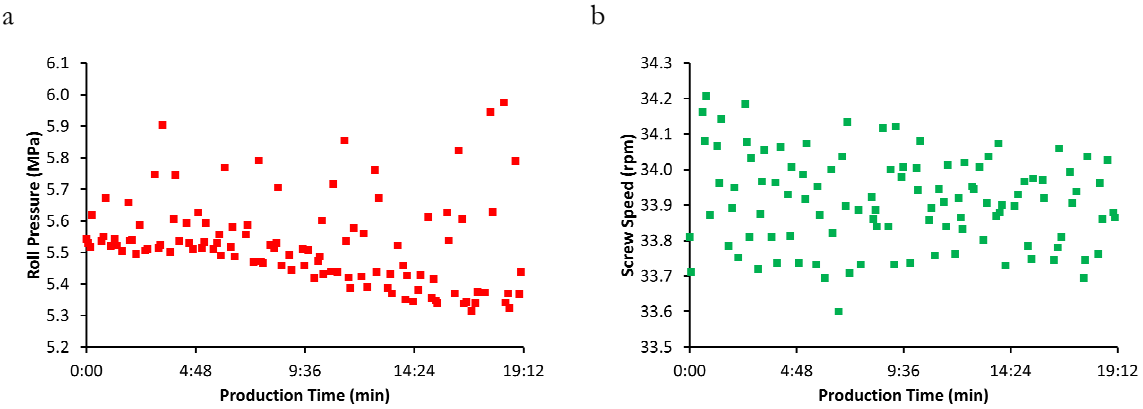

Figure 67: Enlargement of one of the previous example graphs in which the roll pressure (a) and the screw speed (b) during a normal compaction process on the TFC-Lab Micro are plotted separately.

In these figures, not only the scattering of the process conditions is shown, but also, the difficulties of the machine to establish the desire pressure using the pump can be appreciated. This value, for the present graph should be 5 MPa, however, for the whole process

it changes from 5.3 to 5.9 MPa. This range of variation of the TFC-Lab Micro, is the highest observed for all the compactors whose process parameters could be collected (Mini-Pactor®, BRC 25 and 100). For this case, between 6 and 8 points were measured per minute (1 point each 7-10 seconds), meaning that some information is lost. Although the missing points could improve the process stability, from the available data, it can be said, that the TFC-Lab Micro poorly controls the process conditions.

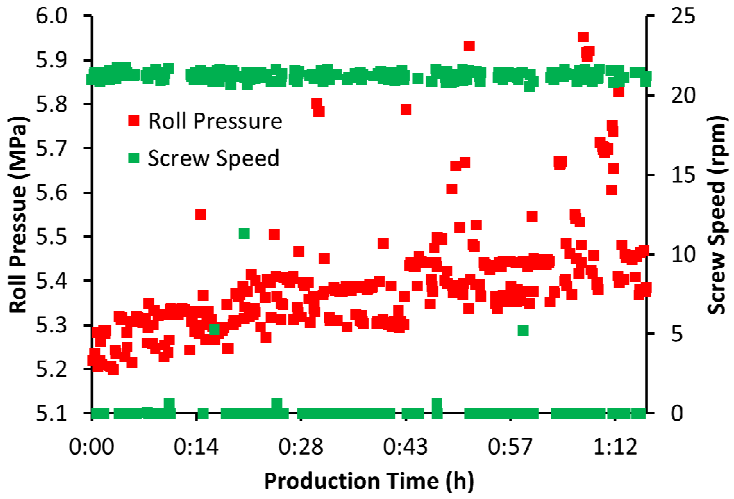

Figure 68: Example graph for a compaction on the TFC-Lab Micro in which it was necessary to stop the process as stickiness took place. Please note that a second axis was applied in order to see how the interruptions (screw speed = 0) affect the process.

In some occasions, the process was stopped because stickiness occurred and the sticking ribbons were removed. Figure 68 shows how the pieces stuck to the rolls were increasing the pressure as they were recompacted, at least for the present case. However for other batches increases and decreases of the roll pressure with the time have been observed, although not necessarily linked to the stickiness. The pressure, which was supposed to be 5 MPa, and again was not possible to set correctly, is changing from a minimum of 5.2 to 5.9 MPa. This scattering is probably also affected by the interruptions of the process. However, it can be again concluded that this compactor has problems with controlling the productions parameters. Furthermore, please note, that no gap control was available, which can be especially critical if the pressure was changing in this manner.

4.2.4.2. RIBBON CHARACTERIZATION

The samples collected were characterized using all methodologies available for ribbon characterization. Before starting the discussion of these results, not only the irregular roll compaction process should be considered, proven at least for the TFC-Lab Micro, but also the problems with the pressure and the linear roll speed, previously described. However, the intention of the present work is still to evaluate the effect of the scale, so these differences should be included also as part of the change of scale.

4.2.4.2.1. APPEARANCE

The ribbons produced with these two compactors, due to the sealing system used, always presented some softer edges that normally detach by themselves. In Figure 69, pictures of ribbons from MCC and mannitol produced in both compactors are shown. In both cases, the ribbon on the left hand side, is the one produced with the TFC-Lab Micro (small scale) and on the right hand side of the photography, the one with the TF-Mini (large scale).

a b

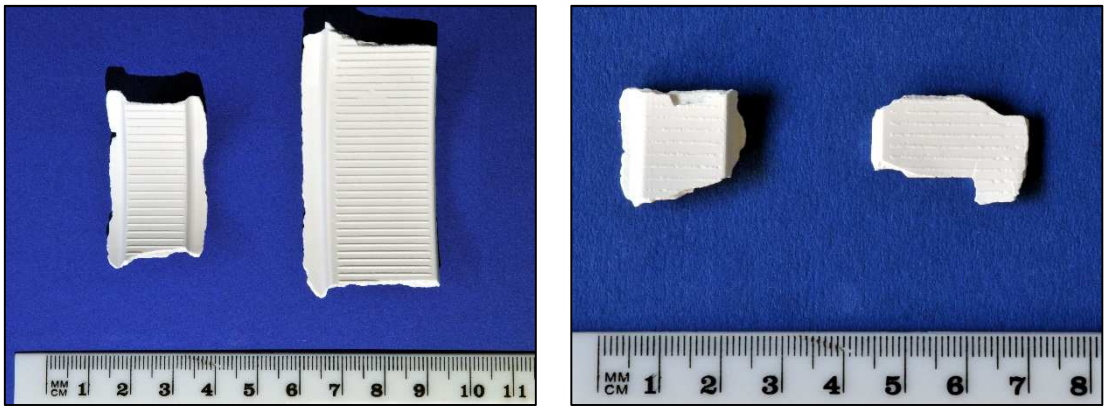

Figure 69: Example of two pieces of ribbons from MCC (a) and mannitol (b) produced with the TFC-Lab Micro (ribbon on the left) and the TF-Mini (ribbon on the right).

In these pictures, it can be seen how the ribbons from MCC are longer than those from mannitol which are normally incomplete, as expected (Yu et al. 2012; Pérez-Gandarillas et al. 2016). Additionally, the pieces produced in the two scales have a similar aspect, apart from the roll width. Nevertheless, these pictures give a general idea of how the ribbons look like, but they are just some examples. In Table 10, all samples produced for this line are considered. For these compactors, no bilamination took place, and thus, all ribbons obtained were integrated. In this manner, the length of the ribbons was considered as the main visual characteristic that was affected by the change in pressure or material compacted. Please note,

as it was for the previous cases, that the classification was made considering the majority of the ribbons, and it is also important to point out that conditions like storage or transport can affect the size of the samples. Ribbons were classified according only to the length in "long" or "short" and depending on the compactor, the limit was established at 1.5 cm for the TFC-Lab Micro and at 2.5 cm for TF-Mini. Although the roll width is 24 mm for the TFC-Lab Micro and 37 mm for the TF-Mini, the edges that can be seen in the previous picture were not considered a proper part of the ribbon, so the lengths that lead to square shapes are those defined. This means that in practise, instead of 24 mm for the small scale and 37 mm for the large one, the ribbon width was approximately 15 mm and 25 mm respectively.

Table 10: Physical appearance of the ribbons produced in both scales. Please note that the cases in which the aspect is different when changing the compactor are highlighted in grey.

CONTENT OF MCC (%)	**CONDITIONS**			**ROLL COMPACTOR**	
	ROLL PRESSURE (MPa)	**RS (rpm)**	**GAP (mm)**	**TF-MINI**	**TFC-LAB MICRO**
0	2	2	1.5	Short	Short
0	5	2	1.5	Short	Short
0	8	2	1.5	Short	Long
15	5	2	1.5	Short	Long
30	5	2	1.5	Short	Short
50	2	2	1.5	Short	Long
50	5	2	1.5	Short	Long
50	8	2	1.5	Long	Long
70	5	2	1.5	Short	Short
85	5	2	1.5	Short	Short
100	2	2	1.5	Long	Long
100	5	2	1.5	Long	Long
100	8	2	1.5	Long	Long

The main conclusion which can be extracted from this table is that the scale normally does not affect the appearance of the ribbons, only in the case of the pure mannitol at 8 MPa, the 15% mixture and the 50% blend at 2 and 5 MPa, but there is not a clear pattern which could explain these cases. This is similar to the case of the L.B. Bohle line, in which no effect of the scale was identified for most of the samples. In that case, all the ribbons were short and on a few occasions bilamination was observed, while for the Freund-Vector ribbons, all were integrated.

4.2.4.2.2. RELATIVE DENSITY

Similar to the previous studies, apart from the effect of the scale, the relative density of the ribbons was analysed considering two other points of view: the impact of the material and the influence of the pressure. Therefore, in both situations, the two machines were always compared in order to understand the influence of the scale and these two factors.

The effect of the material and the scale is plotted in Figure 70 by representing the relative density of the ribbons from all mixtures produced at 5 MPa pressure in both machines. The relative density changes for the same pressure from a minimum of 73.3% to a maximum of 79.0% for the TF-Mini and from 66.8% to 80.2% for the TFC-Lab Micro (most of those values within the acceptability range of 60 to 80%). Therefore, the density varies in a wider range for TFC-Lab Micro. Regarding material effect, the main conclusion that can be extracted is that the relative density tends to decrease with the proportion of MCC, as has already been observed for the previous scale-up studies and in the literature (Chang et al. 2008, Golchert et al. 2013; Iyer et al. 2014b). However, an important difference between the previous families of compactors and Freund-Vector, is the lack of a linear decrease. The global mean for the relative density of the centre point conditions was always decreasing when increasing the percentage of MCC. However, for the present case, and although some differences between both scales can be observed in this respect, for the two compactors the 15% mixture results in higher ribbon densities than for mannitol. If this point were excluded for the TFC-Lab Micro, the decrease in the relative density as the proportion of MCC rises would be more linear. For the TF-Mini, this decrease in relative density (considering all points and standard deviation) is more subtle, even leading to increases at low and high proportions of MCC.

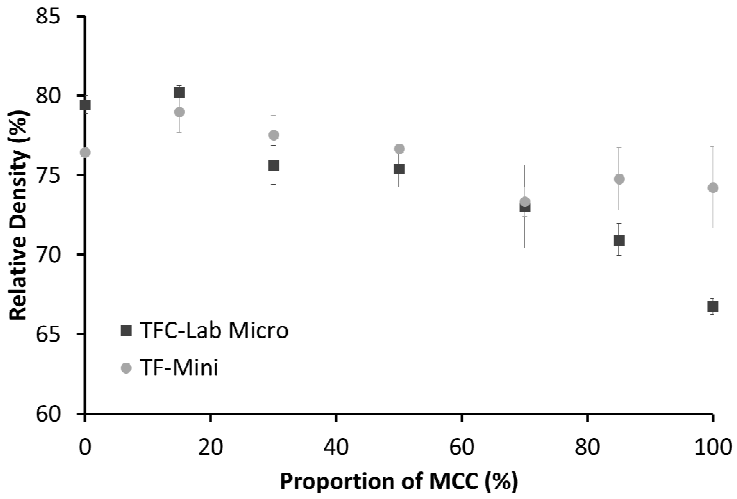

Figure 70: Relative density for all the mixtures for the 5 MPa comparing the two scales of Freund-Vector supplier, mean±s (n = 3).

Furthermore, the pressure has a clear effect on the relative density, and therefore, it was also interesting to see how changing the compaction pressure affects the ribbons produced. In Figure 71 a comparison between the relative density of ribbons from MCC, mannitol and the 50% mixture produced at 2, 5 and 8 MPa in both machines is presented.

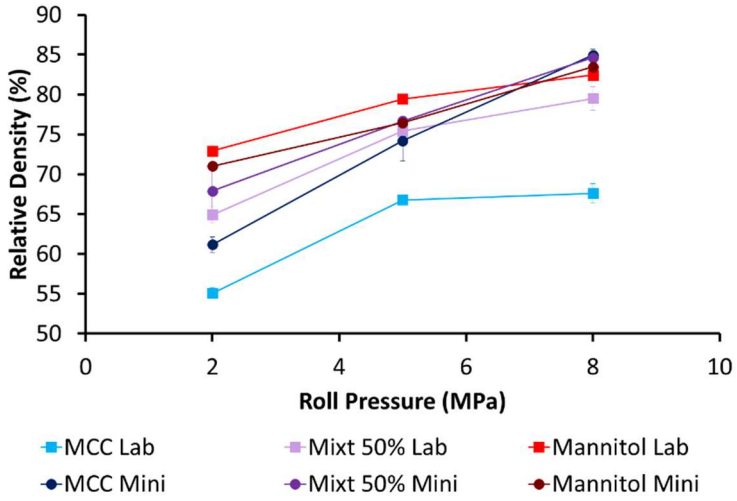

Figure 71: Relative density for the main materials compacted under different pressures comparing the two scales of Freund-Vector supplier. Please note that Lab refers to the TFC-Lab Micro and Mini to the TF-Mini, mean±s (n = 3).

The greater the roll pressure, the higher the relative density changing from a minimum of 55.1 to a maximum of 82.4% for the TFC-Lab Micro (only for MCC at 2 MPa and mannitol at 8 MPa, the density is out of the supposed acceptability range) and from 61.2 to 84.9 for the

TF-Mini (the uses of 8 MPa generates ribbons with densities higher than 80%). The change from the 5 MPa to the 8 MPa is in general weaker, especially for pure MCC at the TFC-Lab Micro. This fact may be due to the difficulty of the machine to really apply such a high pressure or as discussed previously, also because of the poor control. However, in the literature a similar plateau when overcoming a certain pressure has also been described (McAuliffe et al. 2015). In this graph, it can be also seen the general tendency of the MCC to show the lowest relative density, which increases until achieving the highest one for mannitol (the 8 MPa point for the TF-Mini is the only exception). Thus, again the density decreases with the content of MCC.

Dumarey et al. 2011 and Souihi et al. 2013a evaluated different grades and types of MCC and mannitol (including crystalline, spray-dried and granular forms) respectively. In both studies, the formulations contained more than a 55% of one of the previous materials in combination with an API and several other excipients. Compaction was performed in both cases on the TFC-Lab Micro (also known as TFC-Labo) at 5 MPa, 3 rpm of roll speed and the feed screw speed was varied in 3 levels in order to have a feed/roll speed ratio equal to 6, 8 and 10 (meaning 18, 24 and 30 rpm for the feeding screw). In both studies, 3 repetitions of the same compaction conditions with the same formulation (same type and grade of MCC or mannitol) were performed. Although the resulting ribbon density does not depend exclusively on MCC or mannitol, but on the combination of the whole materials in the formulation, some comparisons between their studies and the present one can be made. The range in which the densities were varying was for MCC from 46.5 to 79.3%, while a narrower interval with values between 69.3 and 78.5% was found for mannitol. The differences in the results depend on the grade and type used of the excipient investigated, as well as the feed screw. Both studies showed that the higher the feeding speed, the higher the density. The work of these researchers gives an idea of how MCC of different providers and grades can lead to a broad range of densities. Furthermore, this confirms the low reproducibility of the process, with standard deviations for the 3 repetitions of the centre point of 2.2% for MCC and 1.1% for mannitol.

Although some differences regarding relative density have been discussed, when performing the F and t-test for an $\alpha = 0.05$ and $n = 3$, no statistically significant differences were found for the batches of 15%, 30%, 50% (at 2 and 5 MPa) and 70% mixtures of MCC. This means that for these lots, the change of scale leads to similar relative density, and therefore, those values can be considered equal. Independent of this statistical test, in both representations and if the influence of the scale is considered, it is possible to see that in many cases (although without a statistically significant difference in some instances), the relative

density is mathematically lower for the TFC-Lab Micro (lab-scale) than for the TF-Mini. The few exceptions are for the mannitol and the 15% mixture. However, those results are not expected due to two physical principles. On the one hand, because as has been already discussed, the SCF applied in the case of the TFC-Lab Micro is almost 5 times higher for the same pressure, meaning that the density of the resulting ribbons should be higher for the small scale, or at least not statistically equal. And on the other hand, because the compaction using rolls with larger diameter, will lead to lower densification. Two rolls presenting different diameters will have the same nip angle, which determines where the densification starts. However, for a larger diameter, the roll force is distributed over a greater compaction zone and therefore, the pressure applied to the powder will decrease. This will lead to lower densification of the feed powder and, thus, lower ribbon relative density. However, the results obtained show that for the compactor with larger rolls (TF-Mini), the relative density was higher. Finally, it could be thought that the different dwelling time due to the differences in roll diameter could have an effect, but it would only justify the results obtained for MCC as a plastic material. Therefore, the results do not seem highly trustable, as they are in disagreement with the physical principles explained. Nevertheless, it can be concluded that an adaptation of the process is required in order to successfully scale up the process.

In the studies from Sheskey et al. 2000 and Sheskey et al. 2002, although no relative density was characterized for the ribbons, they also used the TF-Mini as initial scale to transfer their formulation to TF-156 and later to the TF-3012. They concluded that if the roll force per inch and the roll speed are adapted according to the dimensions of the rolls, in order to have the same total roll force and linear speed, the bulk density of the granules (produced with different millers) is in general higher for the lab and pilot compactor (TF-Mini and TF-156 respectively) than for the production scale (TF-3012). And although the miller used can have also an important impact, this means that even if the adaptation is performed some differences can be expected. Nevertheless, this fact should not have such a great impact and not justify completely the denser ribbons of the small scale.

One possible explanation could be that at least one of the conversion factors is wrong, and the relationship between both roll forces are not the ones described, as it is clear from the first graph that the relative density obtained is not from applying a SCF almost 5 times greater. Therefore, if a conversion factor is not correct and the highest roll force corresponded with the large scale, then, although the larger diameter would lead to broader compaction area and thus lower densification, the greater value of roll force could compensate the final pressure. In

other words, a wrong conversion value could justify higher ribbon density values on the large scale, and be in agreement with both physical principles. Another possible reason could be the process control. As has been shown in the previous section, at least for the case of the TFC-Lab Micro, it was proven that the process is not completely stable. Furthermore, it is important to keep in mind that no gap control or any system that allows for knowledge of the roll separation in real time was available, which has been identified in the previous studies as an important factor in roll compaction. This means that not one of the process conditions was accurately controlled, which could lead to a broad range of densities. Therefore, a possible consequence of all of the lack of precise process control is the production of batches with ribbons presenting unexpected relative density values.

4.2.4.2.3. DENSITY DISTRIBUTION

The density distribution of the ribbons compacted at the Freund-Vector compactors is particularly interesting as they present some special edges generated due to the design of the rim rolls. These protrusions were eliminated before performing the measurement with the GeoPyc® because they were not considered proper parts of the ribbon. They resulted from the compaction of powder within the rings of one of the rolls and the corresponding concave border of the other roll. In Figure 72, it can be seen the 3D picture of both ribbons of MCC and mannitol analysed for both compactors. These ribbons correspond to the conditions of 5 MPa roll pressure, 1.5 mm gap and 2 rpm roll speed. Although rim rolls were used for their compaction, MCC ribbons were long and no bilamination took place. In the case of mannitol, during the sample preparation the ribbon corresponding to the TFC-Lab Micro broke in two pieces and both were included in the measurement.

a b

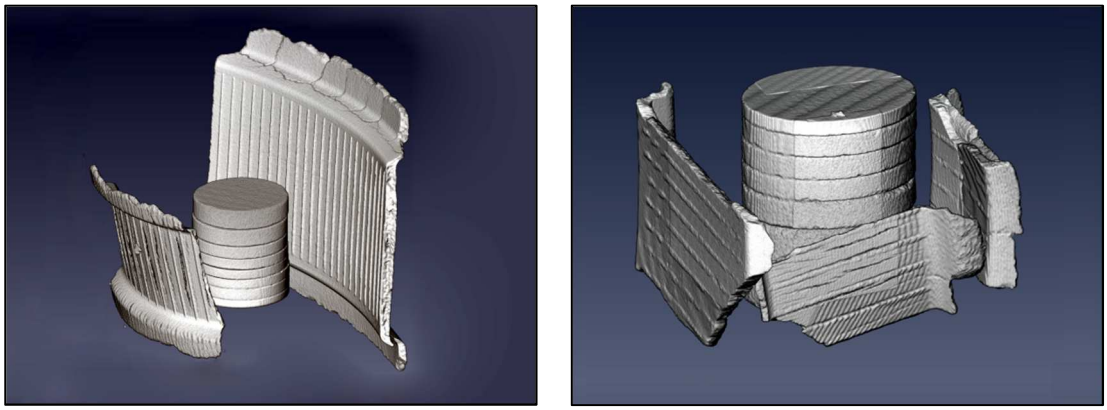

Figure 72: Picture in 3D of the ribbons compacted from MCC (a) and mannitol (b) at both scales of Freund-Vector compactors analysed using μCT.

These images were cut in crosswise (Figure 73) and lengthwise (Figure 74) planes. For the distribution across the ribbon width, and as expected, the protuberances in the samples show a lower density than the rest of the ribbon, reaching even the smallest values. It is especially noteworthy the fact that for both samples produced at the TF-Mini, the harder parts correspond to the connection between these protrusions and the rest of the ribbon. From this point, that would already be part of the edge of the proper ribbon, the distribution is not as clear as for the previous samples, but the density tends to decrease in the centre. However, it seems that the right side is slightly harder than the left one for the MCC ribbons, while the opposite profile is obtained for mannitol ones. Nevertheless, it could be affirmed that a similar pattern is obtained in both scales.

a b

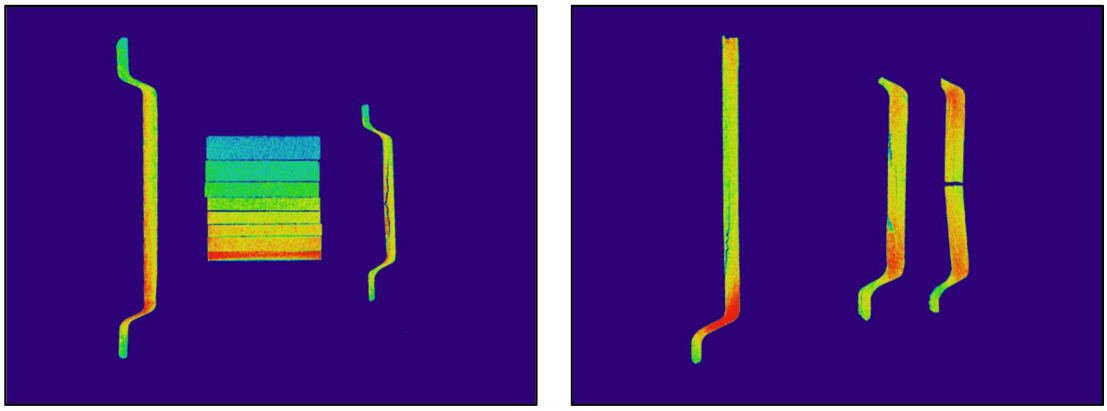

Figure 73: Crosswise cuts in colour of the ribbons from MCC (a) and mannitol (b) compacted at both scales of Freund-Vector compactors. Please note that the ribbon on the left was produced at the TF-Mini and the one on the right at the TFC-Lab Micro.

The latter crosswise plane for mannitol gives a clear example how the density distribution can change depending on where the cut is performed, as two pieces of the small-scale ribbon are collected together. Therefore, the lengthwise pictures were also evaluated. Again a slightly different density can be observed depending on the side considered, resulting in higher values for the left part for both materials. It could be again addressed a higher roll force by one of the rolls. Nevertheless, and as also concluded from the samples of the other compactors, the range in which the densities varied is narrower for the lengthwise distribution than for the crosswise. For MCC ribbons, the peaks generated in the surface due to the use of ribbed rolls can be especially clearly seen. They seem to present a lower density.

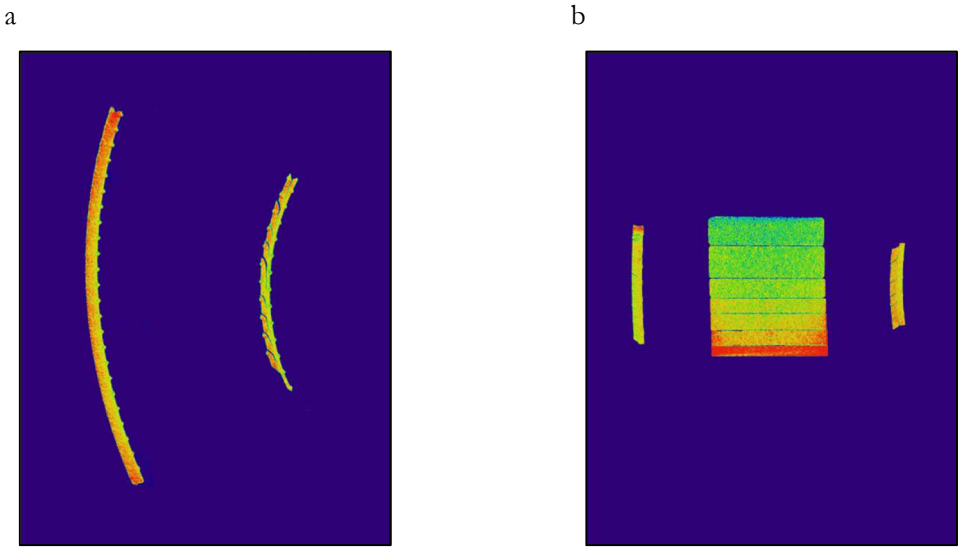

Figure 74: Lengthwise cuts in colour of the ribbons from MCC (a) and mannitol (b) compacted at both scales of Freund-Vector compactors. Please note that the ribbon on the left was produced at the TF-Mini and the one on the right at the TFC-Lab Micro.

In these last pictures, it can be also seen that although no bilamination takes place, several cuts and laminations seem to affect the ribbons. Therefore, it can be already expected that these defects in the ribbons will have an impact on the density distribution profile. In Figure 75, the density values obtained along the ribbon width are presented. In this case, it can be seen how the profiles are not as clear as for the previous compactors especially for MCC. The protuberances of the ribbons made of this material can be identified by the low values at the edges which increase until reaching normally a low peak. These borders are also responsible for the differences in ribbon width that in a few cases reaches real roll width (24 mm for the TFC-Lab Micro and 37 mm for the TF-Mini). For the centre of the sample, the density tends to decrease from left to right in the case of the TF-Mini, and from right to left for the TFC-Lab Micro in approximately a 10% for both cases. As this only depends on the position of the sample while measuring, it could be affirmed that both scales generate similar density distribution, although, the curve does not correspond to the typical expected profile. The internal lamination of the samples could explain these differences. The ribbons of mannitol show a pattern that is easier to interpret, and again similar for both machines. In this case, both ribbons lost one of the protrusions, and for the TF-Mini, a small part of the proper ribbon edge was also in some portions missed. For the TFC-Lab Micro, the remaining protuberance generates a low density which increases until a peak of decrease. Then, in the middle of the proper ribbon, and as expected, the curve shows higher values for the edges than for the centre. In the case of the TF-Mini, this profile is also obtained, being almost symmetrical. The

remained protrusion generates a small increase at the right side of the curve. For this ribbon, it may be surprising to observe such a high density in both edges, when according to the crosswise pictures one of the borders was missed, however, in the 3D picture it can be seen, how for a specific length, the whole ribbon width is almost complete. The peak is a result of the influence of this part, while the colour cuts are just an example.

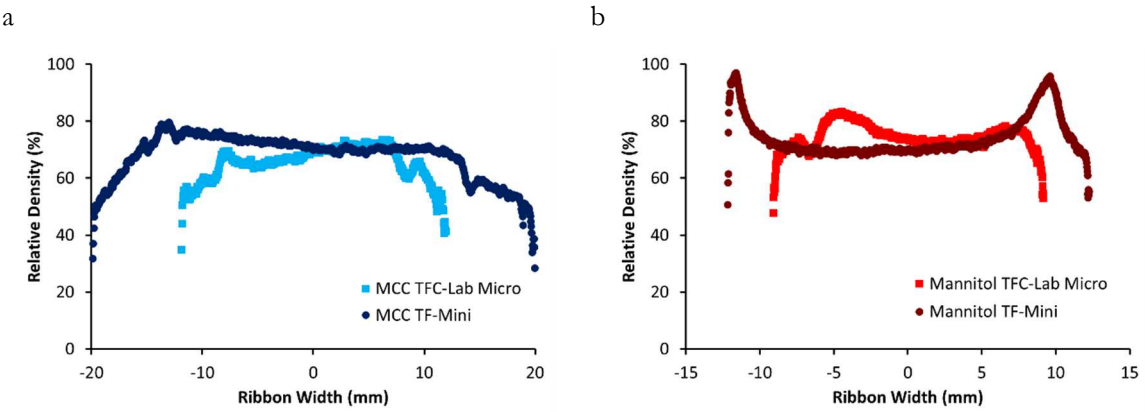

Figure 75: Density distribution along the width of the ribbons from MCC (a) and mannitol (b) compacted at the TFC-Lab Micro and TF-Mini, mean (n = 3).

In Figure 76, a new comparison between the density values obtained with the GeoPyc® and the µCT is again presented. It results again in a higher value for the GeoPyc® which is unexpected. This is especially noteworthy as in the literature, Miguélez-Morán et al. 2009 compared the density obtained with µCT, sectioning method and microhardness (after performing a calibration with tablets) and they found similar values for all techniques.

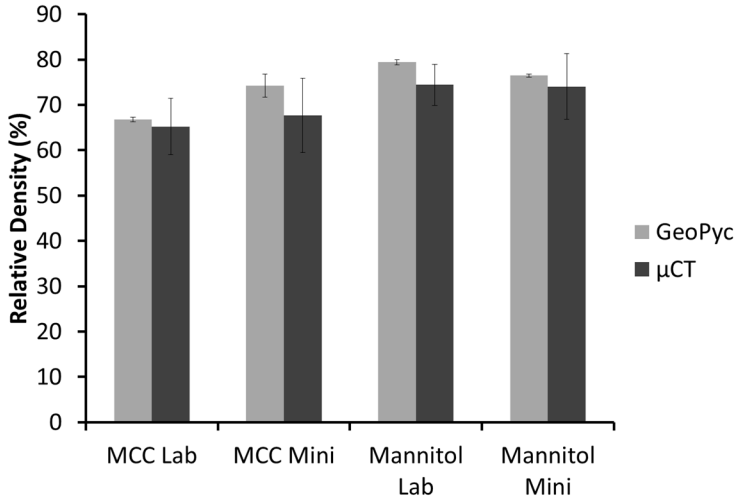

Figure 76: Comparison between the relative density results obtained using the GeoPyc® and the µCT, mean±s (n ≥ 3).

For this reason, the method followed for the calculation of the grey values (for example the limit set) and the calibration with the tablets could again be questionable. However, this could lead to lower densities, making the differences between GeoPyc® and μCT even larger. Therefore, it can be again concluded that both methodologies are not comparable, but they provide different interesting information that helps to deeper investigate the roll compaction process.

4.2.4.2.4. MICROHARDNESS

Due to the short length of some of the ribbons, few samples were complicated to measure. The ribbons produced were characterized regarding HU, following the cross method meaning that the measurements were performed in the highest parts. In Figure 77, the comparison of the HU values for the mixtures produced at 5 MPa is plotted for the two compactors. The microhardness for this pressure evolves from a minimum of 28.3 N/mm^2 to the highest value of 47.0 N/mm^2 for the TFC-Lab Micro, and from 26.6 N/mm^2 to 49.7 N/mm^2 for the TF-Mini. Thus, HU values change in a similar range for both compactors. Due to the confidence interval represented on the graphs, it could be possible to affirm that the differences between the diverse materials are not that strong. Therefore, in this case the effect of the proportion of MCC is not that obvious. If both scales are compared, again the harder ribbons are in general those produced with the TF-Mini.

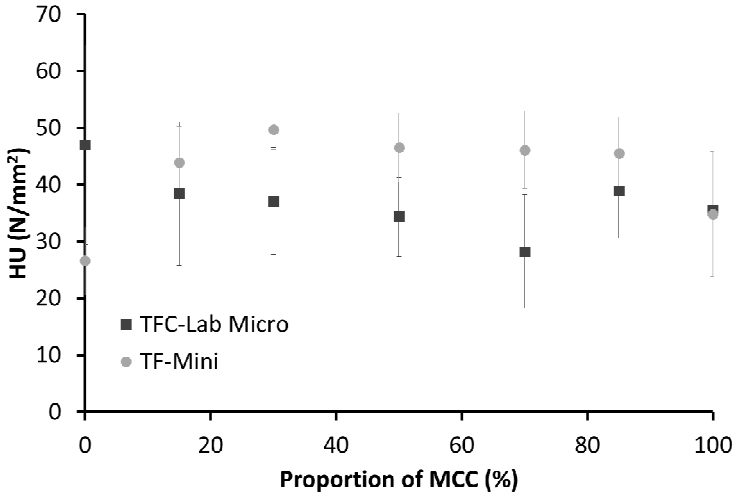

Figure 77: Microhardness for all the mixtures compacted under 5 MPa comparing the two scales of Freund-Vector supplier, mean±CI (n = 36, α = 5%).

The effect of the pressure on the microhardness is depicted in Figure 78. As expected and as it was the case for the relative density, the main conclusion that can be extracted is that

the HU increases with the pressure, and it goes from a minimum of 12.0 to a maximum of 56.5 N/mm^2 for the TFC-Lab Micro and from 15.3 to 81.9 N/mm^2 in the case of the TF-Mini. This means that really high values of microhardness can be achieved, creating doubts about their reliability, especially because in the density distribution profile, the peaks where the measurements are performed, showed lower densities. However, for high SCFs, Wöll 2003 found Martens hardness up to 70 N/mm^2 for MCC, thus, it could be still viable. Furthermore, for the rhombus method applied to the Polygran® centre point ribbons, such a high HU were also found, what could confirm the results then obtained. Apart from the pressure effect, other interesting behaviours were observed while comparing the scales. For pure mannitol and MCC, the mean HU value for all the pressures is higher in the case of the TFC-Lab Micro than for the TF-Mini, although for the pure MCC these differences are unremarkable. This reflects the behaviour expected.

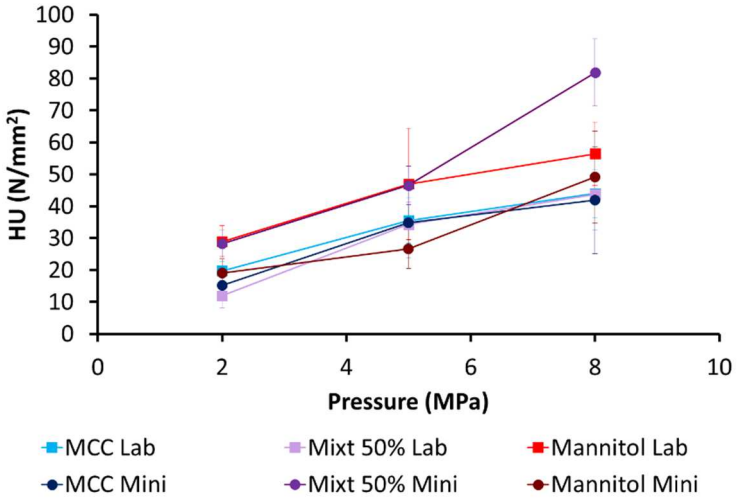

Figure 78: Microhardness for the main materials compacted under different pressures comparing the two scales of Freund-Vector supplier, mean±CI (n = 36, α = 5%).

If the differences between the materials are considered, for the TFC-Lab Micro, the HU value for pure mannitol and for all the pressures is the highest, then it decreases for the mixture and rises again for the pure MCC, although the differences are not that high between these last two. Similarly, for the TF-Mini the HU value for mannitol is lower than for the mixture and the pure MCC shows normally the lowest one but in this case, the differences between the mixture and the pure MCC are higher. Therefore, the effect of the proportion of MCC on the HU is not following a defined tendency. It is important to point out, that all these observations are made without considering the high error bars obtained in some occasions, probably due to the density distribution along the ribbon.

4.2.4.2.5. CORRELATION RELATIVE DENSITY-MICROHARDNESS

In order to mathematically confirm the results obtained regarding relative density and microhardness, both properties were plotted against each other for the TFC-Lab Micro and TF-Mini (Figure 79). If both ribbon attributes are mathematically correlated, this will reaffirm the results obtained although they were not expected from a physical point of view. For both correlations, a positive slope of the best fit curve is obtained, meaning that the two properties are proportionally related. However, in the case of the TFC-Lab Micro (a), the range in which the HU changes is smaller than for the TF-Mini (b). For the later compactor, the 50% mixture compacted at 8 MPa generates a great change in HU for almost the same density as the pure materials. Similarly, for the TFC-Lab Micro, relative densities under 65% generate HU lower than 20 N/mm^2, which after that moment, increases drastically in comparison to the other points.

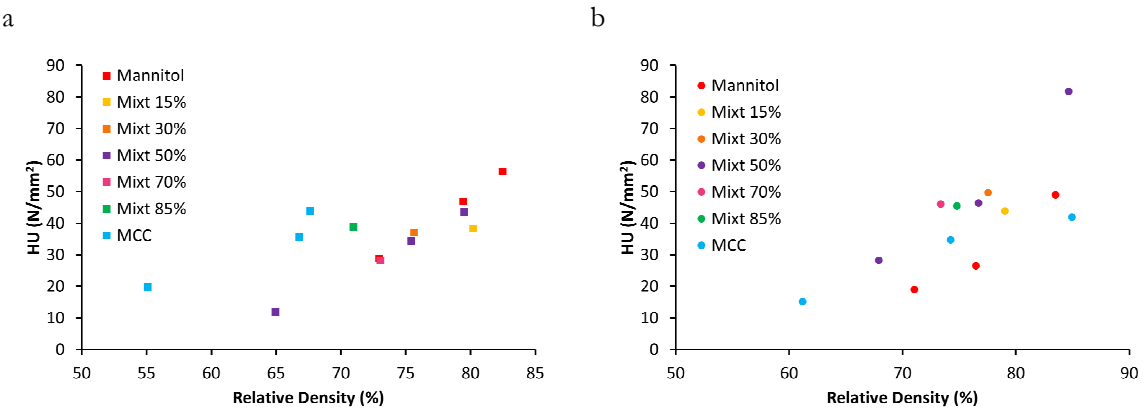

Figure 79: Microhardness results against the relative density for all materials compacted at the TFC-Lab Micro (a) and the TF-Mini (b), mean (n = 3).

Additionally, the t-test for the r was performed for both correlations. This value for the best fit line for each dataset is 0.722 for the TFC-Lab Micro and 0.749 for the TF-Mini. The tabulated value for an $\alpha < 0.01$ and 12 degrees of freedom (all the batches are considered together and they are in total 13), is 0.661, which means that the trend of both curves is statistically significant and not a product of chance. This confirms that although the results for relative density were not expected, those and the HU are correlated and go in the same direction, giving credibility to the results obtained.

4.2.4.3. GRANULE CHARACTERIZATION

Although a larger study regarding GSD was described in the previous chapter, as well as at the beginning of the present section, the ribbons produced at 5 MPa for the main materials were milled into granules. According to the experience gained during the roll compaction process, it was interesting to study the GSD for ribbons with and without a pre-treatment consisting of removing the fines before the milling. This could confirm what has been observed in the small Gerteis study, that the differences in fines could be due to lack of pre-cleaning of the samples.

4.2.4.3.1. GRANULE SIZE DISTRIBUTION

In Figure 80 a comparison of the scale for pure MCC, pure mannitol and the mixture milled with fines is plotted. The GSD obtained for the same process conditions in both compactors were compared in order to understand how the scale affects this property.

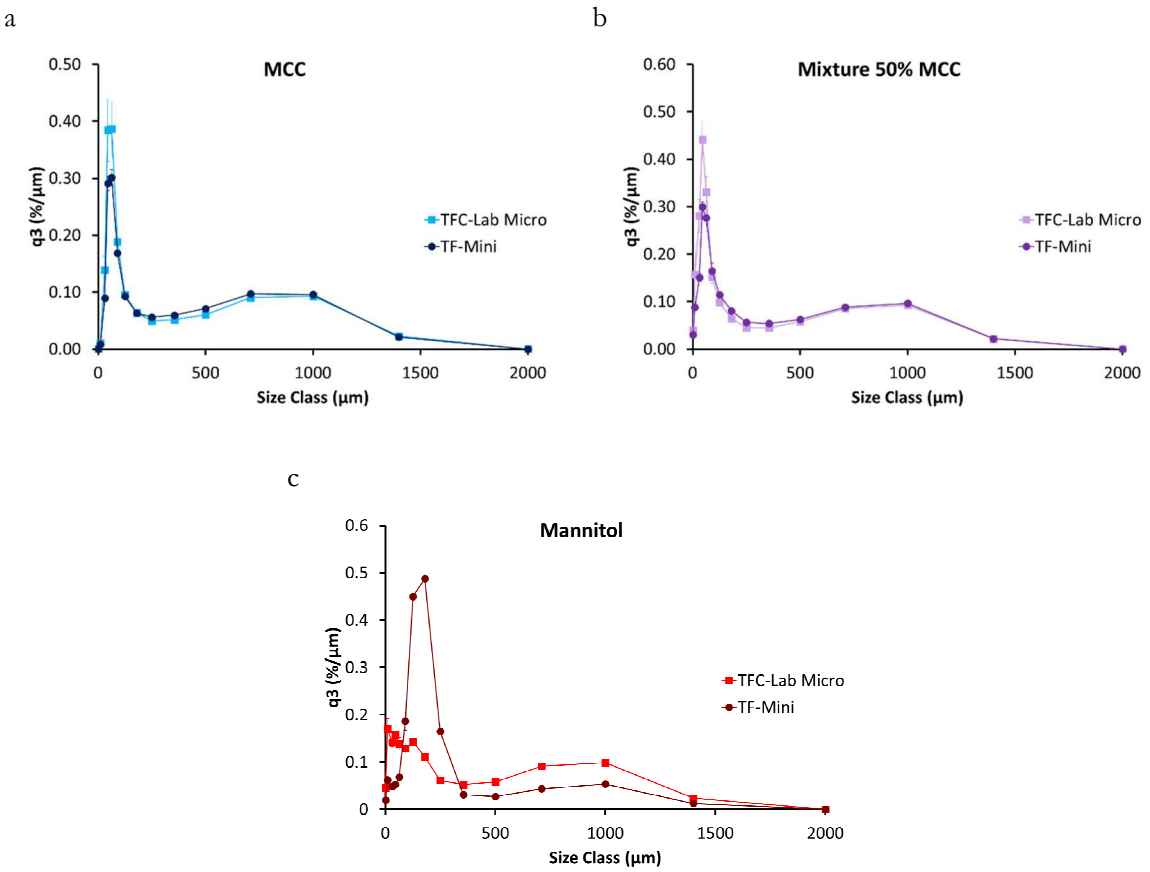

Figure 80: Representation of the q3 curves for MCC (a), 50% mixture (b) and mannitol (c) milled with fines and classified considering the scale of the roll compactor used for their production, mean±s (n = 3).

In these graphs, it can be observed how the GSD follows the same tendency in the case of pure MCC and the mixture, although the TFC-Lab Micro shows a higher amount of fines, which can also be related to the fact that the ribbons from this small-scale compactor are softer than for the TF-Mini. Nevertheless, for mannitol, the two curves look completely different and an enormous amount of fines was found for the TF-Mini. During the production and due to the good flowability of the mannitol together to the horizontal position of the rolls, a constant leak of powder took place. Therefore, these results are affected by this leakage of powder and thus, the information these GSD profiles give is not directly extrapolated from the properties of the ribbons.

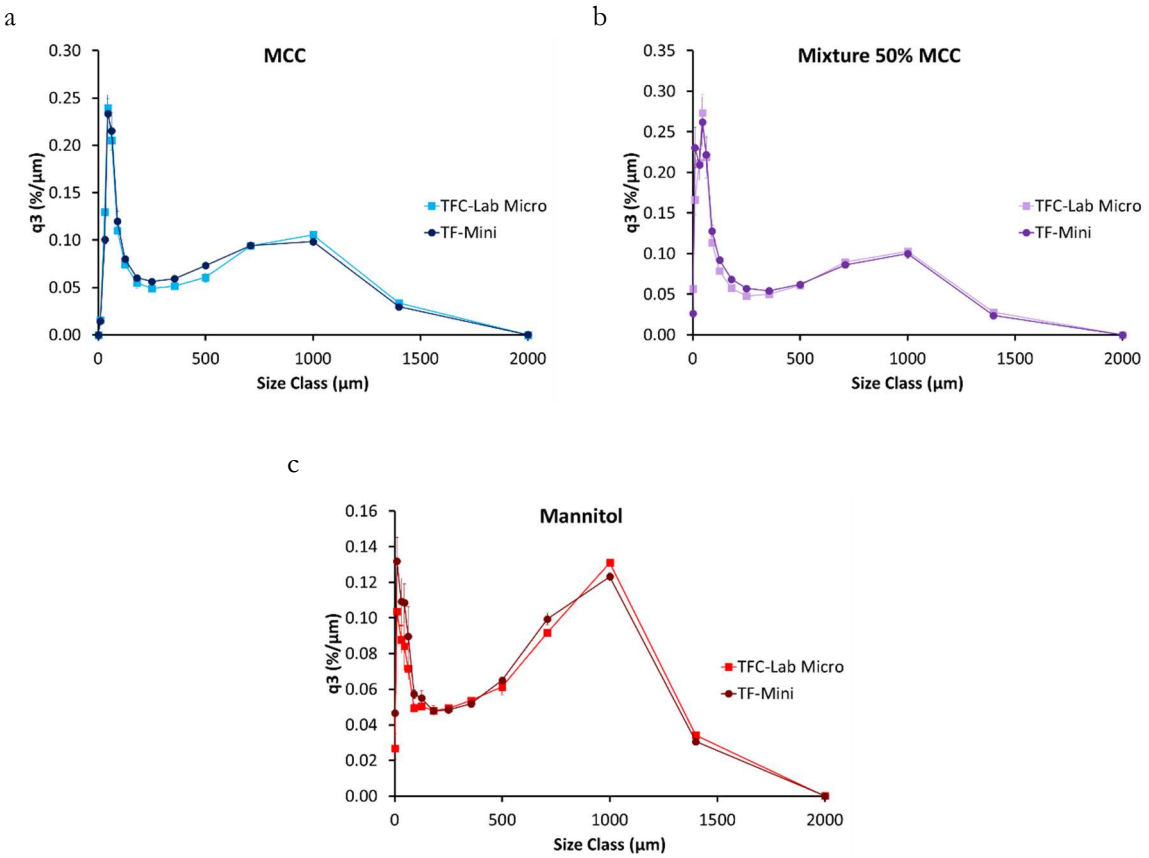

Figure 81: Representation of the q3 curves for MCC (a), 50% mixture (b) and mannitol (c) milled without fines and classified considering the scale of the roll compactor used for their production, mean±s (n = 3).

The granulation process was repeated after cleaning the ribbons from fines and removing the edges produced by the rim rolls. The new graphs obtained are plotted in Figure 81. From these representations, it can be seen how for all the cases, the tendency of q3 representations is the same for each powder, and the curves almost overlap, showing as well, the great differences between milling the ribbons with and without fines. For this reason,

further discussion was performed for the granules obtained from the ribbons cleaned. Nevertheless, it is especially striking that the curves of both scales overlap when the results of ribbon relative density have shown that the values obtained for MCC (66.8% for TFC-Lab Micro and 74.2% for TF-Mini) and mannitol (79.4% for TFC-Lab Micro and 76.5% for TF-Mini) are statistically different. From the Gerteis study, it was learnt that the ribbon relative density and the granule properties (D50 in particular) correlate, which means that different GSD profiles should have been obtained when milling ribbons with different densities. However, Sheskey et al. 2000 and Sheskey et al. 2002 found similar profiles for granules known to have different bulk densities. Nevertheless, they referred to the different granulation conditions used to explain the differences observed. Therefore, it can be possible that the milling process justifies these similarities, but considering the results, it could be concluded that the scale seems not to have an effect on the GSD.

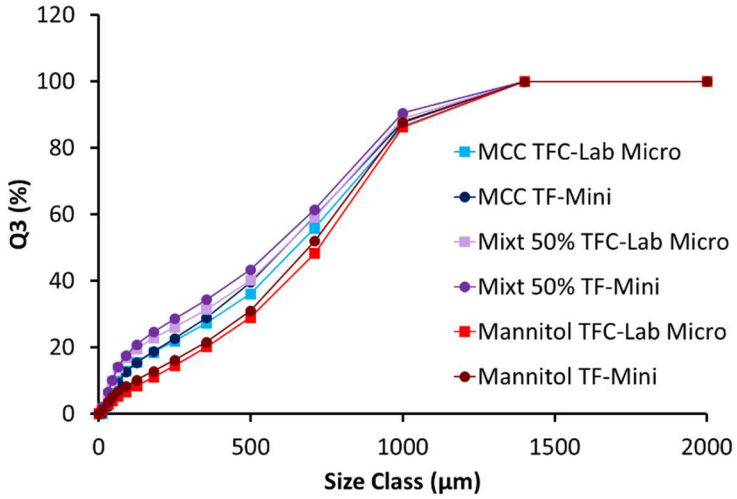

Figure 82: Comparison of the Q3 curve for all the materials and scales, mean (n = 3).

All Q3 curves obtained for the granulation without fines were plotted together in Figure 82 where the 3 materials are compared. Apart from the overlap of the curves, in this graph it can be observed how the mannitol has the higher proportion of large particles, while the mixture shows the greater proportion of smaller particles, being MCC in the middle. This points out the existence of a percolation effect, as was also observed in the study from the previous chapter.

4.2.4.3.2. AMOUNT OF FINES

This lack of impact for the scale is also reflected in the amount of fines obtained. The fines were again defined under 180 µm. For both compactors, the values are similar. The

amounts of fines obtained are collected in Table 11 for the ribbons milled with and without pre-treatment. Considering in the first place the pre-treated ribbons, mannitol obtained the lowest fines fractions in both compactors, while the highest values corresponds to the mixture. Therefore, the percolation effect is again observed, as the lowest values correspond to mannitol, followed by MCC and reaching the maximum for the 50% mixture.

Table 11: Amount of fines for the 5 MPa granules produced from ribbons pre-treated and those directly milled of MCC, mannitol and 50% mixture (n = 3).

MATERIAL	FINES WITH TREATMENT (%)		FINES WITHOUT TREATMENT (%)	
	TFC-LAB MICRO	TF-MINI	TFC-LAB MICRO	TF-MINI
MCC	18.5	18.8	27.3	22.7
Mixture 50%	22.8	24.6	30.6	26.1
Mannitol	11.0	12.8	23.9	51.2

In general, the fines fraction is low, however, this only indicates the amount generated during the milling process. The uncompacted material produced during roll compaction can drastically increase the final amount of fines in the granules, as can also be seen in the table above. The total amount of fines rises between 8 to 12% approximately for the TFC-Lab Micro when excluding the pre-treatment. However, for the TF-Mini the percentage increase is around 2 to 4% for the mixture and MCC respectively, but for the case of the mannitol granules, it becomes a 38% higher. Therefore, not only the differences between scales become larger, but also the total amount of fines increases.

Nevertheless, these fines are not directly related to the efficiency of the roll compaction process. The reason is that the selection of ribbons for the milling process could lead to more or less quantity of raw powder lying on the samples. Therefore, obtaining a representative sample of ribbons with uncompacted material becomes difficult. In order to measure more precisely the amount of fines by avoiding problems when collecting the sample, the initial bag in which the ribbons were collected was sieved using a size of 1 mm. In this manner, the ribbons remain on the sieve and the uncompacted material passes through it. The resulting powder was weighed on a benchtop balance (Sartorius Universal MA AF 200, Sartorius

GmbH, Germany) and the percentage of fines in respect to the total initial sample weight was calculated and presented in Table 12.

Table 12: Amount of fines (considering a 1 mm sieve) for the 5 MPa ribbons MCC, mannitol and 50% mixture in respect to the total initial sample weight.

MATERIAL	FINES FROM RIBBONS (%)	
	TFC-LAB MICRO	TF-MINI
MCC	20.9	3.4
Mixture 50%	18.6	13.0
Mannitol	30.9	65.4

Those values in the table can be affected by the ribbons already milled or by the fact that non individual cleaning ribbon per ribbon was performed at this stage. Nevertheless, the main conclusion is similar to the one that could be extracted from the previous data: the roll compaction process for the TF-Mini is in general more efficient regarding amount of uncompacted powder, however in the case of mannitol, more than the half of material is lost during the compaction. In the particular case of mannitol, the amount of uncompacted material is higher for the present case than for the ribbons without pre-treatment before milling. This probably means that not a representative amount of fines was taken for the milling without pre-treatment, omitting in this manner, an important amount of uncompacted material.

4.2.5. COMPARISON LINES: RELATIVE DENSITY

In this chapter, three individual scale-up studies have been presented. As two of the lines have compactors with similar design, it is interesting to establish some comparisons between the relative density results obtained from Gerteis and L.B. Bohle compactors. The Freund-Vector line will be excluded not only for the differences regarding design, but also because the results obtained seem not to be highly reliable. Actually, there are some differences between the lines investigated in this part. On the one hand, the roll surface and sealing system is different between both lines. On the other hand, the feeding configuration (inclined for Gerteis and horizontal for L.B. Bohle) and the system which applies the SCF differs in both providers. Gerteis uses hydraulic pressure, while L.B. Bohle compactors are equipped with a spindle motor.

4.2.5.1. EFFECT OF SCALE AND MATERIAL

The 3 repetitions of the centre point were used as reference conditions for general data comparison. Global average and standard deviation values of the ribbon relative density for the centre point conditions (6 kN/cm SCF, 2.25 mm gap and 3 rpm roll speed) for MCC, 50% mixture and mannitol were depicted in Figure 83 for the Gerteis (a) and L.B. Bohle (b) compactors. If the influence of the material is taken into consideration, the lowest value is always obtained for the MCC ribbons as already discussed, while the relative density increases for the mixture and reaches the maximum value for the samples of mannitol.

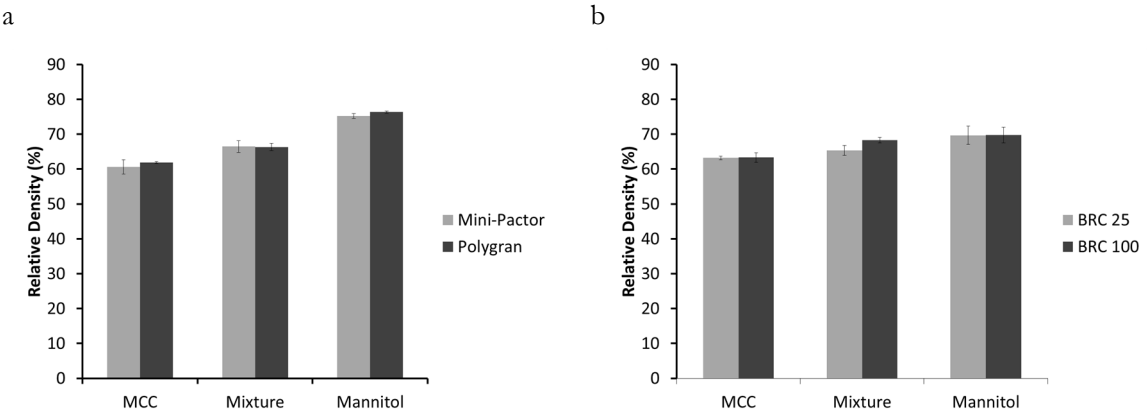

Figure 83: Relative density for MCC, mannitol and the mixture for the centre point conditions comparing the two scales of Gerteis (a) and L.B. Bohle (b) suppliers, mean±s (n = 3).

However, if the same material is compared in both scales, the relative density values for all the powders compacted in the machines from Gerteis are statistically equal for $\alpha = 0.05$ and $n = 3$. For the BRC 25 and 100, a statistically significant difference was found only for the mixture, however, when compacting MCC and mannitol at these conditions, the values obtained are considered to be identical (for $\alpha = 0.05$ and $n = 3$). Standard deviation was found to be slightly higher for the samples produced with the compactors from L.B. Bohle.

In order to further understand the effect of the material, Figures 35 and 62 (page 85 and 116 respectively) can be compared. For both lines, a decrease in the density when increasing the proportion of MCC is again observed, although the decrease is more pronounced for Gerteis compactors, as previously discussed. However, if the Mini-Pactor® and the BRC 25 are compared, generally, the values on the Gerteis compactor are up to a 5.7% higher, only for the 85% mixture and the pure MCC the BRC 25, presents densities up to a 2.6% greater. When comparing the larger scales, the highest values are for the BRC 100 and correspond to the 50% mixtures until the pure MCC. For these 4 cases, the density at the BRC 100 is up to 2.0% higher, however, for mannitol and the 15 and 30% mixture, the Polygran® has values until 6.6% larger. Therefore, a non-clear behaviour can be addressed, but the fact that high proportions of MCC result in denser ribbons when compacting using the L.B. Bohle compactors. Additionally, the F and t-test can be performed (for an $\alpha = 0.05$ and $n = 3$) in order to see if there are variances between both scales, the values resulted statistically equal for all mixtures produced at the Gerteis compactors, however, for the L.B. Bohle those batches produced from 50% and 85% MCC showed statistically significant differences.

4.2.5.2. DIFFERENCES IN SCALE EFFECT

If the coefficient plots obtained for the modification of the DOE including the scale as a factor (Figures 28 and 60, pages 76 and 114 respectively) are compared, the main conclusion that can be extracted is that only MCC compacted at the L.B. Bohle machines is unaffected by the scale. Nevertheless, and although the scale is not significant for all the combinations, it is interesting to stress that this factor has the opposite relationship for the mixture and mannitol when using different lines (for MCC in both families of compactors, the scale has shown an inverse, though not significant, effect). In other words, for the mixture, the scale leads to lower density for the Gerteis compactors, while for the L.B. Bohle an increase on this factor will bring to denser ribbons. For mannitol, the effect is direct for Gerteis and

indirect for L.B. Bohle. This diverse behaviour of the mixture and mannitol is unexpected. The relative density results obtained for the Gerteis compactors gained confidence when the microhardness was confirmed to follow the same tendency. Nevertheless, for L.B. Bohle, no microhardness results are available that could corroborate the direction of the influences of the scale.

If the whole data set is analysed, i.e. all ribbon densities obtained for the 3 materials, approximately half of the batches show a higher density for the small scale for Gerteis ribbons as well as for L.B. Bohle. This means, that the distribution of results is more or less homogenous, i.e. there is not a clear tendency of the small scale (neither the larger) to always present denser ribbons. However, if the densities obtained are classified according to the material, an opposing effect is observed. For MCC, denser ribbons are achieved when compacting with the Mini-Pactor® and the BRC 25 than the respective large scales. However, although the mixture compacted in the Mini-Pactor® also results in denser ribbons, the larger BRC 100 produces samples with higher relative density, compared with the smaller BRC 25. For mannitol, the ribbons compacted in the Polygran® are denser than when using the small scale, but for the L.B. Bohle compactors, the BRC 25 is producing the higher density samples compared with the large scale. In other words, there is no consistent trend between both compactor lines on how the mixture and mannitol behaves when using the small or large scale.

In order to further understand this problem, the same scales for the different materials were compared, i.e. the Mini-Pactor® vs. the BRC 25 and Polygran® vs. BRC 100. This allows for observing if there are similarities in the tendency of the relative density according to the roll configuration. In Table 13 and in order to facilitate the interpretation of results, the values obtained are collected by deducting the relative density of the L.B. Bohle compactor from the corresponding value with the Gerteis machine (Result = Gerteis – L.B. Bohle). This deduction is always performed for specific compaction conditions and using the same material. In other words, the objective is to compare both small and large scales in order to see which family of compactors generates higher densities, and if the trend is the same for all the materials. When calculating the differences between both small scales and both large ones for the main materials, the same trend is observed for MCC and for mannitol, which means that normally for both scales, one family of compactors presents higher density. In other words, for MCC, in most of the cases, the highest value regarding relative density is obtained with the L.B. Bohle compactors, while for mannitol, Gerteis tends to produce denser ribbons. However, this is not the case for the mixture, which shows a different tendency when comparing the small scales

than when relating the large ones. This means that for the small scales, Gerteis shows denser ribbons, while for the large scale, L.B. Bohle shows higher density. A possible reason for these differences could be a partial segregation of the blend or an inappropriate mixing procedure before its compactions.

Table 13: Differences in ribbon relative density when it is deducted from L.B. Bohle compactors the value obtained for Gerteis for the same conditions (production and material). Please note that in this case the small and the large scales are compared between each other. Values positive are marked, meaning that in that case, the density of the Gerteis compactor is higher.

BATCH NUMBER	DIFFERENCES RIBBON DENSITY (%) MINI-PACTOR – BRC 25			DIFFERENCES RIBBON DENSITY (%) POLYGRAN – BRC 100		
	MCC	Mixt 50%	Mannitol	MCC	Mixt 50%	Mannitol
1	-0.79	-1.93	0.62	-2.17	-0.98	5.83
2	-1.32	1.87	2.10	0.37	-0.11	9.02
3	-2.32	3.55	6.29	-3.02	-0.38	5.99
4	-2.84	4.69	5.85	-0.40	0.47	4.58
5	-0.94	0.21	-0.19	-4.84	-2.46	6.80
6	-3.24	4.84	1.61	0.32	-0.73	5.62
7	0.05	1.04	1.35	-5.00	-2.73	6.36
8	-2.57	3.10	1.63	-2.13	-0.85	5.14
9	-2.65	1.09	5.53	-1.46	-1.96	6.58

In a general balance, it can be concluded that the reason why the results go in different directions for both suppliers is unclear. For MCC produced using both families of compactors and under the same conditions, in general lower relative densities are obtained for the Gerteis pieces of equipment than for the BRCs. However, for mannitol the density was normally minor in the case of the L.B. Bohle compactors. An intermediate behaviour can be observed for the mixture, which shows smaller values for the BRC 25 than for the Mini-Pactor® and also lower for the Polygran® than for the BRC 100.

4.2.5.3. CORRELATION MINI-PACTOR®-BRC 25

The Mini-Pactor® and the BRC 25 are compactors not only with a similar design but also the same roll dimensions. Therefore, it is interesting to compare their results obtained in a deeper manner. Nevertheless, it is important to keep in mind that, as described in the literature, the differences in the ribbon density can be due to assembling the compactors with different roll surface (Rambali et al. 2001; Dawes et al. 2012; Iyer et al. 2014a) and/or sealing system (Cunningham et al. 2010; Akseli et al. 2011; Nesarikar et al. 2012a; Mazor et al. 2016; Wiedey et al. 2016). Therefore, the results are not completely comparable, as between both machines there are some differences regarding design as well as diverse sealing systems and roll surfaces were used. Nevertheless, in Figure 84 a correlation between both machines for the relative density regarding the 11-runs DOE is presented.

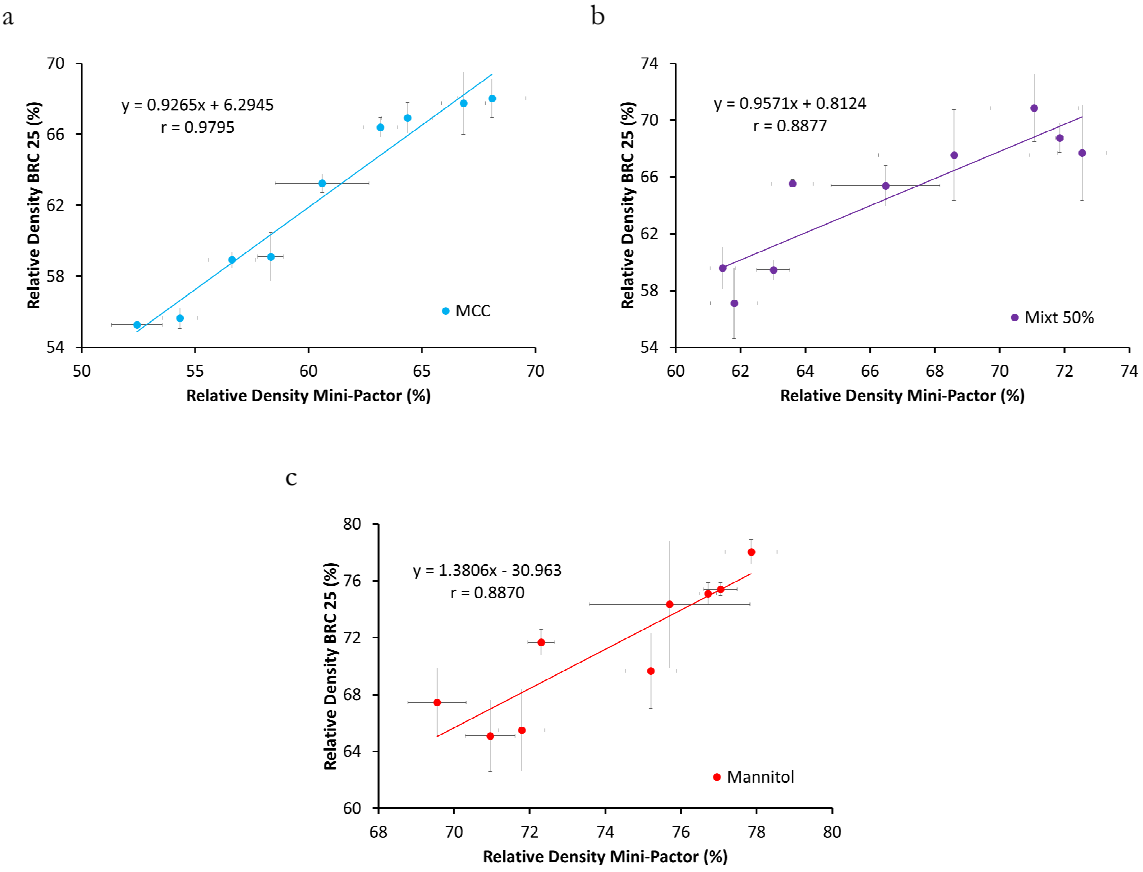

Figure 84: Correlation for relative density of ribbons produced at the same manufacturing conditions between the BRC 25 (L.B. Bohle) in the Y-axis and the Mini-Pactor® (Gerteis) regarding the compaction of MCC (a), the 50% mixture (b) and mannitol (c). The best fit line equation and the correlation coefficient are also presented, mean±s (n = 3).

The correlations are in general good with relatively high r values, which overcome the tabulated value of 0.872 for $\alpha < 0.1\%$ and 8 degrees of freedom. From this aspect the best correlation would be the one obtained for MCC. Regarding the equation of the best fit line, the correlation for the mixture has a slope close to 1 and a Y-intercept almost negligible. Therefore, the latter correlation would be the best of all the ones obtained. As a result of this evaluation, it can be concluded that the relative densities in both compactors is not identical but values in both machines are related to a greater or lesser extent. The differences between both families could be attributed to the diverse compactor designs, the different sealing systems and/or roll surfaces used, which have already been shown to generate varying density distribution profiles.

4.2.6. SUMMARY

Three individual scale-up studies for two compactors developed by Gerteis, L.B. Bohle and Freund-Vectors were performed. Later, the results obtained for the first two lines were compared and discussed together. All scale-up studies tried to evaluate the combined effect of the roll compaction process parameters, the mixture composition and the scale.

For the Gerteis study, the evaluation of the relative density, that was later confirmed to follow similar tendency as the microhardness, led to a general conclusion that denser ribbons are obtained for high SCFs and low gaps, roll speeds and content of MCC. Furthermore, and after evaluating the two complete DOEs for process and mixture investigation, the same profile was observed. The only noteworthy aspect from the comparison of both coefficient plots, was the fact that the proportion of MCC when evaluating the 7 levels of mixtures was more important than even the SCF itself. The significance of the quadratic effects of the SCF and MCC (opposite influence than the initial factor) was also confirmed. Additionally, the inverse effect of the gap-scale and MCC-scale interactions, as well as and the SCF-MCC and the Gap-SCF with a proportional influence, was observed for both analyses or for the one which factors allow the combination. Some of those were not common in both analyses, but those which appear in both coefficient plots lead to the same message. The scale was never significant for the present analyses, nevertheless, its importance was reflected in the significance of the interaction in which it participates. The change in scale was neither affecting the density distribution profile, as for both compactors and materials, curves with higher values in the middle and lower in the edges of the ribbon were found due to the use of cheek plates. Furthermore, the small evaluation of the GSD seems to confirm and correlate with the results of the ribbon relative density as well.

In the case of L.B. Bohle compactors, similar conclusions can be extracted from the analysis of the relative density data. However, in this case, these machines seem to be able to compact MCC mostly with statistically equal densities in both scales. The comparison of ribbon relative density between Gerteis and L.B. Bohle, led to variations when using one line or the other, although not extremely pronounced. The most interesting differences were the lack of significance of the scale in any manner (as pure factor or as part of an interaction) for the MCC compacted only by the L.B. Bohle machines as well as the opposite direction of the scale's effect on the coefficient plots for mixture and mannitol. Regarding density distribution, a clear profile according to the sealing system used was found for the large scale. As rim rolls were used, the ribbon was denser at the edges than in the middle, although this behaviour

could not be addressed for the small-scale ribbon. Nevertheless, due to the great number of cuts and breaks within the ribbon for the small compactor as well as the fact that it was incomplete, it was not possible to conclude that the differences in both profiles are due to the scales used.

The last scale-up study with the Freund-Vector compactors results more difficult to interpret and a higher variability was obtained, what makes these compactors less attractive than the other lines investigated in this thesis. The ribbon relative densities and microhardness seem to follow the same tendency, and they confirm that the results are normally higher for the large scale (TF-Mini). Nevertheless, this was unexpected as according to the conversion factor, the SCF should be higher in the smaller scale and the densification in this compactor should be also higher if the differences in roll diameter are considered. This probably means that at least one of the conversion factors used is wrong. The profile for the density distribution, although different for both materials, was consistent between both scales. The GSD results showed however, no effect of the scale and confirmed as well the great amount of fines that were obtained during the roll compaction.

As the main conclusion from this second chapter, it can be affirmed, that although suppliers, especially like Gerteis and L.B. Bohle, try to facilitate the users of their machines the scalability of the roll compaction process, they normally cannot achieve such an objective, even for materials like MCC which are easy to handle. In this respect, when these manufacturers are designing a new scale, the roll diameter is kept constant and the SCF is used to facilitate the operator the selection of the same conditions in both machines. In spite of these efforts, it has been proven that in order to obtain the same density of the ribbons, an adaptation of the roll compaction process parameters is required.

4.3. MODELLING

4.3.1. INTRODUCTION AND OBJECTIVES

As has been proven in the previous chapter, the scale-up of the roll compaction process is not as simple as the suppliers would like it to be. Depending on the material, the change in scale can be critical or irrelevant for the ribbon properties. For this reason, the ideal way to transfer the process between scales would be the use of models that can be fed with the data from the experiments on the small scale. The fitting of the model would allow for prediction of the production conditions required for obtaining the desired ribbon relative density on the large scale. As previously described, the models can be classified in mechanistic models and approaches based on dimensional analysis.

A model should gather different characteristics. Ideally it is desirable that it should be simple, fast and accurate in order to make its use preferable. Simple refers to easy handling and application of the model. It is desirable that any user can work with the approach of interest and in the case of the mechanistic models, also that the operator is able to understand the principles which it is based on, in order to identify any potential mistake that could be made. Furthermore, a model should be also simple from a practical point of view, i.e. that the results obtained from it, are easy to convert in the conditions that should be set on the new machine to obtain the desirable relative density. Secondly, an approach should be fast to apply. This means not only that the application of the model requires not much time to be run, but also that the data needed for its fitting is also easily and quickly collected. Finally, a model is always preferable that is accurate and gives the same results as the real performance of the experiment. However, it can be complicated to gather all these requirements, especially the last one, and therefore, no perfect model exists.

Several approaches are available in the literature for scaling the roll compaction process up. From all those previously described, the most interesting to test in this thesis is the mechanistic model of Reynolds et al. 2010 and the DVs developed by Rowe et al. 2013 and Boersen et al. 2015. Although other models are presented in the bibliography, those already mentioned were selected according to the accessibility or simplicity of the different approaches. In this section, those models will be applied for the data available from the scale-up studies previously presented. As has been concluded from the discussion in the preceding chapter, the scale-up study performed at the Freund-Vector compactors should be excluded from model evaluation because it was not performed in comparable production conditions as

is the case of the other lines (roll force and linear roll speed are different). Nevertheless, the data from these compactors will be used, due to model requirements. For testing the selected models it was preferably chosen the results corresponding to the ribbon relative density of the 11-runs DOE for the main materials compacted at the Gerteis and L.B. Bohle compactors. Although for the first supplier more data is available, only the experiments related to the 11-runs DOE were selected as they were performed for both lines, and this facilitates the discussion of the models. When needing to feed the data from the Freund-Vector line, the relative density of the main materials also will be used. Independent of the compactor line selected and in order to facilitate the work and graph interpretation, the data used will be always the global mean value, excluding the standard deviation. Finally, in this chapter another model will be proposed for the scaling up of the roll compaction process. This approach will consist on a DV which has been developed based on dimensional analysis.

4.3.2. MODELS IN LITERATURE

4.3.2.1. MECHANISTIC MODEL: REYNOLD'S APPROACH

This is a mechanistic model based on the principles described by Johanson 1965, which basically states that the ribbon relative density can be predicted as a difference in volume between nip area and gap. Therefore, this mechanistic model helps to further understand the process. The most important contributions from the authors to the Johanson's model are the modification of the nip pressure requirement by using the peak pressure (P_{max}) and the inclusion of the feeding system in the approach. This model is the first one tested for scaling the roll compaction process up. Therefore, the objective is to investigate if this approach can successfully predict the ribbon relative density which would be obtained in a larger scale, based on the results from the small scale.

As a prior requirement, this methodology needs shear cell data of the incoming powder, i.e. the effective angle of internal friction (δ_E) and the angle of wall friction (ϕ_W), whose values can be found in Table 14. These parameters are needed to calibrate the model and can be easily and rapidly measured. Nevertheless, those results obtained from the ring shear tester highly depend on the measuring conditions. This means that slightly different setups (diverse preconsolidation loads) would lead to important variations in the resulting angles. For this reason, the methodology followed must be the same for all materials tested together.

Table 14: Measured frictional angles for the starting materials.

MATERIAL	δ_E (°)	ϕ_W (°)
MCC	43.6	11.6
Mixture 50%	41.5	14.4
Mannitol	38.0	14.8

This model allows calculation of a single parameter, P_{max} through equation 7 (page 10), which describes the extent of compacting stress on the material as a result of differences in geometry and operating parameters, providing a basis for transferring process understanding between different roll compactors. In the methodology, the material compaction parameters, K and γ_0, are estimated using ribbon density data. Once estimated, these parameters can be used in the model to predict ribbon densities for different scales of roll compactor as described in the introduction (page 10).

To mimic a typical development workflow, the model was calibrated using the data from the small-scale compactor (the Mini-Pactor® for the Gerteis case and the BRC 25 for L.B. Bohle compactors) and then applied to predict the ribbons density on the large scale. Thus, the material compaction parameters (K and γ_0) are estimated for each small-scale equipment and the model predictions compared with the large-scale equivalents. In Table 15, the K and γ_0 values are presented, as well as the relative density root-mean-square error (RMSE) and the bias expressing the percentage of error. The RMSE refers to the quality of the correlation between the predicted and the observed values. However, the bias represents the percentage difference between the model average prediction and the experimental data, and depending on the sign, the estimation of the model is higher (positive percent) or lower (negative value) than the experimental data measured. In Figure 85, the graphical comparisons between the experimental data obtained for both scales and the predictions given by the model are collected for the different materials and compactors.

Table 15: Values of material compaction parameters together with model results regarding RMSE and the percentage of error for each material produced at the both scales of compactors from Gerteis and L.B. Bohle.

MATERIAL	MODEL	K	γ_0	RELATIVE DENSITY RMSE (%)	RELATIVE DENSITY BIAS (%)
MCC	Gerteis	4.19	0.215	1.7	0.1
	L.B. Bohle	4.59	0.240	1.4	0.1
Mixture	Gerteis	6.75	0.338	1.8	0.9
	L.B. Bohle	5.68	0.294	4.4	-4.0
Mannitol	Gerteis	10.16	0.462	1.6	-1.7
	L.B. Bohle	6.72	0.359	5.2	4.1

The first conclusion that can be extracted from this table is that the RMSEs are in general low, which means a good fitting of the model. It is important to stress out that the RMSEs are primarily affected by the degree of scatter within the raw data rather than deviation from model. If the bias is analysed, for the case of MCC, in both families of compactors, those values are low. This means an excellent prediction of the larger scale compactor by the model as can be seen in Figure 85a with over-predictions of only 0.1%. This points out the easy handling of this material, at least in comparison to the brittle mannitol. However, when increasing the proportion of mannitol, the quality of the prediction decreases. For the mixture (Figure 85b), up to a 4.0% of under-prediction is obtained for the L.B. Bohle compactors, while for the Gerteis compactors an overestimation of 0.9% takes place instead. A similar case is observed for pure mannitol (Figure 85c), where a higher percentage of error is again found for the L.B. Bohle, but in this case, an over-prediction of 4.1% occurs while for the Gerteis an underestimation of 1.7% takes place. This latter value, although higher than for the mixture, is marginal compared to the variation in the raw dataset. For the 50% blend and mannitol, the model predicts more accurately when the compactors from Gerteis are used. However, it is important to point out that the scattering on the results can be also explained by the differences between the two scale-up studies. For the compactors of Gerteis, the increase in the roll width is twice the size of the small scale (from 25 mm to 50 mm), while for the L.B. Bohle machines, the width of the large scale is 4 times higher (from 25 mm to 100 mm). This could explain the higher differences between experimental data and the prediction of the model. Furthermore,

there are some differences between both families regarding compactor design that may also have an impact.

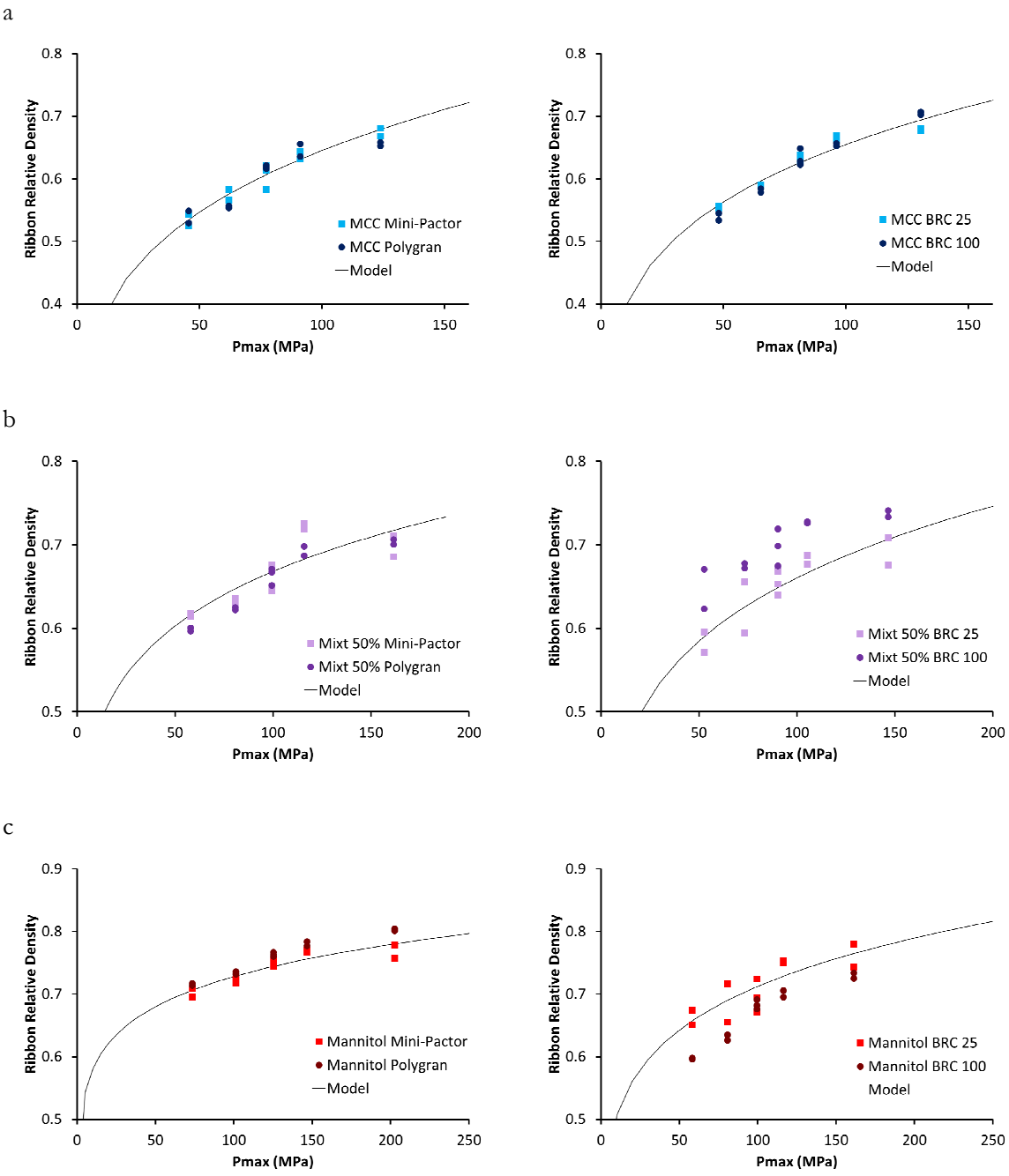

Figure 85: Comparison of the model with the experimental data by presenting the P_{max} estimation vs. the relative density of the ribbons for the Gerteis compactors (left) and L.B. Bohle (right) regarding MCC (a), the 50% mixture (b) and mannitol (c), mean (n = 3).

Another possible reason for these deviations between the suppliers could be the different sealing systems and roll surfaces uses which have an impact on the ribbon relative density and its measurement. Different configurations can affect the nip angle which defines

where the compaction starts. Although the nip angle is constant for a material, the use of different roll surfaces may affect its value and therefore, the densification. The friction angles obtained from the shear cells data are used to calculate the nip angle by finding the point where the slip and no-slip frictional boundary conditions are equal. However, in practise this is probably only relevant for smooth rolls, as the knurling pattern will affect the wall friction and this cannot be easily mimicked by the measurement. Smooth surfaces present lower nip angles, as there is less friction between the powder and the metal surface of the rolls; however, the knurled ones tend to grip the powder and this results in larger nip angles (Johanson 1965; Miller 2005). As the nip angle increases, the roll force is distributed over a larger compaction zone and therefore, the compacting pressure applied to the powder will decrease, leading to lower densification and, therefore, lower ribbon relative density. Therefore, changes in the nip angle caused by differences in the powder interaction with different roll configurations may be the cause of some of the deviations observed in the model.

For the Gerteis equipment, the mixture is under-predicted and the pure mannitol overestimated, while the opposite is seen for the L.B. Bohle compactors. However, the model is highlighting the trends already observed in the raw data. Although no a clear explanation was found for the different directions of the scale's effect for both suppliers (section 4.2.5.2., pages 144-146), it seems that as the material becomes more brittle (i.e. moving from MCC to mannitol), the effect of scale becomes more pronounced in a way that is neither captured by the model. It has already been confirmed in the precedent chapter that the scale affects to a greater or lesser extent, the compaction of the 50, 30, 15% MCC and pure mannitol mainly. This is likely to be caused by complexity in the way the roll configuration (surface and sealing system) interacts with the powder, which could cause changes in the nip angle, leading to an increase or decrease in the peak pressure and therefore, density. These effects may also be exacerbated at increased scale (roll width) due to changes in the lateral pressure distribution, again influencing the size and stress distribution in the compacting zone. Finally, the ribbon pieces for the L.B. Bohle compactors are small, especially for the BRC 25, and thus, the treatment and sampling of them may have an impact. It is possible that the selection of pieces big enough to be handled and the breaking of the BRC 100 samples, (which may have not covered a representative length across the ribbon), would have an impact on the results.

Independent of all the considerations which could try to explain the under- or over-predictions, it can be concluded that the model works accurately and predicts with an assumable error the ribbon relative density. The approach is able to better scale-up the

compactors developed by Gerteis. Apart from that, the model requires few initial properties which are also easily and rapidly obtained. The main inconvenience of the approach according to the data tested, is that although its complexity from physical basis, there are difficulties to adapt to different sealing systems and roll surfaces. Even considering this, the model is giving an acceptable or even excellent prediction of the ribbon relative density and allows the transfer between scales.

4.3.2.2. DIMENSIONAL ANALYSIS

The DVs are attractive for use as they consist of just an equation which can be substituted to obtain the conditions needed to produce ribbons with the same relative density in different scales. However, due to the simplicity behind these, they can be less accurate than the mechanistic models based on physical principles. The most used method to calculate DV is the Buckingham's π theorem consisting of the creation of dimensionless π-products which can be plotted against among them in order to study their relationship and establish the final equation. However, this is not the only methodology and they can be also calculated by other techniques.

4.3.2.2.1. MODIFIED BINGHAM NUMBER

The modified Bingham number Bm* developed by Rowe et al. 2013, is the first DV that will be tested and it is defined by equation 8 (page 12). From this formula, some conclusions can be already extracted before starting the application of the model to the dataset. The first peculiarity of this variable is that it comes from a modification of a relationship already existing in the literature known as Bingham number. It has not been obtained from the Buckingham's π theorem, however, this does not mean that the model is poor regarding the process understanding, as the expression describes the ratio between yield and viscous stresses. Secondly, an aspect that it especially noteworthy is the fact that the terms included in this equation are in some occasions not directly related to the process conditions, material or machine, like is the case of the Cs which is the screw speed constant or the SA_{roll} defined as the surface area of a roller compactor roll. These parameters have to be transformed back into process parameters or roll dimensions. This, in combination with the fact that there is no relationship on the equation for the roll pressure or SCF, makes this DV not highly attractive from a practical point of view. Once the equation is substituted, the result leads to new calculations and transformations, which will not give the roll pressure or SCF. In a daily

performance in a lab, the most important parameter, as has been also proven during the whole thesis, is the SCF, and therefore, producing ribbons with a target relative density without this value seems to be impractical. Nevertheless, this lack of force or pressure term in the expression, has as an advantage that it extends the use of the Bm* to any type of compactor independently of the units used.

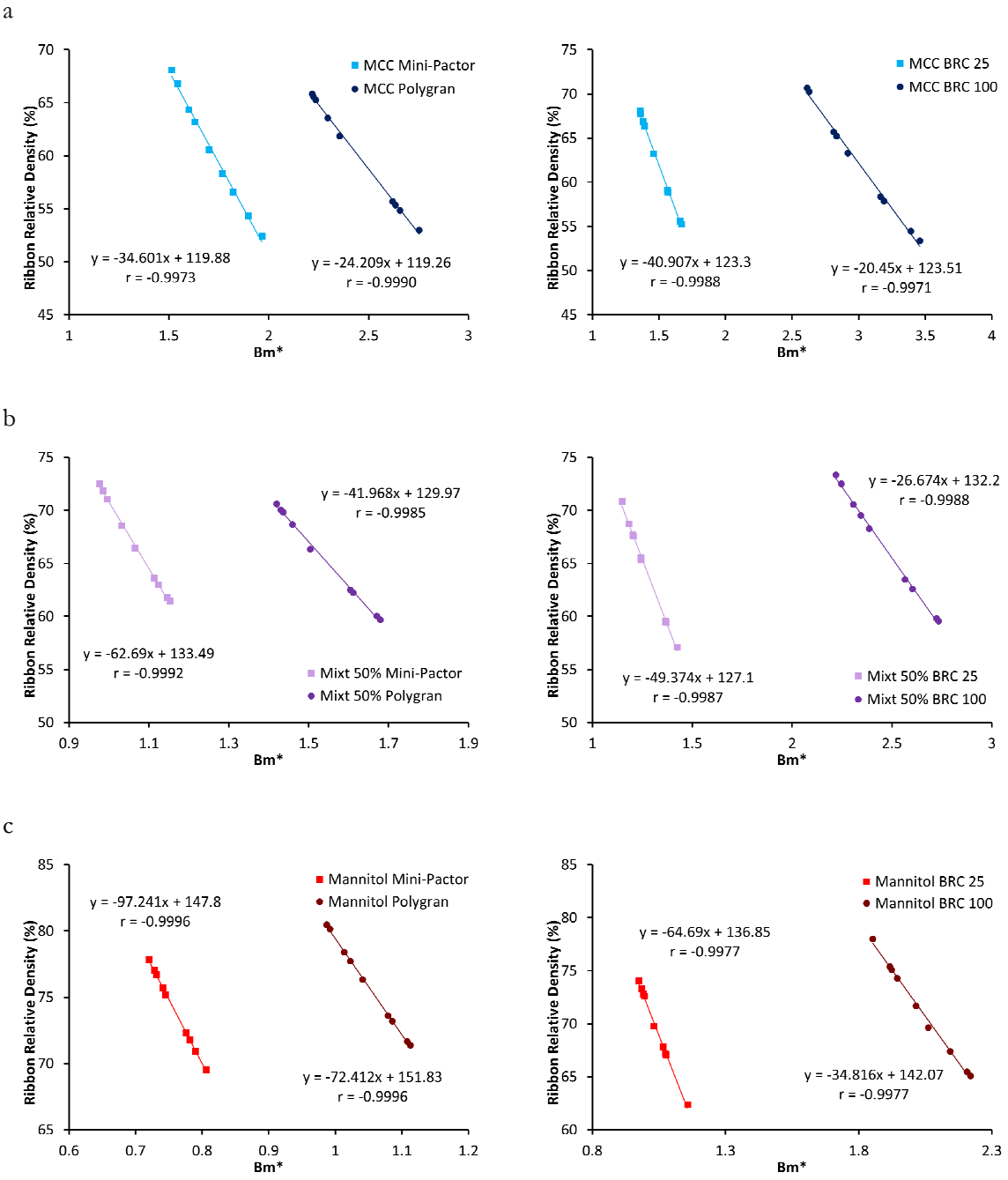

Figure 86: Comparison of the Bm* vs. the relative density of the ribbons for the Gerteis compactors (left) and L.B. Bohle (right) regarding MCC (a), the 50% mixture (b) and mannitol (c), mean (n = 3).

In Figure 86 is presented the correlations between the values obtained for the Bm* and the real ribbon relative densities for Gerteis (on the left) and LB. Bohle (right side) compactors. This type of plot (ribbon relative density against DV value) is the one used to evaluate the quality of the model. The correlations are for both scales and for the main materials: MCC (a), 50% mixture (b) and mannitol (c). The first aspect that draws the attention is the excellent correlations that are obtained with r values never lower than 0.99, overcoming by far the tabulated 0.872 for $\alpha < 0.1\%$ and 8 degrees of freedom (centre point mean was again used). However, the reason why such a perfect correlation is obtained is due to the calculation procedure of the Cs or screw speed constant. This parameter was already described by Reynolds et al. 2010, and it can be experimentally obtained based on the throughput measured or can be mathematically calculated considering the difference in volume. In both cases, the equation 16 is applied independent of the way to obtain the throughput.

$$Cs = \frac{m}{FS} \qquad \text{Eq. 16}$$

where m is the mass rate or mass throughput and FS refers again to the feed screw speed. As the compactors involved in this study count with 2 screws, the FA was selected for this calculation as it is the screw determining the powder taking from the chute. In case of not having measured the throughput in advance, this m value can be calculated from equation 17 depending on the differences in volume:

$$m = \frac{G \cdot W \cdot \pi \cdot D \cdot RS \cdot t \cdot \rho_{rib} \cdot \rho_0}{100} \qquad \text{Eq. 17}$$

where G is the gap width, W the roll width, D the diameter, RS the roll speed, t the time for the throughput (1 min), ρ_{rib} is the ribbon relative density and ρ_0 the true density of the powder. Therefore, for the present evaluation of the model with the data available from this work, the Cs can be calculated as described in equation 18:

$$Cs = \frac{G \cdot W \cdot \pi \cdot D \cdot RS \cdot t \cdot \rho_{rib} \cdot \rho_0}{FS \cdot 100} \qquad \text{Eq. 18}$$

The reason why such an excellent adjustment is obtained is because if this Cs formula was substituted in the equation of the Bm*, most of the elements would be nullified and the resulting expression would be only affected by the ribbon density and the SA_{roll} (expression of the size of the roll). This can be seen in equation 19, where the Bm* formula after the substitution and annulation of the repetitive elements is presented. Therefore, excellent correlations between the Bm* and the ribbon density are obtained because this DV is only

influenced by this property and the compactor dimensions. Therefore, the model does not work properly at least when calculating the throughput, as it results to be redundant or repetitive (the result is included on the model equation). Maybe if the production rate had been measured, the results would be more trustworthy. For their work, Rowe et al. 2013 found the Bm* to be useful for scaling-up the roll compaction process. However, they determined the Cs by performing several calibration experiments later used to deduce how efficiently the material is transported to the gap by the feed screw.

$$Bm^* = \frac{\rho_{rib}}{100} \cdot (SA_{roll})^{0.5} \qquad \text{Eq. 19}$$

Independent of the formula to calculate the Bm*, this model has another practical problem. The idea of this approach is that for a certain relative density a Bm* value is obtained in the small scale. Then, for achieving the same density, another Bm* value in the large scale would be needed. In this manner, the disadvantage of this model, excluding the problem of the repetitive expression, is that it is necessary to obtain the second line in order to predict the density. However, it is not always possible to perform enough amounts of experiments on the large scale in order to obtain this second line which allows the transfer of the process.

4.3.2.2.2. BOERSEN'S DIMENSIONLESS VARIABLE

This DV was developed by Boersen et al. 2015 (from now on, referred as Boersen DV) based on their past experience and the model requirements. Previous investigations from these researchers showed that, in order to model and predict the relative density of a formulation, containing the same excipients, but different APIs, the roll pressure, roll speed, feed screw speed, true density, flowability and the mean particle size are the most critical factors required (Boersen et al. 2014). The roll diameter was included as roll compactor parameter. Furthermore, they excluded all powder attributes and maintained exclusively the true density in the model in order to make the expression dimensionless, what calls into question the real process understanding behind the expression. The DV obtained (equation 9, page 13) was used to test the transfer of the roll compaction process between an Alexanderwerk and a Fitzpatrick for different sieve fractions of MCC as well as its combination with other APIs.

Just by taking a first look to the DV equation it can be concluded that is a simple and practical model. First of all, the formula is not complicated to work with and the terms included are obtained without difficulty from an experimental dataset. Secondly, the majority of the factors are directly related to the process, and thus, it should be easily and rapidly adapted once the prediction has been made, especially as no further transformations are required. The only

criticism that can be made in the first instance, it is that the expression uses roll pressure instead of force, and unfortunately, the SCF cannot be transformed into pressure as the area in which the force is applied is unknown. The ribbon relative densities obtained with the Freund-Vector compactors were used to test the model, although those results were called into question and not many experiments were performed. Therefore, only 3 points per compactor and for the main material are available (for the mixtures just one batch was produced), as these powders were compacted at 2, 5 and 8 MPa. In Figure 87 the correlation of this DV for the Freund-Vector compactors is presented.

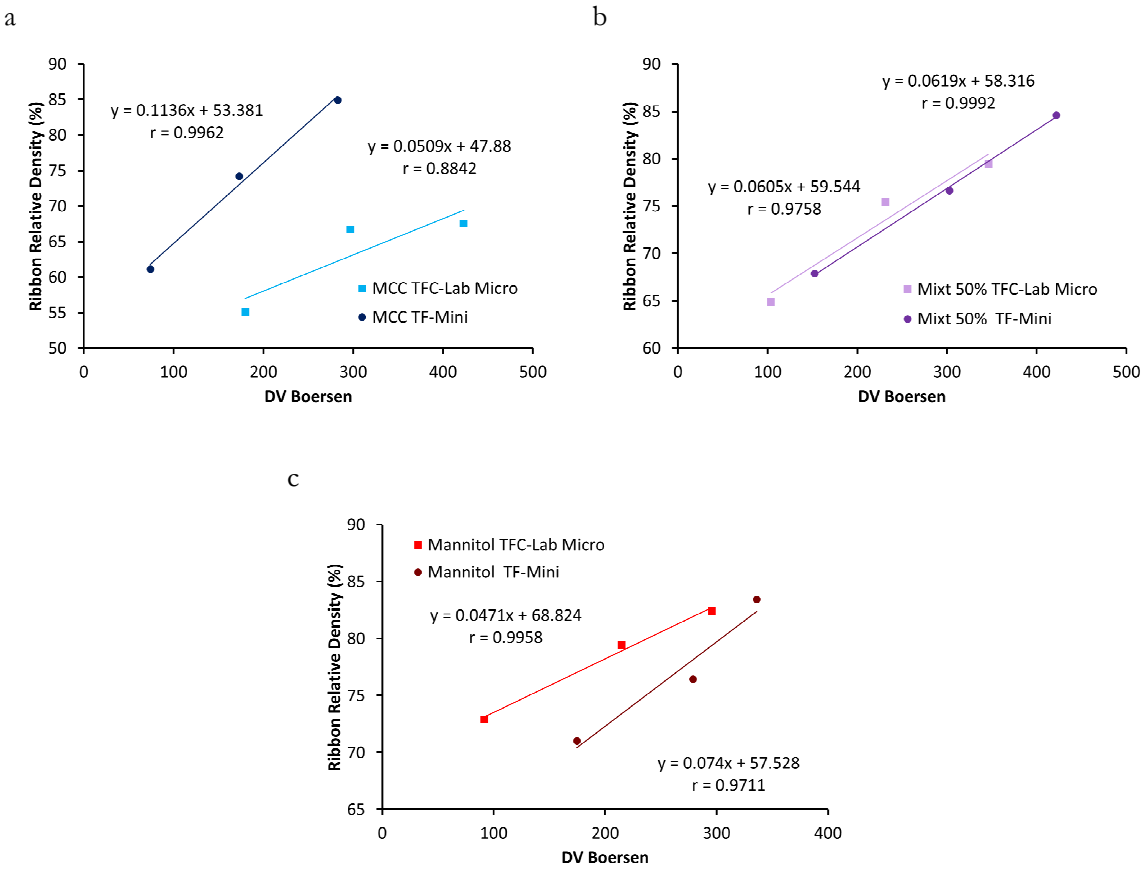

Figure 87: Comparison of the Boersen DV vs. the relative density of the ribbons for the Freund-Vector compactors regarding MCC (a), the 50% mixture (b) and mannitol (c).

According to the Boersen et al. 2015 work, a useful model should lead to a density-DV plot in which all points from both compactors lie on the same line. In other words, the best fit lines of both compactors should overlap or at least be as together as possible. The model works for the case of the mixture (for the other materials the lines are too far away from each other). This would be true only considering that the density results are reliable. Furthermore, to draw a line with just 3 points also brings into question the quality of the best fit line equation

obtained. Therefore, it cannot be indicated if the model does not work for the present case because of its basis or the data used to feed it. Furthermore, it is also important to point out that the correlation between ribbon density and DV that the authors prepared in their work was calculated after adapting the process conditions in the second compactor in order to obtain the same ribbon relative density. This means that ideally for the same DV value, the same ribbon density would be obtained in both machines, but for different process conditions. However, in this thesis, the same production conditions were applied although without the appropriate adaptation, which leads, as can be seen in the graphs, to different DVs for both scales. Nevertheless, the use of a DV is highly interesting because it is a model that is easy and fast to use.

4.3.3. PÉREZ GAGO'S APPROACH

The objective of this part was to develop a DV that could be applied for the compactors which uses SCF instead of roll pressure. In other words, to propose a DV which allows predicting the relative density of the ribbon in larger scales, i.e. scaling the roll compaction process up. In order to obtain the formula presented in equation 14 (page 42), dimensional analysis was used. The Buckingham's theorem requires unfortunately larger amounts of data. This is because in order to define the final terms of the equation, one π product has to be plotted against a second dimensionless group for different combinations of a third π element. Depending on the behaviour of the plot, it could be possible to interpret the relationships within the dimensionless groups and select those which better describe the phenomenon of study, which would help to understand the process further. Unfortunately, the data collected does not fulfil this criterion, and therefore, cannot be applied. However, and after trial-error methodology, the Buckingham's theorem helped to confirm some dimensionless groups, as it could be applied until the step in which the π products are defined, but it is for the next stage when not enough data is available.

Before starting to test the proposed model, it is important to point out, that the objective was to develop a DV with similar characteristics as the Boersen DV. The main advantages of the present equation are similar to those described: it is simple, fast to use and practical, because it includes elements from production conditions, material and type of compactor used. However, this model does not increase the knowledge regarding process understanding, because, and as was the case of the Boersen DV, several parameters which are

identified to have an impact on ribbon density, were organized in a dimensionless expression. If the Buckingham's theorem could have been applied, it would have increased the knowledge regarding the process. It was possible to include the compaction settings by using roll force (which is the result of multiplying the SCF times the roll width, and in this sense, also the scale is reflected), the roll speed, tamping auger speed (which depends on the gap set) and throughput. Then, the material properties with the true density of the powder are also included. At the beginning, the use of other attributes more related to the mechanical behaviour was also considered, but this property is easier to obtain and define the differences on the model. Finally, the dimensions of the compactor are included with the roll diameter and the calculation with the roller width.

The main idea of this DV is based on two properties that the model gathers and that will be justified and discussed in the coming lines with the following figures. On the one hand, the model allows the prediction of the DV in the large scale based on the value previously calculated for the small machine. On the other hand, the distribution of the points when plotting the relative density vs. the DVs is similar for both scales, which could be visually interpreted as the overlap of the two best fit lines obtained for each compactor or its parallel relationship.

In Figure 88 the comparison of the DV values obtained in the small scale against the large one for both Gerteis and L.B. Bohle compactors and the main materials are presented. As can be seen from the r values, the correlations are in general acceptable. To give more confidence to these results, all the cases overcome the 0.872 tabulated value for $\alpha < 0.1\%$ and 8 degrees of freedom. Furthermore, the model has shown that if the point corresponding to 2 kN/cm SCF, 1.5 mm gap and 2 rpm roll speed, were excluded from the model and thus, from this correlation, the r value would increase drastically for most of the cases. This fact is probably because the DV described has an action range defined by lower and upper limits where it losses quality, meaning that the prediction worsens for conditions out of these boundaries. Independent of this exclusion, the model can be considered that allows predicting the DV value in the large scale by calculating the corresponding one in the small machine. Considering the equations of the best-fit lines, it could even be affirmed that the same DV can be obtained on both scales with the same conditions. However, the slope has an important effect. Ideally, it should be 1 and the Y-intercept 0, in order to obtain the same DV value in both scales. For all correlations presented, the corresponding values taken from the equation of the best fit lines are close to the ideal, but they are not perfect. The slope is between 0.54

and 1.43 while the Y-intercept never overcomes the 0.9 value, which can have an effect on the prediction of the DV in the large scale through the value of the small machine. Therefore, and although it cannot be affirmed that the DV is the same on both scales, i.e. it is scale-dependent, in most cases its value on the small machine is similar to the one on the large scale.

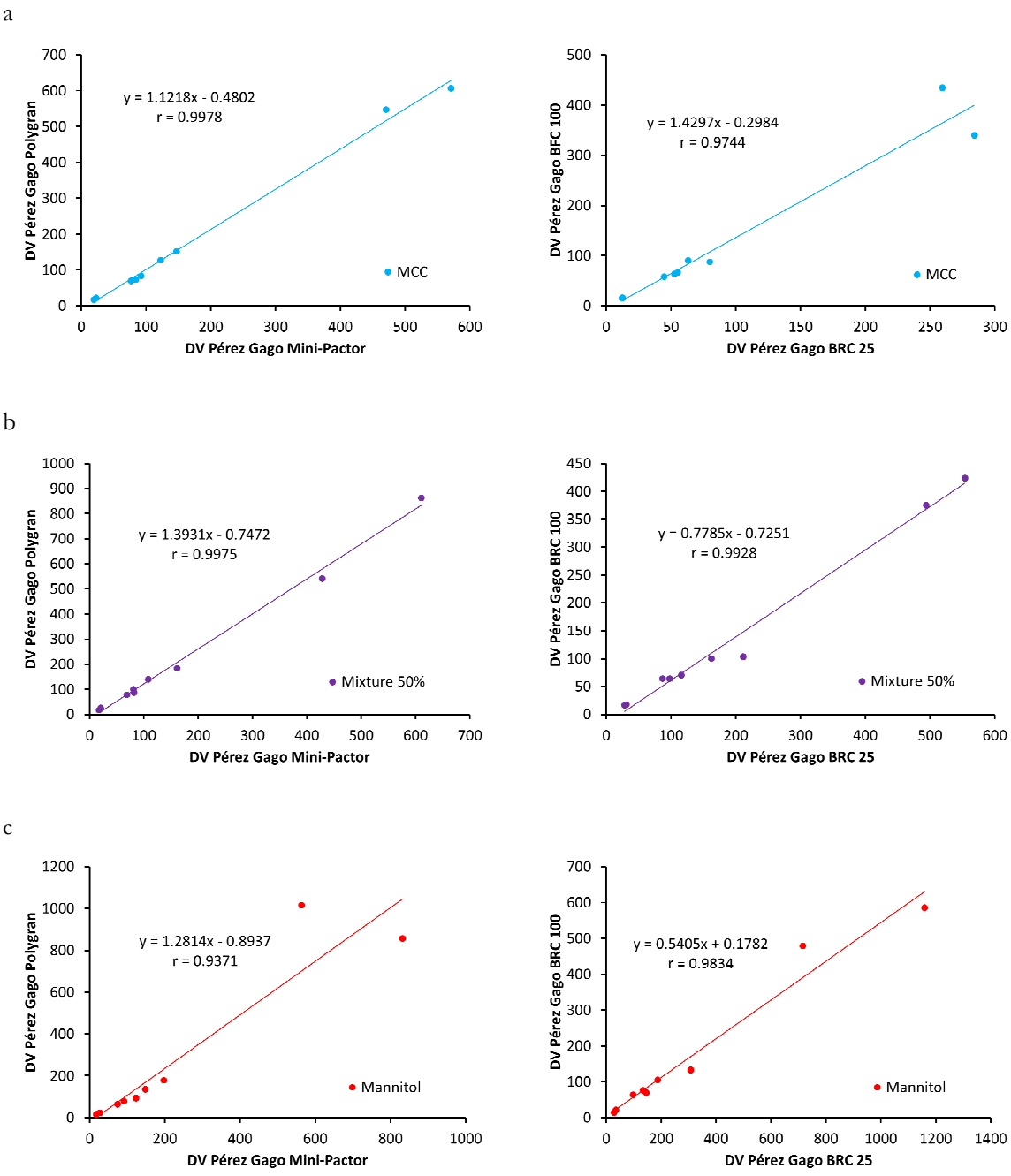

Figure 88: Comparison of the DV proposed obtained in both scales for the Gerteis compactors (left) and L.B. Bohle (right) regarding MCC (a), the 50% mixture (b) and mannitol (c).

After considering the validity of the model to predict the value of the DV in the large scale, the relative density against the calculated DVs for both scales is presented in Figure 89.

Please note that in order to facilitate the handling and testing of the model, the standard deviation of the relative density has been excluded. Its inclusion could affect the model either negatively or positively, but in order to keep it as simple as possible they were not considered. The most noteworthy aspects from these graphs are probably, on the one hand the low r value obtained for all the situations together with the high scattering and, on the other hand, the proximity of the best fit lines for both scales. The value of r never overcomes the 0.54, meaning that all of them are poor correlations. If the t-test were to be performed, no correlation coefficient would pass it, as for an $\alpha < 0.1\%$ and 8 degrees of freedom (9 points) the tabulated value is 0.872, meaning that no significant linear correlation between the ribbon relative density and the DV exists. Nevertheless, there are more trends which describe the distribution of points in a graph than just a straight line.

a

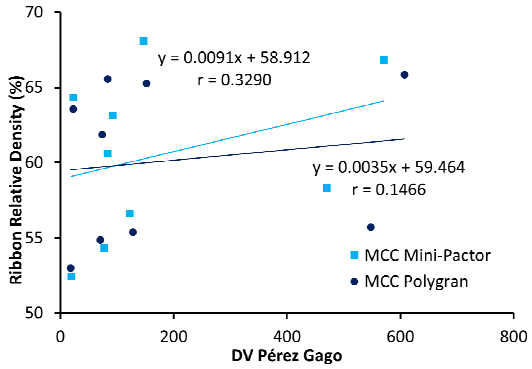

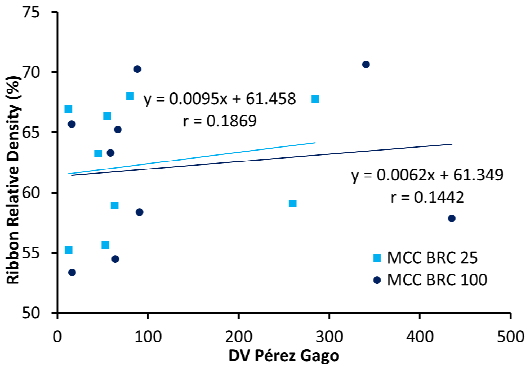

b

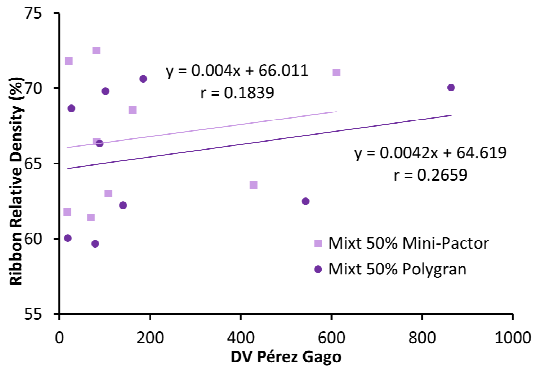

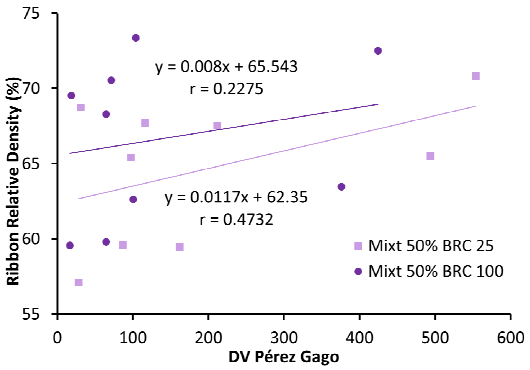

c

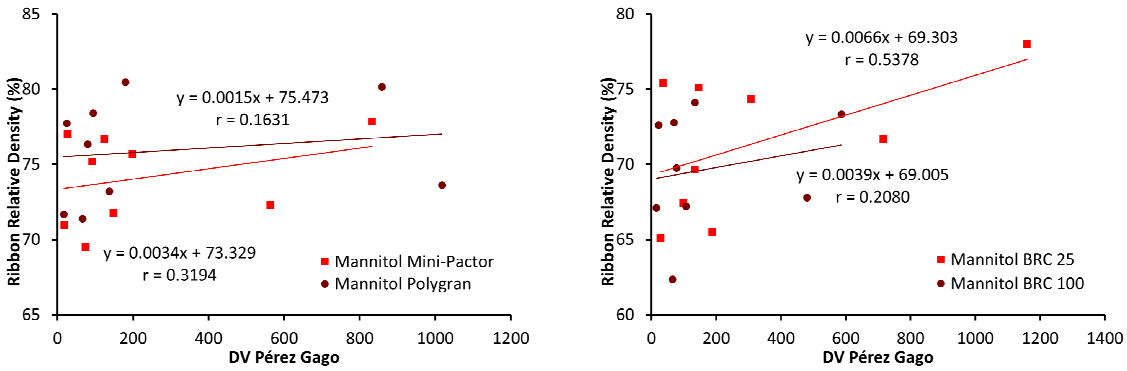

Figure 89: Comparison of the proposed DV vs. the relative density of the ribbons for the Gerteis compactors (left) and L.B. Bohle (right) regarding MCC (a), the 50% mixture (b) and mannitol (c), mean (n = 3).

At this point, the idea behind this model is that a polynomial equation can be found for describing the distribution of the points corresponding to the small scale and it would be comparable to the polynomial of the large scale. This hypothesis comes from the Y-intercepts of the best fit lines, together with the visually similar distribution of the points. When plotting the ribbon relative density against the DV for both scales (Figure 89), on the one hand, the best fit lines tend to be parallel or at least near, due to similar distribution of data points, and on the other hand, similar values of the Y-intercepts are obtained for each pair of compactors for a common material. If considering first the distribution of the points, the models for the L.B. Bohle compactors seem to be poorer than for Gerteis. Furthermore, the quality also seems to get worse when increasing the content of mannitol. When considering the assumption of the Y-intercepts, for the same powder and compactor line, close values are obtained. For example, for the case of the mixture compacted at the BRCs, the Y-intercept value for the BRC 25 is approximately 62.4 and for the BRC 100 is 65.5 which are already relatively close. However, for the mannitol compacted with the same machines, the Y-intercepts are 69.3 and 69.0 for the small and large scale respectively, although in some graphs the last point of the BRC 25 determines the equation. Furthermore, it could be affirmed that the Y-intercept is the factor mostly determining the equation of the best fit line, as the slope is in comparison extremely low, with almost negligible values. At this point, it could be possible to think that there is no relation between the DV and the relative density, as the slope is almost 0, meaning that the line is parallel to the X-axis. However, this would be applicable only if the data points were adjusted to a straight line with a high r value. Nevertheless, it is expected not to be the case, as the main hypothesis of this approach is that the results fit to a polynomial function.

In order to prove mathematically the hypothesis contemplated that a polynomial which described the point's distribution for the small scale would be also applicable for the large one, the mean error was calculated. This mean error is based on the difference obtained between the experimental relative density and the predicted value that using the best fit line equation gives. This means that if the obtained best fit line for a straight line were used to predict the relative density (result that is known that will not be accurate due to the poor best fit line equation), the value calculated would be compared to the experimental one. Then, the error made in this prediction can be obtained. If this is done for every condition and the mean of all the batches is calculated, the mean error is obtained. In Table 16, the value for each material compacted at all the machines is presented. As can be seen, the mean errors are similar. It is especially noteworthy the fact that the mean error decreases with the increase of mannitol content. However, in this case, the only objective of this type of error is to prove that both best fit lines would generate similar differences when making predictions. Therefore, these higher errors for MCC only mean that the points from the best fit line are further away for this material than for the others.

Table 16: Mean errors for each combination of material and compactor, mean (n = 9).

MATERIAL	**MEAN ERROR ON RIBBON RELATIVE DENSITY (%)**			
	MP	**PG**	**BRC 25**	**BRC 100**
MCC	4.48	4.79	4.57	5.55
Mixture 50%	3.70	3.83	3.71	4.70
Mannitol	2.56	3.08	3.29	3.14

Therefore, and considering on the one hand the distribution of points, on the other hand the similar Y-intercepts value and finally the comparable mean error, for the same material compacted at both scales, it could be concluded that the polynomial equation that would describe the small-scale points would be also applicable for the large one. This latter hypothesis together with the prediction of the DV in the large scale, are the pillars of this model. In this manner, the idea of this approach is that after performing the experiments on the small-scale compactor for a specific material, the DV can be calculated and plotted against the relative density. This representation would be described with a polynomial equation that

can be later used to predict the density. Afterwards, the DV at the large scale can be obtained and use to predict the density with the polynomial equation. However, an important criticism of the hypothesis of the polynomial function should be made. The equation of polynomial which could be obtained, would have a degree equal to the number of samples minus 1, meaning that the adjustment will probably highly depend on the amount of data points collected. Furthermore, the complexity of handling the polynomial equation, would increase the problematic nature of the model.

Therefore, this proposed model that combines the prediction of the DV in the bigger scale with the polynomial equation which describes both compactors, would allow predicting the ribbon relative density without the need for performing experiments on the large machine (which was necessary in the case of the results obtained for the Bm*). Nevertheless, this approach is based on several weak assumptions. Additionally, the different application steps of the DV (calculation of DV in large scale, polynomial equation and prediction of ribbon density) result in high deviations, which leads to affirm that this approach is probably not strong enough to be considered as a tool for scaling the process up. Furthermore, as no proper process understanding is behind this expression, correcting the model to improve it would be difficult. Therefore, although DVs seem to be promising tools due to the simplicity and fast application, they cannot beat mechanistic models based on a strong and profound process understanding.

4.3.4. SUMMARY

In this last part of the thesis, three models described in the literature have been evaluated by mostly using the data for MCC, mannitol and the 50% mixture compacted at the Gerteis and L.B. Bohle machines following the conditions of the 11-runs DOE. Furthermore, an approach based on dimensional analysis, and therefore a DV, was proposed as alternative to the models found in the bibliography.

The first approach tested was a mechanistic model developed by Reynolds et al. 2010 which was fitted using material shear data (parameters easily and rapidly to obtain) and calibrated with the ribbon relative density values of the smaller scale. Good fitting between the observed and predicted data was found. For MCC, the model showed excellent prediction with less than 1% error in the estimations. Although the quality of the model decreased for the mixture and mannitol, the predictions were still in good agreement with a maximum margin

of error of 4.1%. However, the model predicts more accurately when the Gerteis compactors are studied, in which case, the maximum bias falls to a 1.7%, and therefore, the great utility of this approach can be proven.

Secondly, two models based on dimensional analysis were tested. The first one was the called Bm* and was described by Rowe et al. 2013. The equation proposed by these researchers showed two small inconveniences, which led to a lack of practical application of it. On the one hand, it does not include any term referred to roll force or pressure. On the other hand, it uses other parameters which are not directly related to the production conditions and thus, it requires further transformations or calculations. Finally, and related to the way of obtaining one of those conflicting terms (Cs), the Bm* equation ends up with a direct relationship with the density, only affected by another parameter related to the compactor's scale. Independent of these limitations and assuming that the model would not be a repetitive equation, it leads to a profile with two lines (one per compactor) which can be used to predict the ribbon density in the large scale. However, the main problem of obtaining these two curves is that it imposes the need of knowing the line corresponding to the large scale, what it is not always so easily done.

Another DV developed by Boersen et al. 2015 showed an equation much simpler and faster to work with in which the roll pressure was used. This was at the same time an inconvenience, as the model cannot be applied to compactors using SCF. Nevertheless, the approach was tested for the data available for the Freund-Vector line, although in this case, it cannot be confirmed if the lack of applicability is due to the model itself, the problems with the initial data or the working flow the authors followed (which is diverse to the way to collect the data in this thesis).

Finally, another DV was unsuccessfully proposed in this work with the objective of describing the scalability of the compactors using SCF. This equation was tried to be kept simple and fast to use as for the previous case. Elements from process conditions, materials and compactor's scale were included. This model is based on the possibility on the one hand, of predicting the DV in the large compactor using the small machines, and on the other hand, of using the predicted value to obtain the relative density in the next scale through the substitution of this value in a polynomial equation. This last aspect could be assumed to be correct according to the similar visual distribution of the points, the values of the Y-intercepts and the mean errors calculated which would confirm the same distribution of the points.

Nevertheless, the approach is based on weak hypothesis which could include the assumption of a high error and, thus, its applicability is called into question.

As a general conclusion and if comparing all approaches presented, the best model by far is the Reynolds's approach, which is able to predict with a low and acceptable error the ribbon relative density and furthermore, it is based in physical and mechanistic backgrounds. The dimensional variables are promising but still need to be improved, as probably, their great advantage, i.e. their simplicity, it is at the same time the main reason why they cannot so accurately predict the ribbon density. Behind their expressions, there is a lack of process understanding that cannot be easily filled.

5. SUMMARY AND OUTLOOK

The present thesis has been focused on investigating the scale-up of the roll compaction process. The effect of plastic/brittle mixtures and process parameters in the products obtained, the impact of the change in scale on ribbon properties and the application of models to try to successfully scale the process up have been considered. A total of 7 mixtures of MCC (plastic material) and mannitol (brittle behaviour) including these proportions: 0, 15, 30, 50, 70, 85 and 100% MCC were investigated. The blends were roll compacted following different process conditions of SCF, gap width and roll speed determined by a previously defined DOE. A total of 6 compactors were used to perform the experiments. These machines are organized in 3 pairs considering the supplier, what means a total of 3 individual scale-up studies.

In the first part of the thesis, the effect of varying the fraction of plastic/brittle material (variation of the proportion of MCC) was evaluated together with the importance of the process parameters. In order to perform this study, a multilevel full factorial design plus 3 repetitions of the centre point was performed for the 7 binary mixtures of MCC and mannitol. The study was mostly focused on granule properties, although the relative density and microhardness (expressed as HU and measured using two different methods) of the centre point ribbons were determined. After plotting the results against the proportion of MCC, it was observed how the ribbon relative density decreases proportionally when increasing the MCC fraction, while for the HU a non-linear effect was identified. The GSD of the granules obtained after milling the ribbons was described by the percentiles D10, D50 and D90, as well as the amount of fines. From the coefficient plots, it was concluded that the higher the SCF, the smaller the gap and the lower the proportions of MCC, the higher the proportion of larger granules and the lower the amount of fines. When comparing the centre point results for those properties against the proportion of MCC, another synergic effect was identified, i.e. the interaction between MCC and mannitol results in values even higher or lower than those of the pure materials. In order to investigate this fact further, the percolation theory was applied to define the percolation thresholds or the proportion of MCC up from which the behaviour of the whole system changes. For microhardness, depending on the measuring method, a percolation threshold was identified at 34% and 26% of MCC, while for the D10 and fines the values were 27% and 28% respectively and finally, the D50 and D90 which were found at 84% and 85% of MCC respectively. As conclusion of this first chapter, the plastic/brittle mixtures

investigated showed different behaviour for most of the properties of ribbons and granules analysed, and therefore, the importance of the MCC/mannitol fraction was proven.

In the second and main part of the thesis, three individual scale-up studies together with the evaluation of process parameters and mixture composition were performed. These studies were classified in Gerteis, L.B. Bohle and Freund-Vectors line, i.e. according to the supplier providing the pair of compactors used. For all compactors assessed, the relative density of the ribbons produced was characterized, as this has been described as a key property. The density distribution, microhardness and in few occasions the GSD, were also investigated to a lesser extent. In general, it was again confirmed that the higher the SCF, the lower the gap and content of MCC, the denser the ribbons. For the first scale-up study, performed using the Gerteis compactors and after evaluating the 2 complete DOEs for process and mixture investigation, the scale was never found to be significant. Nevertheless, the interactions MCC-scale, as well as for the mixture DOE, the gap-scale, were indirectly significant, stressing the importance of this factor in the roll compaction process. However, the density distribution seems not to be affected by the scale, as much as by the sealing system assembled. Similar curves with higher values in the centre and lower in the edges of the ribbon were found for both compactors. For microhardness, the scale was found to be always significant and the evaluation of the GSD confirmed that the profile depends mainly on the relative density of the ribbons. The second scale-up study using L.B. Bohle compactors, led to similar results, although MCC was found not to be significantly affected by the scale or any interaction. The density distribution results were not able to confirm that the profile was unaffected by the scale. However, most probably, the size and irregularity of the piece corresponding to the small scale, may be the reason why both curves look different, especially because the large-scale ribbon showed the expected profile. Finally, the results of the last scale-up study with the Freund-Vector compactors, showed a general tendency of the large scale (TF-Mini) to have denser ribbons with also higher microhardness. However, this result was unexpected, as according to the conversion factor and the roll diameter, the small scale applies a higher roll force and densifies the product more, therefore, probably at least one of the factors used to convert the pressure into roll force was wrong. As main conclusion of this second chapter, it can be confirmed the importance of the scale and the difficulties to transfer the process, in spite of the efforts invested by suppliers like Gerteis and L.B. Bohle, what could lead to the application of a model to successfully scale the process up.

Finally, the third chapter of the thesis has been focused on the modelling of the roll compaction scale-up. A total of three models were selected due to accessibility or simplicity for evaluation of their accuracy for transferring the process. After testing all the approaches it was concluded that the best one is the mechanistic model proposed by Reynolds et al. 2010, giving good fitting and predictions with less than a 4.1% error. Furthermore, this model, only needs the data collected in the small scale to perform the predictions. Some other dimensionless approaches were tested, however they resulted in worse results, probably due to the lack of process understanding in their equations. Therefore, it can be concluded that the roll compaction process can be effectively scaled-up when applying this mechanistic model.

As general conclusion of the whole thesis, the scalability of the roll compaction process for some couples of compactors available on the market has been investigated by identifying the most important parameters affecting the results and adapting then through the application of the mechanistic model proposed. However, much work is still left before being able to affirm that the scalability of the roll compaction process is fully understood. Part of the investigations left includes the assessment of more materials and their mixtures and even formulations with APIs, as well as more compactors should be investigated. Regarding modelling, it could be possible to evaluate more models or according to the experience gained, improve the ones already existing to reduce the prediction error. Furthermore, this work has been mostly focused on ribbon properties, however, the granule characterization should be also further studied, as the final product coming out of the compactors is generally the granules later used for tableting.

6. ZUSAMMENFASSUNG UND AUSBLICK

Die vorliegende Arbeit konzentriert sich auf die Untersuchung des Scale-ups von Walzenkompaktierprozessen. Es wurde der Effekt von Mischungen aus plastischen und sprödbrüchigen Materialien und von den gewählten Prozessparametern auf das Produkt untersucht. Außerdem wurde der Einfluss des Maßstabs auf die Eigenschaften der Schülpen berücksichtigt und unter Anwendung verschiedener Modelle wurde versucht, den Prozess erfolgreich hoch zu skalieren. Es wurden insgesamt 7 Mischungen von mikrokristalliner Cellulose (MCC) (plastisch) und Mannitol (spröde) mit 0, 15, 30, 50, 70, 85 und 100% Anteil an MCC verwendet. Die Mischungen wurden mit verschiedenen Prozesseinstellungen walzenkompaktiert. Die spezifische Kompaktierkraft (SCF), Spaltbreite und Walzengeschwindigkeit wurden durch einen zuvor definierten statistischen Versuchsplan bestimmt. Insgesamt sind 6 verschiedene Walzenkompaktoren für die Durchführung der Experimente benutzt worden. Jeweils zwei Maschinen mit unterschiedlichem Maßstab von drei Lieferanten wurden getestet, woraus insgesamt drei individuelle Scale-up-Studien resultieren.

Im ersten Teil der Arbeit wurde die Auswirkung der Veränderung des Anteils an plastischen/spröden Material (Variation des MCC-Anteils) zusammen mit drei Prozessparametern untersucht. Zur Durchführung dieser Studie wurde ein mehrstufiger vollfaktorieller Versuchsplan mit drei Läufen am Zentralpunkt für die 7 binären Mischungen von MCC und Mannitol gewählt. Die Studie konzentrierte sich hauptsächlich auf die Granulat-Eigenschaften. Zusätzlich wurden die relative Dichte und Mikrohärte (ausgedrückt als HU und mit zwei verschiedenen Methoden gemessen) der Schülpen an den Zentralpunkten gemessen. Die relative Dichte der Schülpen verringert sich linear mit zunehmender MCC-Fraktion, während für die HU ein nichtlinearer Effekt zu erkennen war. Die Partikelgrößenverteilung (PGV) der erhaltenen Granulate wurde durch die Perzentilen D10, D50 und D90 sowie den Feinanteil beschrieben. Aus den Koeffizienten-Diagrammen wurde gefolgert, dass je höher die SCF, je kleiner Spalt und je niedriger die Anteile an MCC sind, desto höher der Anteil an größeren Granulatkörnen ist und desto niedriger der Feinanteil. Beim Vergleich der Zentralpunkte mit dem MCC-Anteil wurde ein anderer synergistischer Effekt identifiziert. Die Interaktion zwischen MCC und Mannitol führte zu Werten, die bei Mischungen höher oder niedriger als die der reinen Materialien waren. Um diese Tatsache tiefergehend zu untersuchen, wurde die Perkolationstheorie angewandt, um die Perkolationsschwellen oder den Anteil an MCC zu definieren, ab dem sich das Verhalten des gesamten Systems ändert. Für die

Mikrohärte wurde, abhängig von der Messmethode, eine Perkolationsschwelle von 34% und 26% MCC identifiziert, während sich für die D10 und die Feinanteile Werte von 27% beziehungsweise 28% ergaben. Für die D50 und D90 schließlich lagen die Perkolationsschwellen bei 84% beziehungsweise 85% MCC. Zusammenfassend ist für den ersten Teil zu sagen, dass die untersuchten plastischen/spröden Mischungen ein unterschiedliches Verhalten für die meisten Eigenschaften der analysierten Schülpen und Granulate zeigten. Dadurch wurde die Wichtigkeit der MCC/Mannitol Antail in den Mischung nachgewiesen.

Im zweiten und Hauptteil der Arbeit wurden drei individuelle Scale-up-Studien zusammen mit der Bewertung der Prozessparameter und der Zusammensetzung der Mischungen durchgeführt. Diese Studien wurden für Gerteis, L.B. Bohle und Freund-Vector-Linie, d.h. in Anlehnung an die Lieferante der Geräte, klassifiziert. Für alle untersuchten Kompaktoren ist die relative Dichte der hergestellten Schülpen charakterisiert worden, da sie als Schlüsseleigenschaft beschrieben wurde. Die Dichteverteilung, die Mikrohärte und in wenigen Fällen die PGV, wurden teilweise ebenfalls untersucht. Für alle Studien wurde bestätigt, dass je höher der SCF, je niedriger der Spalt und der Anteil von MCC, umso höher ist die Dichte der Schülpen. Für die erste Scale-up-Studie, die mit den Gerteis-Kompaktor durchgeführt wurde, und nach der Auswertung der zwei vollständigen Versuchspläne für die Prozess- und Mischungsuntersuchung, wurde die Gerätegroße in keinem Fall als signifikanter Faktor identifiziert. Allerdings waren die Interaktionen MCC x Maßstab sowie für die 50:50 Mischung die Spalt x Skalierung, umgekehrt signifikant, was die Bedeutung des Maßstabs für den Walzenkompaktierungsprozess betont. Jedoch scheint die Größenmaßstab keinen Einfluss auf die Dichteverteilung von Schülpen zu haben, zumindest weniger stark als die verwendeten Abdichtungssysteme. Für beide Kompaktoren wurden ähnliche Kurven mit höheren Dichte-Werten in der Mitte und niedrigen an den Rändern des Schülpen gefunden. Für die Mikrohärte war die Größenmaßstab immer signifikant und die Auswertung der PGV bestätigte, dass das Profil hauptsächlich von der relativen Dichte der Schülpen abhängt. Die zweite Scale-up-Studie mit L.B. Bohle Kompaktoren, führte zu ähnlichen Ergebnissen, obwohl die Skalierung oder ihre Interaktionen für MCC nie signifikant waren. Die Ergebnisse der Dichteverteilung konnten nicht bestätigen, dass das Profil von der Größenmaßstab beeinflusst ist. Allerdings ist durch die Größe und Unregelmäßigkeit der untersuchten Stücke erklärbar, warum beide Kurven anders aussehen, insbesondere, weil die Schülpe der großen Skalierung das erwartete Profil zeigte. Abschließend zeigten die Ergebnisse der letzten Scale-up-Studie mit den Freund-Vector-Kompaktoren die allgemeine Tendenz, dass auf dem

größeren Kompaktor (TF-Mini) dichtere Schülpen mit höherer Mikrohärte produziert wurden. Diese Tatsache war jedoch nicht erwartet werden, da der kleinere Kompaktor in Anlehnung an den Umrechnungsfaktor und den Walzendurchmesser eine höhere Walzenkraft anwendet und das Produkt stärker verdichtet werden sollte. Deswegen war wenigstens einer dieser Faktoren, die verwendet um den Druck in eine spezifische Kompaktierkraft zu konvertieren, wahrscheinlich falsch. Als wichtigste Schlussfolgerung dieses zweiten Kapitels kann die Wichtigkeit der Größenmaßstab bestätigt werden sowie die Schwierigkeiten des Prozesstransfers auf andere Geräte und dies trotz der Anstrengungen der Lieferanten wie Gerteis und L.B. Bohle. Deswegen könnte die Anwendung eines Modells hilfreich sein, um den Prozess erfolgreich zu skalieren.

Das dritte Kapitel befasst sich mit der Modellierung von Walzenkompaktierprozessen. Insgesamt wurden drei Modelle getestet, die aufgrund ihrer Zugänglichkeit oder Einfachheit ausgewählt wurden, um ihre Genauigkeit für die Übertragung des Prozesses zu bewerten. Nach dem Testen aller Ansätze ergibt sich, dass das mechanistische Modell von Reynolds et al. 2010 der beste Ansatz ist, weil es gute Anpassungen und Vorhersagen mit Fehlern kleiner als 4,1% ergibt. Dieses Modell braucht nur die gesammelten Daten des kleinen Größenmaßstabs, um die Vorhersagen durchzuführen. Einige andere dimensionslose Ansätze wurden getestet, jedoch mit schlechteren Ergebnissen aufgrund des fehlenden Prozessverständnisses hinter ihren mathematischen Gleichungen. Deswegen kann gefolgert werden, dass der Prozess der Walzenkompaktierung durch Anwendung dieses mechanistischen Modells effektiv skaliert werden kann.

Die Skalierbarkeit des Walzenkompaktierprozesses wurde für einige Maschinen auf dem Markt untersucht, indem mit dem vorgeschlagenen Modell die wichtigsten Parameter, welche die Ergebnisse beeinflussen, identifiziert wurden. Allerdings bleibt noch viel zu tun, bevor man sagen kann, dass die Skalierbarkeit des Prozesses des Walzenkompaktierens vollständig verstanden ist. Ein Teil der fehlenden Untersuchungen umfasst die Bewertung von mehr Materialien und deren Mischungen und Formulierungen mit Wirkstoffen. Es sollten auch weitere Kompaktoren untersucht werden. In Bezug auf Modellierung könnte es möglich sein, mehr Modelle zu evaluieren oder die schon vorhandenen Ansätze zu verbessern, um den Vorhersagefehler zu reduzieren. Diese Arbeit hat sich hauptsächlich auf die Schülpen-Eigenschaften konzentriert, jedoch könnten auch die Granulatcharakteristika tiefer untersucht werden, da das Endprodukt des Kompaktierens normalweise Granulate sind, die später für die Tablettierung verwendet werden.

7. REFERENCES

Akseli, I., Iyer, S., Lee, H. P. and Cuitino, A. M. (2011). "A Quantitative Correlation of the Effect of Density Distributions in Roller-Compacted Ribbons on the Mechanical Properties of Tablets Using Ultrasonics and X-ray Tomography." AAPS PharmSciTech **12**(3): 834-853.

Allesø, M., Holm, R. and Holm, P. (2016). "Roller compaction scale-up using roll width as scale factor and laser-based determined ribbon porosity as critical material attribute." European Journal of Pharmaceutical Sciences **87**: 69-78.

am Ende, M. T., Moses, S. K., Carella, A. J., Gadkari, R. A., Graul, T. W., Otano, A. L. and Timpano, R. J. (2007). "Improving the content uniformity of a low-dose tablet formulation through roller compaction optimization." Pharmaceutical development and technology **12**(4): 391-404.

Armstrong, N. A. (2009). Mannitol. Handbook of Pharmaceutical Excipients. Rowe, R. C., Sheskey, P. J. and Quinn, M. E. London, Pharmaceutical Press and American Pharmacists Association**:** 424-428.

Austin, J., Gupta, A., McDonnell, R., Reklaitis, G. V. and Harris, M. T. (2013). "The use of near-infrared and microwave resonance sensing to monitor a continuous roller compaction process." Journal of Pharmaceutical Sciences **102**(6): 1895-1904.

Bi, M. D., Alvarez-Nunez, F. and Alvarez, F. (2014). "Evaluating and Modifying Johanson's Rolling Model to Improve its Predictability." Journal of Pharmaceutical Sciences **103**(7): 2062-2071.

Blattner, D., Kolb, M. and Leuenberger, H. (1990). "Percolation Theory and Compactibility of Binary Powder Systems." Pharmaceutical Research **7**(2): 113-117.

Boersen, N., Carvajal, M. T., Morris, K. R., Peck, G. E. and Pinal, R. (2014). "The influence of API concentration on the roller compaction process: modeling and prediction of the post compacted ribbon, granule and tablet properties using multivariate data analysis." Drug Development and Industrial Pharmacy **41**(9): 1470-1478.

Boersen, N., Belair, D., Peck, G. E. and Pinal, R. (2015). "A dimensionless variable for the scale up and transfer of a roller compaction formulation." Drug Development and Industrial Pharmacy **42**(1): 60-69.

Bolhuis, G. K. and Chowhan, Z. T. (1996). Materials for Direct Compaction. Pharmaceutical Powder Compaction Technology Alderborn, G. and Nystrom, C. New York, Marcel Dekker, Inc.**:** 419-500.

Bonny, J. D. and Leuenberger, H. (1993). "Matrix type controlled release systems II. Percolation effects in non-swellable matrices." Pharmaceutica Acta Helvetiae **68**(1): 25-33.

Bryan, J. E. (2005). Theory of Granulation. Handbook of Pharmaceutical Granulation Technology, Second Edition. New York, Marcel Dekker, Inc.**:** 7-78.

Bultmann, J. M. (2002). "Multiple compaction of microcrystalline cellulose in a roller compactor." European Journal of Pharmaceutics and Biopharmaceutics **54**(1): 59-64.

Campbell, G. M., Bunn, P. J., Webb, C. and Hook, S. C. W. (2001). "On predicting roller milling performance: Part II. The breakage function." Powder Technology **115**(3): 243-255.

Caraballo, I., Fernández-Arévalo, M., Holgado, M. A. and Rabasco, A. M. (1993). "Percolation theory: application to the study of the release behaviour from inert matrix systems." International Journal of Pharmaceutics **96**(1): 175-181.

Caraballo, I. (2010). "Factors affecting drug release from hydroxypropyl methylcellulose matrix systems in the light of classical and percolation theories." Expert Opinion on Drug Delivery **7**(11): 1291-1301.

Castellanos Gil, E., Iraizoz Colarte, A., Bataille, B., Brouillet, F. and Caraballo, I. (2009). "Estimation of the percolation thresholds in ternary lobenzarit disodium–dextran–HPMC hydrophilic matrices tablets: Effects of initial porosity." European Journal of Pharmaceutical Sciences **38**(4): 312-319.

Cunningham, J. C., Winstead, D. and Zavaliangos, A. (2010). "Understanding variation in roller compaction through finite element-based process modeling." Computers & Chemical Engineering **34**(7): 1058-1071.

Chang, C. K., Alvarez-Nunez, F. A., Rinella, J. V., Magnusson, L. E. and Sueda, K. (2008). "Roller compaction, granulation and capsule product dissolution of drug formulations containing a lactose or mannitol filler, starch, and talc." AAPS PharmSciTech **9**(2): 597-604.

Dalziel, G., Nauka, E., Zhang, F., Kothari, S. and Xie, M. L. (2013). "Assessment of granulation technologies for an API with poor physical properties." Drug Development and Industrial Pharmacy **39**(7): 985-995.

Dawes, J., Gamble, J. F., Greenwood, R., Robbins, P. and Tobyn, M. (2012). "An investigation into the impact of magnesium stearate on powder feeding during roller compaction." Drug Development and Industrial Pharmacy **38**(1): 111-122.

Dec, R. T., Zavaliangos, A. and Cunningham, J. C. (2003). "Comparison of various modeling methods for analysis of powder compaction in roller press." Powder Technology **130**(1–3): 265-271.

Dumarey, M., Wikstrom, H., Fransson, M., Sparen, A., Tajarobi, P., Josefson, M. and Trygg, J. (2011). "Combining experimental design and orthogonal projections to latent structures to study the influence of microcrystalline cellulose properties on roll compaction." International Journal of Pharmaceutics **416**(1): 110-119.

Esnault, V., Heitzmann, D., Michrafy, M., Oulahna, D. and Michrafy, A. (2013). "Numerical simulation of roll compaction of aerated powders." Chemical Engineering Science **104**: 717-726.

Fahmy, R., Kona, R., Dandu, R., Xie, W., Claycamp, G. and Hoag, S. W. (2012). "Quality by design I: Application of failure mode effect analysis (FMEA) and Plackett-Burman design of experiments in the identification of "main factors" in the formulation and process design space for roller-compacted ciprofloxacin hydrochloride immediate-release tablets." AAPS PharmSciTech **13**(4): 1243-1254.

Falzone, A. M., Peck, G. E. and McCabe, G. P. (1992). "Effects of changes in roller compactor parameters on granulations produced by compaction." Drug Development and Industrial Pharmacy **18**(4): 469-489.

Farber, L., Hapgood, K. P., Michaels, J. N., Fu, X. Y., Meyer, R., Johnson, M. A. and Li, F. (2008). "Unified compaction curve model for tensile strength of tablets made by roller compaction and direct compression." International Journal of Pharmaceutics **346**(1-2): 17-24.

Fernandez Hervas, M. J., Vela, M. T., Gonzalez Rodriguez, M. L. G. and Rabasco, A. M. (1996). "Using the percolation theory to explain the release behavior from inert matrix systems." Drug Development and Industrial Pharmacy **22**(3): 201-210.

FMC BioPolymer (2008). Binders (Data sheet for Avicel® PH 101).

Freeman, T., Vom Bey, H., Hanish, M., Brockbank, K. and Armstrong, B. (2016). "The influence of roller compaction processing variables on the rheological properties of granules." Asian Journal of Pharmaceutical Sciences **11**(4): 516-527.

Freitag, F., Reincke, K., Runge, J., Grellmann, W. and Kleinebudde, P. (2004). "How do roll compaction/dry granulation affect the tableting behaviour of inorganic materials? Microhardness of ribbons and mercury porosimetry measurements of tablets." European Journal of Pharmaceutical Sciences **22**(4): 325-333.

Freitag, F., Runge, J. and Kleinebudde, P. (2005). "Coprocessing of powdered cellulose and magnesium carbonate: Direct tableting versus tableting after roll compaction/dry granulation." Pharmaceutical Development and Technology **10**(3): 353-362.

Fuertes, I., Miranda, A., Millan, M. and Caraballo, I. (2006). "Estimation of the percolation thresholds in acyclovir hydrophilic matrix tablets." European Journal of Pharmaceutics and Biopharmaceutics **64**(3): 336-342.

Gamble, J. F., Tobyn, M., Dennis, A. B. and Shah, T. (2010). "Roller compaction: Application of an in-gap ribbon porosity calculation for the optimization of downstream granule flow and compactability characteristics." Pharmaceutical Development and Technology **15**(3): 223-229.

García Muñoz, S., MacGregor, J. F. and Kourti, T. (2005). "Product transfer between sites using Joint-Y PLS." Chemometrics and Intelligent Laboratory Systems **79**(1–2): 101-114.

Ghorab, M. K., Chatlapalli, R., Hasan, S. and Nagi, A. (2007). "Application of thermal effusivity as a process analytical technology tool for monitoring and control of the roller compaction process." AAPS PharmSciTech **8**(1).

Golchert, D., Bines, E. and Carmody, A. (2013). "Evaluation of some compression aids in tableting of roller compacted swellable core drug layer." International Journal of Pharmaceutics **453**(2): 322-328.

Grund, J., Körber, M. and Bodmeier, R. (2013). "Predictability of drug release from water-insoluble polymeric matrix tablets." European Journal of Pharmaceutics and Biopharmaceutics **85**(3, Part A): 650-655.

Guigon, P. and Simon, O. (2003). "Roll press design - influence of force feed systems on compaction." Powder Technology **130**(1-3): 41-48.

Guigon, P., Simon, O., Saleh, K., Bindhumadhavan, G., J. Adams, M. and Seville, J. P. K. (2007). Chapter 5 Roll pressing. Handbook of Powder Technology. A.D. Salman, M. J. H. and Seville, J. P. K., Elsevier Science B.V. **Volume 11:** 255-288.

Gupta, A., Peck, G. E., Miller, R. W. and Morris, K. R. (2004). "Nondestructive Measurements of the Compact Strength and the Particle-Size Distribution after Milling of Roller Compacted Powders by Near-Infrared Spectroscopy." Journal of Pharmaceutical Sciences **93**(4): 1047-1053.

Gupta, A., Peck, G. E., Miller, R. W. and Morris, K. R. (2005a). "Effect of the variation in the ambient moisture on the compaction behavior of powder undergoing roller-compaction and on the characteristics of tablets produced from the post-milled granules." Journal of Pharmaceutical Sciences **94**(10): 2314-2326.

Gupta, A., Peck, G. E., Miller, R. W. and Morris, K. R. (2005b). "Influence of ambient moisture on the compaction behavior of microcrystalline cellulose powder undergoing uni-axial compression and roller-compaction: A comparative study using near-infrared spectroscopy." Journal of Pharmaceutical Sciences **94**(10): 2301-2313.

Guy, A. (2009). Cellulose, Microcrystalline. Handbook of Pharmaceutical Excipients. Rowe, R. C., Sheskey, P. J. and Quinn, M. E. London, Pharmaceutical Press and American Pharmacists Association**:** 129-133.

Hamad, M. L., Bowman, K., Smith, N., Sheng, X. H. and Morris, K. R. (2010). "Multi-scale pharmaceutical process understanding: From particle to powder to dosage form." Chemical Engineering Science **65**(21): 5625-5638.

He, X., Secreast, P. J. and Amidon, G. E. (2007). "Mechanistic study of the effect of roller compaction and lubricant on tablet mechanical strength." Journal of Pharmaceutical Sciences **96**(5): 1342-1355.

Heiman, J., Tajarobi, F., Gururajan, B., Juppo, A. and Abrahmsen-Alami, S. (2015). "Roller Compaction of Hydrophilic Extended Release Tablets-Combined Effects of Processing Variables and Drug/Matrix Former Particle Size." AAPS PharmSciTech **16**(2): 267-277.

Herting, M. G. and Kleinebudde, P. (2007a). "Roll compaction/dry granulation: Effect of raw material particle size on granule and tablet properties." International Journal of Pharmaceutics **338**(1-2): 110-118.

Herting, M. G., Klose, K. and Kleinebudde, P. (2007b). "Comparison of different dry binders for roll compaction/dry granulation." Pharmaceutical Development and Technology **12**(5): 525-532.

Hervieu, P., Dehont, F., Jerome, E., Delacourte, A. and Guyot, J. C. (1994). "Granulation of Pharmaceutical Powders by Compaction - An Experimental-Study." Drug Development and Industrial Pharmacy **20**(1): 65-74.

Hilden, J., Earle, G. and Lilly, E. (2011). "Prediction of roller compacted ribbon solid fraction for quality by design development." Powder Technology **213**(1–3): 1-13.

Inghelbrecht, S., Remon, J. P., deAguiar, P. F., Walczak, B., Massart, D. L., VandeVelde, F., DeBaets, P., Vermeersch, H. and DeBacker, P. (1997). "Instrumentation of a roll compactor and the evaluation of the parameter settings by neural networks." International Journal of Pharmaceutics **148**(1): 103-115.

Inghelbrecht, S. and Remon, J. P. (1998a). "Roller compaction and tableting of microcrystalline cellulose drug mixtures." International Journal of Pharmaceutics **161**(2): 215-224.

Inghelbrecht, S. and Remon, J. P. (1998b). "The roller compaction of different types of lactose." International Journal of Pharmaceutics **166**(2): 135-144.

Iyer, R. M., Hegde, S., Singhal, D. and Malick, W. (2014a). "A novel approach to determine solid fraction using a laser-based direct volume measurement device." Pharmaceutical Development and Technology **19**(5): 577-582.

Iyer, R. M., Hegde, S., Dinunzio, J., Singhal, D. and Malick, W. (2014b). "The impact of roller compaction and tablet compression on physicomechanical properties of pharmaceutical excipients." Pharmaceutical Development and Technology **19**(5): 583-592.

Johanson, J. R. (1965). "A Rolling Theory for Granular Solids." Journal of Applied Mechanics: 842-848.

Khorasani, M., Amigo, J. M., Sun, C. C., Bertelsen, P. and Rantanen, J. (2015). "Near-infrared chemical imaging (NIR-CI) as a process monitoring solution for a production line of roll compaction and tableting." European Journal of Pharmaceutics and Biopharmaceutics **93**: 293-302.

Kleinebudde, P. (2004). "Roll compaction/dry granulation: pharmaceutical applications." European Journal of Pharmaceutics and Biopharmaceutics **58**(2): 317-326.

Kushner, J., Langdon, B. A., Hiller, J. I. and Carlson, G. T. (2011). "Examining the Impact of Excipient Material Property Variation on Drug Product Quality Attributes: A Quality-By-Design Study for a Roller Compacted, Immediate Release Tablet." Journal of Pharmaceutical Sciences **100**(6): 2222-2239.

Leuenberger, H., Bonny, J. D. and Kolb, M. (1995). "Percolation effects in matrix-type controlled drug release systems." International Journal of Pharmaceutics **115**(2): 217-224.

Leuenberger, H. (1999). "The application of percolation theory in powder technology." Advanced Powder Technology **10**(4): 323-352.

Levin, M. (2005). "How to Scale Up Scientically: Scaling Up Manufacturing." Pharmaceutical Technology **3**: S4-S12.

Lim, H., Dave, V. S., Kidder, L., Neil Lewis, E., Fahmy, R. and Hoag, S. W. (2011). "Assessment of the critical factors affecting the porosity of roller compacted ribbons and the feasibility of using NIR chemical imaging to evaluate the porosity distribution." International Journal of Pharmaceutics **410**(1-2): 1-8.

Liu, Y. and Wassgren, C. (2016). "Modifications to Johanson's roll compaction model for improved relative density predictions." Powder Technology **297**: 294-302.

Liu, Z., Bruwer, M. J., MacGregor, J. F., Rathore, S. S. S., Reed, D. E. and Champagne, M. J. (2011). "Scale-up of a Pharmaceutical Roller Compaction Process Using a Joint-Y Partial Least Squares Model." Industrial & Engineering Chemistry Research **50**(18): 10696-10706.

Malkowska, S. and Khan, K. A. (1983). "Effect of Re-Compression on the Properties of Tablets Prepared by Dry Granulation." Drug Development and Industrial Pharmacy **9**(3): 331-347.

Mansa, R. F., Bridson, R. H., Greenwood, R. W., Barker, H. and Seville, J. P. K. (2008). "Using intelligent software to predict the effects of formulation and processing parameters on roller compaction." Powder Technology **181**(2): 217-225.

Mazor, A., Pérez-Gandarillas, L., de Ryck, A. and Michrafy, A. (2016). "Effect of roll compactor sealing system designs: A finite element analysis." Powder Technology **289**: 21-30.

McAuliffe, M. A. P., Omahony, G. E., Blackshields, C. A., Collins, J. A., Egan, D. P., Kiernan, L., Oneill, E., Lenihan, S., Walker, G. M. and Crean, A. M. (2015). "The use of PAT and off-line methods for monitoring of roller compacted ribbon and granule properties with a view to continuous processing." Organic Process Research and Development **19**(1): 158-166.

Micromeritics (2001). GeoPyc 1360 Operator's Manual.

Michrafy, A., Diarra, H., Dodds, J. A., Michrafy, M. and Penazzi, L. (2011). "Analysis of strain stress state in roller compaction process." Powder Technology **208**(2): 417-422.

Miguélez-Morán, A. M., Wu, C. Y. and Seville, J. P. K. (2008). "The effect of lubrication on density distributions of roller compacted ribbons." International Journal of Pharmaceutics **362**(1–2): 52-59.

Miguélez-Morán, A. M., Wu, C. Y., Dong, H. S. and Seville, J. P. K. (2009). "Characterisation of density distributions in roller-compacted ribbons using micro-indentation and X-ray micro-computed tomography." European Journal of Pharmaceutics and Biopharmaceutics **72**(1): 173-182.

Miller, R. W. (2005). Roller Compaction Technology. Handbook of Pharmaceutical Granulation Technology, Second Edition. Parikh, D. M. New York, Marcel Dekker, Inc**:** 159-190.

Morrison, R. D., Shi, F. and Whyte, R. (2007). "Modelling of incremental rock breakage by impact – For use in DEM models." Minerals Engineering **20**(3): 303-309.

Mosig, J. and Kleinebudde, P. (2014). "Evaluation of lubrication methods: How to generate a comparable lubrication for dry granules and powder material for tableting processes." Powder Technology **266**: 156-166.

Muliadi, A. R., Litster, J. D. and Wassgren, C. R. (2012). "Modeling the powder roll compaction process: Comparison of 2-D finite element method and the rolling theory for granular solids (Johanson's model)." Powder Technology **221**: 90-100.

Nesarikar, V. V., Vatsaraj, N., Patel, C., Early, W., Pandey, P., Sprockel, O., Gao, Z. H., Jerzewski, R., Miller, R. and Levin, M. (2012a). "Instrumented roll technology for the design space development of roller compaction process." International Journal of Pharmaceutics **426**(1-2): 116-131.

Nesarikar, V. V., Patel, C., Early, W., Vatsaraj, N., Sprockel, O. and Jerzweski, R. (2012b). "Roller compaction process development and scale up using Johanson model calibrated with instrumented roll data." International Journal of Pharmaceutics **436**(1-2): 486-507.

Nkansah, P., Wu, S. J., Sobotka, S., Yamamoto, K. and Shao, Z. J. (2008). "A novel method for estimating solid fraction of roller-compacted ribbons." Drug Development and Industrial Pharmacy **34**(2): 142-148.

Osborne, J. D., Althaus, T., Forny, L., Niederreiter, G., Palzer, S., Hounslow, M. J. and Salman, A. D. (2013). "Investigating the influence of moisture content and pressure on the bonding mechanisms during roller compaction of an amorphous material." Chemical Engineering Science **86**: 61-69.

Patel, B. A., Adams, M. J., Turnbull, N., Bentham, A. C. and Wu, C. Y. (2010). "Predicting the pressure distribution during roll compaction from uniaxial compaction measurements." Chemical Engineering Journal **164**(2–3): 410-417.

Pérez-Gandarillas, L., Mazor, A., Souriou, D., Lecoq, O. and Michrafy, A. (2015). "Compaction behaviour of dry granulated binary mixtures." Powder Technology **285**: 62-67.

Pérez-Gandarillas, L., Pérez-Gago, A., Mazor, A., Kleinebudde, P., Lecoq, O. and Michrafy, A. (2016). "Effect of roll-compaction and milling conditions on granules and tablet properties." European Journal of Pharmaceutics and Biopharmaceutics **106**: 38-49.

Peschl, I. A. S. Z. and Colijn, H. (1977). "New rotational shear testing technique." Journal of Powder and Bulk Solids Technology **1**(3): 55-60.

Peter, S., Lammens, R. F. and Steffens, K.-J. (2010). "Roller compaction/Dry granulation: Use of the thin layer model for predicting densities and forces during roller compaction." Powder Technology **199**(2): 165-175.

Ragnarsson, G. (1996). Force-Displacement and Network Measurements. Pharmaceutical Powder Compaction Technology Alderborn, G. and Nystrom, C. New York, Marcel Dekker, Inc.**:** 77-97.

Rambali, B., Baert, L., Jans, E. and Massart, D. L. (2001). "Influence of the roll compactor parameter settings and the compression pressure on the buccal bio-adhesive tablet properties." International Journal of Pharmaceutics **220**(1-2): 129-140.

Retsch (2012). Bedienungsanleitung / Handbuch Korngrößenmesssystem Camsizer® und Camsizer® XT. Retsch Technology GmbH, Haan (Germany).

Reynolds, G., Ingale, R., Roberts, R., Kothari, S. and Gururajan, B. (2010). "Practical application of roller compaction process modeling." Computers & Chemical Engineering **34**(7): 1049-1057.

Roquette (2006). Pearlitol®. Mannitol for pharmaceutical applications.

Rowe, J. M., Crison, J. R., Carragher, T. J., Vatsaraj, N., McCann, R. J. and Nikfar, F. (2013). "Mechanistic Insights into the Scale-Up of the Roller Compaction Process: A Practical and Dimensionless Approach." Journal of Pharmaceutical Sciences **102**(10): 3586-3595.

Sakwanichol, J., Puttipipatkhachorn, S., Ingenerf, G. and Kleinebudde, P. (2012). "Roll compaction/dry granulation: Comparison between roll mill and oscillating granulator in dry granulation." Pharmaceutical Development and Technology **17**(1): 30-39.

Samanta, A. K., Ng, K. Y. and Heng, P. W. S. (2012). "Cone milling of compacted flakes: Process parameter selection by adopting the minimal fines approach." International Journal of Pharmaceutics **422**(1–2): 17-23.

Samanta, A. K., Karande, A. D., Ng, K. Y. and Heng, P. W. S. (2013). "Application of Near-Infrared Spectroscopy in Real-Time Monitoring of Product Attributes of Ribbed Roller Compacted Flakes." AAPS PharmSciTech **14**(1): 86-100.

Sheskey, P., Pacholke, K., Sackett, G., Maher, L. and Polli, J. (2000). "Roll compaction granulation of a controlled-release matrix tablet formulation containing HPMC: Effect of process scale-up on robustness of tablets, tablet stability, and predicted in vivo performance." Pharmaceutical Technology **24**(11): 30-52.

Sheskey, P., Pacholke, K., Sackett, G. and Maher, L. (2002). Lab-Scale to Full Production Scale Evaluation of a Controlled-Release Formulation Based on Hypromellose and Manufactured Using Roll Compaction Technology. 198-02080-0602AMS. USA, The Dow Chemical Company.

Shi, W. and Sprockel, O. L. (2016). "A practical approach for the scale-up of roller compaction process." European Journal of Pharmaceutics and Biopharmaceutics **106**: 15-19.

Shlieout, G. (2000). "New Aspects in the Roller Compaction Technology. Part 3: Dry Granulation with a Gerteis 3-W-Polygran Roll Compactor and Description of the Functional Units and Operation Modes." Pharmaceutical Technology Europe: 24-35.

Simon, O. and Guigon, P. (2003). "Correlation between powder-packing properties and roll press compact heterogeneity." Powder Technology **130**(1-3): 257-264.

Sinko, C. M., Carlson, G. T. and Gierer, D. S. (1995). "The identification of percolation and mechanical thresholds during the compaction of hydroxypropyl methylcellulose: Comparison to thresholds determined from out-of-die indentation experiments." International Journal of Pharmaceutics **114**(1): 85-93.

Smith, T. J., Sackett, G., Sheskey, P. and Liu, L. (2009). Development, Scale-up, and Optimization of Process Parameters: Roller Compaction. Developing Solid Oral Dosage Forms**:** 715-724.

Soh, J. L. P., Wang, F., Boersen, N., Pinal, R., Peck, G. E., Carvajal, M. T., Cheney, J., Valthorsson, H. and Pazdan, J. (2008). "Utility of multivariate analysis in modeling the effects of raw material properties and operating parameters on granule and ribbon properties prepared in roller compaction." Drug Development and Industrial Pharmacy **34**(10): 1022-1035.

Souihi, N., Dumarey, M., Wikstrom, H., Tajarobi, P., Fransson, M., Svensson, O., Josefson, M. and Trygg, J. (2013a). "A quality by design approach to investigate the effect of mannitol and dicalcium phosphate qualities on roll compaction." International Journal of Pharmaceutics **447**(1-2): 47-61.

Souihi, N., Josefson, M., Tajarobi, P., Gururajan, B. and Trygg, J. (2013b). "Design space estimation of the roller compaction process." Industrial and Engineering Chemistry Research **52**(35): 12408-12419.

Souihi, N., Nilsson, D., Josefson, M. and Trygg, J. (2015a). "Near-infrared chemical imaging (NIR-CI) on roll compacted ribbons and tablets – multivariate mapping of physical and chemical properties." International Journal of Pharmaceutics **483**(1–2): 200-211.

Souihi, N., Reynolds, G., Tajarobi, P., Wikström, H., Haeffler, G., Josefson, M. and Trygg, J. (2015b). "Roll compaction process modeling: Transfer between equipment and impact of process parameters." International Journal of Pharmaceutics **484**(1-2): 192-206.

Sprockel, O. L. and Stamato, H. J. (2011). Design and scale-up of dry granulation processes. Chemical Engineering in the Pharmaceutical Industry: R&D to Manufacturing. Ende, D. J. a.

Stauffer, D. and Aharony, A. (1994). Introduction: Forest Fires, Fractal Oil Fields, and Diffusion. Introduction to Percolation Theory. London, Taylor and Francis**:** 1-14.

Tan, B. M. J., Chan, L. W. and Heng, P. W. S. (2016). "Determination of the Nip Angle in Roller Compactors With Serrated Rolls." Journal of Pharmaceutical Sciences **105**(6): 1967-1975.

Teng, Y., Qiu, Z. and Wen, H. (2009). "Systematical approach of formulation and process development using roller compaction." European Journal of Pharmaceutics and Biopharmaceutics **73**(2): 219-229.

von Eggelkraut-Gottanka, S. G., Abu Abed, S., Muller, W. and Schmidt, P. C. (2002). "Roller compaction and tabletting of St. John's wort plant dry extract using a gap width and force controlled roller compactor. II. Study of roller compaction variables on granule and tablet properties by a 3(3) factorial design." Pharmaceutical Development and Technology **7**(4): 447-455.

Wagner, C. M., Pein, M. and Breitkreutz, J. (2015). "Roll compaction of granulated mannitol grades and the unprocessed crystalline delta-polymorph." Powder Technology **270**: 470-475.

Weyenberg, W., Vermeire, A., Vandervoort, J., Remon, J. P. and Ludwig, A. (2005). "Effects of roller compaction settings on the preparation of bioadhesive granules and ocular minitablets." European Journal of Pharmaceutics and Biopharmaceutics **59**(3): 527-536.

Wiedey, R. and Kleinebudde, P. (2016). "The Density Distribution in Ribbons from Roll Compaction." Chemical Engineering & Technology (in preparation).

Wöll, F. (2003). Entwicklung von Methoden zur Charakterisierung von Schülpen, Martin-Luther-Universität Halle-Wittenberg.

Wu, C. Y., Hung, W. L., Miguelez-Moran, A. M., Gururajan, B. and Seville, J. P. K. (2010). "Roller compaction of moist pharmaceutical powders." International Journal of Pharmaceutics **391**(1-2): 90-97.

Yu, S., Gururajan, B., Reynolds, G., Roberts, R., Adams, M. J. and Wu, C.-Y. (2012). "A comparative study of roll compaction of free-flowing and cohesive pharmaceutical powders." International Journal of Pharmaceutics **428**(1–2): 39-47.

Yu, S., Adams, M., Gururajan, B., Reynolds, G., Roberts, R. and Wu, C.-Y. (2013). "The effects of lubrication on roll compaction, ribbon milling and tabletting." Chemical Engineering Science **86**: 9-18.

Zhang, J., Pei, C., Schiano, S., Heaps, D. and Wu, C.-Y. (2016). "The application of terahertz pulsed imaging in characterising density distribution of roll-compacted ribbons." European Journal of Pharmaceutics and Biopharmaceutics **106**: 20-25.

Zheng, Z. X., Xia, W. and Zhou, Z. Y. (2013). "Experimental and Numerical Modeling for Powder Rolling." Reviews on Advanced Materials Science **33**(4): 330-336.

Zinchuk, A. V., Mullarney, M. P. and Hancock, B. C. (2004). "Simulation of roller compaction using a laboratory scale compaction simulator." International Journal of Pharmaceutics **269**(2): 403-415.

Zlokarnik, M. (1991). Dimensional Analysis and Scale-up in Chemical Engineering. Heidelberg, Springer Berlin Heidelberg.

Zohuri, B. (2015). Dimensional Analysis and Self-Similarity Methods for Engineers and Scientists. Switzerland, Springer International Publishing.

8. ACKNOWLEDGMENTS

8.1. DECLARATION OF INTEREST

This work was supported by the IPROCOM Marie Curie initial training network, funded through the People Programme (Marie Curie Actions) of the European Union's Seventh Framework Programme FP7/2007-2013/ under REA grant agreement No. 316555. This work would have not been possible without the great efforts invested by Prof. Dr. Dr. h.c. Peter Kleinebudde, whose ideas, guidelines and corrections have not only enriched this thesis, but made it feasible. However, there are more people who have contributed to a greater or lesser extent to achieve the results here presented, whose participation should be mentioned and acknowledged.

The author would like to start by thanking the host institutions where parts of this work were performed, for allowing the successful development of the collaborations, the access to their facilities and in most of the cases, provide the raw materials. In the first place, to thank Bayer Pharma AG located in Berlin (Germany) and the team of Dr. Susanne Skrabs, especially Dr. Sarah Just, Dr. Dejan Djuric and Christian Nienerza for their different roles in the work performed at the Polygran®. Secondly, to thank the University of Surrey (Prof. Charley Wu and his group, especially Ms. Serena Schiano) and AstraZeneca in Macclesfield (Dr. Gavin Reynolds and his group, especially Dr. Andreja Mirtič) both located in UK, for their advice and assistance during the Freund-Vector scale-up study. Finally, to acknowledge L.B. Bohle for kindly offering their facilities and machines to perform the L.B. Bohle study, and especially to Dr. Hubertus Rehbaum, Andreas Altmeyer and Philipp Harbaum for their different contributions to this work.

The author would like also to thank Raphael Wiedey for his assistance, help and predisposition in performing the measurements on the μCT, as well as the data collection, treatment and visualization. Similarly, acknowledge Dr. Rok Šibanc for the development and improvement of the software to extract the grey values. To thank Kitti Csordás for the production of the batches of MCC and the 50% mixture in the BRC 25, as well as Felix Franken for characterizing of the porosity of the samples corresponding to the 15% mixture produced at the Polygran®. Special acknowledgement goes to Dr. Gavin Reynolds and AstraZeneca for allowing the use of their tool, for providing the calibration data, for running the model, for forwarding the data and for performing the evaluation of the approach. Additionally, to thank him as well as for contributing to this thesis with some lines which allow

the clarification of the explanation or application of his approach. Similarly, to thank Orlando Pérez Gago for collaborating in the development of the Pérez Gago dimensionless variable, as well as for his advising, help and support during the whole process. To thank Dr. Klaus Knop for his assistance in taking the pictures of the ribbons presented in this work. And finally, to thank Katie Slater and Emily Brennan for the English revision and correction of this PhD thesis and Hannah Lou Reimer for her help in translating the "Summary and Outlook" section into German.

8.2. PERSONAL ACKNOWLEDGMENTS

My extraordinary supervisor Prof. Dr. Dr. h.c. Peter Kleinebudde, who I thank from the bottom of my heart. I am grateful to him from the moment he took the time to read my application for this position until the last minute he spent in improving this thesis. However, there are many things I would like to thank him for this 3 and a half years. Prof. Kleinebudde, thanks for giving me this amazing opportunity of not only being in a European project in which I have learnt a lot and grown in the scientific and personal field, but also thanks for choosing me to join, as I heard when I was still in Spain, one of the best research groups in Europe; thanks for trusting me even when I hesitate about my abilities; for having always a smile and good mood, even when you were busy or stressed; for all hours spent on questions, discussion and corrections; for your patience and for finding always a solution; for continuing to teach me something new day by day not only in the scientific aspect but also in the personal one; for allowing me to go to all conferences to present my results and to collaborate with many colleagues through the secondments, for being an admirable scientist, person and boss and finally, for everything else that you have done in order to make this work possible. Thanks for being like a professional father for me, I could never thank you enough for this chance.

My second supervisor and excellent scientist Prof. Dr. Jörg Breitkreutz, who has been always there for any comment, question or petition. Thanks for all the important and interesting contributions in Focus Groups, PhD seminars and similar discussions which have also improved this work; for all guidelines and help in conferences; for the corrections in German and in general, thanks for being there always with a great smile and good mood. I am really glad to have had the chance of working with you, and thanks to that, I have also grown and developed myself.

The IPROCOM coordinator Prof. Chuan-Yu (Charley) Wu, who has invested great efforts to make this multidisciplinary European project possible. Thanks Charley for organizing this consortium; for keeping working hard day by day; for not losing motivation, and transmitting this feeling to all of us, for accepting me as a member and for giving me the opportunity of collaborating with your team. In general, thanks for doing your best to make the project as successful as it is. Similarly, I would like to thank the IPROCOM project managers Dr. Ling Zhang and the former Dr. Chunlei (Marvin) Pei, for the fantastic organization, for all the kind reminders about our individual project duties and for having always nice words and being willing to help.

All other excellent IPROCOM supervisors Dr. Abderrahim Michrafy, Dr. Olivier Lecoq, Dr. Gavin Reynolds, Dr. Aleksander Mendyk, Dr. Charles Radeke, Dr. Torsten Kraft, Prof. Hugh Stitt, Dr. Michele Marigo, Dr. Crina Grosan, Prof. Vaclav Snasel and Prof. Ajith Abraham, as well as the members of the international advisory board, Prof. Karen Hapgood, Prof. Wei Ge and Prof. Antonios Zavaliangos. All them are prominent figures in their field and I would like to thank all of you for the interesting feedback, for giving another perspective to our work and for the wonderful time spent during the project meetings. I would especially like to thank Charley, Gavin, Abder and Aleksander for the collaborations, some may not be part of this thesis, but from which I have always learnt. Similarly, also to thank all partners who have made this project a great consortium and the host institutions of the meetings, who have always welcomed us with open arms.

My IPROCOM colleagues and friends Serena Schiano, Kitti Csordás, Lucía Pérez Gandarillas, Luca Orefice, Alon Mazor, Simone Loreti, Raphael Schubert, Varun Kumar Ojha, Hossam Zawbaa, Pezhman Kazemi, Hassan Khalid, Dr. Zilin Yan, Dr. Sebastian Gonzalez and Dr. Andreja Mirtič, as well as our "adopted" member of IPROCOM Dr. Alexander Krok, especially thanks for him for having the patience to show me the basis of the dimensional analysis. I am really thankful of having worked together in this project with these 15 fantastic researchers from all over the world. Thanks boys and girls for all the scientific discussions, for giving different points of view to our work, for learning and growing up together, for all the personal conversations and the moments of fun during the meetings. Especially thanks to Serena, Andreja, Kitti, Lucía, Alon, Simone, Varun, Hossam and Pezhman with whom I have the luck of working a bit more closely with, thanks for choosing me to collaborate together, for your help and patience during the secondments and for finding always moments to be friends during the working hours.

Alle meine Heinrich-Heine-Universität Doktoranden Kollegen genauso wie Postdocs, Master und Diploma Studenten, die mit mir seit August 2013 gearbeitet haben. Vielen Dank für das warme Willkommen, für die Hilfe am Anfang, wenn ich verloren war, für die wissenschaftlichen Diskussionen und Vorschläge in den Seminaren, für die lustige Anekdoten und die schöne Zeit hier zusammen, für die Geduld mit meinem Deutsch, für die Reisen zu Konferenzen und Meetings und, generell, vielen Dank für die Freundlichkeit und Anhänglichkeit, die ihr mit mir gehabt habt.

Alle meine „Granulation Focus Group" Kollegen, Dr. Christian Mühlenfeld, Dr. Moritz Wagner, Dr. Johanna Mosig, Dr. Julian Quodbach, Dr. Carolin Eckert, Dr. Carmen Stromberg, Dr. Gustavo Petrovick, Daniel Sieber, Dr. Robin Meier, Johanna Peters, Kitti Csordás, Haress Mangal, Simon Grote, Raphael Wiedey, Kira Adam, Alessia Lazzari, Oscar Arndt, Dr. Rok Šibanc und Hanna Lou Reimer. Ich bedanke mich nicht nur für die wissenschaftlichen Diskussionen, Ideen und Hilfe, sondern auch für die Mühe, Englisch in der Focus Group zu benutzen und die Geduld jetzt mit meinem Deutsch. Ich möchte auch alle meine „Mini-Pactor® Kollegen" für die Hilfe, Beratung und Zusammenarbeit danken. Ein besonderes Dankeschön für Dr. Johanna Mosig und Dr. Moritz Wagner für die Einführung am Walzenkompaktor, die Geduld mit den Fragen und im Allgemeinen, die Hilfe am Anfang der Promotion beim Kennenlernen der Grundlagen des Trockengranulierens und der Funktionsweise des Mini-Pactors®.

Meine Bürokollegen, besonders Dr. Robin Meier und Svenja Korthues, für die schöne Arbeitsatmosphäre, für alle die professionellen und persönlichen Gespräche, für alle die Übersetzungen von Briefen, Emails und so weiter, genauso wie alle die Anrufe auf Deutsch, für die Geduld mit den Fragen über die deutsche Sprache und allgemein, vielen Dank für die Freundlichkeit und die lustige Zeit zusammen.

Alle meine anderen Arbeitskollegen, Dr. Klaus Knop, Karin Matthée, Dorothee Eikeler, Annemarie Schmitz, Dorothee Hetkämper-Flockert und Stefan Stich, und auch die ehemaligen Mitglieder Prof. Dr. Markus Thommes und Prof. Dr. Miriam Pein-Hackelbusch. Ich bedanke mich für die wunderbare Arbeitsatmosphäre, für die Bereitschaft zu assistieren und für das Interesse an meinem Deutsch Niveau, das ich in dieser Zeit verbessert habe dank ihrer Hilfe. Ich möchte besonders Dr. Klaus Knop danken für seine Hilfe bei wissenschaftlichen, photographischen, PC-bezogenen und vielen anderen Problemen, aber auch für seine gute Laune und Geduld während der Jahre mit mir. Ich bedanke mich für alles.

All my foreign friends from the university, normally guests than I have the luck to work with or PhD students from other departments. I would like to thank Branko, Kasama, Cristina, Alessia, Marta, Manuel, Juan Pablo, Jin and Aki, for the nice times we shared together, everything that we have learnt together, for always lending a helping hand and in general, for your friendship. A special acknowledgement to my great friend and colleague since almost the beginning, Alessia Lazzari (who I am sure will become Dr. in 2018) for all her support, her optimist and energy, her good mood and big smiles, for always having nice words and patience, for teaching me a bit of Italian and for having always big hugs for me, especially in the worse moments. Grazie mille per tutto amore!

Mis antiguos profesores del departamento de Farmacia y Tecnología Farmacéutica de la Universidad de Santiago de Compostela (USC), el Dr. Francisco Javier Otero Espinar, el Prof. Dr. Ángel Joaquín Concheiro Nine, el Prof. Dr. Ramón Martínez Pacheco, la Dra. Carmen Isabel Álvarez Alonso y la Dra. Mariana Landín Pérez, por toda su ayuda y apoyo durante el proceso de solicitud de la plaza de doctorado en Alemania como durante el mismo, por creer en mí y estar orgullosos de mí y en general, por estar siempre ahí. Una mención especial merece sin duda alguna, mi supervisora de la Tesina y gran amiga de mis tiempos en el laboratorio de la USC, la Dra. María José Campaña Seoane, no solo porque sin ella, no me habría lanzado de cabeza a esta aventura, si no por todo su apoyo y amistad a lo largo de estos 3 años y medio, por alegrarse de mi progreso y por estar siempre ahí a pesar de la distancia. ¡Muchas gracias!

Mi maravillosa y única familia, por todo su apoyo desde el primer momento que comenté la posibilidad de dejar la comodidad de España para aventurarme en Alemania a hacer el doctorado, hasta la última llamada por teléfono para concretar los detalles de la defensa. Gracias a todos, Papá, Mamá, Or, Celia y Santi, al igual que mi Abuela, mi padrino Berna y mi familia política, especialmente Carmiña. Gracias a todos por apoyarme en esta pequeña locura y animarme en los momentos más duros. Gracias no solo por entenderlo, lo que ya de por sí no es fácil (sobre todo para los pequeños), si no por estar orgullosos de mí (y me consta que incluso presumir un poco), por las horas hablando de las dificultades a lo largo este camino, por estar siempre ahí, 24 horas al día, 7 días a la semana, y básicamente, gracias por quererme y confiar así de ciegamente en mí. A pesar de los kilómetros, saber que estáis ahí apoyándome, me da fuerza día tras día. ¡Os quiero mucho a todos!

Mi marido, amor de mi vida y compañero de aventuras, Cristian Rodríguez Mirazo. Gracias tesoro, desde el momento que decidiste renunciar a todo en España para venir

conmigo, hasta el último abrazo de apoyo o palabra de ánimo. Muchas gracias por seguirme en este viaje a lo desconocido, por ser el hombro en que llorar, por abrirme los ojos esos días en que hubiera hecho las maletas y vuelto a España, por estar orgulloso de mí, por siempre creer que todo va a salir bien, por ser el pilar que me fortalece, por todo tu cariño, amor y apoyo sin descanso; gracias simplemente por ser como eres y por quererme ciega e incondicionalmente. ¡Te quiero muchísimo bonito!